Population heterogeneity in Saccharomyces cerevisiae and Escherichia coli lab scale cultivations simulating industrial scale bioprocesses

Heins, Anna-Lena; Carlqvist, Magnus; Gernaey, Krist V.; Eliasson Lantz, Anna

Publication date:
2014

Document Version
Peer reviewed version

Population heterogeneity in *Saccharomyces cerevisiae* and *Escherichia coli* lab scale cultivations simulating industrial scale bioprocesses

PhD Thesis

by

Anna-Lena Heins

February 2014

Department of Systems Biology, Technical University of Denmark

Supervisors: Associate Professor Anna Eliasson Lantz,

Professor Krist V. Gernaey (DTU Chemical and Biochemical Engineering),

Assistant Professor Magnus Carlquist (Lund University)

Preface

This thesis was prepared at the Department of Systems Biology, at the Technical University of Denmark (DTU) as partial fulfillment of the requirement for acquiring the degree of Doctor of Philosophy (Ph.D.)

The here presented work was carried out from January 2011 till February 2014. Associate Professor Anna Eliasson Lantz (DTU Systems Biology) was the principal supervisor for the project with Professor Krist V. Gernaey (DTU Chemical Engineering) and Assistant Professor Magnus Carlquist (Lund University) as co-supervisors.

This Ph.D. project was financed by the Danish Council for Strategic Research in the frame of the project "Towards robust fermentation processes by targeting population heterogeneity at microscale" (project number: 09-065160).

Kongens Lyngby, 2014

Anna-Lena Heins

Acknowledgements

First I would like to thank my three supervisors Anna Eliasson Lantz, Krist V. Gernaey and Magnus Carlquist for giving me the opportunity of doing this project. Furthermore I'm grateful for all the guidance, support, optimism and always an open ear especially during the last months. A special thanks also for the long work meetings in Denmark and Sweden.

Moreover I was really lucky to be part of a project that involved a lot of different people which were all fun to work with! Thanks for the fun workshops, group meetings, long fermentation nights, bus or car rides with samples, sample measurement days, conferences, work meetings and always nice chats ☺! A special thanks to you Rita, Luisa, Marta, Andrijana, Shanshan, Ted and Ines. Also to Anna S. who joined the heterogeneity group for a short while.

I also want to thank all my colleagues from the former CMB for being welcoming and always nice, helpful and anytime open for a talk. Special thanks goes to Stig, Lars, Paiman, Peter, Phillippe, Tomas and Gerit for always being up for socialising as well as to my two offices mates Louise and Zofia for a lot of fun, motivational talks and always finding good excuses to not work ;)!

A big thanks also goes to all the people that were there for lunch, afternoon breaks and especially outside working hours and always up for crazy things! Thanks for all the nice evenings, nights, days, weekend trips$_{\text{Because I Can}}$ and moments! Thanks for the motivation, head ups and for just always being there Koletti, Sarah, Oli, Hande, Watsy, Thas (thanks for always fixing stuff), Andrea, Aleks and Brauney$_{\text{Because I can}}$! Special thanks also to the girls and my danish family!

Als letztes aber natürlich nicht am unwichtigsten danke ich meiner Familie dafür dass sie mich immer unterstützt und für mich da ist auch wenn ich manchmal nichts von mir hören lasse ;).

Abstract

Today it is well known that a population of cells in a bioreactor is heterogeneous, opposite to traditional belief, and thus exhibiting distributions of single cell properties e.g. cell size, viability and metabolic activity rather than having a set of characteristics that can be described by averaged values. Population distributions always exist, but are significantly pronounced due to a combination of metabolic and stress responses of single cells travelling throughout the reactor experiencing gradients of substrate, pH and oxygen caused by non-ideal mixing in industrial scale bioprocesses. This thesis aimed at reaching a deeper understanding of how microbial physiology and cell dynamics are affected by the spatial heterogeneity in a bioreactor. Therefore large scale fermentation was simulated in laboratory scale using two of the most industrially relevant organisms *E. coli* and *S. cerevisiae*. Single cell distributions of cell size and fluorescence - originating from growth, cell membrane robustness and ethanol reporter strains or different fluorescence stains (for e.g. viability and metabolic activity) - were thereby followed by applying flow cytometry. Cell responses were studied in different cultivations modes, in steady state at different growth rates and in response to glucose perturbation in continuous culture, simulating the feeding zone of a large scale fed-batch fermentation and in batch culture to characterise the single cell behaviour in a dynamic environment. Furthermore, a two compartment chemostat setup, simulating different zones seen in large scale cultivations, was developed and studied under different compartmentalization conditions. The observed population heterogeneity distributions were, opposite to the common approach using mean values, described and validated in a quantitative manner through newly developed parameters, using percentile analysis followed by multivariate statistics as well as using a modeling approach.

In general the applied reporter strains as well as fluorescence stains in combination with flow cytometry showed to be valuable tools to study population heterogeneity in the different setups simulating large scale fermentation that can potentially be used in development and optimisation of industrial scale processes. Differences in growth and membrane robustness due to varying growth conditions and between slow and fast growing cells, different metabolic activities on different substrates and phenomena during compartmentalization which are hidden in a normal chemostat could be successfully visualised and quantified.

Resumé

Modsat den tidligere traditionelle opfattelse er det i dag velkendt at en population af celler i en bioreaktor er heterogen. Cellerne i populationen er forskellige og derfor finder man fordelinger af enkel celle egenskaber, f.eks. celle størrelse, levedygtighed og metabolisk aktivitet, i modsætning til karakteristikker der kan blive beskrevet af gennemsnitlige værdier. Der vil altid være en vis heterogenicitet i en celle population, men heterogeniciteten bliver mere tydelig på grund af forskel i metabolske og stress responser hos enkelte celler når de bevæger sig igennem reaktoren og udsættes for gradienter af substrat, pH og oxygen, forårsaget af en ikke-ideel omrørning i industri-skala bioreaktorer. Denne afhandling sigter efter at opnå en større forståelse af hvordan mikrobiel fysiologi og celle dynamik er påvirket af spatial heterogenicitet i en bioreaktor. Derfor blev industriskala fermenteringer simuleret i laboratorieskala, hvor der blev anvendt to af industriens mest relevante organismer, *E. coli* and *S. cerevisiae*. Enkel celle fordelinger af celle størrelse og fluorescens – udsprunget fra henholdsvis vækst-, cellemembran robusthed- og ethanol- reporter stammer eller fra forskellige fluorescens indfarvninger (for at detektere f.eks. levedygtighed og metabolisk aktivitet) – blev dermed fulgt ved at anvende flødescytometri.

Cellernes respons blev studeret i forskellige fermenterings opstillinger; i steady state ved varierende vækst rate og efter glukose pulser i kontinuerlige gæringer, med formål at simulere fodringszonen af en storskala fed-batch fermentering samt i batch for at karakterisere cellepopulationens adfærd i et dynamisk miljø. Dertil blev en to-kammer kemostat opstilling, med hensigt at simulere de forskellige zoner som opstår i storskala reaktorer, udviklet og studeret under forskellige betingelser. Den observerede population heterogenicitets fordelningen, kunde beskrives kvantitativt ved brug af ny-udviklede matematiske parametre, percentil analyse i kombination med multivariat statistik samt ved modellering.

Generelt set viste sig de anvendte reporter stammer, såvel som fluorescens indfarvningsmetoderne, i kombination med flødescytometri at være værdifulde værktøjer til at studere populations heterogenicitet i forskellige setups, simulerende storskala fermentering. Strategier brugt i denne afhandling har potentiale til at blive anvendt i udvikling og optimering af storskala processer. Følgende er succesfuldt blevet visualiseret og kvantificeret: Forskelle i vækst og membranrobusthed under varierende vækstbetingelser og mellem langsomt og hurtigt voksende celler; forskellige metabolske aktiviteter på forskellige substrater og fænomener relateret til hurtigt skift mellem

vækstbetingelser, som normalt er skjulte i en regulær kemostat. Desuden vil den opnåede fysiologiske indsigt kunne bruges i udformning af fremtidlige proces optimerings strategier.

Table of contents

1. Chapter

Outline and aim of the thesis

1.1 Aim of the thesis

The aim of this thesis was to achieve a deeper understanding of how the spatial heterogeneity often seen in industrial fermentation processes influences microbial physiology, and in particular how population heterogeneity and cell dynamics are affected. The underlying phenomena were investigated at single cell level by experimental simulation of large-scale fermentation conditions in laboratory scale. In addition, tools to perform population heterogeneity studies in a quantitative manner were developed and validated in the frame of this thesis.

Traditionally microbial physiology in fermentation processes has been described using averaged values which fail to characterise the real situation in a bioreactor[1]. Heterogeneous populations have been found, for example with cells in different stages of the cell cycle and with varying activity, which may lower the biomass yield in scale-up of aerobic processes and in addition enlarge by-product formation[2,3]. In contrast, it was found that large-scale processes with higher heterogeneity are more robust, exhibiting a higher cell viability compared to lab-scale experiments[4]. The underlying reason for both phenomena is a combination of metabolic and stress responses of the cells resulting from glucose, pH and oxygen gradients throughout the reactor causing a highly dynamic environment and hence a heterogeneous population[3]. Based on these findings the central hypothesis arises that there is an optimal level of population heterogeneity that leads to more robust processes while still sustaining a high productivity. But currently, the understanding of population heterogeneity is very limited and seldom researched in detail.

To get a deeper understanding of the interplay between environmental conditions and cell responses at the single cell level, two of the most industrially relevant organisms for production of recombinant proteins and biopharmaceuticals, *Escherichia coli* and *Saccharomyces cerevisiae*, were studied in different cultivation modes. The enterobacterium *E. coli* is widely used for the production

of recombinant proteins, and numerous of them have been approved for use as biopharmaceuticals for the treatment of infectious diseases or endocrine, nutritional and metabolic disorder disease groups like e.g. insulin for the treatment of diabetes mellitus or the human hormone somatostatin[5]. Due to its advantageous physiology and characteristics (fast growth, rapid expression as well as ease to culture and genetically modify) it has also become a model organism for prokaryotes and therefore its genetics is better understood than those of other microorganisms[6]. However, *E. coli* also exhibits some disadvantageous features, for example the inability to glycosylate the produced proteins and the formation of inclusion bodies, which inactivates proteins. Furthermore, acetate that is produced by *E. coli* as by-product in mixed acid fermentation not only reduces overall process yields but also results in cell toxicity[6]. The well-known yeast *S. cerevisiae* is both used as an eukaryotic model organism and for production of various biotechnological products[7,8]. Some industrial processes aim at *S. cerevisiae* itself (for bread, wine and beer production) or products naturally produced by yeast e.g. ethanol, whereas for others like the production of recombinant proteins and biopharmaceuticals, new metabolic pathways need to be introduced into yeast[7]. For the latter case *S. cerevisiae* exhibits advantageous characteristics compared to prokaryotes because the produced proteins are mostly excreted (extracellular) and *S. cerevisiae* can furthermore glycosylate them in a similar way as mammalian cells, though still not all proteins produced by yeast can be accepted by humans[6]. Further valuable properties of *S. cerevisiae* are its GRAS (generally regarded as safe) status, considerably rapid and high density growth in defined medium, high yields and productivity in processes and its stability as production strain making it a cost efficient production host[6]. Even though *S. cerevisiae* as production host also shows some obstacles, e.g. that the production of recombinant proteins also triggers conformational stress responses and produced proteins sometimes fail to reach their native conformation, many approved protein products are available like hormones (e.g. insulin), vaccines (e.g. hepatitis B virus surface antigen) and virus-like particles (VLPs)[5]. As in the case of *E. coli*, most of the recombinant pharmaceuticals from yeast are targeting the treatment of either infectious diseases or endocrine, nutritional and metabolic disorders[5].

My studies have focused on exploring causes and influences of cell population heterogeneity of the two organisms during experimental lab-scale simulation of large-scale fermentation processes. Hereby the focus was mainly on cultivations with glucose as substrate. Primarily, continuous cultivations (chapter 4, 6 and 8), which are used to investigate single cell responses to different growth rates and to simulate gradients seen in industrial scale fed-batch fermentation by

perturbations with substrate pulses, were used for my population heterogeneity studies. Another way of simulating large-scale fed-batch and/or continuous cultivations is the use of multi-compartment reactors (mostly referred to as scale-down reactors), which have been shown to be a valuable tool to study cellular responses to gradients[9] and were employed for work described in this thesis (chapter 8). Furthermore, for strain characterization (chapter 4), to follow changes in growth rate and single cell physiology over time (chapter 5 and 7) or study the influence of different conditions (aerobic/anaerobic, pH and glucose concentration) on physiology, batch cultivations were used.

During the performed cultivations, population performance and physiology were studied both at the average population and at the single-cell level. Physiological heterogeneities during cultivation in different process modes were studied by using flow cytometry (for method description, see chapter 2a) gathering information about cell size, morphology as well as fluorescence intensity correlated to specific cell properties. Fluorescent dyes were used to study metabolic activity, viability and respiration of single cells in cultivation processes (chapter 4 and 7). Furthermore, transcription based reporter strains expressing green respectively blue fluorescent protein (GFP, BFP) were used to study heterogeneities in growth and physiological responses to ethanol and glucose levels (detailed description see chapter 2a). As an additional feature the GFP reporter strain could be used to study freeze-thaw stress tolerance due to the pH sensitivity of GFP as a fluorescent reporter. The BFP fluorescence however is pH independent (chapter 8).

1.2 Outline of the thesis in brief

At first, a short introduction to the tools and methods used in the scope of this thesis, partly based on a review paper which is included in the appendix, is given (chapter 2a). The *E. coli* and *S. cerevisiae* strains employed, the major measurement tool flow cytometry and the fluorescence strains to assess single cell property distributions are introduced. Thereafter, studies of population heterogeneity at single cell level in cultivation processes at different scales and with different process modes presented in literature will be reviewed (chapter 2b). The sample analysis and experimental setup used for different population heterogeneity studies in this thesis are then shortly introduced (chapter 3). Experimental results are presented in the chapters four to eight. The major findings of my studies will be summarised and future perspectives will be discussed in chapter nine. In the appendix other publications that were generated during my PhD project but are not included in this thesis are provided.

In chapter four, the characterization of the *S. cerevisiae* growth reporter strain FE440 and its potential as a tool to investigate single-growth rate heterogeneities within a population during batch and continuous cultivation was described. Thereafter, to obtain an objective overview of the degree of heterogeneity seen under different conditions in batch cultivation of *S. cerevisiae* FE440 in lab-scale, a data analysis method combining interval analysis with principal component analysis was developed (chapter 5). To investigate the physiological responses to sudden changes from glucose-limited to glucose excess conditions glucose pulses were introduced to steady state cultures of *E. coli* and *S. cerevisiae* growth reporter strains to investigate the resulting impact on single cell physiology. To objectively quantify the overall resulting heterogeneity, both in steady state and as a result of the glucose pulse, descriptive mathematical tools were developed (chapter 6). In chapter seven, a combination of five different fluorescent stains targeting different metabolic properties and an *E. coli* growth reporter strain were applied to investigate the effect of acetate on population heterogeneity in large scale fermentation. Therefore, the cells were grown in batch cultivations with acetate respectively glucose as carbon source. To further simulate industrial production conditions and the appearance of substrates gradients, a continuous scale down setup has been modeled *in silico* and subsequently developed in the lab by connecting two stirred tank reactors (STRs) to each other (chapter 8). This two-compartment reactor set-up was applied to further study physiology responses to fluctuating conditions using the FE440 growth reporter strain as well as a *S. cerevisiae* ethanol reporter strain expressing BFP.

1.3 References

1. Fernandes, R. L. *et al.* Experimental methods and modeling techniques for description of cell population heterogeneity. *Biotechnol. Adv.* **29,** 575–599 (2011).

2. Bylund, F., Collet, E., Enfors, S.-O. & Larsson, G. Substrate gradient formation in the large-scale bioreactor lowers cell yield and increases by-product formation. *Bioprocess Eng.* **18,** (1998).

3. Enfors, S. O. *et al.* Physiological responses to mixing in large scale bioreactors. *J. Biotechnol.* **85,** 175–185 (2001).

4. Hewitt, C. J., Nebe-von Caron, G., Nienow, a W. & McFarlane, C. M. The use of multi-parameter flow cytometry to compare the physiological response of Escherichia coli W3110 to glucose limitation during batch, fed-batch and continuous culture cultivations. *J. Biotechnol.* **75,** 251–264 (1999).

5. Ferrer-Miralles, N., Domingo-Espín, J., Corchero, J. L., Vázquez, E. & Villaverde, A. Microbial factories for recombinant pharmaceuticals. *Microb. Cell Fact.* **8,** (2009).

6. Demain, A. L. & Vaishnav, P. Production of recombinant proteins by microbes and higher organisms. *Biotechnol. Adv.* **27,** 297–306 (2009).

7. Krogh, A. M. *et al.* Adaptation of Saccharomyces cerevisiae expressing a heterologous protein. *J. Biotechnol.* **137,** 28–33 (2008).

8. Nielsen, J. & Jewett, M. C. Impact of systems biology on metabolic engineering of Saccharomyces cerevisiae. *FEMS Yeast Res.* **8,** 122–131 (2008).

9. Papagianni, M. Methodologies for Scale-down of Microbial Bioprocesses. *J. Microb. Biochem. Technol.* **05,** 1–7 (2011).

2. Chapter a

Background of tools for single cell analysis

2.1 Study of general physiology and single cell properties in bioprocesses

As mentioned above, cell population heterogeneity resulting from a changing environment inside the bioreactor implies the co-existence of cells at different physiological states. It is of outmost importance to characterize the physiological state of single cells in a population and to monitor the presence of potential unproductive subpopulations for industrial fermentation processes since in a number of bioprocesses cell growth, and closely related to it physiology, is tightly correlated to productivity[1]. Information about cell physiology is a prerequisite for process optimization to achieve robust and high-yielding production. Traditionally, this knowledge has been acquired by on-line respectively at-line measurement of a number of parameters characterizing the process (e.g. pH and T) or the performance of the microorganism indirectly (e.g. cell density, sugar consumption, product formation). However, with the significant improvements of the techniques for molecular biology and systems level analysis, the physiological state of cells may be investigated in much greater detail (see chapter 2b). This may for example involve assessment of the change in expression levels of individual genes throughout a process, either by global transcriptomics or by following the expression of specific genes of particular relevance[1]. Therefore, the traditional methods are today known as general practices which are applied as a basis in every bioprocess and normally more advanced methods are applied for deeper cell analysis (see chapter 2b). Single-cell analysis of microbial populations is an advanced method that lately has received much attention, and a number of studies focusing on quantification of single-cell properties have been reported in the last years (see chapter and review by Schmid *et al.* (2010)[2]). Most single-cell studies generally aim at characterisation of the microenvironment in the vicinity of individual cells (applying traditional methods), whereas understanding the underlying phenomena of population heterogeneity, the mechanisms or origin of the observed changes between cells is rarely done up to now (reviewed by Fernandes *et al.* (2011)[1]). Such methodologies can be of different nature and involve a broad range of characteristics, which in combination give information about the response of populations to their immediate environment.

In this thesis, different analytical methods, traditional as well as single cell methods were applied. Most of the traditional methods are nowadays general practice in monitoring bioprocess operations like the online measurement of the off gas composition as well as on-line recording of controlled process parameters including dissolved oxygen, pH, stirrer speed and temperature. Moreover, at-line measurement of optical density, cell biomass dry weight and substrate consumption, product formation and by-product formation using high performance liquid chromatography (HPLC), are well established. This is the reason why these methods are not discussed in more detail here. The following sections rather focus on tools specifically related to single cell analysis, and on the methodologies applied in the work reported in this thesis. First a short introduction to flow cytometry – a technique which in my work was used for all measurements of single cell properties - is given due to its general importance for the thesis. Afterwards the tools that were used to make population heterogeneity accessible via flow cytometry, e.g. reporter strains and fluorescent dyes, are shortly introduced.

2.2 Tools used to study single cell properties in bioprocesses

2.2.1 Basic principles of flow cytometry

A flow cytometer (FC) is a robust high-throughput instrument that counts, sorts and examines particles in suspensions, such as bacteria and yeast cell cultures[1]. It can be used to measure a variety of structural and functional single cell features at high speed in real time, which allows its application for the study of phenotypic diversity of individual cells[1] and with it the assessment of population heterogeneity[3]. Hereby it relies on the properties of light scattering, and fluorochrome excitation and emission[1]. Different protocols have been developed in order to study diverse cell properties such as size, intracellular pH, protein content and membrane potential in single cells within an entire population using flow cytometry in combination with fluorescent dyes ([1] and reviewed in chapter 2b).

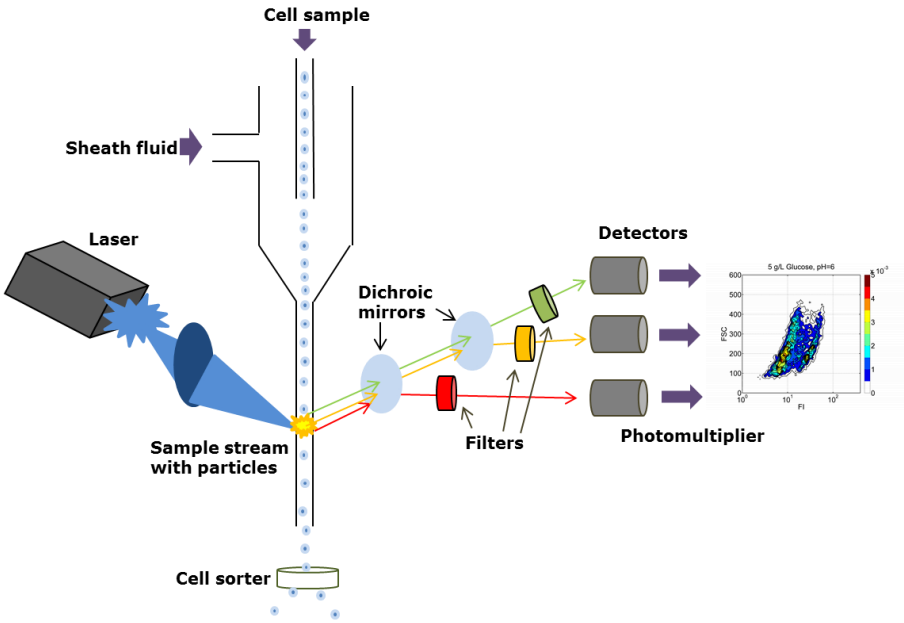

Figure 1 – Schematic presentation of a flow cytometer: including fluidics, light source, optics and electronic parts.

A flow cytometer (figure 1) consists of four core parts, the fluidics, the light source, the optics and the electronic part[4]. The fluidics contains a flow chamber that provides and maintains a constant laminar stream of liquid in the system which is use to transport the cells. The cell sample is injected into the flow chamber stream (Sheath fluid) and aligned by hydrodynamic focusing[4]. Thereafter the cells pass one after each other through a laser beam that is orthogonal to the flow. This allows the detection of up to 10 000 cells /s [3]. When the light impacts the cells, the focused light of the laser is scattered in both forward and sideways directions. The forward-scattered light (FSC) can be correlated to cell size in yeast[5]. For bacterial cells it provides hints about cell morphology[6]. The side-scattered light (SSC) is affected by several parameters, including granularity, cell size and cell morphology[4]. The scattered light will be directly collected whereas cell fluorescence originating from e.g. staining of specific cell characteristics (see chapter 7) or from reporter genes (applied in all chapters) needs to be filtered by optical filter units for specific wavelength detection before collection (e.g. 488 nm for GFP fluorescence)[4]. For this purpose separate fluorescence channels are present, which allows certain cell components and properties to be selectively assayed[3]. The resulting fluorescence light will then be processed through the photomultiplier converting the recorded optical signal into an electrical impulse that will be sent to the data processing system. The scattered light and the fluorescence signals can be combined in various ways to enable the observation of subpopulations carrying different traits. To sort subpopulations or cells with user-

specified properties, flow cytometry can also be combined with a sorting unit which offers the possibility of separating selected cells from the rest of the population[4].

When visualizing the collected flow cytometry data, bivariate plots or single parameter plots (histograms) are created in most cases (figure 2) using one of the various available softwares for data processing. But also multivariate data analysis methods have been developed to improve the extraction of information from data obtained by multi-parameter flow cytometry analysis[7]. In this thesis Matlab was exclusively used for processing of the single-cell data, obtained as fcs-files from the FC. To get a general overview of the data the above mentioned biplots or single parameter plots (histograms) were used in the this thesis (figure 2). For the biplots two properties of the cell population, normally FSC and GFP fluorescence, were plotted against each other to evaluate the relation between these parameters. Additionally, when evaluating the shape of a population distribution of a chosen property, histogram plots were utilised. Hereby the number of events/cells recorded in each fluorescence channel, which are 1024 for the flow cytometer used in this thesis, were plotted. Series of histograms plotted in the same graph – either stacked or stacked offset - allow the direct comparison of the shape as well as e.g. the detection of shifts of the whole population over time. For the deeper investigation of the shape of the population distributions, an alternative and only rarely applied way of plotting distribution data was also used in the scope of this thesis, namely the cumulative distribution function plot (cdf-plot, figure 2 right). The cdfplot represents the cumulative sum of the number of events/cells recorded in sequential channelnumbers and is normalised by the sum of the total number of recorded cells, thus resulting in a sigmoidal shaped distribution curve. This way of plotting facilitates shape comparisons if two distributions are similar and also clarifies the existence of subpopulations, because even small changes in the distribution are visible as shifts in the slope of the curve.

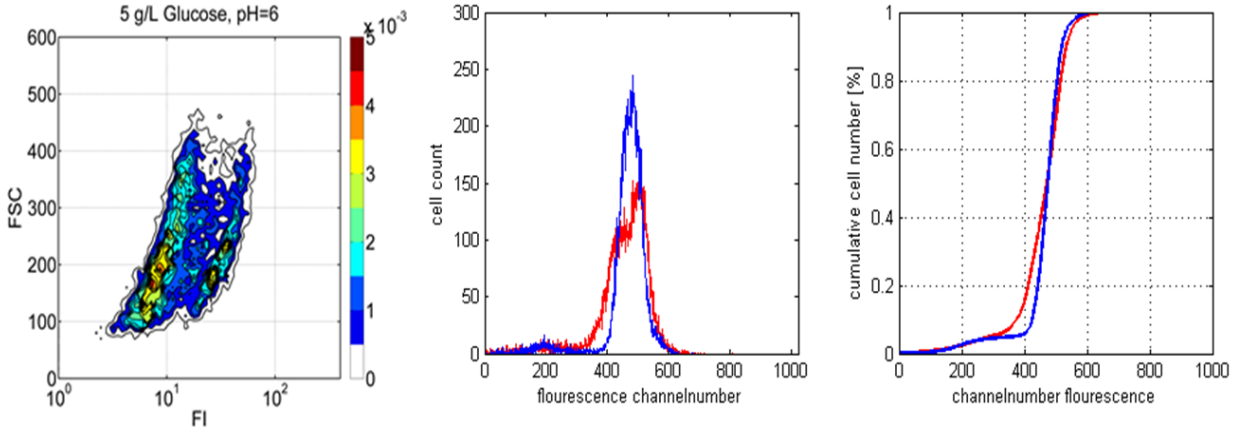

Figure 2 – Visualisation of flow cytometry data: Classical flow cytometry data are plotted as biplots (left) or single parameter histograms (middle). An alternative way to plot distribution data is the cumulative distribution function plot (right).

2.2.2 Reporter strains, a tool to study population heterogeneity

For the understanding of the cell physiology, different reporter systems have been proven to be useful tools to monitor events occurring inside the cells (see chapter 2b). Using reporter systems, gene regulation/expression can be visualised in an alternative and simpler way than using time-consuming and expensive global methods (e.g. Northern blotting, fingerprinting methods or DNA microarrays)[1,8]. Reporter strains typically express a protein or enzyme whose activity can be easily assayed (e.g. fluorescent protein GFP or BFP)[1] for example by the use of flow cytometry analysis. The use of reporter genes can provide different kinds of cellular information, e.g. protein localization, formation of protein complexes, polypeptide folding, protein stability and intracellular pH[9–11]. Nevertheless, most common reporter gene systems are used to obtain information of the gene transcription frequency (RNA formation) and/or gene dose of the protein respectively enzyme of interest[1]. Since reporter systems are strain dependent according to e.g. codon usage and protein maturation the choice should be well considered depending on which parameters to address. Normally the procedure of choosing a reporter system - meaning the procedure aiming at combining a promoter from a suitable target gene with an e.g. fluorescent reporter protein - begins with a literature search for whole-genome transcriptomics data. These data are reviewed for promoters which exhibit a large and fast response as well as a low background signal connected to the state of cells of interest. If possible these data should afterwards be confirmed from several independent sources to avoid biased data interpretation.

In the scope of this thesis, two *S. cerevisiae* and two *E. coli* reporter strains with the expression of a green respectively blue fluorescent protein (GFP, BFP), were applied for different studies and their characteristics are summed up in table 1. Both *E. coli* reporter strains, and one of the *S. cerevisiae* reporter strains are transcription based,-GFP growth reporters. The growth reporter strains carry the GFP gene chromosomal integrated for yeast (additionally also an extra copy of the promoter of choice) respectively on the plasmid for *E. coli* downstream of growth related promoters, and are useful tools to study physiology since they provide an estimate of the growth of non-steady–state cultures[12]. In my work, I used the strains to study how environmental changes influence reporter gene expression and consequently also influence the growth of the microorganisms.

The *S. cerevisiae* growth reporter strain FE440 expresses a chromosomal integrated yEGFP3 gene (yeast optimized GFP)[13] under the control of the ribosomal promoter *RPL22a* (further described in chapter 4 and also used in chapter 5, 6 and 8). Ribosomal protein synthesis in *S. cerevisiae* is believed to be regulated at transcription level[14] implying that the amount of mRNA is correlated to the amount of ribosomal protein. Since the ribosome biogenesis is affected by the growth rate of the cell, transcription of the ribosomal protein genes should be correlated to growth[15], and thus GFP expression is a marker for growth in this case (chapter 4). In addition, when applying freeze-thaw stress the reporter strain can also be used to examine cell wall robustness, since fluorescence from the intracellular GFP, which is pH dependent, is reduced in cells with permeabilised cell membrane due to changes of the intracellular pH (chapter 4).

As mentioned before, both of the *E. coli* strains are growth reporter strains. The *E. coli* Fis reporter strain is based on the *fis* promoter (applied in chapter 6), whose product controls the expression of a transcriptional activator of the ribosomal RNA by recruiting the RNA polymerase to the promoter[16]. This strain carries an unstable variant of GFP[17] and the genes are expressed from a low copy number plasmid. GFP expression in the *E. coli* Fis reporter strain has been shown to respond to changes in growth conditions since *fis* expression is immediately replying to nutrient up-and downshift and thereby regulated by growth[18–21]. The second *E. coli* reporter strain rrnBP1P2 (applied in chapter 7) also expresses an unstable GFP and the promoter is Fis. Fis acts as a transcription factor that activates the *rrnB* promoter[18]. Also for this reporter strain GFP fluorescence has been seen to correlate to growth.

The second *S. cerevisiae* reporter strain is an ethanol reporter strain expressing a BFP (Johansen, unpublished). Hereby the BFP expression is controlled by the promoter for phosphoenolpyruvate

carboxykinase 1 (PCK1). PCK1 catalyzes the conversion of oxaloacetate via guanosine triphosphate (GTP) to phosphoenolpyruvate as the first and rate-limiting step of the gluconeogenesis. Transcriptome studies have demonstrated that the expression of PCK1 is upregulated during ethanol consumption after diauxic shift and repressed by the presence of glucose[22,23] and hence the BFP signal will increase when glucose has been depleted and cells are utilising ethanol. Compared to the other reporter strains that express a GFP, the use of TagBFP, whose fluorescence is pH independent, results in that the strain cannot be used for determination of membrane robustness as no reduction in fluorescence signal can be seen in cells exposed to freeze-thaw stress.

Table 1 - Overview of reporter strains: used in the scope of the thesis including characteristics as organism, promoter used to express the reporter gene, type of integration, type of reporter and reference if already published.

Strain	Organism	Promoter	Reporter gene	Type of integration	Type of reporter	Reference
FE440	*S. cerevisiae*	RPL22a	GFP	Chromosomal	Growth reporter	Chapter 4 [24]
Sc-PCK1-B	*S. cerevisiae*	PCK1	BFP	Chromosomal	Ethanol reporter	(Johansen, unpublished)
MG1655/pGS20PrrnBGFPAAV	*E. coli*	Rrnb	GFP	Plasmid	Growth reporter	Han *et al.* (2013)
MG1655/pGS20fisGFPAAV	*E. coli*	Fis	GFP	Plasmid	Growth reporter	Han *et al.* (2013)

2.2.3 Fluorescent dyes that enable description of microbial properties at single cell level

Fluorescent dyes allow for determination and monitoring of several cell properties including structural respectively functional parameters (e.g. viability, DNA content)[1]. In combination with flow cytometry, fluorescent dyes can contribute to obtain increased knowledge about population heterogeneity and dynamics, because single cell distributions of the stained properties will be recorded. Furthermore, the application of a combination of different fluorescent stains simultaneously can be used to unveil functional differences between bacterial cells[25]. Several stains are available to study single cell characteristics but up to now they have mostly been applied in fluorescence microscopy or pure flow cytometry studies (without fermentation) and only in a few cases for the assessment of population heterogeneity in fermentation processes (see chapter 2b).

However many of them have great potential to be established for on-line monitoring of bioprocesses[1]. For example, the novel fluorogenic Redox Sensor Green, which was also applied for my studies (chapter 7), can be used as an indicator for the respiratory ability of cells.

Cellular viability is one of the most relevant physiological parameters to be assessed in any kind of biological studies and also of high importance for the performance of industrial fermentation processes. Therefore viability stains nowadays are one of the most commonly and often the only type of stain used in bioprocess monitoring in combination with flow cytometry/online flow cytometry. Especially in industrial fed-batch and continuous processes, where viability is a crucial parameter to ensure a robust high yielding process they have a wide range of applications (see chapter 2b and e.g. [26,27]). Membrane integrity is the most commonly used indicator in the assessment of viability and is based on the capacity of cells with intact membranes to exclude the fluorescent dye[1]. The most frequently applied example is Live/Dead staining[28] respectively propidium iodide (PI) (figure 3), which has also been applied in the scope of this thesis (chapter 4 and 7) together with bis-(1,3-dibarbituric acid)-trimethine oxanol ($DiBAC_4(3)$). $DiBAC_4$ selectively enters cells with depolarised membrane/lack of membrane potential (figure 3)[29].

Cellular respiration is another important cell parameter that is commonly studied in staining experiments. The stain of choice for the determination of respiratory activity is mostly, despite of many critical issues concerning toxicity and accuracy, 5-cyano-2,3-ditolyltetrazolium chloride (CTC). CTC forms red-fluorescing formazan crystals inside the cell when reduced by the electron transport system in bacterial cells (figure 3)[1]. CTC has also been applied in the scope of this thesis together with SYBR Green (SYBR), a cyanine dye, which binds to nucleic acids in cells (figure 3 and chapter 7).

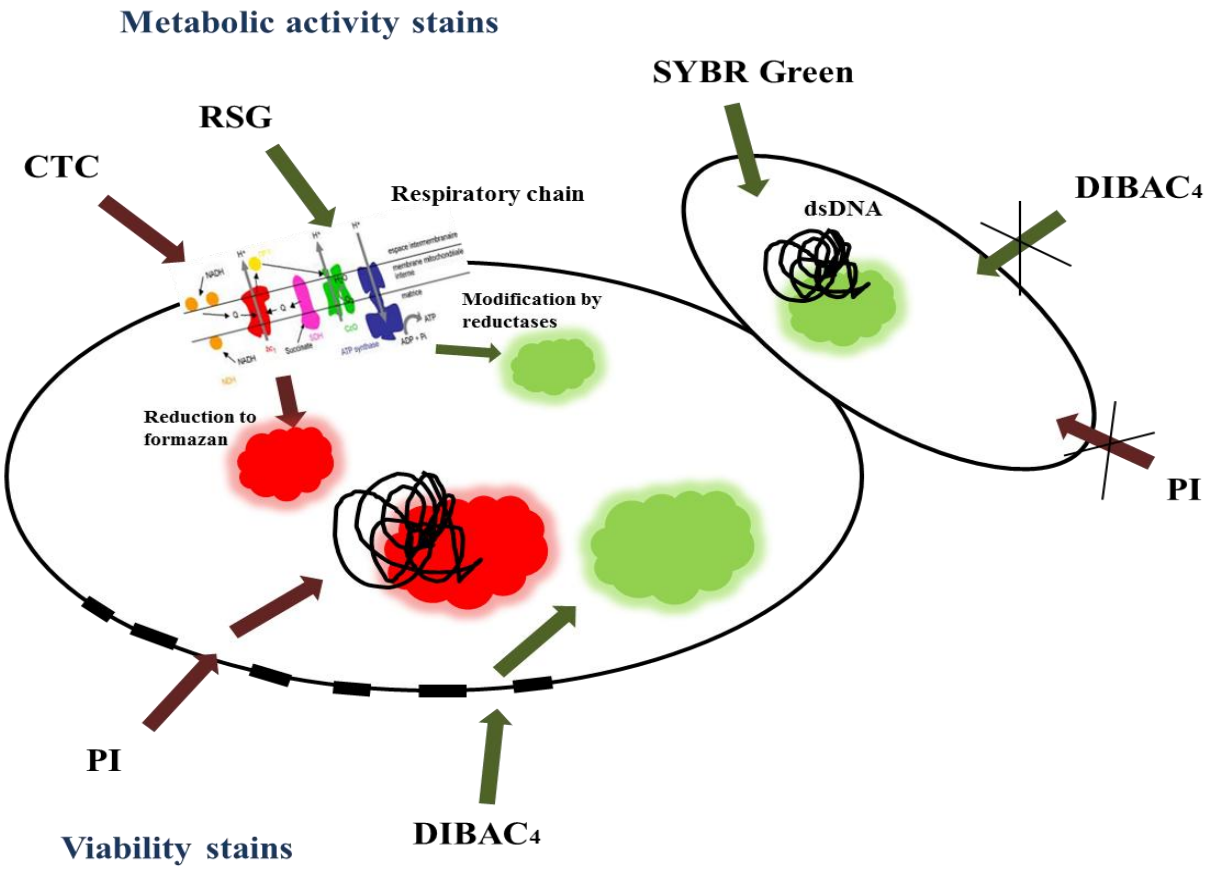

Figure 3 – Stains used in the scope of the thesis and their targets: including the viability stains propidium iodide (PI) and $DIBAC_4$ as well as the metabolic activity stains CTC, RSG (Redox sensor green) and SYBR green.

2.3 References

1. Fernandes, R. L. *et al.* Experimental methods and modeling techniques for description of cell population heterogeneity. *Biotechnol. Adv.* **29,** 575–599 (2011).

2. Schmid, A., Kortmann, H., Dittrich, P. S. & Blank, L. M. Chemical and biological single cell analysis. *Curr. Opin. Biotechnol.* **21,** 12–20 (2010).

3. Díaz, M., Herrero, M., García, L. a. & Quirós, C. Application of flow cytometry to industrial microbial bioprocesses. *Biochem. Eng. J.* **48,** 385–407 (2010).

4. Rieseberg, M., Kasper, C., Reardon, K. F. & Scheper, T. Flow cytometry in biotechnology. *Appl. Microbiol. Biotechnol.* **56,** 350–360 (2001).

5. Porro, D., Brambilla, L. & Alberghina, L. Glucose metabolism and cell size in continuous cultures of Saccharomyces cerevisiae. *FEMS Microbiol. Lett.* **229,** 165–171 (2003).

6. Gottfredsson, M., Erlendsdóttir, H., Sigfússon, Á., Gottfredsson, S. & Erlendsdo, H. Characteristics and Dynamics of Bacterial Populations during Postantibiotic Effect Determined by Flow Cytometry Characteristics and Dynamics of Bacterial Populations during Postantibiotic Effect Determined by Flow Cytometry. *Antimicrob. Agents Chemother.* **42,** 1005–1011 (1998).

7. Davey, H. M., Jones, A., Shaw, a D. & Kell, D. B. Variable selection and multivariate methods for the identification of microorganisms by flow cytometry. *Cytometry* **35,** 162–168 (1999).

8. Misteli, T. & Spector, D. L. Applications of the green fluorescent protein in celll biology and biotechnology. *Nat. Biotechnol.* **15,** (1997).

9. Chien, C. T., Bartel, P. L., Sternglanz, R. & Fields, S. The two-hybrid system: a method to identify and clone genes for proteins that interact with a protein of interest. *Proc. Natl. Acad. Sci. U. S. A.* **88,** 9578–9582 (1991).

10. Fields, S. & Song, O. A novel genetic system to detect protein-protein interactions. *Nature* **340,** (1989).

11. Waldo, G. S., Standish, B. M., Berendzen, J. & Terwilliger, T. C. Rapid protein-folding assay using green fluorescent protein. *Nat. Biotechnol.* **17,** 691–695 (1999).

12. Brauer, M. J. *et al.* Coordination of Growth Rate , Cell Cycle , Stress Response , and Metabolic Activity in Yeast. *Mol. Biol. Cell* **19,** 352–367 (2008).

13. Cormack, B. P. *et al.* Yeast-enhanced green fluorescent protein (yEGFP): a reporter of gene expression in Candida albicans. *Microbiology* **143,** 303–311 (1997).

14. Fazio, A. *et al.* Transcription factor control of growth rate dependent genes in Saccharomyces cerevisiae: a three factor design. *BMC Genomics* **9,** (2008).

15. Regenberg, B. *et al.* Growth-rate regulated genes have profound impact on interpretation of transcriptome profiling in Saccharomyces cerevisiae. *Genome Biol.* **7,** (2006).

16. Han, S., Delvigne, F., Brognaux, A., Charbon, G. E. & Sorensen, S. J. Design of growth-dependent biosensors based on destabilized GFP for the detection of physiological behavior of Escherichia coli in heterogeneous bioreactors. *Biotechnol. Prog.* (2013). doi:10.1002/btpr.1694

17. Andersen, J. B. *et al.* New Unstable Variants of Green Fluorescent Protein for Studies of Transient Gene Expression in Bacteria New Unstable Variants of Green Fluorescent Protein for Studies of Transient Gene Expression in Bacteria. *Appl. Environ. Microbiol.* **64,** 2240–2246 (1998).

18. Han, S., Delvigne, F., Brognaux, A., Charbon, G. E. & Sørensen, S. J. Design of growth-dependent biosensors based on destabilized GFP for the detection of physiological behavior of Escherichia coli in heterogeneous bioreactors. *Biotechnol. Prog.* **29,** 553–563 (2013).

19. Bradley, M. D., Beach, M. B., de Koning, a P. J., Pratt, T. S. & Osuna, R. Effects of Fis on Escherichia coli gene expression during different growth stages. *Microbiology* **153,** 2922–2940 (2007).

20. Richins, R. & Chen, W. Effects of FIS overexpression on cell growth, rRNA synthesis, and ribosome content in Escherichia coli. *Biotechnol. Prog.* **17,** 252–257 (2001).

21. Zhi, H., Wang, X., Cabrera, J. E., Johnson, R. C. & Jin, D. J. Fis stabilizes the interaction between RNA polymerase and the ribosomal promoter rrnB P1, leading to transcriptional activation. *J. Biol. Chem.* **278,** 47340–47349 (2003).

22. DeRisi, J. L., Iyer, V. R. & Brown, P. O. Exploring the Metabolic and Genetic Control of Gene Expression on a Genomic Scale. *Science (80-.).* **278,** 680–686 (1997).

23. Daran-Lapujade, P. *et al.* Role of transcriptional regulation in controlling fluxes in central carbon metabolism of Saccharomyces cerevisiae. A chemostat culture study. *J. Biol. Chem.* **279,** 9125–9138 (2004).

24. Carlquist, M. *et al.* Physiological heterogeneities in microbial populations and implications for physical stress tolerance. *Microb. Cell Fact.* **11,** (2012).

25. Nebe-von-Caron, G., Stephens, P. J., Hewitt, C. J., Powell, J. R. & Badley, R. a. Analysis of bacterial function by multi-colour fluorescence flow cytometry and single cell sorting. *J. Microbiol. Methods* **42,** 97–114 (2000).

26. Hewitt, C. J., Nebe-Von Caron, G., Nienow, a W. & McFarlane, C. M. Use of multi-staining flow cytometry to characterise the physiological state of Escherichia coli W3110 in high cell density fed-batch cultures. *Biotechnol. Bioeng.* **63,** 705–711 (1999).

27. Wang, J. *et al.* Genetic engineering of Escherichia coli to enhance production of L-tryptophan. *Appl. Microbiol. Biotechnol.* **97,** 7587–7596 (2013).

28. Boulos, L., Desjardins, R. & Barbeau, B. Methods LIVE / DEAD ® Bac Light E : application of a new rapid staining method for direct enumeration of viable and total bacteria in drinking water. *J. Appl. Microbiol.* **37,** 77–86 (1999).

29. Laflamme, C., Lavigne, S., Ho, J. & Duchaine, C. Assessment of bacterial endospore viability with fluorescent dyes. *J. Appl. Microbiol.* **96,** 684–692 (2004).

2. Chapter b

Population heterogeneity in bioprocesses studied at single cell level: industrial scale simulated in the lab using basic and advanced setups

Heins A.-L. [1], Carlquist M.[1,3], Gernaey K.V. [2], Eliasson Lantz A.[1]

[1] Department of Systems Biology, Technical University of Denmark, 2800 Kongens Lyngby, Denmark

[2] Department of Chemical Engineering, Technical University of Denmark, 2800 Kongens Lyngby, Denmark

[3] Present address: Department of Chemistry, Division of Applied Microbiology, Lund University, 221 00 Lund, Sweden

Written as review

Status: Manuscript in preparation

Abstract

This review focuses on the setups and tools that are used to study population heterogeneity in bench scale. Population heterogeneity is a phenomenon that is especially observable in large scale industrial fermentation processes. Hereby mostly studies that use *E. coli* and/or *S. cerevisiae* are taken into account due to their relevance as industrial production hosts for biomass, bulk chemicals, enzymes and recombinant proteins. After a summary on how population heterogeneity is studied in classical process or lab scale setups of batch, fed-batch and continuous culture (chemostat), specific setups developed or potentially valuable for the study of single cell heterogeneities are presented. This includes microbioreactors (MBRs), single cell reactors/flow chambers, scale down reactors (SDRs, also referred to as multi compartment reactors) as well as special setups that are based on continuous cultivation. These setups are chosen as they have special characteristics which would be suitable or are already used to study single cells in a controlled environment under e.g. extreme growth conditions, following rapid changes originating from external perturbations of the stable environment or automated sampling followed by investigation of single cell distributions. Flow cytometry is presented, since it is a technique that is often used as a central measurement tool for the different kinds of studies on cell heterogeneity due to its increasing importance for single cell analysis, but also other tools like fluorescence sensors and fluorescence microscopy are mentioned. Methods are focusing on the use of fluorescence stains, reporter strains or other methods to access population heterogeneity. Additionally possibilities for data analysis that are other than the classical presentation of mean values are depicted.

Table of contents

2.1 Introduction

Microbial cells, primarily genetically modified, are nowadays extensively used in industrial scale fermentation processes for the production of diverse goods like biomass, bulk products e.g. bioethanol, pharmaceuticals or recombinant proteins[1,2]. Yeast, especially *S. cerevisiae*, as well as bacteria like *E. coli* are applied in several of these different processes[3–6].

Together with the steadily rising demand for sustainable high yielding production processes, also the demand for robustness of biotechnological production systems/hosts increases, which consequently needs to be well characterised and controllable. Optimization of fermentation parameters is therefore crucial. The development in instrumental tools enabled the study of single cells involved in production processes in bioreactors, and consequently it is generally known today that cultures originally perceived as homogeneous, in fact show a heterogeneous behavior

(reviewed in[7,8]): population properties are distributed rather than following, as generally assumed, averaged characteristics[9,10]. These distributions originate from gradients, especially seen in large scale industrial processes, of e.g. substrate, pH, oxygen or other factors changing the environment of cells. Gradients arise due to non-ideal mixing creating local microenvironments in the reactor which induce dynamic changes to the single cell distribution[10–12]. But population heterogeneity is also a generally accepted phenomenon in bench scale cultivations and in even smaller scale in e.g. biofilms which are reviewed elsewhere[13]. As a consequence of population heterogeneity elevated stress responses of cells circulating throughout the reactor, reduced yields and productivities as well as increases by-product formation were observed, but also higher cell robustness, especially at low growth rates, as well as quick adaption to new conditions, making population heterogeneity a two-sided phenomenon[11,12,14–17]. Therefore the investigation to improve its understanding and subsequently enable the control of heterogeneity is of high importance to optimise production processes as well as develop new microbial cell factories.

To approach single cell heterogeneity flow cytometry (FC) has become a valuable tool and has therefore been frequently reviewed elsewhere[18,19]. A flow cytometer is a robust high-throughput instrument that counts, sorts and examines up to 10 000 cells per second[10,18]. It has been extensively used in mammalian cell research before, but is also adapted for the study of bacterial and yeast cell size and morphology as well as in combination with e.g. fluorescence stains or reporter strains[20]. Other tools and a deeper description of flow cytometry for the measurement of single cell properties have been reviewed elsewhere[10,21–23].

This review aims at giving a summary of lab scale cultivation setups that are used to study population heterogeneity in fermentation processes, which includes primarily the application of flow cytometry, with a special focus on *E. coli* and *S. cerevisiae*. The intention is to show the potential of single cell studies in bioreactors to reveal more detailed cell physiological characteristics which are normally hidden in classical physiology studies and control strategies of fermentation processes. First an overview of the current status of population heterogeneity studies and tools to study it in industrial biotechnology labs and large scale batch, fed-batch and continuous cultivation will be given. Afterwards special setups that can potentially be used or are already applied to study population heterogeneity are presented and likewise studies done will be summed up. Moreover, in the discussion possible future strategies to control population heterogeneity as well as the need for deeper and more objective data analysis will be discussed.

2.2 Population heterogeneity, microbial physiology and production studied at single cell level

In this first part of the review studies to access population heterogeneity or monitor special single cell properties that have been performed using a basic reactor setup in different cultivation modes will be summarised. This includes studies done under the changing conditions in batch cultivation, in the for production most frequently used setup of fed-batch cultivation as well as in continuous cultivation (Chemostat) (for short definitions of the setups see glossary box). Hereby studies have been grouped into targeting heterogeneity in cell size and cell cycle, physiological state and production respectively single cell productivity.

2.2.1 Cell size and cell cycle heterogeneity

The investigation of general physiology, concerning cell properties, like optical density, dry weight and extracellular metabolites (e.g. using high performance liquid chromatography (HPLC)) as well as off-gases released by the organism are nowadays complemented with the study of single cell parameters. The introduction of flow cytometry for the analysis of cultivation broth samples enabled an additional measurement of distributions of e.g. cell size, morphology and cell cycle progression[24].

The first single cell cycle investigations of *S. cerevisiae* and *E. coli* on different carbon sources were performed in shake flasks analyzing samples at-line by applying flow cytometry for cell size and protein distributions (fluorescein isothiocyanate (FITC) staining) and coulter counter for cell count[25–27]. Furthermore bud scar analysis was performed. Later, additional analysis of the budding index and cell cycle distributions revealed that *S. cerevisiae* cells are bigger and enter the S-phase faster when growing on glucose than when growing slower on ethanol[28]. Furthermore with the frequent integration of flow cytometry into continuous cultivation processes single cell heterogeneities in general physiology have also been studied in a steady state environment[24]. This was in many studies supported by the use of the measurement of the expression of fluorescence originating from reporter strains (GFP and BFP), stained properties or immuno-fluorescent methods. Cell size studies of both *E. coli* and *S. cerevisiae* were mainly based on investigations of cell cycle kinetics at different growth rates (range from D = 0.07 h^{-1} to 0.43h^{-1}) and were combined

with staining for protein content using FITC, mitramycin and/or ethidium bromide to assess the budding index or distribution of single cell division[29–31].

Later cell division and growth heterogeneities in well controlled batch reactors have been further examined as well by the application of different reporter strains expressing GFP whose expression can be analysed using flow cytometry. An example is the monitoring of cell division of single cells of *E. coli* using a GFP dilution method[32].

A combined approach of experimental and mathematical description (population balance model coupled to unstructured model) of the dynamics of cell size and cell cycle position distributions of *S. cerevisiae* in batch experiments showed good agreement between data and model, thus indicating the suitability of the model as well as leading to considerations for development of additional combined approaches[33]. Details about the research in cell cycle progression of yeast including modeling of growing yeast populations and the application of flow cytometry in batch experiments for measurement of cellular properties, have been reviewed elsewhere[34].

2.2.2 Heterogeneity in physiological state

Since the cell physiology (see 2.1. in e.g. cell size) is found to be clearly influenced by the dynamic growth conditions in a batch reactor but also during fed-batch and continuous cultures (mainly as stress response), the environmental influences on the single cell physiological state are frequently studied as well. Especially the assessment of the level of single cell viability is nowadays a commonly used method in process control and optimization to ensure high process efficiency of *S. cerevisiae* and *E. coli*. Normally at-line flow cytometry in combination with one or more viability stains (e.g. propidium iodide (PI), ethidium bromide (EB), BOX (Bis-oxonol), Rhodamine123 (RH123) etc.) and/or metabolic activity stains (e.g. 3,3-dihexylocarbocyanine iodide (DIOC6) for membrane integrity and potential or Dihydrorhodamine123 (DHR)) or fluorescence sensors was applied. Hereby the level of viability in different growth phases[35–37] or in response to various kind of stress e.g. UV-light, agitation, susceptibility to copper toxicity, weak acids, dissolved oxygen level or heat shock[38–43] was evaluated. The result of combining stains that target different properties is that cells can be classified into different physiological state categories like e.g. alive, dead and alive but not culturable by simple gating/overlaying of measured distribution plots of cell properties. An example is a drop in viability due to cell death at the end of the fed-batch phase of a high density *E. coli* production process found in some processes or cells that were alive but lost their ability to divide in a process producing the recombinant protein promegapoietin or in Fab

production[36,44,45]. This knowledge can then be used to e.g. generate segregated models of population dynamics in a batch process[35]. Also, one approach used multivariate statistics to predict population responses to different stresses[39].

Furthermore, with the application of a combination of different viability stains it could be shown that cells in large scale fed-batch processes, experiencing a dynamic environment (gradients of glucose, oxygen etc.) were less affected in viability than cells grown in well mixed lab scale experiments[46,47]. Opposite to this, nothing similar could be detected during batch or continuous culture[46].These findings lead to the suggestion to use an on-line flow cytometer[46] or at least to introduce the application of more on-line fluorescent measuring sensors, as e.g. the biomass sensor and on-line HPLC analyzer monitoring recombinant protein production by *E. coli* used by Gustavsson et al. (2012)[48] to improve process control.

To realize constant production with high productivity and viability, also process optimization concerning the control strategy and conditions the microorganism experience is of high importance. For this reason perturbation studies with e.g. pulses of substrate (e.g. ethanol or glucose), a toxic compound or a sudden change in oxygen level[49] and the resulting physiological responses to concentration heterogeneities[10] have been performed frequently. For example the general physiological response of *S. cerevisiae* and *E. coli* cells to glucose pulses in glucose-limited chemostat culture (D= 0.05 h^{-1} and 0.1 h^{-1}) has been studied evaluating glucose and oxygen uptake as well as the metabolic fluxes[50–53].

Additionally, many studies dealing with proteome and transcriptome as well as metabolome analysis with fully labeled C^{13} carbon of e.g. *E. coli*[54–56] and *S. cerevisiae*[52,57] have been performed in fed-batch cultivations or in the stable steady state environment of the chemostat at different dilution rates (focus on dilution rate range D = 0.02-0.33 h^{-1}). The aim of such studies has mainly been to investigate the transcriptional or proteomic changes of *E. coli* and *S. cerevisiae,* for example studying the influence of growth rate, oxygen level or carbon source (e.g. glucose, ethanol, maltose or acetate) respectively a combination of all three[58] on e.g. gene expression[24,59–62]. In the course of such investigations, *S. cerevisiae* cells isolated during the bioethanol production phase of a fed-batch process by density gradient centrifugation were found to consist of two distinct subpopulations, which were further analysed using transcriptome analysis as well as fluorescence microscopy for evaluating viability and metabolic activity (methylene blue, Calcuflor and FUN1 staining)[63]. It was found that one population was uniform in size with high respiratory activity

whereas the other one was heterogeneous in size as well as less respiratory active, which led to the conclusion that the production is uncoupled from growth while the cells show similar characteristics in morphology and metabolism as when entering stationary phase[63].

Stress response distributions of single cells in batch, fed-batch and continuous cultivation have also been further examined by the application of different reporter strains expressing BFP or GFP whose expression can be assessed using flow cytometry and correlated to a specific cell response. Examples are the application of *S. cerevisiae* stress reporter strains based on the heat shock protein Hsp104, the stress response protein Hsp12 or an *E. coli* stress reporter strain (bioluminescence construct yciG::LuxCDABE) to investigate heterogeneities of stress responsive gene expression and stress tolerance of individual cells[64,65]. Also, in response to e.g. pulses of glucose of different intensities (0.08, 0.4 and 1g/L) or NaCL, ethanol and elevated temperature in glucose limited chemostats at different dilution rates[65–67]. A *S. cerevisiae* dual reporter system to map growth and cell robustness (assessed via exposure to freeze-thaw stress) heterogeneities based on a ribosomal protein promoter (RPL22a) made it possible to distinguish between different cell growth phases in batch fermentation by the level of fluorescence intensity, study the single cell response to glucose pulses as well as subpopulations with high and low cell membrane robustness could be detected[14]. It may be applied to identify more robust subpopulations for process design of more effective bioprocesses.

2.2.3 Heterogeneity in Production

Apart from the assessment of the influence of the process environment (see 2.2.) on the cell population in bioreactors the investigation of single cell heterogeneities in the production of e.g. recombinant proteins itself is also of importance to ensure a high yielding process. A few attempts using reporter genes to follow recombinant protein production by *E. coli* in fed-batch cultivation in combination with special sensors were made, e.g. applying an operon fusion of GFP and chloramphenicol acetyltransferease (CAT) (under control of pBAD promoter or arabinose (araBAD) operon)[68] or GFP respectively BFP monitoring the expression of a stress related promoter. Both fluorescent proteins were found to be a valuable tool to monitor processes as reporter genes for recombinant protein production in *E. coli*[69]. In general these reporter genes could also be used in combination with at-line flow cytometry or as suggested elsewhere with on-line flow cytometry[46] to get a better understanding of population heterogeneity and single cell behavior in e.g. large scale fed-batch processes, and would as a consequence enable further process

optimization. Studies like this have been done in batch cultivation e.g. the study of the dynamics in glucose uptake of *E. coli* single cells using a fluorescent glucose analogue (2-NBDG (2-(N-(7-nitrobenz-2-oxa-1,3-diazol-4-yl)amino)-2-deoxyglucose)) which is taken up by the cells and can afterwards be measured as intracellular fluorescence that can then indirectly be correlated to product formation[70]. Furthermore the investigation of the physical and metabolic consequences of inclusion body formation in batch cultures of *E. coli* producing a recombinant protein (the isopropylthiogalactopyranoside-inducible model eukaryotic protein AP50), using dual colour staining for membrane polarisation and permeability which can also be used as a tool for on-line monitoring of potential production processes[71]. Additionally the NADH dependent culture fluorescence and plasmid stability in recombinant protein production followed by the fluorescence decline when a fluorescent substrate is degraded by the produced enzyme (e.g. fluorescein di-*beta*-D-glucopyranoside (FDGlu)) has been studied in chemostat culture[72,73].

Moreover, combining metabolic and physiological perturbation responses with gene expression analysis can reveal information for the improvement of production processes through the design of new strains[10]. Examples are transcriptomics studies of glucose pulses respectively repeated glucose pulses in glucose limited chemostats of *E. coli* and *S. cerevisiae*[65,67,74].

.

Table 1- population heterogeneity studied in fermentation processes using batch, fed-batch or chemostat mode: The table is divided into studies investigating heterogeneity in cell size and cell cycle, physiological state or production/productivity of single cells. In each section studies are listed in chronological order. Abbreviations: BFP: Blue fluorescent protein; BI: budding index; CFU: Colony forming units; DAPI: 4',6-diamidino-2-phenylindole; EB: Ethidium bromide; GFP: Green fluorescent protein; FC: flow cytometry; FITC: Fluorescein isothiocyanate; FSC: Forward scatter; PI: Propidum iodide; RH123: Rhodamine123; SSC: Side scatter;

Reference	**Organism**	**DEF/RICH medium**	**Type of heterogeneity studied**	**Tools used to study heterogeneity**	**Fermentation mode/ scale**	**Data analysis**
Cell size and cell cycle heterogeneity						
Skarstad *et al*. (1983)	*E. coli*	M9 medium, glucose	Cell cycle kinetics	FC (EB, FSC, mitramycin), CFU	Chemostat	Correlation between DNA, cell size and cell count in different cell cycle stages
Vanoni *et al*. (1983) Lord and Wheals (1980)	*S. cerevisiae*	YEP and YNB medium, different carbon sources	DNA content, protein content	FC (FITC staining), bud scar analysis	Shake flask 0.5 L	Fried algorithm analysis of DNA distributions, histogram plots of measured distributions, modeling of unequal division of yeast
Ranzi *et al.* (1986)	*S. cerevisiae*	D = 0.07-0.43h^{-1}, YEP medium, glucose	Protein content, cell volume	FC (PI, FITC), coulter counter	Chemostat , 0.75 L	Biplots and histograms of measured properties
Åkerlund *et al*. (1995)	*E. coli*	LB or M9 medium, glucose or acetate	Cell size, DNA content	FC (DAPI, FSC), fluorescence microscopy	Shake flask	Time series of histogram plots
Larsson *et al.* (1996) Bylund *et al.* (1998)	*S. cerevisiae* *E. coli*	Minimal medium, glucose	biomass productivity, recombinant protein production	rapid sampling at different locations	Fed-batch, 30 m^3, 12 m^3	CFD modeling, product formation, measured properties plotted over time
Zhao *et al.* (1998)	*E. coli* *S. cerevisiae*	2XGYT complex medium or YPD medium, both with glucose	Growth rate, cell size, SSC, growth, DNA content	Online spectrometer, automated online FC (GFP, FSC, SSC, FITC), rapid sampling,	Batch, 1 L	Histogram and landscape plots for measured property distributions

Howlett and Avery (1999)	*S. cerevisiae*	YPD-medium, glucose, D= 0.1h^{-1}	Cell cycle stage, viability, protein content	FC (FSC, PI, FITC)	Chemostat	Biplots, histogram plots, gating for different cell cycle stages with percentale analysis and for positive stained cells
Porro *et al*. (2003)	*S. cerevisiae*	Minimal medium, glucose, D= 0.08-0.3h^{-1}	Cell size, protein, viability	FC (FSC, PI, FITC)	Chemostat 0.8 L	BI, measured properties plotted against dilution rate
Cipolina *et al.* (2005 & 2007)	*S. cerevisiae*	Rich/poor medium, glucose/ethanol, D= 0.05h^{-1}	Cell size, DNA content, viability, transcriptomics	FC (FSC,FITC, PI), coulter counter (cell count)	Shake flask, chemostat	BI, FSC, RNA/DNA content distributions, histogram plots, mean values plotted over time
Roostalu *et al*. (2008)	*E. coli*	LB-medium, glucose	cell division, viability, cell size	FC (GFP, SSC, PI)	Shake flask 0.5 L	Series of histograms and biplots of measured properties, peak shift analysis
Tibyrenc *et al*. (2010)	*S. cerevisiae*	Defined medium, 200-300g/L glucose	Cell size & viability	FC(FSC, PI), coulter counter, fluorescence microscopy, online measurement of biomass	Batch 2 L	Multivariate statistical analysis of data, partial least square method, viability and cell size histogram plots
Fernandes Lencastre *et al*. (2012)	*S. cerevisiae*	Minimal medium, glucose	Cell size and cell cycle stage, DNA content,	BI, FC (FITC, PI)	Batch, 1.5 L	population balance model coupled to unstructured model, time series of histogram plots and biplots
Heterogeneity in physiological state						
Hewitt *et al.* (1998, 1999& 2000)	*E. coli*	Synthetic medium, glucose	Growth, physiological state, cell size, viability	Multiparameter FC (PI, EB, RH123, FSC, SSC, BOX)	Fed-batch, 2.5 L and 20 m^3	Biplots of stained properties, gating for positively and negatively stained cells
Hewitt *et al.* (1998)	*E. coli*	D= 0.2h^{-1}, SM medium, glucose	Cell size, cell membrane	FC (PI, BOX, RH123,FSC), microscopy	Chemostat 4 L	Microscopic pictures, biplots of measured properties, gating for positive cells
Nebe-von-Caron *et al*. (2000)	*Bacteria*	Various	Viability, metabolic state, vitality, metabolic activity, cell size	Multiparameter FC (PI, BOX, RH123, EB, FSC, SSC), cell sorting	Fedb-batch, various	Biplots of measured properties, 3D plots over time, correlation analysis of metabolic traits, plots of mean and CV
Enfors *et al.* (2001)	*E. coli*	Glucose-ammonia salt medium	Stress response, viability	FC (PI, BOX), mRNA analysis	Fed-batch, 22 m^3 and scale down	CFD simulation, gene expression tables, biplots of measured properties, gating for positive and negative cells

Attfield *et al*. (2001)	*S. cerevisiae*	GYP medium, glucose,	stress response & tolerance, viability	Reporter strain (HSP104), FC (PI, GFP), fluorescence microscopy	Shake flask	Biplots, histograms, gating for viable cells, percentage and expression plotted over time
Abu-Absi *et al.* (2002)	*S. cerevisiae*	SD minimal medium, glucose	Stress response, cell count, cell size, viability	Automated FC (GFP, FSC, SSC, PI), frequent sampling	Batch, 2 L	Biplots for measured properties, 3D plots for property time frequency
Kacmar et al. (2004)	*S. cerevisiae*	SD minimal medium, glucose	Cell size, viability, GFP fluorescence/production	Automated FC (PI, FSC, GFP), 3 different reporter strains, frequent sampling	Batch, 1.5 L	Biplots for measured properties, manual gating, mean and CV plotted over time, percentage viability, fluorescence color map plots
Nisamedtinov *et al.* (2008)	*S. cerevisiae*	SM medium, glucose, D=0.14h^{-1}	Stress response	Fluorescence reader (GFP fluorescence), reporter strain (HSP12p)	Chemostat, 1 L	Mean values plotted over time
Benbadis *et al.* (2009)	*S. cerevisiae*	YPD medium, glucose,	Stress response	Global transcriptome analysis, subpopulation evaluation	Fed-batch	Subpopulation analysis
Winder *et al*. (2011)	*E. coli*	MSX medium, glucose	Metabolic fingerprinting, viability,	FT-IR analysis, CFU	Fed-batch, 1.25 L	Cluster analysis and PCA, mean values plotted over time
Amilastre *et al*. (2012)	*S. cerevisiae*	Mineral medium	Viability, biomass formation	FC(Methylene blue staining)	Fed-batch, continuous, 1,3 & 5 L	Model of temperature impact on production
Carlquist *et al.* (2012)	*S. cerevisiae*	Delft minimal medium, glucose, glucose pulse	Cell size, growth, cell robustness, viability	FC (FSC, SSC, GFP, PI), dual reporter strain (RPL22a)	Batch and continuous 2 L	Budding index, biplots and histogram plots, percentage analysis, mean values plotted over time
Freitas *et al*. (2013)	*S. carlsbergensis*	MC medium, glucose	Viability	Multi-parameter FC (PI, RH123)	Shake flask, 1 L	Biplots and histograms with squared gating
Heterogeneity in production						
DeLisa *et al.* (1999)	*E. coli*	Defined or semi-defined medium, glucose	Recombinant protein production	Reporter strain (GFP sensor, activity assay)	Fed-batch, 2 L	Data comparison from different sources and plotted over time

Natarajan and Srienc (1999)	*E. coli*	M9 minimal medium, glucose	Glucose uptake	FC (fluorescent substrate, FSC)	Batch, 2 L	Model of distributions, mean values plotted over time, biplots and histogram plots
Chau *et al*. (2001)	*S. cerevisiae*	Complex medium, glucose, D= $0.1h^{-1}$	Plasmid stability, viability, protein content, cell size	FC (plasmid fluorescence, PI, FITC), electron microscopy	Chemostat , 2 L	Histogram plots, biplots, gating for percentage of positively stained cells
Reischer *et al.* (2004)	*E. coli*	D= $0.1h^{-1}$, minimal medium, glucose	BFP & GFP protein production	ELISA, reporter strains for recombinant protein production	Chemostat , 7 L	Mean values plotted over time
Abel *et al.* (2004)	*S. cerevisiae*	D= $0.2h^{-1}$, synthetic medium, glucose	NADH dependent fluorescence	Fluorescence reader	Chemostat , 2.5 L	Mean values plotted over time, histogram plots for fluorescence
Lewis *et al*. (2004)	*E. coli*	LB-medium, glucose	Cell size, membrane permeability	reporter strain (recombinant protein production), FC (FSC, PI, BOX)	Batch, 4 L	Histograms and biplots of measured properties, squared gating of subpopulations
Wållberg *et al*. (2005) Sunstroem et al. (2004)	*E. coli*	Minimal medium, glucose	Viability, Recombinant protein production	Multiparameter FC (immunofluorescent labelling, FSC, PI, BOX),CFU	Fed-batch, 5 L	Histograms plots of measured properties, mean values plotted over time
Want *et al*. (2008)	*E. coli*	Minimal medium, glucose	Viability, growth, recombinant protein production	FC (PI, BOX), ELISA for product formation	Fed-batch, 3 L	Biplots for measured properties, mean values plotted over time
Sunya *et al.* (2012) 1+2, (2013) Sunya	*E. coli*	D= $0.15h^{-1}$, minimal medium, glucose	GFP fluorescence	Fluorescence reader (GFP fluorescence), reporter strain	Chemostat , 1 L	Mean values plotted over time
Gustavssen *et al*. (2013)	*E. coli*	Semi synthetic medium, glucose	Biomass, GFP fluorescence, recombinant protein production	Online sensor for biomass	Fed-batch, 4 L	Measured values plotted in time plots, model for process control

2.3 Specialised setups to simulate large scale in lab scale

This part focuses on the presentation of setups that have specifically been developed to study single cells or population heterogeneity, as well as setups that are used or could potentially be used to investigate population heterogeneity, and are based on the above described continuous cultivation principle. These setups include the study of cells grown under extreme conditions (e.g. retentostat) as well as under isolated/ idealized growth conditions (e.g. single cell reactor).

2.3.1 Setups using continuous culture

In this section setups are described that are based on continuous cultivation and have not been mentioned above because they have a special feature which is beneficial for studying population heterogeneity or they have already been used to access population heterogeneity at single cell level.

2.3.1.1 Turbidostat

The Turbidostat (for a short definition, see the glossary box) has, apart from that it permits direct observation of fluctuations in the specific growth rate, several advantages that can be used to study population heterogeneity, including a higher volumetric productivity than a chemostat, a stable culture behaviour at high dilution rates close to the critical dilution rate, and a high selection pressure[75]. The latter feature enables its application for strain development/selection e.g. the selection for *S. cerevisiae* mutants with higher acetate respectively higher ethanol tolerance by gradually increasing the concentration of the respective compound and furthermore also selection for strains with the highest growth rate[76,77]. As continuous process the turbidostat was also used to study different production processes in small scale using fluorescent reporters strains or proteins like e.g. the production of human proinsulin by *S. cerevisiae* where the expression was regulated by a promoter that is repressed when glucose is present[78]. This revealed single cell production rate distributions.

Furthermore, various studies of the metabolic fluxes applying flux analysis and/or studies of the central carbon metabolism in *E. coli*[79–81] have been conducted. Interestingly, only very few modeling attempts of the conditions in a turbidostat have been made[82–84]. However, the reason might be that the turbidostat is not as popular as the chemostat[85]. Potential challenges when developing a model for such system are some of the disadvantages of the system, like the nonlinear correlation between biomass and optical density, fouling of the sensors which tampers the

measurement and the fact that the sensors are also sensitive to air bubbles or other particles in the culture[75]. Although some attempts to overcome these problems led to an improvement, like the measurement of growth by-products[85], a biomass measurement system based on dielectric permittivity (so called Permittistat[75]) or the use of an external, replaceable tube for optical density measurements[86], still mostly population averaged values and no single cell distributions are measured. However, for the study of oscillations in turbidostats in *S. cerevisiae* and *E. coli*[75,87,88] cell size and viability distributions (using methylene blue and fluorescence microscopy respectively FC) were recorded. Furthermore, for the analysis of the oscillation signaling system in *E. coli* a fluorescent reporter system which allowed single cell analysis was used[88].

2.3.1.2 Retentostat

The retentostat (for a short definition, see the glossary box) was developed for specific study of microbial physiology at extreme low/near-zero specific growth rates[89] which allows the distinction between carbon starvation and calorie restriction, which is not possible in a conventional chemostat, while other parameters like agitation, aeration and pH can be tightly controlled[90]. Because the substrate is constantly fed, a retentostat does not lead to starvation and is different from resting cell states where there is little or no metabolic activity[91,92].

The retentostat system has mainly been applied to study the maintenance requirements (general physiology and DNA/RNA content) of several bacterial systems like e.g. *E. coli*[93] without studying population heterogeneity in particular. The experiments revealed that physiology of these prokaryotes at extremely low specific growth rates could not be accurately predicted by extrapolation of the results obtained in a conventional chemostat at higher specific growth rates, which was also forecasted by Konopka (2000)[94] who reviewed physiological cell characteristics at low growth rate and principles of nutrient starvation. The most frequently studied organism in a retentostat up to now is *S. cerevisiae* because its behavior at near-zero growth rates is a rather unexplored field of yeast research[92]. A couple of studies, whose results were in good agreement with conventional chemostat studies, were performed[90–92] starting with the investigation of the physiology of *S. cerevisiae* in an anaerobic glucose limited retentostat (D=0,025 h^{-1}). Thereby also population distributions of cells were analysed concerning viability (CFU and live/dead staining) and metabolic activity (FITC and cFDA) measured by fluorescence microscopy. In addition, calculations of the maintenance requirements were done and were supplemented with the quantification of general physiology including storage compounds. Later, additional genome wide-

transcriptional analysis was performed to compare *S. cerevisiae* cells grown at near-zero specific growth rate with faster growing and stationary phase yeast cultures as well as with cells under starvation compared to cells that have been grown under extreme calorie restriction (by switching off the glucose feed)[90,91]. A similar study has also been done for *L. lactis* decreasing the specific growth rate from 0,025h^{-1} to 0,0001h^{-1}[95].

2.3.1.3 Cytostat

The cytostat (for a short definition, see the glossary box) can be controlled at very low cell concentrations which only negligibly change the composition of the medium in the bioreactor, making the cell environment precisely defined by the feed. This allows also the investigation of the effect of nutrients or toxic compounds (e.g. drugs or inhibiting products) on the cell culture[85] as well as the selection of more robust/tolerant strain towards a specific compound[96,97]. The cytostat has also been modeled[98]. Examples for this are investigations of the cell size increase in *S. cerevisiae* due to high ethanol concentration[85] or the selection for *S. cerevisiae* strains with higher acetate tolerance during ethanol production[99,100]. These studies were mainly followed by RNA microarray analysis and general physiology.

But additionally, with the connected flow cytometer it is possible to measure single cell property distributions and the appearance of subpopulations (presented in biplots and histogram plots, mean and CV, cdfplots are also plotted) instead of just population average properties for example for cell size, cell membrane robustness (PI-staining) and metabolic activity (FITC), or one can apply stress reporter strains (GFP, promoter pTEF,S65T)[97,101]. In the experiments performed in these studies, cells are frequently withdrawn automatically (every 15min) from the bioreactor and collected in a microchamber with two different outlets, one with a membrane for exchange of liquid for stains (PI or others) and washing while the cells are retained in the chamber and one connected to a sampling loop of known volume with which the cells are pumped into the flow cytometer[97]. These kinds of studies have been performed using *S. cerevisiae* as well as *E. coli*, each expressing GFP and stained for different properties (FITC, PI)[82,97] thus revealing subpopulations which potentially could be sorted.

It should be mentioned that the system applying automated sampling in connection to the use of an on-line flow cytometer has also been used in batch fermentation[82,102].

2.3.1.4 Bioscope

The bioscope system (for a short definition, see the glossary box) which was developed by Visser et al. (2002) and Mashego et al. (2006)[103,104] allows the elucidation of short-term in vivo kinetics of a continuous microbial culture in steady state via perturbation experiments. It is an improved version of a system developed by Buziol et al. (2001)[105], who created a system for stimulus response experiments and uses the stopped flow technique originally developed by Koning and van Dam (1992)[106]. The technique allows rapid sampling without disturbing the main culture since the perturbation takes place outside the reactor[103,107]. A detailed description of the characteristics and building blocks of the system can be found elsewhere[103,104]. Up to date the system was exclusively applied for metabolome and general physiology studies and showed results in good agreement with conventional chemostat perturbation experiments. Firstly the metabolic response of *S. cerevisiae* and *P. chrysogenum* to pulses of glucose, ethanol as well as electron donor and acceptor (glucose and acetaldehyde) was examined in aerobic glucose and ethanol limited steady state cultures (D= $0.05h^{-1}$). Samples were rapid and automatically withdrawn and quenched for intra- and extracellular metabolites, both in steady state and over a time period of 180 s following the perturbation. Such experiments lead among others to the calculation of the NAD/NADH ratio in the cytosol[104,108,109]. Furthermore a method for the assessment of the intracellular pH could be established using perturbation with benzoic acid and ethanol or glucose[74,110]. Later, after the introduction of some changes in the system concerning increased oxygen transfer and adjusted sampling intervals to the faster response of bacteria, the dynamics of a large range of central metabolites of *E.coli* could be followed[111].

2.3.2 Miniaturised Setups

2.3.2.1 Microbioreactors

Microbioreactors (MBRs) are still quite new experimental tools that are typically operated with a volume between 50µL-2mL, although the strict definition of MBRs defines a volume of less than 1mL[112,113]. But due to the demand for more advanced sample analysis partly at-line or at the end of the process MBR platforms with parallelised reactors (microtiterplates with 8 or 48 wells) that are designed like MBRs can have a volume up to 12 mL[114–117]. Such reactors are also described in this section, although they are strictly speaking not MBRs. A detailed investigation and evaluation of the future potential and applicability of today's MBRs including recommendations for use are reviewed elsewhere[112,113]. In general MBRs are disposable and miniaturised versions of bench scale reactors that combine the easy handling of shake flask experiments with the controllability of bench

scale reactors[118].This has some practical and financial advantages as it reduces the overall process cost, concerning material and energy use as well as space requirement for equipment[113]. But MBRs also have some advantages due to their inherent characteristics. For example, the mixing (achieved with miniature versions of impeller, gas-induced or magnetic stirrer as well as peristaltic mixers[116,119]) can due to the small volume, almost be considered to be ideal without significant gradients of glucose, oxygen or pH, which allows the investigation of single cell dynamics in a controlled environment[10]. Additionally MBRs exhibit some thermal advantages allowing quick temperature changes, headspace aeration without bubble formation as well as due to this often precise online monitoring of general process parameters and general cell characteristics like pH, temperature, DOT (dissolved oxygen tension) and OD (optical density)[10,114,120,121]. Furthermore a conductometric method for on-line CO_2 measurement in a MBR batch culture of *C. albicans* was developed[119]. Due to the sensitivity of the signals in MBRs it is also possible to monitor real time cell responses by measuring fluorescence from reporter strains with fluorescence sensors or a microscope (reviewed elsewhere[122]) as well as using fluorescence readers which are especially developed for MBRs[10,114,120,123]. Also a fiber-optic on-line monitoring system of OD and fluorescence during MBR and shaken MTPs cultivations, called BioLector, was developed[124]. It enabled monitoring of the dry weight/ optical density development as well as GFP expression (on-line reporter for protein expression) in batch and fed-batch (linear and exponential feed) cultivation of *E. coli* in a microbioreactor array (200µL)[115,124,125]. Moreover results showed good agreement with a 1 L bench scale reactor cultivation, which was also proven with other MBRs using fed-batch fermentation of *E. coli* (2 mL compared to 1 L) for e.g. the production of a plasmid DNA vaccine vector (p VAX1-GFP)[121,126]. Continuous cultivations of *E. coli* and *S. cerevisiae* could also be successfully scaled down in MBRs (8 µL respectively droplets (BAY (Bacteria, Archaea, Yeast) reactor)), and included also applying fluorescent growth reporter strains, measuring general physiology (OD, DW, offline: HPLC) as well as off-line application of stains for viability (EB, PI and SYTO9)[120,127]. Also topology optimization was applied for process optimization of recombinant protein production by *S. cerevisiae* investigated in a MBR[128]. With all these features and characteristics MBRs can be used for high throughput bioprocess development and optimization simulating distinct conditions which cells might experience in large scale reactors[10,124,126]. As an example it has been shown that a MBR (volume: 50 µL) can be used for DNA microarray analysis to obtain differential gene expression profiles during the exponential growth phase of *E. coli* [129]. The applicability of a parallel micro-chemostat array for investigation of the *S. cerevisiae* proteome

in response to UV irradiation as also been demonstrated[123]. Together with similar approaches, this will enable the rapid assessment of environmental factors responsible for spatial heterogeneity in microbial populations[10].

Also, using an array of parallel controlled MBRs respectively microtiterplates (MTPs) equipped as MBRs allows the time efficient performance of a high number of experiments with good scalability and optimization strategies using CFD modeling[114]. Examples are batch and fed-batch (linear and exponential feed) cultivations of *E. coli* and *S. cerevisiae* in a block with 48 parallel miniaturised stirred tank reactors (volume: 8-12 mL) which is autoclavable in place and provides possibilities for on-line monitoring of controlled parameters (pH, temperature, DOT) and physiology (OD, GFP fluorescence), double sided pH control as well as automated sampling[114,116,117].

2.3.2.2 Envirostat

An Envirostat is a microfluidic bioreactor based on a microfluidic chip, on which cells are separated into microtiter wells and then cultivated. It is a device to study cellular physiology and single cell responses to environmental perturbations without disturbance of the whole cell population traits[130]. CFD simulations are used to ensure controlled constant environmental conditions (medium composition changes below 0,001%, hence homogenous reactor) with constant medium supply flow, temperature control and cell trapping via negative dielectrophoresis (nDEP)[130]. Through on-line monitoring of the optical density (OD), growth heterogeneities of single cells can be investigated by assuming a correlation between OD and growth rate. Furthermore, the specific growth rate can also be derived by recording budding events over time[130,131]. Additionally, the system is equipped with an inverted microscope to record pictures respectively videos, and there is a possibility of taking samples for post growth analysis (transcriptome, proteome and metabolome). The envirostat has been applied to study growth kinetic time trends of single cells of *S. cerevisiae* and its descendants in glucose concentration independent population experiments[130,131]. To enable additionally the time resolved protein secretion by an individual cell, the envirostat was coupled to a confocal microscope[131]. In the latter setup the secretion of a scFv-eGFP fusion protein by singularised and trapped *S. pombe* cells could be followed and secreting cells could be differentiated from non-secreting cells. The latter feature can be potentially used in process optimization of proteins secretion[131]. Lately, the envirostat system was extended to cover a wider range of cell types[132] resulting in the first contactless cultivation procedure of a single bacterial cell. The procedure, which cytometrically measures cell dimensions for single cell growth rate calculation, was demonstrated growing *Bacillus subtilis*, *E.* coli and *Corynebacterium glutamicum*

amongst others. It could be consistently shown, that growth of single cells is significantly higher compared to growth rates observed in cell populations, like conventional batch cultivations or shake flask experiments[132,133].

2.3.2.3 Single cell reactors and flow chamber

Single cell reactors or flow chamber experiments are the next step down in volume from microbioreactors and are a quite new and upcoming field in single cell research within the last ten years[134]. The basic principle involves the trapping of single cells in membrane covered (to allow medium flow in and out while retaining cells) microchannels or flow chambers (microfluidic devices) which are mounted on a lab-on-chip or simple microscope slide[135,136]. Some devices consist of several of those channels allowing the parallel cultivation of several single cells or also having different channels or chambers for cultivation and in place analysis and moving the cells between the channels by means of optical tweezers[135,137]. Additionally some systems have channels to remove daughter cells after cell division through shear force in order to follow several cell generations[134,138]. The cultivation process is observed via phase-contrast or fluorescence microscopy allowing to record pictures respectively videos followed by image analysis[135,138,139]. Up to now single cell reactors and flow chamber setups are mainly used for studies of *E. coli* in continuous culture as well as once for yeast investigating e.g. biofilm formation[140], the effect of salt or other compounds on growth[138] or growth responses to environmental change over several cell generations (up to 50)[136,139]. This enables continuous observation and comparison of genetically identical cells concerning kinetic parameters and distributions as well as some physiological characteristics[137]. It should thus help in the clarification of heterogeneous phenomena, for example unequal cell division and cell differentiation. The control and data analysis of these systems is still critical but it allows following of the cell size/cell volume or length increase over time, estimation of individual doubling and lag-time as well as to record GFP expression exhibited by cells or special tagged cell parts[135,136,138,139].

2.3.3 Scale down reactors

For the simulation and the development of future large scale processes as well as for optimization of already existing industrial scale processes (mostly fed-batch processes) scale down reactors have been reported to represent a better tool than conventional bench scale reactors[10]. With a scale down reactor, which refers in this case to a multi-compartment reactor, gradients of substrate, oxygen and pH in large scale processes can be simulated by selecting appropriate points for oxygen inlet, nitrogen sparging and/or substrate feed[10,141]. The general characteristics of scale down reactors and

methodologies including regime analysis have been reviewed elsewhere[141]. Different approaches have been developed depending on the type of study; STR (stirred tank reactor) coupled to a PFR (plug flow reactor), two or more STRs in series, a STR with separated internal compartments, tubular loop reactors[142] and STRs with randomly fluctuating substrate addition[141].

2.3.3.1 PFR and STR

The most commonly used setup is the STR coupled to a PFR because it combines the stable environment of the STR and the time varying conditions of the PFR which is especially useful for population heterogeneity studies since it allows the creation of gradients of various reactor parameters (e.g. pH, oxygen, substrate concentration)[142]. Several studies investigated glucose gradients since most optimization studies first aim at overcoming this problem, especially in industrial fed-batch processes[141]. George et al (1993)[143] simulated aerobic ethanol production due to glucose excess of *S. cerevisiae* in a scale down setup with a PFR connected with circulation to a well-mixed aerated STR. Due to insufficient mixing, which was simulated by adding a glucose feed at the inlet of the PFR (high glucose/low oxygen concentration), heterogeneities arose which lowered the biomass yield and increased ethanol production. This experimental setup corresponded well to the situation cells experience in large scale fed-batch *E. coli* cultivation (in this case for acetate accumulation), which enabled the analysis of stress responses experienced by the cells travelling throughout the different zones of the reactor as well as analysis of viability (PI and BOX staining)[11,144].

Later, Delvigne et al. (2006a, 2006b & 2006c)[145–147] developed, for both *E. coli* and *S. cerevisiae*, a combination of stochastic microbial growth and bioreactor mixing models to explore the hydrodynamic effect of the bioreactor on microbial growth and this allowed the explanation of the scale down effect associated with glucose fluctuations. By combining the two model parts the profile of concentrations that a cell was subjected to during its cultivation in the bioreactor were obtained. Verification experiments in scale down reactors using a STR connected to four different unmixed plug flow sections: a silicone tubing, a glass bulb, two glass bulbs in series and two glass bulbs in parallel with continuous circulation between both parts were in good agreement with the modeling results[145–148].

The latest approaches include the assignment of reporter strains of *E. coli* as whole microbial cell biosensors to investigate the response of the single cells to glucose and oxygen gradients. This is then followed by the modeling of the GFP expression which is coupled to the expression of specific

growth, nutrient up- and downshift or stress related genes (like the sigma factor rpoS or rrnB and fis, respectively) by using an on-line flow cytometer[149–151], which has also been reviewed recently[23]. Also GFP leakage in *E. coli* biosensors (cisE promoter response to nutrient up and down shift) was found to be applicable to assess microbial viability in scale down experiments additionally to PI-staining used for all experiments[152].

Apart from glucose gradient studies the setup has been used to study the general physiological responses to e.g. oxygen gradients in *B. subtilis* fermentation [153] and *Yarrowia lipolytica* lipase production[154] in large scale fed-batch processes as well as for the investigation of pH gradients in *B. subtilis* fermentation[155].

2.3.3.2 2STRs

Another widely used setup for scale down reactors consists of two STRs coupled to each other with continuous circulation inbetween[141]. Several studies have been done varying the circulation times as well as the volume ratio between the reactors simulating different sizes of the glucose feeding zone with more or less effective mixing with feeding that was only applied in the reactor with the smaller volume. In this way decreased yields and elevated by-product formation as also seen in a setup with STR and PFR[143]were found for *S. cerevisiae*[156]. Also instantaneous elevated levels of stress related oxygen limitation and heat-shock genes were found for *E. coli* cells passing through the high glucose zone (STR with glucose inlet)[16]. Consequently, the system offers a tool for monitoring of process related changes in the transcriptional regulation of genes[156]. Apart from glucose gradients, oscillations in the dissolved oxygen concentration in *E. coli* fermentation were studied with a setup with one aerobic and one anaerobic STR with a volume ratio 1:2 (correspond to 88% of the cells experience anaerobic conditions) applying a stress reporter strain which expresses GFP[12]. In this way population heterogeneity as a response to changing oxygen availability could be studied. Studies just considering physiology changes as result of oxygen gradients have also been conducted for different organisms, like *E. coli* and *Penicillum chrysogenum*[157,158].

Table 2- special setups to study population heterogeneity in lab scale simulating large scale fermentation: The setups have been grouped under separate headings in chronological order. Abbreviations: BFP: Blue fluorescent protein; BI: budding index; CFU: Colony forming units; EB: Ethidium bromide; GFP: Green fluorescent protein; FC: flow cytometry; FITC: Fluorescein isothiocyanate; FSC: Forward scatter; PI: Propidum iodide; RH123: Rhodamine123; SSC: Side scatter;

Fermentation mode	**Organism**	**medium**	**Type of heterogeneity studied**	**Tools used to study heterogeneity**	**Reactor scale**	**Data analysis**
TURBIDOSTAT						
Tøttrup and Carlsen (1989)	*S. cerevisiae*	YEP medium, ethanol	Proinsulin production	Reporter strain (fluorescence reader and ELISA for fluorescence)	2.5 L, 3, 5 and 300 L	Timeplots of production rate, yields
Aarnio *et al.* (1990)	*S. cerevisiae*	YPD medium, glucose	growth rate	Online measurement of growth rate	1 L	Growth rate distribution plotted
Markx *et al.* (1991) Davey *et al.* (1995)	*S. cerevisiae*	Complex medium, sucrose, glucose	Growth rate, viability, bud count, cell size, biomass	Online monitoring, fluorescence microscopy (MB), bud count, coulter counter	0.75 L	BI, percentage of viable cells plotted over time, correlation analysis between different recorded parameters
Ullman *et al.* (2012)	*E. coli*	M9 minimal medium, glucose	Single cell expression	Transcriptomics	Lab-on-chip	Image analysis
RETENTOSTAT						
Tappe *et al.* (1996&1999)	*N. europaea, N. winogradskyi*	Inorganic medium, ammonium	See below	See below, but automated sampling and staining	0.5 L, internal biomass retention	See below
Boender *et al.* (2009)	*S. cerevisiae*	D= <0.001h-1,	Viability, metabolic	CFU, fluorescence microscopy (PI,	2 L	Mean properties plotted over time

		YPD medium, glucose	activity	FITC)		
Boender *et al*. (2011) 1+2	*S. cerevisiae*	See above	See above, gene expression analysis, metabolome	See above FC(PI, CFDA)	See above	See above, metabolix fluxes and expression levels compared
Chesbro *et al*. (1999) Ercan *et al*. (2013)	*E. coli* *L. lactis*	Minimal medium, glucose	Viability, DNA/RNA, protein	FC (PI, FITC)	1 L	Timeplots for mean measured properties
CYTOSTAT						
Zhao *et al*. (1998)	*S. cerevisiae*, *E. coli*	Complex medium, glucose	Growth rate	Online monitoring of growth rate, automated FC (PI, FITC)	See below	See below
Gilbert *et al.* (2009) Kacmar *et al*. (2006) Kacmar *et al*. (2004) Pena *et al.* (2012)	*S. cerevisiae*	SD- medium, glucose	growth rate, viability, robustness, metabolic fingerprinting, GFP fluorescence	Metabolic analysis, FC (FITC, PI, FSC, GFP), comparison of reporter strains, online monitoring (PI and GFP)	0.4 L	Cumulative distribution plots of measured properties and analysis of shifts, biplots, mean and CV plotted over time, biplots for stained properties
BIOSCOPE						
Mashego *et al*. (2006) 1+2 Nasution *et al*. (2006) De Mey *et al*. (2010) Visser *et al*. (2002) Lange *et al*. (2001)	*S. cerevisiae*, *P. chrysogenum*, *E. coli*	Minimal medium, glucose, D= 0.05h^{-1} or 0.1h^{-1}	metabolome	rapid sampling, Glucose perturbation compared to conventional chemostat	4 L	Metabolic profiles, general physiology
Kresnowati *et al.* (2006 &2008)	*S. cerevisiae*	See above	See above, but pulses of ethanol and glucose	See above, evaluation of intracellular pH	4 L	See above, calculation of intracellular pH

Miniaturised Setups						
SINGLE CELL REACTORS and FLOW CHAMBER						
Inuoe *et al.* (2001)	*E. coli*	M9LB medium, glucose	Growth of single cells	On-line monitoring under microscope	<1mL, parallel microchambers	Image analysis
Wakamoto *et al.* (2001)	various	Various	See above	See above	Mircochambers	See above
Groisman *et al*. (2005)	Various	Various	Single cell growth, GFP fluorescence	Lab-on-chip for single cell growth, fluorescence microscopy	See above	Image analysis
Elfwing *et al*. (2005) Jang *et al*. (2011)	*E. coli*, other bacteria	LB medium, glucose	Single cell growth, cell division, single cell protein secretion	On-line monitoring under microscope	<1 mL	Image analysis, doubling time analysis, protein production plotted
Long *et al*. (2012)	*E. coli*	M9-minimal medium, glucose	See above	See above	6000 cell trapping channels	See above
Denervaud *et al*. (2013)	*S. cerevisiae*	SD-medium, glucose	Growth, GFP expression	Proteome, microscopy	Microchemostat	Image analysis
ENVIRONSTAT						
Kortmann *et al.* (2008) 1+2 Dusny *et al*. (2012) Fritzsch *et al.* (2013)	*S. cerevisiae* *E. coli* and other bacteria	Minimal medium, glucose	Single cell growth rate	Lab-on-chip, on-line monitoring of biomass, microscopy (pictures, videos)	MTPs	CFD modeling, Image analysis, growth rate distributions, fitting of distributions to growth rate population
Kortmann *et al*. (2009)	*S. pombe*	See above	Single cell recombinant protein production	See above	See above	See above, production of single cell calculated

MICROBIOREACTOR						
Parallel MBRs/MTPS						
Buchenauer *et al.* (2009) Gebhardt *et al.* (2011) Puskeiler *et al.* (2005) Weuster-Botz *et al.* (2005)	*E. coli* *S. cerevisiae* *E. coli*	TB-medium, glycerol YEPD-medium Mineral medium, glucose	Growth rate	BioLector pH, biomass monitored on-line, magnetic stirring fluorescence reader	48 well MTP (8-12mL), batch, fed-batch (exponential& constant feed)	Timeplots of measured properties, comparison to large scale
Van Leeuwen *et al.* (2009)	*C. utilis*	Minimal medium, glucose	Growth rate, CO_2-production	See above, on-line CO_2 measurement	96 well MTP	See above
MBRs						
Kostov *et al.* (2000)	*E. coli*	LB-medium, glucose	Growth rate	On-line monitoring (OD, pH, DO)	8 mL	Timeplots for measured data, comparison to 1L scale
Edlich *et al.* (2009)	*S. cerevisiae*		Growth rate, viability	On-line monitoring (DO, OD), fluorescence kit and reader (PI, SYTO9)	8 µL, continuous cultivation possible	Percentage of viable cells, timeplots of measured properties, comparison to large scale
Kensy *et al.* (2009) Funke *et al.* (2010)	*E. coli*	WR-medium, glycerol	Growth rate, protein production	BioLector software	200 µL, batch and fed-batch	Timeplots of values, comparison to 1L scale
Au *et al.* (2011)	BAY (bacteria, archaea, yeast)	Various	Growth rate, viability, fluorescence	On-line monitoring, viability assay, reporter strains (microscope)	Droplet, semi, continuous	See above
Bower *et al.* (2012)	*E. coli*	Semi-defined medium	Growth rate, protein production	On-line monitoring (pH, OD, temperature)	1 mL, fed-batch	See above
SCALE DOWN REACTORS						
PFR+STR						
Amanullah *et al.* (2000)	*B. subtilis*	Defined medium,	biomass and product	product formation assay	STR 2 L/PFR 0.05 L	Timeplots of measured data, comparison to normal fed-

		glucose	formation			batch process
Enfors *et al.* (2001)	*E. coli*	Mineral salt medium, ammonium	Stress response, viability	FC (PI, BOX), stress gene expression analysis	2 L	Biplots gating for viable percentage
Delvigne *et al.* (2006 1,2& 3, 2009, 2011) Han *et al.* (2013) Lejeune *et al.* (2010)	*E. coli* *S. cerevisiae*	Mineral medium, glucose	Cell count, Stress response, viability, GFP leakage, growth rate	FC (FSC, SSC, GFP, PI), subpopulation analysis, stress and growth reporter strain	1 L	Timeplots of all mean measured properties, frequency distribution of mean concentration, stochastic models for scale down in comparison to normal fed-batch and chemostat
Brognaux *et al.* (2012)	*E. coli*	Mineral medium, glucose	GFP fluorescence	Three different reporter strains (FC)	Mini scale down system, fed-batch, 0.2 L	Modeling of results and compared to lab scale, scale down and conventional reactor
2 STRS						
Larsson and Enfors (1985, 1988)	*P. chrysogenum*	Complex medium	Response to oxygen gradients	General physiology	2x15 dm^3	Modeling, timeplots of general physiology, oxygen uptake rate
Sweere *et al.* (1988)	*S. cerevisiae*	Minimal medium, glucose	Growth	General physiology	Different volume ratio and recirculation times	Glucose and oxygen uptake, timeplots
Lara *et al.* (2006)	*E. coli*	Mineral medium, glucose	Stress gene response	Fluorescence reader, qRT-PCR	0.8 L anaerobic, 0.4 L aerobic	Mean fluorescence, gene expression levels
TURBULAR LOOP REACTOR						
Papagianni *et al.* (2003)	*A. niger*	Minimal medium, glucose	Response to oxygen and pH gradients	General physiology, microscopy	3.5-9 L	Image analysis

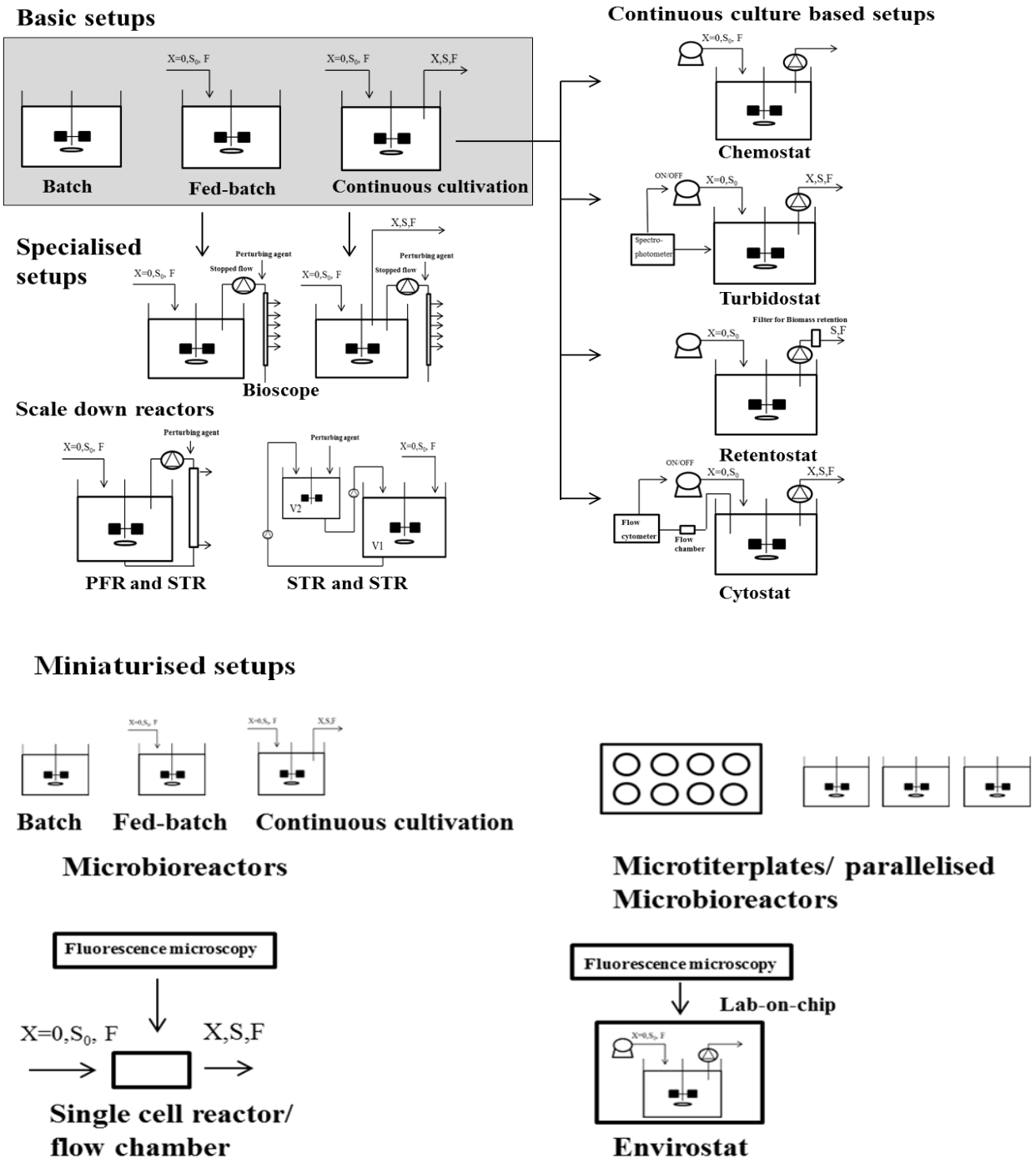

Figure 1- Overview of setups used to investigate single cell population heterogeneity that are described in this review. Short definitions of the basic and continuous culture based setups are found in the glossary box respectively in the particular chapters describing the setups. The grey box marks basic setups. Abbreviations: STR: stirred tank reactor; PFR: plug flow reactor.

2.4 Discussion and outlook

2.4.1 Further application possibilities of the presented setups

The setups for simulation of population heterogeneity – a phenomenon especially found to influence large scale industrial production processes – presented in the scope of this review are of different nature and are in different stages of actually being applied in process research and development. While there are various studies using the basic setups as batch, fed-batch and chemostat in a scaled down version compared to industry, specialised setups e.g. cytostat, retentostat or the bioscope are only used in a limited number of studies but have a tremendous potential for extended future use. But also combinations of the basic setups with more advanced sampling techniques (automated, rapid sampling) or on-line monitoring of single cell properties could be integrated into cultivation processes to further improve the access to experimental data on rapid physiology changes. These setups are especially valuable when reporter strains and/or stains (applied as single stains or as a combination of several stains) are applied as single cell expression targeting special features of interest can be monitored on-line. A valuable tool for the assessment of rapid physiology changes could be the bioscope system. Up to now the application of the system, as reviewed here, is limited to metabolome studies. However, it could be easily applied for the study of dynamic responses on population heterogeneity level in combination with at-line flow cytometry analysis applying e.g. reporter strains. The only limitation would be that in order to be able to detect single cell responses the sampling time would need to be adjusted to the generation time of the fluorescent protein, which is e.g. in case of GFP around 40 min[69]. This could be avoided by using setups like the cytostat that use an on-line flow cytometer since in this case fluorescence could be monitored on-line permanently. The cytostat is generally broadly applicable within single cell physiology studies but its development is still at the beginning[97]. However, it could be used to monitor the expression of a certain gene of interest which is e.g. stress response related as well as by applying more stains apart from PI in the microchamber sampling unit. Furthermore, a cell sorter could be integrated in the system to sort for single cell subpopulations with desired properties that can afterwards be analysed in more detail. To study cells under more extreme growth conditions a turbidostat or retentostat could be applied. The turbidostat could hereby be used to investigate single cell behavior and responses to perturbations during growth at maximum specific growth rates, which might be of interest for industrial processes that aim at producing growth related products, due to the increased volumetric productivity. Also the potential high cell densities achieved in a turbidostat resemble e.g. industrial high density fed-batch process conditions. On the

other hand the retentostat could be used to study the opposite phenomenon of single cells growing at near-zero growth rates, which might have future potential for creating new cell factories as well as for the investigation of processes with a production that is uncoupled to growth, or in general for a more detailed investigation of cell robustness. However, more measurements like, cell size distribution, reporter strains, fluorescent stains and biosensors should be included in the studies. At present there is room for considerable development as well as a need for modeling approaches to make studies better controllable and predictable.

In general all these setups provide, when performed in lab scale considerable amounts of detailed data and comparing all scales (figure 2), these setups have the biggest potential to be combined with different sampling methods and analysis.

Furthermore scale down reactors can be used for several different approaches with different settings and building blocks (Combination of narrow property distributions in PFR and zones with high and low parameter values depending on the position in the reactor in a STR). Studies also showed that they can mimic the behavior of industrial scale processes and can be modeled which makes scale down reactors a useful tool for studying population heterogeneity and process optimization. Future application could include extended use of reporter systems/microbial cell biosensors and also expand scale down reactors up to now run as fed-batch processes towards other process modes like the chemostat. An attempt was made recently to couple two STRs to each other with continuous circulation between them, where one reactor represented the feeding zone with glucose inlet and the other one the remaining reactor volume with outlet and aeration (unpublished results).

A tremendous potential for future use in bioprocess development and optimization also lies in miniaturised setups like microbioreactors, arrays of microtiter plates(MTPs), lab-on-chip setups (e.g. environstat) or single cell reactors[134]. Especially setups following single cells like the environstat or single cell reactors and flow chambers improve the possibilities in single cell research, because it allows the characterization of single cells in an isolated environment, which can be extended to study e.g. single cell protein expression (figure 2). Setups like this, although loosing mostly the high throughput of flow cytometry because they use microscopy, describe processes with high sample frequency (figure 2). Furthermore it might simplify the investigation of regulatory and physiological responses to genetic and environmental perturbations[130]. But these relatively new devices need further improvement in process control, sampling and data analysis. However due to the small volume it will be a challenge to integrate more advanced sampling for e.g. gene

expression analysis as well as proteome or metabolome analysis. To circumvent this problem more on-line monitoring tools in combination with reporter strains could be applied.

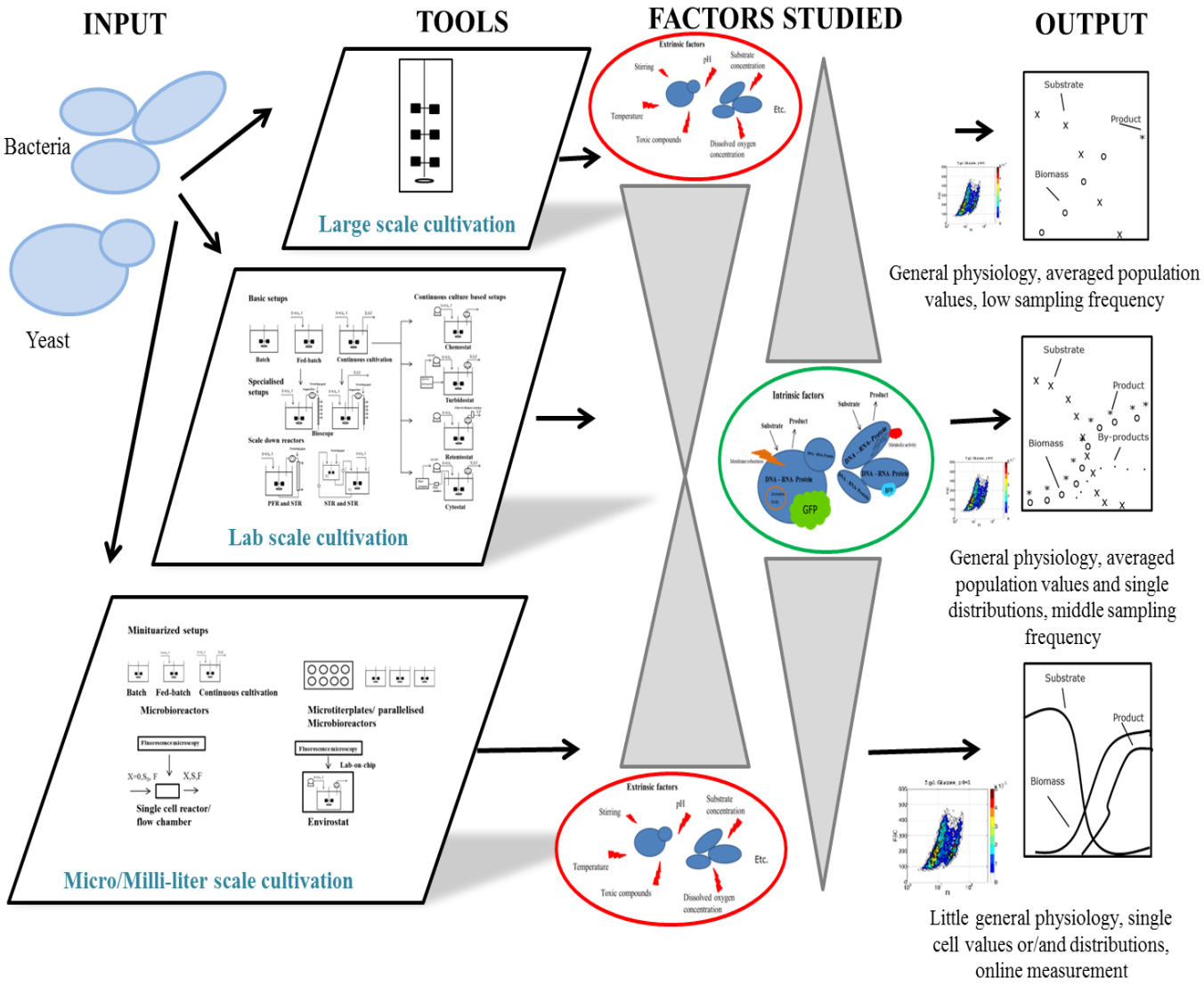

Figure 2- Comparison of investigation of single cells population heterogeneity at different scales: evaluating tools, factors studied (extrinsic and intrinsic) and the output**.** With the decrease in scale more valuable single cell data can be collected with decreasing respectively increasing influence of intrinsic and extrinsic factors which is reflected in the output going from mostly general physiology data to single values and distributions.

2.4.2 Need for more advanced data analysis

Studies at single cell level mentioned in the scope of this review generate bog amounts of data, especially when involving flow cytometry with regular sampling to follow a whole cultivation

process. These data are normally evaluated using biplots of cell size against a measured fluorescent property distribution e.g. GFP fluorescence or single parameter histogram plots, which are manually gated for positive stained cells (see table 1 and 2, column data analysis). Thereafter values are mostly scaled down to mean values or in rare cases coefficient of variance (CV) values, which fail to describe the real phenomena in the bioreactor. As a consequence the potential of the data collected using advanced setups that make population heterogeneity assessable are subjectively analysed which makes comparison of results from different studies difficult as well as reproducibility questionable. Therefore, the need for more objective data analysis and unbiased systematic tools to describe population heterogeneity arose in several studies and reviews[10,14,23,33]. This would in the end also facilitate the use of these methods for optimization of industrial processes. Data analysis methods like this are general practice in mammalian cell research and have been reviewed elsewhere[159]. Additionally to data analysis also the mathematical modeling efforts to account for the heterogeneity in bioprocesses is scarce and not sufficiently explored thus far to validate model predictions for cell property distributions against experimental data, which has also been reviewed[160].

Some approaches have been developed to overcome these problems in e.g. developing simple mathematical parameters to describe the distribution shape of single cell properties in a quantitative way (Heins et al., unpublished). Furthermore a basic kinetic model was coupled to a single cell model to account for single cell distributions during batch cultivations of *S. cerevisiae*[33].

2.4.3 General usefulness of the presented setups and tools for industry and outlook

In conclusion, the reviewed methods and setups to investigate population heterogeneity hold great potential to be further developed or/and combined, and thereby hopefully enable better control of this phenomenon in the future. Moreover, if data analysis and modeling tools will be improved these setups can also be used in industrial process development and optimization applying reporter strains as well as different fluorescence stains evaluated by flow cytometry on-line or at-line. For the production process itself the application of reporter strains might be critical but more on-line monitoring methods could be applied. Also, adding cell sorting of subpopulations observed during bioprocesses to allow more detailed characterization of them could be helpful and consequently be used for strain population engineering, which lately caught increased attention.

Glossary box: short definition of cultivation setups

Batch: Batch cultivations are characterised by different growth phases exhibiting different growth rates and cell characteristics, which makes the batch cultivation a good tool to characterise and study the behavior of cells in a dynamic environment. Normally performed in well-controlled industrial (e.g. for recombinant protein production) or bench scale reactors but especially in earlier days less controlled cultures in shake flask were also considered sufficient.

Fed-batch: Fed-batch cultivation, which are traditionally operated with a continuous feed of substrate but no removal of old medium, are widely and preferably used in industrial production processes for e.g. amino acids, nucleic acids and heterologous recombinant proteins, because high cell densities and productivities can be achieved[36]. Examples for industrial production processes are reported in the literature[37,161,162].

Continuous culture

Two different ways of continuous culture are mainly used nowadays to investigate single cell behavior in a controlled stable environment, the turbidostat and the chemostat. But also more specialised setups are applied and have the potential to be applied for single cell investigations.

Chemostat: In the more frequently used chemostat in single cell analysis, the dilution rate is fixed by controlled pumping in of the inlet feed[85]. The dilution rate equals the growth rate under these conditions and the medium is designed so that cell growth is nutrient limited by e.g. glucose or ethanol as substrate[85]. After three to five volume changes in the reactor, steady state is normally assumed, meaning that the concentration of metabolites and gases (oxygen, carbon dioxide) do not change over time, which makes the chemostat a valuable tool to investigate single cell behaviour in a stable steady state environment[10].

Turbidostat: A Turbidostat, is a continuous process in which the medium is, in contrast to the chemostat, is rich in all nutrients and the growth rate is the maximal specific growth rate the organism is capable of under the given conditions[163]. The feed is feedback controlled by the optical density or biomass concentration which means that fresh medium is only applied when the biomass respectively optical density exceeds a set point but also that a high cell concentration is required[163]. At this cell density secretion products accumulate and nutrients are consumed such that the extracellular environment at steady state deviates significantly from the feed medium composition[85].

Retentostat: A Retentostat or sometimes referred to as recycle fermenter or recyclostat[92], which was first proposed by Herbert (1961), is a variation of the chemostat with the difference that the effluent outlet is replaced by a polypropylene filter so that all cells are retained inside the bioreactor[90]. Consequently, the biomass concentration in the bioreactor will constantly increase while the growth-limiting energy substrate is fed with a constant low rate that is sufficient for maintenance of cellular viability and integrity but insufficient for growth[91,92]. If operated for a prolonged time the glucose available per cell is decreasing and finally a situation is attained where the specific growth rate becomes zero (below 0.01 h^{-1}) and the substrate consumption equals the maintenance energy requirement[90,92].

Cytostat: A cytostat, is a modification of the turbidostat, where the inlet feed is controlled by an automated flow cytometer directly connected to the bioreactor which is measuring, monitoring and controlling its cell number concentration[85]. Originally, the cytostat process control was developed for mammalian cell culture and used for diverse applications like the production of monoclonal antibodies[164] or the continuous culture of Chinese hamster ovary (CHO) cells[97]. In the latter case the original cytostat, whose use was limited to high cell concentrations and had the disadvantage that the cell concentration needed to be achieved indirectly by a correlation, was further developed by connecting an automated flow cytometer with flowchamber to the bioreactor to use it for the control of the cell concentration[85]. In this way the cytostat can be controlled at very low cell concentrations which only negligibly change the composition of the medium in the bioreactor making the cell environment precisely defined by the feed.

Bioscope: The bioscope sampling loop is connected to a fed-batch or continuously operated bioreactor, from which it is fed with a constant flow (normally 1-3 mL/min) of bioreactor broth which is then mixed with a small amount of perturbing agent (perturbation start, e.g. substrate, inhibitors, uncoupled agents)[103]. Afterwards the perturbed broth flows through a long channel and samples are taken automatically at different locations along the bioscope, which resembles a PFR, corresponding to different incubation times after perturbation (0-100s, sampling port every 3s)[103]. This setup allows the performance of perturbation experiments of various kind and intensity evaluating in vivo kinetics during large scale continuous and fed-batch experiments within the same experiment with high reproducibility and possible application of different sampling protocols[103,104].

2.5 References

1. Ferrer-Miralles, N., Domingo-Espín, J., Corchero, J. L., Vázquez, E. & Villaverde, A. Microbial factories for recombinant pharmaceuticals. *Microb. Cell Fact.* **8,** (2009).

2. Chemler, J. a, Yan, Y. & Koffas, M. a G. Biosynthesis of isoprenoids, polyunsaturated fatty acids and flavonoids in Saccharomyces cerevisiae. *Microb. Cell Fact.* **5,** (2006).

3. Demain, A. L. The business of biotechnology. *Ind. Biotechnol.* **3,** 269–283 (2007).

4. Demain, A. L. & Vaishnav, P. Production of recombinant proteins by microbes and higher organisms. *Biotechnol. Adv.* **27,** 297–306 (2009).

5. Krogh, A. Stability of heterologous protein production by Saccharomyces cerevisiae in continuous cultures. (2009).

6. Hensing, M. C., Rouwenhorst, R. J., Heijnen, J. J., van Dijken, J. P. & Pronk, J. T. Physiological and technological aspects of large-scale heterologous-protein production with yeasts. *Antonie Van Leeuwenhoek* **67,** 261–279 (1995).

7. Lara, A. R., Galindo, E., Ramirez, O. T. & Palomares, L. A. Living with heterogeneities in bioreactors: understanding the effects of environmental gradients on cells. *Mol. Biotechnol.* **34,** 355–381 (2006).

8. Müller, S., Harms, H. & Bley, T. Origin and analysis of microbial population heterogeneity in bioprocesses. *Curr. Opin. Biotechnol.* **21,** 100–113 (2010).

9. Lidstrom, M. E. & Konopka, M. C. The role of physiological heterogeneity in microbial population behavior. *Nat. Chem. Biol.* **6,** 705–712 (2010).

10. Fernandes, R. L. *et al.* Experimental methods and modeling techniques for description of cell population heterogeneity. *Biotechnol. Adv.* **29,** 575–599 (2011).

11. Enfors, S. O. *et al.* Physiological responses to mixing in large scale bioreactors. *J. Biotechnol.* **85,** 175–185 (2001).

12. Lara, A. R., Galindo, E., Ramírez, O. T. & Palomares, L. A. Living With Heterogeneities in Bioreactors Living With Heterogeneities in Bioreactors. *Mol. Biotechnol.* **34,** (2006).

13. Muller, S., Harms, H. & Bley, T. Origin and analysis of microbial population heterogeneity in bioprocesses. *Curr. Opin. Biotechnol.* **21,** 100–113 (2010).

14. Carlquist, M. *et al.* Physiological heterogeneities in microbial populations and implications for physical stress tolerance. *Microb. Cell Fact.* **11,** (2012).

15. Bylund, F., Collet, E., Enfors, S.-O. & Larsson, G. Substrate gradient formation in the large-scale bioreactor lowers cell yield and increases by-product formation. *Bioprocess Eng.* **18,** (1998).

16. Schweder, T. *et al.* Monitoring of genes that respond to process-related stress in large-scale bioprocesses. *Biotechnol. Bioeng.* **65,** 151–159 (1999).

17. Larsson, G. *et al.* Substrate gradients in bioreactors: origin and consequences. *Bioprocess Eng.* **14,** 281–289 (1996).

18. Díaz, M., Herrero, M., García, L. a. & Quirós, C. Application of flow cytometry to industrial microbial bioprocesses. *Biochem. Eng. J.* **48,** 385–407 (2010).

19. Müller, S. & Nebe-von-Caron, G. Functional single-cell analyses: flow cytometry and cell sorting of microbial populations and communities. *FEMS Microbiol. Rev.* **34,** 554–587 (2010).

20. Rieseberg, M., Kasper, C., Reardon, K. F. & Scheper, T. Flow cytometry in biotechnology. *Appl. Microbiol. Biotechnol.* **56,** 350–360 (2001).

21. Schmid, A., Kortmann, H., Dittrich, P. S. & Blank, L. M. Chemical and biological single cell analysis. *Curr. Opin. Biotechnol.* **21,** 12–20 (2010).

22. Herzenberg, L. a, Tung, J., Moore, W. a, Herzenberg, L. a & Parks, D. R. Interpreting flow cytometry data: a guide for the perplexed. *Nat. Immunol.* **7,** 681–685 (2006).

23. Delvigne, F. & Goffin, P. Microbial heterogeneity affects bioprocess robustness: Dynamic single-cell analysis contributes to understanding of microbial populations. *Biotechnol. J.* **9,** 61–72 (2014).

24. Cipollina, C. *et al.* Revisiting the role of yeast Sfp1 in ribosome biogenesis and cell size control: a chemostat study. *Microbiology* **154,** 337–346 (2008).

25. Vanoni, M., Vai, M., Popolo, L. & Alberghina, L. Structural heterogeneity in populations of the budding yeast Saccharomyces Structural Heterogeneity in Populations of the Budding Yeast Saccharomyces cerevisiae. *J. Bacteriol.* **156,** 1282–1291 (1983).

26. Lord, P. G. & Wheals, A. E. Asymmetrical division of Asymmetrical Division of Saccharomyces cerevisiae. *J. Bacteriol.* **142,** 808–818 (1980).

27. Akerlund, T., Nordström, K. & Bernander, R. Analysis of cell size and DNA content in exponentially growing and stationary-phase batch cultures of Escherichia coli. *J. Bacteriol.* **177,** 6791–6797 (1995).

28. Cipollina, C., Alberghina, L., Porro, D. & Vai, M. SFP1 is involved in cell size modulation in respiro-fermentative growth conditions. *Yeast* **22,** 385–399 (2005).

29. Skarstad, K., Steen, H. B. & Boye, E. Cell cycle parameters of slowly growing Escherichia coli B / r studied by flow Cell Cycle Parameters of Slowly Growing Escherichia coli B / r Studied by Flow Cytometry. *J. Bacteriol.* **154,** 656–662 (1983).

30. Porro, D., Brambilla, L. & Alberghina, L. Glucose metabolism and cell size in continuous cultures of Saccharomyces cerevisiae. *FEMS Microbiol. Lett.* **229,** 165–171 (2003).

31. Ranzi, B. M., Cornragno, C. & Martegani, E. Analysis of Protein and Cell Volume Distribution in G I u cose- Li m it ed Continuous Cultures of Budding Yeast. *Biotechnol. Bioeng.* **XXVIII,** 185–190 (1986).

32. Roostalu, J., Jõers, A., Luidalepp, H., Kaldalu, N. & Tenson, T. Cell division in Escherichia coli cultures monitored at single cell resolution. *BMC Microbiol.* **8,** (2008).

33. Lencastre Fernandes, R. *et al.* Cell mass and cell cycle dynamics of an asynchronous budding yeast population: experimental observations, flow cytometry data analysis, and multi-scale modeling. *Biotechnol. Bioeng.* **110,** 812–826 (2013).

34. Porro, D., Vai, M., Vanoni, M., Alberghina, L. & Hatzis, C. Analysis and modeling of growing budding yeast populations at the single cell level. *Cytometry. A* **75,** 114–120 (2009).

35. Quiros, C., Herrero, M., Garcia, L. A. & Diaz, M. Application of flow cytometry to segregated kinetic modeling based on the physiological states of microorganisms. *Appl. Environ. Microbiol.* **73,** 3993–4000 (2007).

36. Hewitt, C. J., Nebe-Von Caron, G., Nienow, a W. & McFarlane, C. M. Use of multi-staining flow cytometry to characterise the physiological state of Escherichia coli W3110 in high cell density fed-batch cultures. *Biotechnol. Bioeng.* **63,** 705–711 (1999).

37. Wang, J. *et al.* Genetic engineering of Escherichia coli to enhance production of L-tryptophan. *Appl. Microbiol. Biotechnol.* **97,** 7587–7596 (2013).

38. Freitas, C., Neves, E., Reis, A., Passarinho, P. C. & da Silva, T. L. Use of multi-parameter flow cytometry as tool to monitor the impact of formic acid on Saccharomyces carlsbergensis batch ethanol fermentations. *Appl. Biochem. Biotechnol.* **169,** 2038–2048 (2013).

39. Tibayrenc, P., Preziosi-Belloy, L. & Ghommidh, C. Single-cell analysis of S . cerevisiae growth recovery after a sublethal heat-stress applied during an alcoholic fermentation. *J. Ind. Microbiol. Biotechnol.* 687–696 (2011). doi:10.1007/s10295-010-0814-6

40. Amillastre, E., Aceves-Lara, C.-A., Uribelarrea, J.-L., Alfenore, S. & Guillouet, S. E. Dynamic model of temperature impact on cell viability and major product formation during fed-batch and continuous ethanolic fermentation in Saccharomyces cerevisiae. *Bioresour. Technol.* **117,** 242–250 (2012).

41. Berney, M. *et al.* Specific Growth Rate Determines the Sensitivity of Escherichia coli to Thermal , UVA , and Solar Disinfection. *Appl. Environ. Microbiol.* **72,** 2586–2593 (2006).

42. Hewitt, C. J., Boon, L. a, McFarlane, C. M. & Nienow, a W. The use of flow cytometry to study the impact of fluid mechanical stress on Escherichia coli W3110 during continuous cultivation in an agitated bioreactor. *Biotechnol. Bioeng.* **59,** 612–620 (1998).

43. Howlett, N. G. & Avery, S. V. Flow cytometric investigation of heterogeneous copper-sensitivity in asynchronously grown Saccharomyces cerevisiae. *FEMS Microbiol. Lett.* **176,** 379–386 (1999).

44. Sundström, H. *et al.* Segregation to non-dividing cells in recombinant Escherichia coli fed-batch fermentation processes. *Biotechnol. Lett.* **26,** 1533–1539 (2004).

45. Want, A., Thomas, O. R. T., Kara, B., Liddell, J. & Hewitt, C. J. Studies related to antibody fragment (Fab) production in Escherichia coli W3110 fed-batch fermentation processes using multiparameter flow cytometry. *Cytometry. A* **75,** 148–154 (2009).

46. Nebe-von-Caron, G., Stephens, P. J., Hewitt, C. J., Powell, J. R. & Badley, R. a. Analysis of bacterial function by multi-colour fluorescence flow cytometry and single cell sorting. *J. Microbiol. Methods* **42,** 97–114 (2000).

47. Hewitt, C. J., Nebe-Von Caron, G., Axelsson, B., McFarlane, C. M. & Nienow, a W. Studies related to the scale-up of high-cell-density E. coli fed-batch fermentations using multiparameter flow cytometry: effect of a changing microenvironment with respect to glucose and dissolved oxygen concentration. *Biotechnol. Bioeng.* **70,** 381–390 (2000).

48. Gustavsson, R. & Mandenius, C.-F. Soft sensor control of metabolic fluxes in a recombinant Escherichia coli fed-batch cultivation producing green fluorescence protein. *Bioprocess Biosyst. Eng.* **36,** 1375–1384 (2013).

49. Sweere, A. P. J. *et al.* Modelling the dynamic behaviour of Saccharomyces cerevisiae and its application in control experiments. *Appl. Microbiol. Biotechnol.* 116–127 (1988).

50. Taymaz-Nikerel, H., van Gulik, W. M. & Heijnen, J. J. Escherichia coli responds with a rapid and large change in growth rate upon a shift from glucose-limited to glucose-excess conditions. *Metab. Eng.* **13,** 307–318 (2011).

51. Theobald, U., Mailinger, W., Baltes, M., Rizzi, M. & Reuss, M. In vivo analysis of metabolic dynamics in Saccharomyces cerevisiae : I. Experimental observations. *Biotechnol. Bioeng.* **55,** 305–316 (1997).

52. Wu, L. *et al.* Quantitative analysis of the microbial metabolome by isotope dilution mass spectrometry using uniformly 13C-labeled cell extracts as internal standards. *Anal. Biochem.* **336,** 164–171 (2005).

53. Zakrzewska, A. *et al.* Genome-wide analysis of yeast stress survival and tolerance acquisition to analyze the central trade-off between growth rate and cellular robustness. *Mol. Biol. Cell* **22,** 4435–4446 (2011).

54. Raman, B., Nandakumar, M. P., Muthuvijayan, V. & Marten, M. R. Proteome analysis to assess physiological changes in Escherichia coli grown under glucose-limited fed-batch conditions. *Biotechnol. Bioeng.* **92,** 384–392 (2005).

55. Yoon, S. H., Han, M.-J., Lee, S. Y., Jeong, K. J. & Yoo, J.-S. Combined transcriptome and proteome analysis of Escherichia coli during high cell density culture. *Biotechnol. Bioeng.* **81,** ombined transcriptome and proteome analysis of Esc (2003).

56. Winder, C. L. *et al.* Metabolic fingerprinting as a tool to monitor whole-cell biotransformations. *Anal. Bioanal. Chem.* **399,** 387–401 (2011).

57. Daran-Lapujade, P. *et al.* Role of transcriptional regulation in controlling fluxes in central carbon metabolism of Saccharomyces cerevisiae. A chemostat culture study. *J. Biol. Chem.* **279,** 9125–9138 (2004).

58. Fazio, A. *et al.* Transcription factor control of growth rate dependent genes in Saccharomyces cerevisiae: a three factor design. *BMC Genomics* **9,** (2008).

59. Kolkman, A., Olsthoorn, M. M. a, Heeremans, C. E. M., Heck, A. J. R. & Slijper, M. Comparative proteome analysis of Saccharomyces cerevisiae grown in chemostat cultures limited for glucose or ethanol. *Mol. Cell. Proteomics* **4,** 1–11 (2005).

60. Brauer, M. J. *et al.* Coordination of Growth Rate , Cell Cycle , Stress Response , and Metabolic Activity in Yeast. *Mol. Biol. Cell* **19,** 352–367 (2008).

61. Regenberg, B. *et al.* Growth-rate regulated genes have profound impact on interpretation of transcriptome profiling in Saccharomyces cerevisiae. *Genome Biol.* **7,** (2006).

62. Tai, S. L. *et al.* Two-dimensional transcriptome analysis in chemostat cultures. Combinatorial effects of oxygen availability and macronutrient limitation in Saccharomyces cerevisiae. *J. Biol. Chem.* **280,** 437–447 (2005).

63. Benbadis, L., Cot, M., Rigoulet, M. & Francois, J. Isolation of two cell populations from yeast during high-level alcoholic fermentation that resemble quiescent and nonquiescent cells from the stationary phase on glucose. *FEMS Yeast Res.* **9,** 1172–1186 (2009).

64. Attfield, P. V, Choi, H. Y., Veal, D. a & Bell, P. J. Heterogeneity of stress gene expression and stress resistance among individual cells of Saccharomyces cerevisiae. *Mol. Microbiol.* **40,** 1000–1008 (2001).

65. Sunya, S., Delvigne, F., Uribelarrea, J.-L., Molina-Jouve, C. & Gorret, N. Comparison of the transient responses of Escherichia coli to a glucose pulse of various intensities. *Appl. Microbiol. Biotechnol.* **95,** 1021–1034 (2012).

66. Nisamedtinov, I. *et al.* The response of the yeast Saccharomyces cerevisiae to sudden vs. gradual changes in environmental stress monitored by expression of the stress response protein Hsp12p. *FEMS Yeast Res.* **8,** 829–838 (2008).

67. Sunya, S., Gorret, N., Delvigne, F., Uribelarrea, J.-L. & Molina-Jouve, C. Real-time monitoring of metabolic shift and transcriptional induction of yciG::luxCDABE E. coli reporter strain to a glucose pulse of different concentrations. *J. Biotechnol.* **157,** 379–390 (2012).

68. DeLisa, M. P., Li, J., Rao, G., Weigand, W. a & Bentley, W. E. Monitoring GFP-operon fusion protein expression during high cell density cultivation of Escherichia coli using an on-line optical sensor. *Biotechnol. Bioeng.* **65,** 54–64 (1999).

69. Reischer, H., Schotola, I., Striedner, G., Pötschacher, F. & Bayer, K. Evaluation of the GFP signal and its aptitude for novel on-line monitoring strategies of recombinant fermentation processes. *J. Biotechnol.* **108,** 115–125 (2004).

70. Natarajan, a & Srienc, F. Dynamics of glucose uptake by single Escherichia coli cells. *Metab. Eng.* **1,** 320–333 (1999).

71. Lewis, G., Taylor, I. W., Nienow, A. W. & Hewitt, C. J. The application of multi-parameter flow cytometry to the study of recombinant Escherichia coli batch fermentation processes. *J. Ind. Microbiol. Biotechnol.* **31,** 311–322 (2004).

72. Lú Chau, T., Guillán, A., Roca, E., Núñez, M. J. & Lema, J. M. Population dynamics of a continuous fermentation of recombinant Saccharomyces cerevisiae using flow cytometry. *Biotechnol. Prog.* **17,** 951–957 (2001).

73. Abel, C. *et al.* Transient behaviour of continuously cultivated Baker ' s yeast during enforced variations of dissolved oxygen and glucose concentrations. *J. Biotechnol.* **33,** 183–193 (1994).

74. Kresnowati, M. T. A. P., Groothuizen, M. K. & Winden, W. A. Van. Measurement of Fast Dynamic Intracellular pH in Saccharomyces cerevisiae Using Benzoic Acid Pulse. *J. Biotechnol.* **97,** 86–98 (2007).

75. Davey, H. M. *et al.* Oscillatory, stochastic and chaotic growth rate fluctuations in permittistatically controlled yeast cultures. *Biosystems.* **39,** 43–61 (1996).

76. Aarnio, T. H., Suihko, M. L. & Kauppinen, V. S. Isolation of acetic acid-tolerant Baker's yeast variants in a turbidostat. *Appl. Biochem. Biotechnol.* **27,** 55–63 (1991).

77. Avrahami-Moyal, L., Engelberg, D., Wenger, J. W., Sherlock, G. & Braun, S. Turbidostat Culture of Saccharomyces cerevisiae W303-1A under Selective pressure elicited by ethanol selects for mutations in SSD1 and UTH1. *FEMS Yeast Res.* **12,** 521–533 (2013).

78. Tøsttrup, H. V & Carlsen, S. A Process for the Production of Human P r oi n su I i n i n Saccharom yces cere vjsjae. *Biotechnol. Bioeng.* **35,** 339–348 (1989).

79. el-Mansi, E. M. & Holms, W. H. Control of carbon flux to acetate excretion during growth of Escherichia coli in batch and continuous cultures. *J. Gen. Microbiol.* **135,** 2875–2883 (1989).

80. Holms, H. Flux analysis and control of the central metabolic pathways in Escherichia coli. *FEMS Microbiol. Rev.* **19,** 85–116 (1996).

81. Laurinavichene, T. V, Chanal, A., Wu, L. F. & Tsygankov, a a. Effect of O2, H2 and redox potential on the activity and synthesis of hydrogenase 2 in Escherichia coli. *Res. Microbiol.* **152,** 793–798 (2001).

82. Zhao, R., Natarajan, A. & Srienc, F. A flow injection flow cytometry system for on-line monitoring of bioreactors. *Biotechnol. Bioeng.* **62,** 609–617 (1999).

83. Zhao, Z., Wang, T. & Chen, L. Dynamic analysis of a turbidostat model with the feedback control. *Commun. Nonlinear Sci. Numer. Simul.* **15,** 1028–1035 (2010).

84. Guo, H. & Chen, L. Periodic solution of a turbidostat system with impulsive state feedback control. *J. Math. Chem.* **46,** 1074–1086 (2008).

85. Kacmar, J., Gilbert, A., Cockrell, J. & Srienc, F. The cytostat: A new way to study cell physiology in a precisely defined environment. *J. Biotechnol.* **126,** 163–172 (2006).

86. Sorgeloos, P., Van Outryve, E., Persoone, G. & Cattoir-Reynaerts, A. New type of turbidostat with intermittent determination of cell density outside the culture vessel. *Appl. Environ. Microbiol.* **31,** 327–331 (1976).

87. Markx, G. H., Davey, C. L. & Kell, D. B. The permittistat: a novel type of turbidostat. *J. Gen. Microbiol.* **137,** 735–743 (1991).

88. Atkinson, M. R., Savageau, M. a, Myers, J. T. & Ninfa, A. J. Development of genetic circuitry exhibiting toggle switch or oscillatory behavior in Escherichia coli. *Cell* **113,** 597–607 (2003).

89. Van Verseveld, H. W. *et al.* Modeling of microbial substrate conversion, growth and product formation in a recycling fermentor. *Antonie Van Leeuwenhoek* **52,** 325–342 (1986).

90. Boender, L. G. M. *et al.* Extreme calorie restriction and energy source starvation in Saccharomyces cerevisiae represent distinct physiological states. *Biochim. Biophys. Acta* **1813,** 2133–2144 (2011).

91. Boender, L. G. M. *et al.* Cellular responses of Saccharomyces cerevisiae at near-zero growth rates: transcriptome analysis of anaerobic retentostat cultures. *FEMS Yeast Res.* **11,** 603–620 (2011).

92. Boender, L. G. M., de Hulster, E. a F., van Maris, A. J. a, Daran-Lapujade, P. a S. & Pronk, J. T. Quantitative physiology of Saccharomyces cerevisiae at near-zero specific growth rates. *Appl. Environ. Microbiol.* **75,** 5607–5614 (2009).

93. Chesbro, W., Evans, T. & Eifert, R. Very slow growth of Very Slow Growth of Escherichia coli. *J. Bacteriol.* **139,** (1979).

94. Konopka, a. Microbial physiological state at low growth rate in natural and engineered ecosystems. *Curr. Opin. Microbiol.* **3,** 244–247 (2000).

95. Ercan, O., Smid, E. J. & Kleerebezem, M. Quantitative physiology of Lactococcus lactis at extreme low-growth rates. *Environ. Microbiol.* **15,** 2319–2332 (2013).

96. Bull, A. T. The renaissance of continuous culture in the post-genomics age. *J. Ind. Microbiol. Biotechnol.* **37,** 993–1021 (2010).

97. Kacmar, J. & Srienc, F. Dynamics of single cell property distributions in Chinese hamster ovary cell cultures monitored and controlled with automated flow cytometry. *J. Biotechnol.* **120,** 410–420 (2005).

98. Gilbert, A. & Srienc, F. Optimized evolution in the cytostat: a Monte Carlo simulation. *Biotechnol. Bioeng.* **102,** 221–231 (2009).

99. Gilbert, A., Sangurdekar, D. P. & Srienc, F. Rapid strain improvement through optimized evolution in the cytostat. *Biotechnol. Bioeng.* **103,** 500–512 (2009).

100. Peña, P. V, Glasker, S. & Srienc, F. Genome-wide overexpression screen for sodium acetate resistance in Saccharomyces cerevisiae. *J. Biotechnol.* **164,** 26–33 (2013).

101. Kacmar, J., Zamamiri, A., Carlson, R., Abu-Absi, N. R. & Srienc, F. Single-cell variability in growing Saccharomyces cerevisiae cell populations measured with automated flow cytometry. *J. Biotechnol.* **109,** 239–254 (2004).

102. Abu-Absi, N. R., Zamamiri, A., Kacmar, J., Balogh, S. J. & Srienc, F. Automated flow cytometry for acquisition of time-dependent population data. *Cytometry. A* **51,** 87–96 (2003).

103. Visser, D. *et al.* Rapid sampling for analysis of in vivo kinetics using the BioScope: a system for continuous-pulse experiments. *Biotechnol. Bioeng.* **79,** 674–681 (2002).

104. Mashego, M. R., van Gulik, W. M., Vinke, J. L., Visser, D. & Heijnen, J. J. In vivo kinetics with rapid perturbation experiments in Saccharomyces cerevisiae using a second-generation BioScope. *Metab. Eng.* **8,** 370–383 (2006).

105. Buziol, S. *et al.* New bioreactor-coupled rapid stopped-flow sampling technique for measurements of metabolite dynamics on a subsecond time scale. *Biotechnol. Bioeng.* **80,** 632–636 (2002).

106. De Koning, W. & van Dam, K. A method for the determination of changes of glycolytic metabolites in yeast on a subsecond time scale using extraction at neutral pH. *Anal. Biochem.* **204,** 118–123 (1992).

107. Lange, H. C. *et al.* Improved rapid sampling for in vivo kinetics of intracellular metabolites in Saccharomyces cerevisiae. *Biotechnol. Bioeng.* **75,** 406–415 (2001).

108. Mashego, M. R., van Gulik, W. M. & Heijnen, J. J. Metabolome dynamic responses of Saccharomyces cerevisiae to simultaneous rapid perturbations in external electron acceptor and electron donor. *FEMS Yeast Res.* **7,** 48–66 (2007).

109. Nasution, U., Gulik, W. M. Van, Kleijn, R. J. & Winden, W. A. Van. Measurement of Intracellular Metabolites of Primary Metabolism and Adenine Nucleotides in Chemostat Cultivated Penicillium chrysogenum. *Interscience* (2006). doi:10.1002/bit

110. Kresnowati, M. T. a P., Suarez-Mendez, C. M., van Winden, W. a, van Gulik, W. M. & Heijnen, J. J. Quantitative physiological study of the fast dynamics in the intracellular pH of Saccharomyces cerevisiae in response to glucose and ethanol pulses. *Metab. Eng.* **10,** 39–54 (2008).

111. De Mey, M. *et al.* Catching prompt metabolite dynamics in Escherichia coli with the BioScope at oxygen rich conditions. *Metab. Eng.* **12,** 477–487 (2010).

112. Gernaey, K. V *et al.* Monitoring and control of microbioreactors: an expert opinion on development needs. *Biotechnol. J.* **7,** 1308–1314 (2012).

113. Schäpper, D., Alam, M. N. H. Z., Szita, N., Eliasson Lantz, A. & Gernaey, K. V. Application of microbioreactors in fermentation process development: a review. *Anal. Bioanal. Chem.* **395,** 679–695 (2009).

114. Weuster-Botz, D. *et al.* Methods and milliliter scale devices for high-throughput bioprocess design. *Bioprocess Biosyst. Eng.* **28,** 109–119 (2005).

115. Buchenauer, a *et al.* Micro-bioreactors for fed-batch fermentations with integrated online monitoring and microfluidic devices. *Biosens. Bioelectron.* **24,** 1411–1416 (2009).

116. Puskeiler, R., Kaufmann, K. & Weuster-Botz, D. Development, parallelization, and automation of a gas-inducing milliliter-scale bioreactor for high-throughput bioprocess design (HTBD). *Biotechnol. Bioeng.* **89,** 512–523 (2005).

117. Gebhardt, G., Hortsch, R., Kaufmann, K., Arnold, M. & Weuster-Botz, D. A new microfluidic concept for parallel operated milliliter-scale stirred tank bioreactors. *Biotechnol. Prog.* **27,** 684–690 (2011).

118. Xie, D. in *Methods Mol. Biol.* (Cheng, Q.) **834,** (Springer New York, 2012).

119. Leeuwen, M. Van & Heijnen, J. J. Development Of a System for the On-Line Measurement of Carbon Dioxide Production in Microbioreactors : Application to Aerobic Batch Cultivations of Candida utilis. *Am. Inst. Chem. Eng.* (2009). doi:10.1021/bp.145

120. Edlich, A. *et al.* Microfluidic reactor for continuous cultivation of Saccharomyces cerevisiae. *Biotechnol. Prog.* **26,** 1259–1270 (2010).

121. Bower, D. M., Lee, K. S., Ram, R. J. & Prather, K. L. J. Fed-batch microbioreactor platform for scale down and analysis of a plasmid DNA production process. *Biotechnol. Bioeng.* **109,** 1976–1986 (2012).

122. Fritzsch, F. S. O., Dusny, C., Frick, O. & Schmid, A. Single-Cell Analysis in Biotechnology, Systems Biology, and Biocatalysis. *Annu. Rev. Chem. Biomol. Eng. Vol 3* **3,** 129–155 (2012).

123. Dénervaud, N. *et al.* A chemostat array enables the spatio-temporal analysis of the yeast proteome. *Proc. Natl. Acad. Sci. U. S. A.* **110,** (2013).

124. Funke, M. *et al.* Bioprocess control in microscale: scalable fermentations in disposable and user-friendly microfluidic systems. *Microb. Cell Fact.* **9,** (2010).

125. Kensy, F., Engelbrecht, C. & Büchs, J. Scale-up from microtiter plate to laboratory fermenter: evaluation by online monitoring techniques of growth and protein expression in Escherichia coli and Hansenula polymorpha fermentations. *Microb. Cell Fact.* **8,** (2009).

126. Kostov, Y., Harms, P., Randers-Eichhorn, L. & Rao, G. Low-cost microbioreactor for high-throughput bioprocessing. *Biotechnol. Bioeng.* **72,** 346–352 (2001).

127. Au, S. H., Shih, S. C. C. & Wheeler, A. R. Integrated microbioreactor for culture and analysis of bacteria, algae and yeast. *Biomed. Microdevices* **13,** 41–50 (2011).

128. Schäpper, D. *et al.* Topology optimized microbioreactors. *Biotechnol. Bioeng.* **108,** 786–796 (2011).

129. Boccazzi, P. *et al.* Gene expression analysis of Escherichia coli grown in miniaturized bioreactor platforms for high-throughput analysis of growth and genomic data. *Appl. Microbiol. Biotechnol.* **68,** 518–532 (2005).

130. Kortmann, H. *et al.* The Envirostat - a new bioreactor concept. *Lab Chip* **9,** 576–585 (2009).

131. Kortmann, H., Blank, L. M. & Schmid, A. Single cell analysis reveals unexpected growth phenotype of S. cerevisiae. *Cytometry. A* **75,** 130–139 (2009).

132. Fritzsch, F. S. O. *et al.* Picoliter nDEP traps enable time-resolved contactless single bacterial cell analysis in controlled microenvironments. *Lab Chip* **13,** 397–408 (2013).

133. Dusny, C., Fritzsch, F. S. O., Rosenthal, K., Frick, O. & Schmid, A. quantitative physiology with isolated single cells and micropopulations in controlled microenvironments employing a picoliter bioreactor. *Conf. Contrib.* 1576–1578 (2012).

134. Jang, K. *et al.* Development of a microfluidic platform for single-cell secretion analysis using a direct photoactive cell-attaching method. *Anal. Sci.* **27,** 973–978 (2011).

135. Inoue, I., Wakamoto, Y., Moriguchi, H., Okano, K. & Yasuda, K. On-chip culture system for observation of isolated individual cells. *Lab Chip* **1,** 50–55 (2001).

136. Groisman, A. *et al.* A microfluidic chemostat for experiments with bacterial and yeast cells. *Nat. Methods* **2,** 685–689 (2005).

137. Wakamoto, Y., Inoue, I., Moriguchi, H. & Yasuda, K. Analysis of single-cell differences by use of an on-chip microculture system and optical trapping. *Fresenius. J. Anal. Chem.* **371,** 276–281 (2001).

138. Elfwing, A., Lemarc, Y., Baranyi, J. & Ballagi, A. Observing Growth and Division of Large Numbers of Individual Bacteria by Image Analysis. *Appl. Environ. Microbiol.* **70,** 675–678 (2004).

139. Long, Z. *et al.* Microfluidic chemostat for measuring single cell dynamics in bacteria. *Lab Chip* **13,** 947–954 (2013).

140. Teodósio, J. S., Simões, M., Melo, L. F. & Mergulhão, F. J. Flow cell hydrodynamics and their effects on E. coli biofilm formation under different nutrient conditions and turbulent flow. *Biofouling* **27,** 1–11 (2011).

141. Papagianni, M. Methodologies for Scale-down of Microbial Bioprocesses. *J. Microb. Biochem. Technol.* **05,** 1–7 (2011).

142. Papagianni, M., Mattey, M. & Kristiansen, B. Design of a tubular loop bioreactor for scale-up and scale-down of fermentation processes. *Biotechnol. Prog.* **19,** 1498–1504 (2003).

143. George, S., Larsson, G. & Enfors, S.-O. A scale-down two-compartment reactor with controlled substrate oscillations: Metabolic response of Saccharomyces cerevisiae. *Bioprocess Eng.* **9,** 249–257 (1993).

144. Bylund, F., Guillard, F., Enfors, S.-O., Trägårdh, C. & Larsson, G. Scale down of recombinant protein production: a comparative study of scaling performance. *Bioprocess Eng.* **20,** (1999).

145. Delvigne, F., Destain, J. & Thonart, P. Toward a stochastic formulation of microbial growth in relation to bioreactor performances: case study of an E. coli fed-batch process. *Biotechnol. Prog.* **22,** 1114–1124 (2006).

146. Delvigne, F., Destain, J. & Thonart, P. A methodology for the design of scale-down bioreactors by the use of mixing and circulation stochastic models. *Biochem. Eng. J.* **28,** 256–268 (2006).

147. Delvigne, F., Lejeune, A., Destain, J. & Thonart, P. Stochastic Models To Study the Impact of Mixing on a Fed-Batch Culture of Saccharomyces cere W isiae. *Biotechnol. Prog.* 259–269 (2006).

148. Lejeune, A., Delvigne, F. & Thonart, P. Influence of bioreactor hydraulic characteristics on a Saccharomyces cerevisiae fed-batch culture: hydrodynamic modelling and scale-down investigations. *J. Ind. Microbiol. Biotechnol.* **37,** 225–236 (2010).

149. Delvigne, F., Boxus, M., Ingels, S. & Thonart, P. Bioreactor mixing efficiency modulates the activity of a prpoS::GFP reporter gene in E. coli. *Microb. Cell Fact.* **8,** (2009).

150. Han, S., Delvigne, F., Brognaux, A., Charbon, G. E. & Sørensen, S. J. Design of growth-dependent biosensors based on destabilized GFP for the detection of physiological behavior of Escherichia coli in heterogeneous bioreactors. *Biotechnol. Prog.* **29,** 553–563 (2013).

151. Brognaux, A. *et al.* Direct and indirect use of GFP whole cell biosensors for the assessment of bioprocess performances: design of milliliter scale-down bioreactors. *Biotechnol. Prog.* **29,** 48–59 (2012).

152. Delvigne, F. *et al.* Green fluorescent protein (GFP) leakage from microbial biosensors provides useful information for the evaluation of the scale-down effect. *Biotechnol. J.* **6,** 968–978 (2011).

153. Junne, S., Klingner, A., Kabisch, J., Schweder, T. & Neubauer, P. A two-compartment bioreactor system made of commercial parts for bioprocess scale-down studies: impact of oscillations on Bacillus subtilis fed-batch cultivations. *Biotechnol. J.* **6,** 1009–1017 (2011).

154. Kar, T., Destain, J., Thonart, P. & Delvigne, F. Scale-down assessment of the sensitivity of Yarrowia lipolytica to oxygen transfer and foam management in bioreactors: investigation of the underlying physiological mechanisms. *J. Ind. Microbiol. Biotechnol.* **39,** 337–346 (2012).

155. Amanullah, a, McFarlane, C. M., Emery, a N. & Nienow, a W. Scale-down model to simulate spatial pH variations in large-scale bioreactors. *Biotechnol. Bioeng.* **73,** 390–399 (2001).

156. Sweere, A. P. J., Matla, Y. A., Zandvliet, J., Luyben, C. A. M. & Kossen, N. W. F. Applied Microbiology Biotechnology. *Appl. Microbiol. Biotechnol.* **28,** 109–115 (1988).

157. Larsson, G. & Enfors, S. Influence of oxygen starvation on the respiratory capacity of Penicillium chrysogenum. *Appl. Microbiol. Biotechnol.* **21,** 228–233 (1985).

158. Larsson, G. & Enfors, S.-O. Studies of insuffiecient mixing in bioreactors: Effects of limiting oxygen concentrations and short term oxygen starvation on Penicillium chrysogenum. *Bioprocess Eng.* **3,** 123–127 (1988).

159. Pedreira, C. E., Costa, E. S., Lecrevisse, Q., van Dongen, J. J. M. & Orfao, A. Overview of clinical flow cytometry data analysis: recent advances and future challenges. *Trends Biotechnol.* **31,** 415–425 (2013).

160. Koutinas, M., Kiparissides, A., Pistikopoulos, E. N. & Mantalaris, A. Bioprocess systems engineering : transferring traditional process engineering principles to industrial biotechnology. *Comput. Struct. biotechnoloy* **3,** (2012).

161. Gao, T., Wong, Y., Ng, C. & Ho, K. L-lactic acid production by Bacillus subtilis MUR1. *Bioresour. Technol.* **121,** 105–110 (2012).

162. Kim, S.-J., Seo, S.-O., Jin, Y.-S. & Seo, J.-H. Production of 2,3-butanediol by engineered Saccharomyces cerevisiae. *Bioresour. Technol.* **146,** 274–281 (2013).

163. Szybalski, W. & Bryson, V. Genetic studies on microbial cross resistance to toxic agents. I. Cross resistance of Escherichia coli to fifteen antibiotics. *J. Bacteriol.* **64,** 489–499 (1952).

164. Fazekas de St Groth, S. Automated production of monoclonal antibodies in a cytostat. *Methods Enzymol.* **121,** 360–375 (1986).

3. Chapter

Experimental design

3.1 Experimental Design/ Lab scale simulation of large-scale fermentation

In the scope of this thesis, different aspects of large scale fermentation conditions were experimentally simulated in lab-scale to investigate effects of environmental conditions on population heterogeneity using different process types (batch, fed-batch, continuous cultivation). Additionally a new setup for two compartment chemostat culture was developed (referred to as scale down reactor). Slightly different procedure protocols were applied depending on the particular study and they are shortly introduced in the following sections.

3.1.1 *S. cerevisiae* cultivations

S. cerevisiae cultivations were performed in batch mode (figure 1 setup I, used in chapters 4 and 5), as conventional chemostat followed by glucose perturbation (figure 1 setup II, used in chapters 4, 6 and 8) as well as continuous cultivation in a two compartment reactor (figure 1 setup III, used in chapter 8). For continuous cultivations in scale down reactors (two compartment chemostat), additionally a fed-batch phase was introduced to achieve a higher biomass before the switch to chemostat for cultivations with high glucose concentration in the feed. Common to all cultivations was the growth medium used, which in the case of *S. cerevisiae* was a defined mineral medium after Verduyn *et al*. (1992)[1] with glucose as carbon source. Furthermore, irrespectively of the process type the preculture procedure was the same for all performed experiments. The strain was first streaked out on a yeast nitrogen base plate and grown for at least two days. Thereafter, a single colony was used to inoculate a shake flask preculture which was grown until mid-exponential phase and subsequently used to inoculate the bioreactor (figure 1).

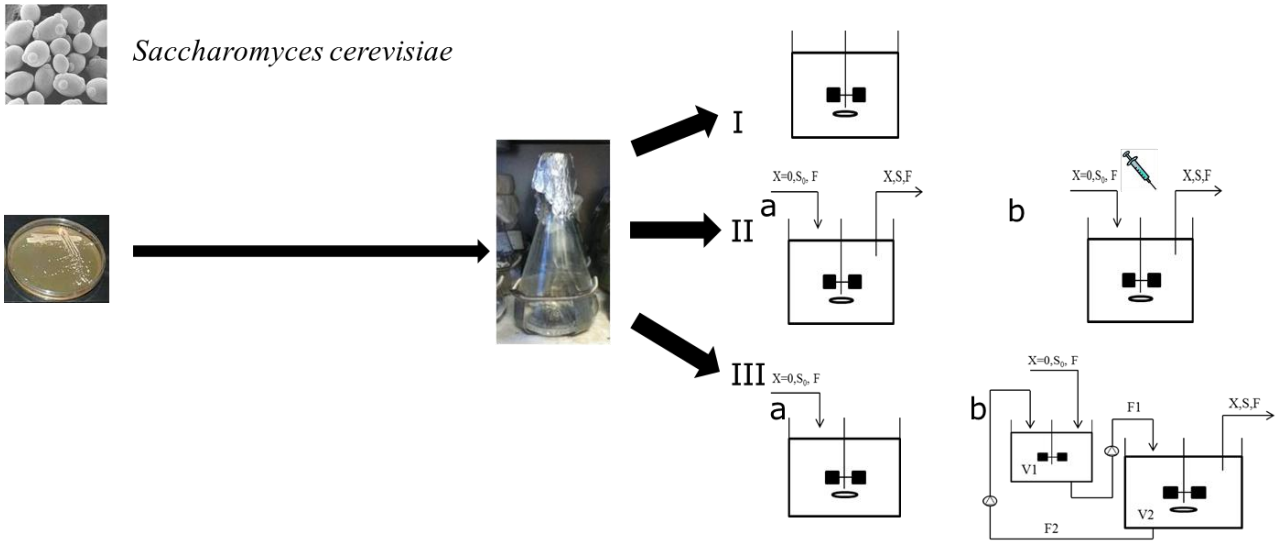

Figure 1 - Experimental setup summary: Different experimental setups used for *S. cerevisiae* cultivations.

For *S. cerevisiae* experiments mainly the growth reporter strain FE440[2] was used, which was first characterized in stirred tank batch cultivations (figure 1 setup I, used in chapter 4) under the growth conditions which were defined as standard conditions (pH 5; aeration: 1 v/vm; stirring: 600 rpm; 5g/L glucose as carbon source) in the frame of this thesis. If not otherwise noted, cultivations have been performed using standard conditions (see table 1). Later on, to evaluate the influence of different parameters on population heterogeneity, batch experiments were performed in stirred tank reactors under different conditions (see table 1, figure 1 setup I, used in chapter 5).

Furthermore, continuous cultivations (figure 1, setup II) evaluating steady state at different dilution rates were executed. In this way the dependency of the GFP fluorescence expression on cell growth of the reporter strain FE440 could be investigated (chapter 4 and 6). Thereafter the steady state cultures were perturbed with glucose (chapter 6) to simulate the occurrence of a sudden rise in carbon concentration which the cells might experience in large scale fed-batch and continuous cultivation due to non-ideal mixing, especially close to the feed point[3].

For the simulation of static zones and the further investigation of substrate gradients a new type of scale down reactor setup for two-compartment continuous cultivation consisting of two interconnected stirred tank reactors (figure 1 setup III) was developed in the course of the thesis. For a current status on scale down reactor studies, chapter 2 should be consulted. Hereby, the feeding zone of the continuous process was represented by a 0.5 L reactor with low oxygen and

high glucose concentration whereas the rest of the reactor with high oxygen and low glucose concentration was represented by a 5 L reactor (working volume: 3 L). Both reactors were connected to each other via a recirculation loop. The experiments in the system were run with three different dilution rates applying different feed concentrations and recirculation between the two reactors following a factorial design plan (for details, see chapter 8). Besides the growth reporter strain FE440, also the ethanol reporter strain Sc-PCK1-B was used in some of the experiments (chapter 8). Because the feed concentration in continuous mode was higher than for the standard conditions used during the batch, a fed-batch phase to achieve an increase in biomass was introduced applying a 300 g/L glucose feed to avoid later washout of the biomass or a delay in reaching steady state. As a comparison, conventional chemostats were performed under the same conditions.

3.1.2 *E. coli* cultivation

Cultivations with *E. coli* were either performed in batch (figure 2 setup I, chapter 7) or continuous mode (figure 2 setup II, chapter 6). Similar to *S. cerevisiae* cultivations a defined mineral growth medium was applied for all performed experiments[4]. However both glucose (chapter 6 and 7) and acetate (chapter 7) were used as carbon source. Standard conditions were defined as pH 5, aeration: 1 v/vm, stirring: 1000 rpm and 5 g/L glucose as carbon source.

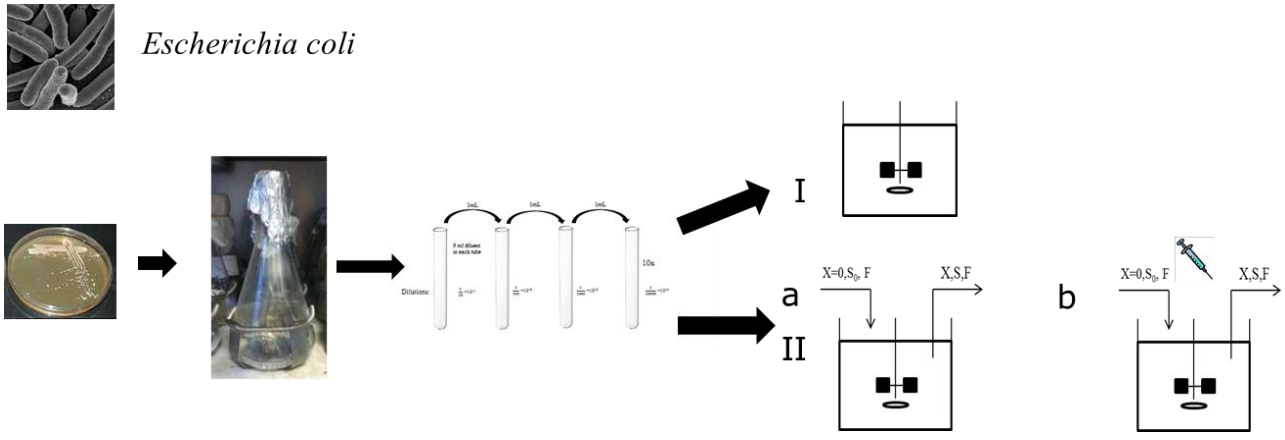

Figure 2 - Experimental setup summary: Different experimental setups used for *E. coli* cultivations

Also the preculture procedure was common to all *E. coli* experiments. The strain was streaked out on a Luria Bertani (LB) plate, incubated for at least two days and then inoculated for a two-step preculture procedure. First, an overnight culture in LB medium was prepared, which in the second

step was used to inoculate a dilution series with 10-fold steps. Subsequently, the optical density from the dilution series grown overnight was measured and the dilution with an optical density between 0.4 and 0.6 was used to inoculate the bioreactor.

To compare the influence of different carbon sources on single cell physiology and heterogeneity in metabolic activity, respiration and viability batch experiments with acetate respectively glucose were performed under standard conditions (figure 2 setup I, chapter 7). For both types of batch experiments the rrnB reporter strain was used.

Furthermore, continuous cultivations (figure 2 setup II) under standard conditions evaluating steady state followed by glucose perturbation at three different dilution rates were performed using the *fis* promoter reporter strain (for details, see chapter 6). This study was conducted in parallel with the corresponding *S. cerevisiae* investigation and steady state experiments and also served the investigation of substrate gradients in large scale fermentation.

Table 1 - Overview of cultivation procedures: used in the different experimental chapters of the thesis including cultivation mode, carbon source(s), cultivation conditions, reporter strain, stains and type of sampling. Abbreviations: OD: optical density, DW: dry weight, HPLC: high performance liquid chromatography, FC: flow cytometry. * Standard conditions for *S. cerevisiae* experiments were: aerobic; pH 5; aeration: 1 v/vm; stirring: 600 rpm; 5g/L glucose as carbon source. For *E. coli*: aerobic; pH 7; aeration: 1 v/vm; stirring: 1000 rpm; 5g/L glucose as carbon source

	Chapter 4	**Chapter 5**	**Chapter 6**	**Chapter 7**	**Chapter 8**
Cultivation mode	Batch, Chemostat	Batch	Chemostat	Batch	Fed-batch, Chemostat/two-compartment Chemostat
Carbon source	Glucose	Glucose	Glucose	Glucose and acetate	Glucose
Cultivation conditions	Standard conditions*	Variation of carbon source, pH and aeration otherwise standard conditions*	Standard conditions*	Standard conditions* apart from carbon source	Factorial design for D, carbon source and recirculation, otherwise standard conditions*
Reporter strain	FE440	FE440	FE440 and RrnB	Fis	FE440 and PCK1
Stain	PI	-	-	PI, CTC, SYBR, RSG, $DiBAC_4(3)$	-
Sampling (OD, DW, HPLC, FC)	+	+	+	+	+
FC sample analysis	Fresh and frozen cells	Fresh and frozen cells	Fresh and frozen cells	Fresh cells	Frozen cells

3.1.3 Parameters analysed for the study of general physiology and single cell properties

As mentioned earlier, in my studies both traditional and advanced methods for monitoring physiology and population behaviour in the model bioprocesses were applied. Sampling procedures were adjusted to the particular process type and the organism used. Common to all performed experiments was the on-line measurement of the off-gas composition including oxygen, carbon dioxide and ethanol via a mass spectrometer as well as on-line recording of process parameters including dissolved oxygen, pH, stirrer speed and temperature (figure 3). Moreover, the at-line sampling procedure included sampling for optical density (OD_{600}), dry weight (DW) and HPLC for all studies (figure 3 and table 1). Hereby samples for OD_{600} and DW were analysed directly, whereas samples for HPLC analysis were filtered and frozen in -20°C until analysis. HPLC samples of *E. coli* and *S. cerevisiae* cultivations revealed the concentrations of substrate (glucose or acetate) as well as of the major metabolites produced (acetate, pyruvate, lactate, glycerol, ethanol and formate).

Flow cytometry (FC) samples were either kept on ice or at room temperature (referred to as fresh cells) (chapter 4, 5, 6 and 7) until analysis or frozen in -80°C (referred to as frozen cells) with subsequent thawing on ice (Chapter 4, 5, 6 and 8) and storage in buffer with different pH (chapter 6). Hereby, the procedure differed depending on the organism and experimental setup (table 1 and particular chapters). Afterwards the flow cytometry samples were either analysed directly to measure Forward scatter, Side scatter as well as GFP fluorescence (all chapters) of the reporter or for two experimental studies also stained for different cell properties (table 1). The stains applied were 5-cyano-2,3-ditolyltetrazolium chloride (CTC), SYBR Green (SYBR), Propidium Iodide (PI), Bis-(1,3-dibutylbarbituric acid) trimethine oxonol ($DiBAC_4(3)$) and Redox Sensor Green (RSG) (see chapters 4 and 7 for further details).

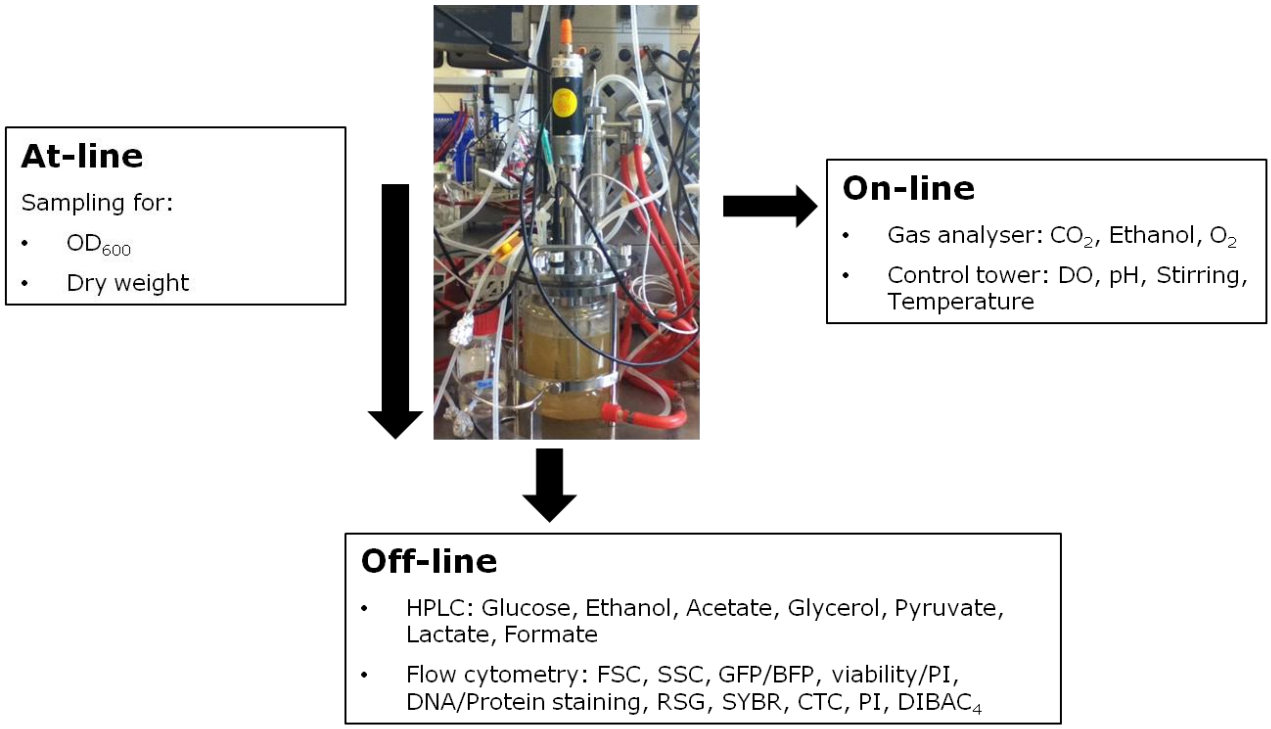

Figure 3 – Sampling from the bioreactor: At-line, On-line and Off-line collected data and samples from cultivation in a bioreactor. Depending on the setup not all types of data respectively samples were collected (see corresponding chapters).

Also the sampling frequency for at-line and off-line analysis was dependent on the particular process type. For batch cultivation sampling following the different growth phases (lag-, exponential growth on glucose and ethanol respectively acetate, diauxic shift and stationary phase) was done every 1-1,5h (chapter 4 and 7) or sampling intervals were timed to record at least three data points in each growth phase (chapter 5). During continuous cultivation samples were taken over at least three residence times to confirm steady state whereas during glucose perturbation frequent sampling with time intervals depending on the dilution rate was performed (details see chapter 4 and 6). In chapter 8 continuous cultivations (ordinary chemostats and in scale down reactors) were performed and the cultivations followed starting from the batch and fed-batch phase over the switch to chemostat (0. residence times) until 9 residence times. Sampling was done once every residence time for the chemostat phase and every 2 hours during the exponential growth in batch and fed-batch phase.

3.2 References

1. Verduyn, C., Postma, E., Scheffers, W. a & Van Dijken, J. P. Effect of benzoic acid on metabolic fluxes in yeasts: a continuous-culture study on the regulation of respiration and alcoholic fermentation. *Yeast* **8,** 501–517 (1992).

2. Carlquist, M. *et al.* Physiological heterogeneities in microbial populations and implications for physical stress tolerance. *Microb. Cell Fact.* **11,** (2012).

3. Enfors, S. O. *et al.* Physiological responses to mixing in large scale bioreactors. *J. Biotechnol.* **85,** 175–85 (2001).

4. Xu, B., Jahic, M. & Blomsten, G. Glucose over flow metabolism and mixed-acid fermentation in aerobic large-scale fed-batch processes with Escherichia coli. *Appl. Microbiol. Biotechnol.* **51,** 564–571 (1999).

4. Chapter

Physiological heterogeneities in microbial populations and implications for physical stress tolerance

Magnus Carlquist[3], Rita Lencastre Fernandes[2], Søren Helmark[5], Anna-Lena Heins[1], Luisa Lundin[4], Søren J Sørensen[4], Krist V Gernaey[2] and Anna Eliasson Lantz[1]*

[1] Department of Systems Biology, Technical University of Denmark, 2800 Kongens Lyngby, Denmark

[2] Department of Chemical Engineering, Technical University of Denmark, 2800 Kongens Lyngby, Denmark

[3] Department of Chemistry, Division of Applied Microbiology, Lund University, 221 00 Lund, Sweden

[4] Molecular Microbial Ecology Group, Department of Biology, University of Copenhagen, 1370K Copenhagen, Denmark

[5] Fermenco ApS, 2800 Kongens Lyngby, Denmark

Written as journal paper

Status: Published in microbial cell factories since 16. July 2012

MICROBIAL CELL FACTORIES

RESEARCH Open Access

Physiological heterogeneities in microbial populations and implications for physical stress tolerance

Magnus Carlquist[1,2], Rita Lencastre Fernandes[3], Søren Helmark[4], Anna-Lena Heins[1], Luisa Lundin[5], Søren J Sørensen[5], Krist V Gernaey[3] and Anna Eliasson Lantz[1*]

Abstract

Background: Traditionally average values of the whole population are considered when analysing microbial cell cultivations. However, a typical microbial population in a bioreactor is heterogeneous in most phenotypes measurable at a single-cell level. There are indications that such heterogeneity may be unfavourable on the one hand (reduces yields and productivities), but also beneficial on the other hand (facilitates quick adaptation to new conditions - i.e. increases the robustness of the fermentation process). Understanding and control of microbial population heterogeneity is thus of major importance for improving microbial cell factory processes.

Results: In this work, a dual reporter system was developed and applied to map growth and cell fitness heterogeneities within budding yeast populations during aerobic cultivation in well-mixed bioreactors. The reporter strain, which was based on the expression of green fluorescent protein (GFP) under the control of the ribosomal protein RPL22a promoter, made it possible to distinguish cell growth phases by the level of fluorescence intensity. Furthermore, by exploiting the strong correlation of intracellular GFP level and cell membrane integrity it was possible to distinguish subpopulations with high and low cell membrane robustness and hence ability to withstand freeze-thaw stress. A strong inverse correlation between growth and cell membrane robustness was observed, which further supports the hypothesis that cellular resources are limited and need to be distributed as a trade-off between two functions: growth and robustness. In addition, the trade-off was shown to vary within the population, and the occurrence of two distinct subpopulations shifting between these two antagonistic modes of cell operation could be distinguished.

Conclusions: The reporter strain enabled mapping of population heterogeneities in growth and cell membrane robustness towards freeze-thaw stress at different phases of cell cultivation. The described reporter system is a valuable tool for understanding the effect of environmental conditions on population heterogeneity of microbial cells and thereby to understand cell responses during industrial process-like conditions. It may be applied to identify more robust subpopulations, and for developing novel strategies for strain improvement and process design for more effective bioprocessing.

Keywords: Population heterogeneity, Cell fitness, Cell membrane robustness, Flow cytometry, Budding yeast, Reporter strain, Cell factory optimisation

* Correspondence: ael@bio.dtu.dk
[1]Center for Microbial Biotechnology, Department of Systems Biology, Technical University of Denmark, DK-2800 Kgs. Lyngby, Denmark
Full list of author information is available at the end of the article

Background

Traditionally, a microbial population has been considered homogeneous in optimisation studies of fermentation processes. Bioprocess measurements are typically obtained as an "average" of the whole cell population, thereby neglecting the effects and phenomena at the individual cell level. However, research has shown that a typical microbial population in a bioreactor is heterogeneous in most phenotypes measurable at a single-cell level [1-3]. There are indications that such heterogeneity may be unfavourable on the one hand (reduces yields and productivities), but also beneficial on the other hand (facilitates quick adaptation to new conditions - i.e. increases the robustness of the fermentation process) [4,5]. Therefore, understanding and control of microbial population heterogeneity is of major importance for improving biological production processes, and this has led to an increased interest from industry for methods to monitor population heterogeneity [6,7].

Phenotypic heterogeneity occurs even if the microenvironment surrounding the cells is constant, and it is driven by factors such as differences in cell cycle and cell ageing. Furthermore, stochastic gene transcription, translation and post-translational modifications have an impact [2]. In industrial scale fermentation processes, phenotypic heterogeneity is further amplified as a result of deficient mixing, which leads to zones with diverse environmental conditions [8]. The microbial cells, thus, experience sudden changes in the environmental conditions as they circulate from one zone to the other. These changes may pose different types of stress (e.g. oxidative, temperature, pH) on the cells and affect their metabolism and fitness [4,8,9]. The heterogeneous environment in large-scale fermenters may lead to repeated cycles of production/re-assimilation of overflow metabolites and repeated induction/relaxation of stress responses resulting in reduced biomass yield and productivity [4,10].

Stress tolerance has previously been shown to differ depending on the physiological state of the cell, i.e. which growth phase the cells were in prior to exposure to the stress factor. For example, yeast cells in respiratory ethanol growth phase have been found to be more tolerant to freeze-thaw stress than cells in respiro-fermentative glucose growth phase during aerobic batch cultivation [11]. This may be due to differences in cell membrane robustness, which is a key phenotypic trait that determines how well the cell can cope with physical stresses (such as heat, mechanical, osmotic or freezing) [12]. Many cellular stress responses are unique for the specific stress, however, there is also a global induction of cell responses leading to cross-tolerance towards non-related stresses; a phenomenon known as the environmental stress response (ESR) [13]. In a recent study by Zakrezewska *et al.* [14], tolerance to different stresses has been shown to be inversely correlated to cell growth rate, i.e. cells growing at a slow rate display a higher resistance to a number of stresses (e.g. heat, acid, oxidative) irrespectively of the cause for the reduced growth rate. The inverse correlation to growth rate was speculated to be related to the fact that the pool of cellular resources (energy, material) is limited and needs to be distributed as a trade-off between the two cellular functions growth and survival. In a population, the individuals differ in physiological state and are therefore equipped differently to cope with subsequent exposure to harsh conditions [15] that may occur in large-scale fermentation processes or in succeeding bioprocessing operations.

The aim of the present work was to map physiological state and cell robustness distributions within a microbial population, using budding yeast *Saccharomyces cerevisiae* as model organism. *S. cerevisiae* has an outstanding importance in industrial bioprocesses. It has been used in baking and alcoholic brewing for centuries, but is also used in a wide range of newer biotechnology production applications, such as production of heterologous proteins (e.g. insulin and different vaccines) and commodity chemicals. Most of the pharmaceutical proteins produced by microbial eukaryotic cells so far approved by the FDA or EMEA are almost exclusively based on production by *S. cerevisiae* [16].

To be able to shed light into whether population heterogeneity could be a consequence of the trade-off in cell economy for growth and robustness, a dual reporter system was developed that allowed for studying the prevalence of subpopulations which are differently prepared for changes in environmental conditions. The dual reporter system was based on:

(A) the expression of green fluorescent protein (GFP) [17,18] under control of the ribosomal protein promoter RPL22A, thereby making cellular GFP level proportional to growth;
(B) loss of GFP signal in cells with permeabilised plasma membranes after exposure to physical stress.

The dual nature of the reporter strain was validated by staining with propidium iodide (PI), which clearly demonstrated that cells with permeabilised plasma membrane lost GFP signal and were PI positive, while cells with remained level of GFP were PI negative.

As a case study, the relationship between physiological heterogeneity of a microbial population and the prerequisite of the population to tolerate subsequent freeze-thaw stress (as a model of physical stress) was characterised on a single cell level. It was found that subpopulations with different level of cell membrane robustness and tolerance towards physical stress co-existed in a population, and that the distribution was changing dynamically between different

phases of cultivation. The results have implications for biological processing where intact cell membranes are desirable, for example in pharmaceutical protein production. In addition, the presented methodology more generally provides an additional dimension in optimisation of microbial cell factories.

Results and discussion

Population dynamics during batch cultivation

In order to capture the dynamic growth responses in a population during the different growth phases of batch cultivation, a reporter strain based on the expression of GFP under the control of the promoter for the ribosomal protein gene RPL22a was used. The RPL22a promoter was chosen based on that ribosomal protein gene transcription has previously been found to be linearly correlated to growth rate, as determined by transcriptome analysis of cells grown in continuous cultivation mode under different limiting conditions [19-21]. Furthermore, ribosomal protein synthesis is believed to be regulated at the transcription level [22], which makes promoters for ribosomal proteins the ideal choice for construction of growth reporter strains.

To investigate the behaviour of the growth reporter strain during different growth phases, batch cultivations in well-controlled stirred tank reactors were performed and the physiology was monitored both on the whole population by standard methods and on a single-cell level by flow cytometry (see Materials and Methods). The reporter strain exhibited expected growth behaviour in defined mineral media, i.e. four distinct growth phases were observed. Growth first occurred on glucose, which was exhausted after 19 hours (Figure 1). Cells then underwent a diauxic shift and growth occurred on ethanol until stationary phase was reached approximately after 35–40 hours. The growth rate and biomass yield of the reporter strain did not differ from the control strain that did not express GFP, hence demonstrating that expression of GFP was not a burden to the cell (data not shown).

The mean GFP level defined as mean cellular fluorescence intensity measured by flow cytometry was initially quite stable around ca. 215 channel number units during growth on glucose (Figure 1). As the cells entered diauxic shift, the fluorescence decreased with approximately 30 channel number units in 2 hours. The turn-over of intracellular GFP is a result of the sum of gene transcription, gene translation as well as mRNA transcript degradation and protein degradation. Thus, the relatively rapid decrease in GFP level upon glucose depletion which coincides with a momentarily detainment of cell proliferation rate during the diauxic shift, demonstrated that the RPL22a promoter activity and GFP synthesis were rapidly down-regulated during this growth phase. The half-life of the GFP version used in the present study has previously been reported to be approximately 7 hours [23], which is coherent with the fluorescence decrease observed upon glucose depletion (approximately 15% decrease in 2 hours, Figure 1). Besides protein degradation, the decrease in GFP level may also to some extent be ascribed to dilution by cell division [24]. After the diauxic shift, the mean fluorescence continued to decrease, although at a lower rate than upon glucose depletion, which indicates that the RPL22a promoter activity and GFP synthesis were re-initiated to some extent during exponential growth on ethanol until the carbon source was depleted and stationary phase was reached. The mean fluorescence in stationary phase (ca. 70 channel number units) remained ca 10 times higher for the reporter strain compared to the auto fluorescence of the control strain.

The differences in GFP level at different growth phases confirmed that the growth reporter could be used to distinguish cells in different propagation modes, i.e. distinguish cells growing on glucose from cells growing on ethanol or in stationary phase. However, whether the lowered GFP level during growth on ethanol is a result of the lower growth rate and that the regulation of the RPL22a promoter is a part of the 'universal' growth rate response (GRR) as defined by Slavov and Botstein (2011) [25], or if the regulation of RPL22a is specific for the carbon source or other extrinsic factors is not clear. In the study performed by Slavov and Botstein (2011), RPL22a was found *not* to be a part of the 'universal' GRR, i.e. the transcription of RPL22a was strongly up-regulated at higher growth rates on glucose and slightly down-regulated at higher growth rates on ethanol [26]. It is therefore likely that the decreased level of GFP after the diauxic shift (Figure 1) is not strictly due to the lower growth rate per se, but also a response to the change in carbon source and the change from respiro-fermentative to respiratory metabolism. Another support for the interpretation that the regulation of the RPL22a promoter is not exclusively related to the growth rate is the observation that the GFP level decreased steadily during growth on ethanol despite the fact that the growth rate did not decrease until late exponential phase. On the other hand, the gradual decrease in GFP level during ethanol growth may additionally be due to dilution by cell division [24]. Albeit that other aspects might have influence on the regulation of the RPL22a promoter in addition to the growth rate, the reporter strain can be used to distinguish cells at different growth conditions (e.g. growth on glucose, growth on ethanol, no growth) which may be useful during optimisation of large-scale bioprocess conditions. Effects due to different stirring and feeding can be evaluated by following the response by the reporter system thereby used to guide

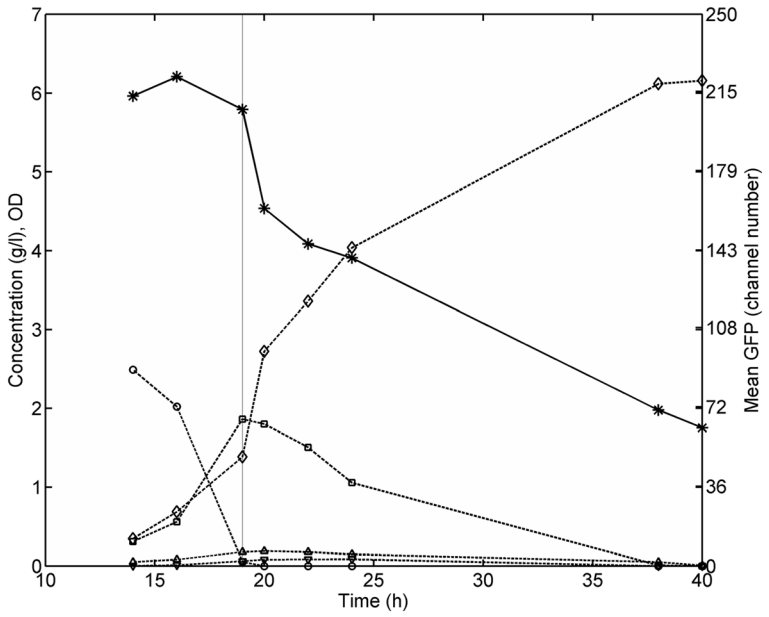

Figure 1 Mean fluorescence, biomass formation, substrate utilisation and product formation during aerobic batch cultivation of the *S. cerevisiae* reporter strain in defined mineral media. Symbols: Mean GFP fluorescence (*snowflakes*); OD_{600} (*open diamonds*); Glucose (*open circles*); Acetate (*open triangle pointing upwards*); Ethanol (*open squares*); Glycerol (*open triangles pointing downwards*). *The vertical line marks the time point glucose depletion was observed.*

process development. The reporter system may enable identification of cell growth physiology at single-cell level from different zones of a large-scale reactor, for example if cells are being trapped in ethanol (or alternatively glucose) rich zones for longer time periods.

To enumerate whether cell to cell variations in RPL22a promoter activity could be ascribed to more than differences in cell size, a percentile analysis similar to the method previously reported by Sumner *et al.* [27] was performed. For such an analysis, the events measured in the flow cytometry for each sample were first categorised in 10%-percentiles based on the forward scatter (FSC) signal; then for each percentile the mean FSC and GFP level were calculated and plotted against each other (Figure 2; see Additional file 1: Figure S1-2 for further information on how the percentile analysis was made). In Figure 2, the different coloured lines correspond to the sample time points, and each marker indicates the mean FSC and GFP for cells belonging to a given FSC percentile interval (e.g. the mean FSC and GFP of the cells presenting a FSC between the 10^{th} and 20^{th} percentile, for each time point, is indicated with an open circle). From the percentile analysis, a clear correlation between GFP level and FSC was observed for all time points, with larger cells in general having a higher GFP level (Figure 2). However, cell size was not the only determinant of GFP level as there was a discrepancy from the linearity, especially at higher FSC percentiles. The difference in GFP level that cannot be explained by cell size alone may be an artefact from the flow cytometry analysis (particularly at the 90-100% percentile), meaning that the deviation may simply be explained by the presence of cell aggregates, which are read as a single event thereby giving a false reading of the GFP level. On the other hand, it may also well indicate *non*-stochasticity and the presence of subpopulations with different regulation of RPL22a promoter activity. In relation to this, it could be speculated that larger cells with higher fluorescence propagate at a higher rate, at least during glucose assimilation, which would be in agreement with earlier observations that RPL22a transcription in glucose-limited chemostats correlated to growth rate [19,25]. Moreover, differences in cell cycle phase may contribute to the *non*-linear GFP level-cell size correlation (in general high FSC percentiles may contain a higher fraction of budding cells, which are larger than non-budding cells). In this work the budding index (BI), i.e. the fraction of budding cells in the population, was not measured, however it has been reported in the literature that for cultures in exponential growth on glucose the BI is approximately 70-80% [28,29]. This implies that budding cells would most likely be present also in the FSC percentile intervals as low as 20–30 or 30-40% and that influence by cell cycle therefore is not likely to have a large influence on the correlation discrepancies. The results reported here are however not conclusive, and additional analysis is needed to clearly state whether two cells of approximately the same FSC would present different GFP level due to the fact that one is budding and the other is not.

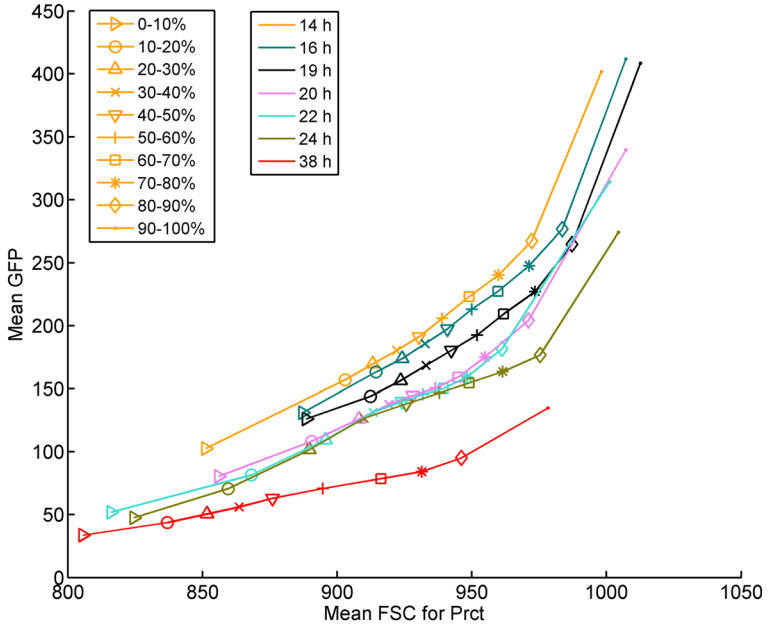

Figure 2 Mean GFP level as a function of mean FSC for each percentile during aerobic batch cultivation. For each time point there is a line (*in a different colour*) with markers for each percentile. Details of the percentile analysis can be found in the methods section and the Additional file 1: Figure S1-2.

Another circumstance highlighted from the percentile analysis was that the slope of the GFP level-cell size correlation differed depending on growth phase, with a lower slope during ethanol assimilation than before the diauxic shift (Figure 2). At the same time, a trend towards smaller cells throughout the cultivation could be observed. The decreased GFP level-cell size slope illustrates a decrease in growth heterogeneity, which may be a consequence of the fact that the whole population relocates resources to get prepared for survival rather than propagation. In general, the GFP level decreased to a relatively higher extent in larger cells than smaller cells, which may be interpreted as the larger cells underwent a larger physiological change (both growth and cell size decreased) as a response to the shift in environmental conditions.

Cell to cell variation in cell membrane robustness

As a case study for determining heterogeneities in cell membrane robustness and cellular capacity to withstand physical stress, the population was exposed to freeze-thaw stress and the degree of cell membrane permeabilisation was quantified by flow cytometry after cell staining with propidium iodide (PI). It has previously been shown that there is a connection between tolerance to freeze-thaw stress and other physical stresses (H_2O_2 oxidative stress; calcofluor white as cell wall-challenging reagent) [30]. Therefore, cells displaying high tolerance to freeze-thaw stress are also likely to withstand other seemingly unrelated types of specific stresses since the response to most stress factors relies at least partly on the ESR [13]. Thus, mapping of subpopulations with elevated capacity to freeze-thaw stress is of high relevance for reaching more robust bioprocesses where multiple factors pose pressure on cell membrane integrity.

Prior to the freeze-thaw stress, over 95% of the cells were PI negative demonstrating an undamaged cell membrane phenotype (Figure 3). However, after freeze-thaw stress a significant amount of cells had permeabilised cell membranes and were thus stained with PI. The degree of cell membrane permeabilisation varied within the population and could be divided in two categories: PI negative (PI fluorescence intensity <=10), and PI positive (PI fluorescence intensity >10). Cell membrane robustness was clearly linked to the specific growth phase the cells were in prior to applying freeze-thaw stress; in general cells growing on glucose were more sensitive than cells growing on ethanol, and cells in stationary phase. The fraction of PI negative cells increased from below 20% during the exponential glucose growth phase to around 80% in stationary phase and a corresponding decrease of the PI positive subpopulation in the same time interval was seen. This is in accordance with a previously published study made on the whole population level, where viability after freeze-thaw stress was measured on cells in different growth phases [11]. Furthermore, it is in line with the hypothesis that there is an inverse correlation between growth and robustness as has been

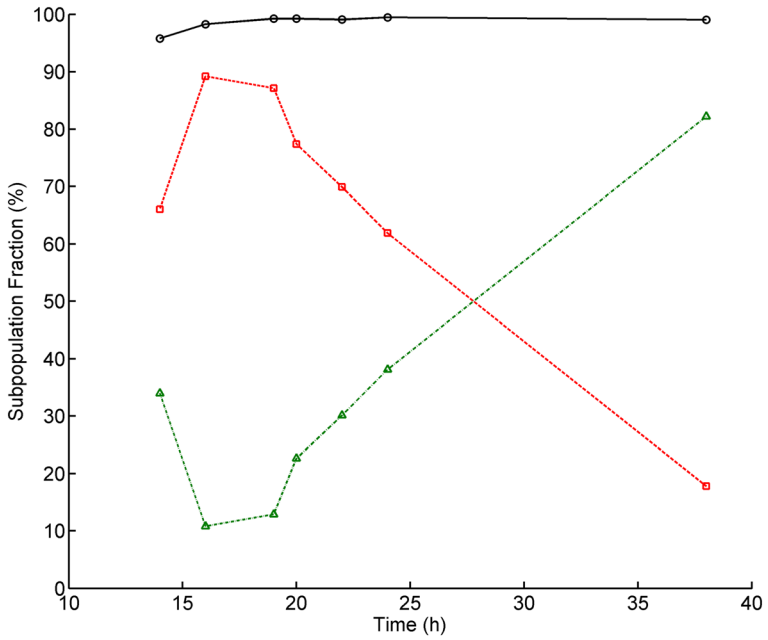

Figure 3 Distribution of PI-stained cells prior to and after freeze-thaw stress exposure plotted against point of harvest during aerobic batch cultivation. Symbols: PI negative cells prior to freeze-thaw stress (*circles*), PI negative cells (*triangles*) and PI positive cells (*squares*) after freeze-thaw stress.

previously suggested [25]. The trade-off between growth and robustness can be further substantiated by the inverse correlation between the RPL22a promoter activity prior to stress and freeze-thaw stress tolerance (Figure 4). However, the rapid increase in cell membrane robustness after the diauxic shift may also be a consequence of the ESR, which previously has been shown to be activated during diauxia and increase tolerance to multiple stresses [13].

Level of cell membrane robustness was also found to be correlated to cellular GFP level after exposure to freeze-thaw stress. Permeabilised cells significantly lost GFP fluorescence, while the PI negative subpopulation with intact cell membrane kept similar fluorescence intensity to untreated cells (Figure 5). The loss in GFP fluorescence in cells with permeabilised cell membrane may be due to leakage of intracellular GFP [31] and it may additionally be due to a decrease in intracellular pH which quenches the fluorescence signal [32]. Regardless of the specific cause, the measurable loss of GFP signal means that PI staining becomes redundant and that cell membrane robustness can be estimated by GFP level alone. In fact, this demonstrates that the reporter strain can be used as a dual reporter system for mapping heterogeneities in both growth (GFP level prior to stress exposure) and cell membrane robustness (distribution of subpopulations with high/low GFP level after stress exposure). The redundancy of PI was clear for the experimental set-up used in this study, and it may be useful for other investigations of cell membrane robustness on a single cell level; however, further experiments are needed to confirm that the dual nature of the reporter system also is applicable for other cases of physical stress.

Changes in cell membrane robustness by glucose perturbation

To study how heterogeneity in cell membrane robustness of the population is influenced by a dynamic environment often seen in larger scale cultivations, an experiment mimicking glucose gradients was performed. Cells were grown in continuous mode with $D = 0.2\ h^{-1}$ (which is below the dilution rate where overflow metabolism occurs [33,34]) and subjected to a glucose pulse. Cells were harvested at different time points during the pulse and subsequently exposed to freeze-thaw stress. As demonstrated above, the GFP signal could directly be used as a measure of cell membrane robustness and no additional staining was applied for these experiments. During steady state, the mean fluorescence was constant and the cells displayed two separate subpopulations with varying degree of cell membrane robustness (ca 80-85% of subpopulation P1, high mean fluorescence, intact cell membrane; ca 15-20% of subpopulation P2, low mean fluorescence, permeabilised cell membrane) (Figures 6, 7). The degree of cells with permeabilised cell membrane was thus significantly lower than for a population during batch growth on glucose, which is consistent with the inverse relationship between growth rate and cell robustness. Furthermore, the steady

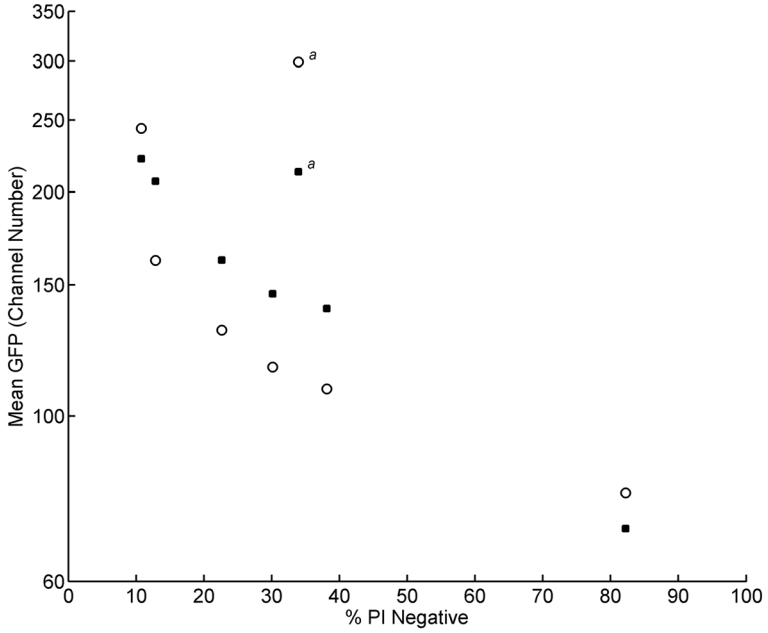

Figure 4 Inverse correlation between growth and cell membrane robustness. Mean GFP level of the whole population prior to freeze-thaw stress (*empty symbols*) as a function of the percentage of PI negative cells after freeze-thaw stress; and the mean GFP of the PI negative cells after freeze-thaw stress (*full symbols*) as a function of the percentage of PI negative cells after freeze-thaw stress. [a] These outlying data points are from the first sample of aerobic batch cultivation.

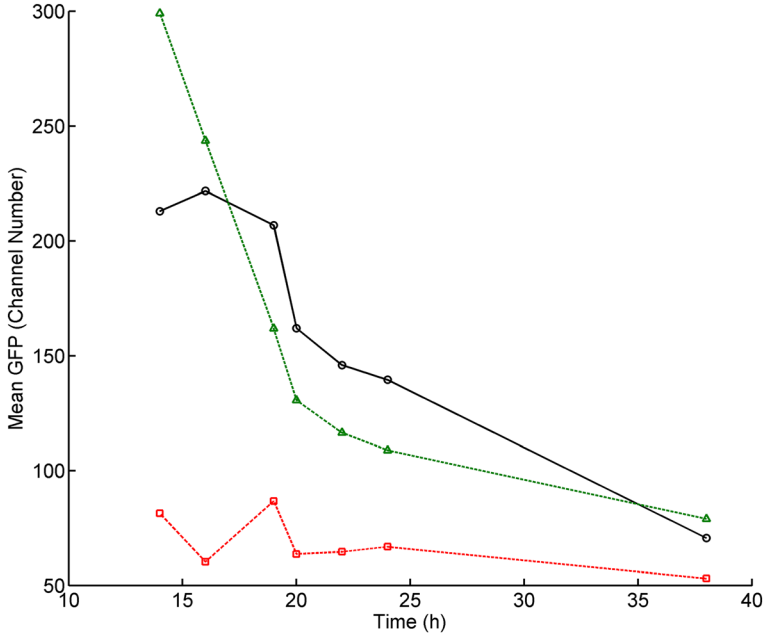

Figure 5 Effect of freeze-thaw stress on GFP signal. Mean GFP level of the entire population prior to freeze-thaw stress (*circles*) and mean GFP level of PI negative cells (*triangles*) and PI positive cells (*squares*) after freeze-thaw stress plotted against point of harvest during aerobic batch cultivation. The GFP signal was significantly decreased in cells that have been permeabilised by the stress exposure, hence making PI staining redundant to estimate number of cells with intact membranes.

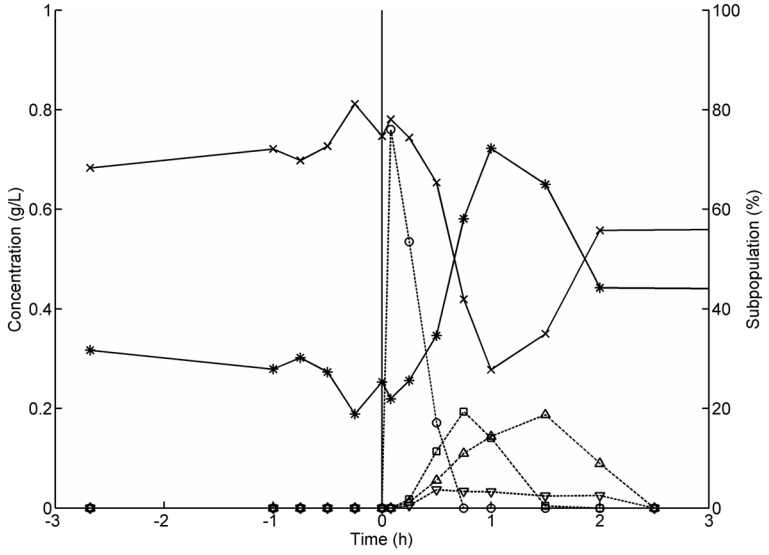

Figure 6 Dynamic responses of subpopulations and metabolites in glucose gradient experiments mimicking large-scale cultivation conditions. An aerobic glucose-limited chemostat was perturbed with a low concentration glucose pulse. Cells were sampled from the bioreactor and exposed to freeze-thaw stress and subsequently analysed with flow cytometry. Symbols: Subpopulation P1 (high GFP level, intact cell membranes) (*crosses*); Subpopulation P2 (low GFP level, permeabilised cell membranes) (*snowflakes*); Glucose (*open circles*); Acetate (*open diamonds*); Ethanol (*open squares*); Glycerol (*open triangles*).

distribution of subpopulations demonstrates that continuous cultivation, where the environment is constant and the average cell population grows with a constant growth rate, is the preferred experimental setup when comparing physiology of different strains, since dynamic changes in physiology otherwise seen in batch mode are minimised. Continuous cultivation may also be used to investigate how subpopulation distribution is affected by growth rate

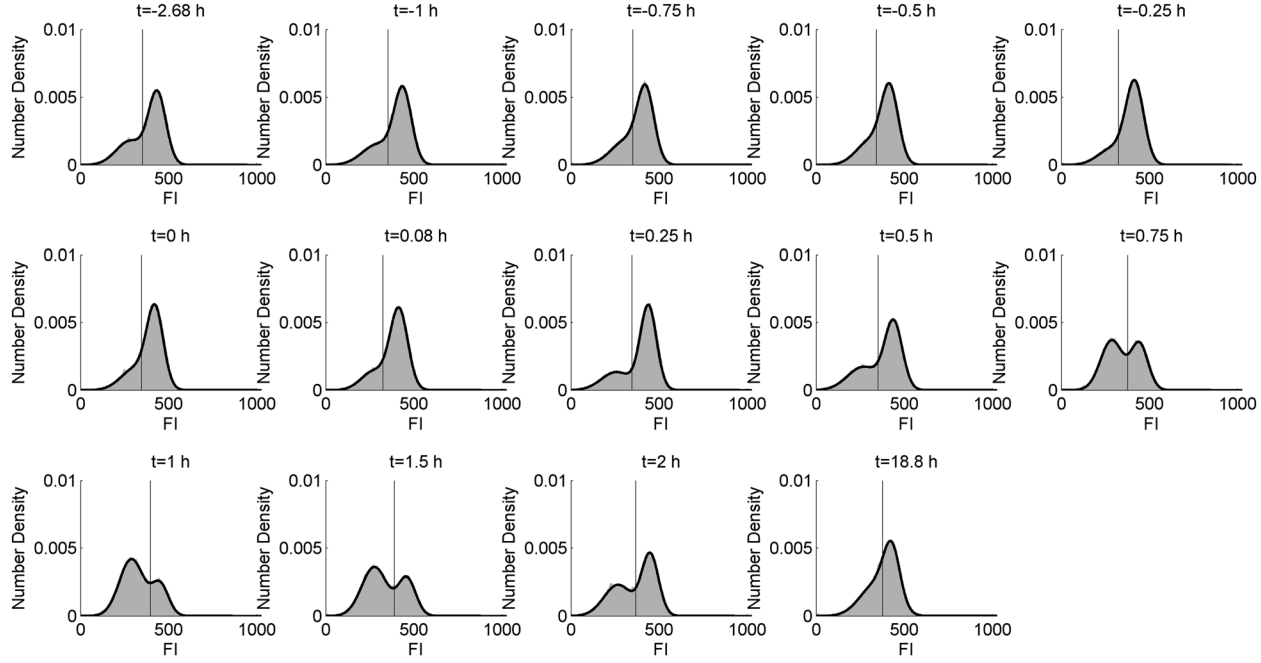

Figure 7 GFP histograms illustrating the distribution of subpopulations with different degree of cell membrane robustness following the glucose pulse. GFP histograms (*grey area*). FI = Fluorescence intensity. The black lines correspond to the fitted mixture of two Gaussian distributions. The vertical line corresponds to the subpopulation classification threshold.

as it allows for changing the growth rate while keeping other conditions constant and this knowledge can then be applied in development and design of a fed-batch process.

At time point zero, a pulse of 10 mL highly concentrated glucose solution was added and the glucose concentration inside the bioreactor instantly increased from ca 0 g/L to 0.8 g/L. Directly after the pulse, glucose was consumed and ethanol, acetate and glycerol were produced at different rates, as has been observed previously [35]. After glucose depletion, ethanol and acetate consumption occurred. During the pulse, the cells rapidly experienced a variation from a low to a high glucose concentration, which is similar to what a cell may experience in fed-batch cultivations as the cell is transported from the bottom of a bioreactor – a low glucose environment – to the top, which normally is close to the feeding point and hence has a high glucose concentration [36]. Approximately 15 minutes after glucose was added, a drop in the P1 subpopulation (intact cell membranes) and an increase in the P2 subpopulation (permeabilised cell membranes) fractions were observed (Figures 6, 7). The P2 subpopulation increased to 63% of the entire population 45 min after the glucose pulse was added. This demonstrates that a sudden change in glucose concentration has a profound effect on cell fitness distribution, since an increased number of cells with lower fluorescence and consequently lower cell membrane robustness emerged. The shift from steady state growth with $D = 0.2\ h^{-1}$ to batch mode and hence higher growth rate led to that a substantial part of cellular resources were redistributed to promote an increased growth rate, and consequently, the population became more sensitive to freeze-thaw stress. A difference in subpopulation distribution at steady states before and after the pulse was observed (68% P1 before compared to 59% P1 after the pulse), despite similar biomass and carbon dioxide profiles. The mechanism underlying the difference in subpopulation distribution at the different steady states before and after the pulse is not clear, however, it is probable that steady state after the pulse had not yet been reached on all levels despite constant biomass concentration, as has been observed previously [33].

Conclusions

A dual reporter system in budding yeast was constructed and used to measure population heterogeneities in growth and cell membrane integrity after physical stress, using freeze-thaw stress as a model. A clear inverse correlation between growth and cell membrane robustness was observed and the two antagonistic phenotypes co-existed in the population, demonstrating that the population was prepared for different types of variations in environmental conditions.

Cells in stationary phase displayed the highest cell membrane robustness and tolerance to freeze-thaw stress. For cells that were actively proliferating, the percentage of the subpopulation with low cell membrane robustness was lower in continuous cultivation mode as compared to a population growing in batch mode. However, the low membrane robustness phenotype could be easily induced for cells growing under glucose limiting conditions by a sudden increase of glucose at a low concentration. Distribution of the two subpopulations with high and low membrane robustness was modulated quickly as a response to the low-level fluctuation in glucose concentration. This suggests that spatial heterogeneities of glucose concentration in a fermentation tank may be detrimental for cell membrane robustness and physical stress tolerance. Furthermore this demonstrates the importance of rapid methods for monitoring effects of small sudden changes on microbial cultures at a single-cell level

To the best of our knowledge this is the first time that the existence of subpopulations with different tolerance towards physical stress and a reporter system to analyse distributions of cell membrane robustness in budding yeast have been reported. The developed system is useful for optimisation studies for more efficient production in microbial cell factories or for optimising physical state of a population at point of harvest, thus increasing resistance to adverse conditions during downstream processing where intact cells are desired, for example for the production of baker's yeast. Furthermore, a high fraction of cells with robust membrane phenotype may be important in secretory production of recombinant proteins where release of contaminating intracellular proteins is highly unwanted [37]. Contrary, in production processes having a cell-lysis step to liberate the product a high percentage of a less robust subpopulation may be preferred.

Methods

Strains

Escherichia coli strain MC1000 [*araD139* Δ(*ara-leu*)*7679 galU galK lac 174 rpsL thi-1*] [38] was used for subcloning before yeast transformation. Plasmids and *S. cerevisiae* strains are summarised in Table 1. All strains were stored in 15% glycerol stocks in liquid media at –80°C. *S. cerevisiae* strains were plated on YNB-agar plates (6.7 g/L yeast nitrogen base (Difco, USA), 20 g/L glucose and 20 g/L agar) and incubated for 2 days at 30°C before use.

Molecular biology techniques

PCR was performed using Phusion® DNA polymerase from Finnzymes (Espoo, Finland) and all other enzymes for cloning were purchased from Fermentas International Inc (Canada) and used following the recommendations of the manufacturer. Purification of DNA fragments from agarose gels was performed using the DNA Extraction Kit

Table 1 *S. cerevisiae* strains and plasmids used in this study

Strains	Relevant genotype	Ref.
CEN.PK 113-5D	Mat**a** SUC2 MAL2-8^{c} *ura3-52*	[39]
FE440	CEN.PK 113-5D with *ura3-52*:: URA3-P_{RPL22A}-yEGFP-T_{CYC1} chromosomal integration	This study
FE522	CEN.PK 113-5D with *ura3-52*::URA3 chromosomal integration	This study
Plasmids		
pBR322		[40,41]
pFe131	pBR322 with CEN1-ARS4-URA3	This study
pFe134	pFe131 with P_{RPL22A}-yEGFP-T_{CYC1}	This study

from Fermentas International Inc (Canada). Plasmid DNA was isolated from *E. coli* by using ZyppyTM Plasmid Miniprep Kit, Zymo Research (California, USA). Chromosomal DNA from *S. cerevisiae* was purified using YeaStarTM Genomic DNA Kit from Zymo Research (California, USA). Sequencing of DNA constructs was done by Macrogen (Seoul, Korea). Cells of *E. coli* were transformed by electroporation using a Bio-Rad Micropulser^{TM} and the recommended procedure of the manufacturer. *S. cerevisiae* cells were made competent, frozen in sorbitol buffer and transformed by electroporation according to the protocol of Suga *et al.* [42]. Southern blotting was done with the digoxigenin method by Roche (Indianapolis, IN, USA) using a digoxigenin labeled yEGFP PCR probe and hybridization at 65°C.

Construction of reporter strains

A 2200 bp EcoRI-PaeI fragment of CEN4-ARS1 was obtained by PCR with pCM188 as template [43] and a 1143 bp URA3 fragment flanked by *Pae*I and *Bam*HI/*Sal*I was obtained with pEMBLyex4 as template [44]. pBR322 [41] was cut with *Eco*RI and *Sal*I and the larger 4085 bp fragment was purified. The CEN4-ARS1 and URA3 fragments were cut with *Pae*I, ligated in vitro and cloned in the purified *Eco*RI-*Sal*I fragment of pBR322 resulting in plasmid pFe131. Then the RPL22A promoter was amplified as a 444 bp *Bam*HI-*Hind*III fragment with CEN.PK 113-5D chromosomal DNA as template, a 730 bp yEGFP3 fragment flanked by *Hind*III in the 5' end and *Xho*I-*Xba*I sites divided by two stop codons in the 3' end was amplified with pYGFP3 [17] as template and the CYC1 terminator was amplified as a 268 bp *Xba*I-*Sal*I fragment with pCM188 as template. The RPL22A promoter fragment was cut with *Hind*III, the yEGFP3 fragment was cut with *Hind*III and *Xba*I, the CYC1 terminator fragment was cut with *Xba*I and the three fragments were ligated in vitro and the combined 1442 bp fragment was purified from an agarose gel. This fragment was then cloned with *Bam*HI-SalI in pFe131 resulting in pFe134. For chromosomal integrations a 2585 bp URA3-RPL22A-yEGFP3-TCYC1 fragment was amplified with primers FP212 and FP169 with pFe134 as template and transformed to CEN.PK 113-5D resulting in strain FE440, whereas the control strain FE522 was obtained by transforming CEN.PK 113-5D with a 1143 bp URA3 fragment obtained by PCR with primers FP212 and FP213 and with pFe131 as template. Primers for chromosomal integrations are shown in Table 2. Correct chromosomal integration was verified by sequencing and Southern blotting.

Batch cultivations

Batch cultivations were performed in duplicate using Sartorius 1 L bioreactors (Sartorius Stedim Biotech, Germany) with a working volume of 1.0 L. The pH and DOT electrode (Mettler Toledo, OH, USA) were calibrated according to standard procedures provided by the manufacturer. Inocula of *S. cerevisiae* strains were prepared by transferring colonies from fresh YNB-plates into 500 mL Erlenmeyer flasks containing 100 mL defined mineral media [45] supplemented with 10 g/L glucose and incubating in a shake incubator set to 150 rpm and 30°C. Precultures were grown until reaching mid exponential phase (approximately 10 hours) and then used directly for inoculation (starting $OD_{600nm} = 0.001$) of the bioreactor containing defined mineral media [45] supplemented with 5 g/L glucose. Cultivation conditions were set to the

Table 2 Primers used for *S. cerevisiae* chromosomal integrations

Primer	Sequence 5'-3'
FP169, r	TATAAAGGCCATGAAGCTTTTTCTTTCCAATTT TTTTTTTTTCGTCATTA
	TAGAAATCATTACGACCGAGATTCCCGGGTAA TTGGCCGCAAATTAAAGC
FP212, f	GATTCGGTAATCTCCGAGCAGAAGGAAGAACGA AGGAAGGAGCAC
	CAGCTATGACCATGATTACG
FP213, r	TTTTTCGTCATTATAGAAATCATTACGACCGAG ATTCCCGGGTAA
	TTTTTGATCGGGTAATAACTG

The underlined sequence is complementary to the PCR template; the remaining part of the sequence is complementary to the ura3-52 chromosomal site in CEN.PK113-5D.

following; aeration 1 v/v/min; temperature 30°C; stirring 600 rpm and pH 5.0 (pH was controlled by automatic addition of 2 M KOH). Samples for OD_{600nm}, high performance liquid chromatography (HPLC) and flow cytometry analysis were withdrawn approximately every 1 hour. Samples for OD_{600} were analysed directly while samples for HPLC were kept at −20°C. Samples for flow cytometry were centrifuged for 1 minute at 3000 *g* and 4°C, and resuspended in saline solution. Cells were then kept in saline solution on ice for maximum 45 minutes until they were stained with PI (10 μg/mL) [46]. In brief, cell samples were stained by the addition of PI stock solution and subsequently incubated in darkness for 20 min at room temperature and analysed by flow cytometry. As positive control for cells with permeabilised plasma membranes was ethanol (70%) treated cells (100% of cells were PI positive; PI >100 ch. nr.).

Glucose gradient simulation

Continuous cultivations were performed using a Sartorius 2 L bioreactor (Sartorius Stedim Biotech, Germany) with a working volume of 1.5 L. Cultivation parameters were set as described above. After an initial batch phase, the continuous operation mode was started when glucose was nearly depleted and the carbon dioxide production started to peak. The dilution rate (D) was set to 0.2 h^{-1}, which was below the dilution rate where overflow metabolism occurs [33]. Steady state was observed after feeding ca 5 reactor volumes, and biomass and carbon dioxide were constant for at least 20 hours. When steady state was reached, 10 mL of concentrated glucose was swiftly added to the bioreactor by using a sterile syringe, which resulted in an increase in glucose concentration from ca 0 g/L to 0.8 g/L. Samples were taken before, during and after glucose addition and analysed by HPLC. Cell samples were exposed to freeze-thaw stress as described below and analysed by flow cytometry.

Freeze-thaw stress experiments

Samples were withdrawn from the bioreactor using a sterile syringe and then instantly mixed with an equal volume of 30% glycerol solution, resulting in a cell suspension with 15% glycerol. Cell suspensions were subjected to freezing by placement in a freezer set to −80°C. After complete freezing for at least 4 hours, cell samples were taken out of the freezer and placed in a water bath with controlled temperature at 37°C until samples were entirely thawed. After thawing, cells were centrifuged for 1 minute at 3000 *g* and 4°C, and resuspended in saline solution, and kept on ice for maximum 45 min until analysis. Cells were stained with PI (10 μg/mL) as described above and analysed by flow cytometry.

Analyses

Growth was monitored by measuring OD_{600nm} with a Shimadzu UV mini 1240 spectrophotometer (Shimidzu, Kyoto, Japan). The concentrations of glucose, acetate, ethanol, glycerol, pyruvate and succinate were determined by HPLC (Agilent 1100, Agilent Technologies, CA, USA) with a 300 mm × 7.8 mm Aminex HPX-87 H ion exchange column (Bio-Rad, Hercules, CA, USA), refractive index detector (RID Agilent 1200, Agilent Technologies, CA, USA) and UV detector (Agilent 1100, Agilent Technologies, CA, USA) set to 210 nm. The mobile phase was 5 mM H_2SO_4 (aq.), temperature 60°C and flow rate 0.6 mL/min. The composition of the outgoing gas from batch cultivations was monitored by a 1311 Fast response Triple-gas monitor (Innova Air tech technologies, Ballerup, Denmark).

A BD FACSAria III (Becton-Dickinson, NJ, USA) flow cytometer was used for single-cell analysis. Excitation wavelength for the laser used was 488 nm. Fluorescence emission levels were measured using a band pass filter at 530/30 nm (FITC) and 616/23 (PI). Light scattering and fluorescence levels were standardized using 2.5 μm fluorescent polystyrene beads. 10,000 events were recorded with a rate of approximately 1,000 events per second. Processing and analysis of flow cytometry raw data was performed by using MatLab ® R2009b (The MathWorks, Inc., Natick, MA, USA). The measurement files, exported as fcs files by the flow cytomer FACSAria III, were imported into MatLab®, using a "fcs data reader" routine (by L.Balkay, University of Debrecen, Hungary), available on MatLab® File Exchange website. The classification of cells into a high and a low fluorescence subpopulation was based on fitting a gaussian mixture of two components to the GFP fluorescence histograms (using a nonlinear least square curve fitting algorithm available in MatLab® R2009b). The relative weight of the two gaussian distributions in the mixture were used as prior probabilities in the definition of the classification rule that minimizes the expected cost of misclassification [47].

Additional file

Additional file 1: S1. Percentile analysis.

Competing interests

The authors declare that they have no competing interests.

Authors' contributions

MC and RLF participated in the design of the study, physiological experiments, flow cytometry analysis and drafted the manuscript. SH carried out the strain constructions. ALH participated in the physiological experiments and flow cytometry analysis. LL participated in the flow cytometry analysis. SJS participated in the design of the study. KVG participated in the design of the study and its coordination. AEL conceived the study, and participated in its design and coordination and helped to draft the manuscript. All authors read and approved the final manuscript.

Acknowledgements
ERA-IB (ERA-NET Industrial Biotechnology) is gratefully acknowledged for financial support in the frame of the project"Targeting population heterogeneity at microscale for robust fermentation processes" (project number EIB.08.031). The Danish Council for Strategic Research is gratefully acknowledged for financial support in the frame of the project "Towards robust fermentation processes by targeting population heterogeneity at microscale" (project number 09–065160).

Author details
[1]Center for Microbial Biotechnology, Department of Systems Biology, Technical University of Denmark, DK-2800 Kgs. Lyngby, Denmark. [2]Division of Applied Microbiology, Department of Chemistry, Lund University, SE-22100 Lund, Sweden. [3]Center for Process Engineering and Technology, Department of Chemical and Biochemical Engineering, Technical University of Denmark, DK-2800 Kgs. Lyngby, Denmark. [4]Fermenco ApS, Kgs. Lyngby, DK-2800 Kgs. Lyngby, Denmark. [5]Molecular Microbial Ecology Group, Department of Biology, University of Copenhagen, Sølvgade 83H, DK-1370K Copenhagen, Denmark.

Received: 22 March 2012 Accepted: 19 June 2012
Published: 16 July 2012

References

1. Lencastre Fernandes R, Nierychlo M, Lundin L, Pedersen AE, Puentes Tellez PE, Dutta A, Carlquist M, Bolic A, Schapper D, Brunetti AC, Helmark S, Heins AL, Jensen AD, Nopens I, Rottwitt K, Szita N, Van Elsas JD, Nielsen PH, Martinussen J, Sørensen SJ, Lantz AE, Gernaey KV: **Experimental methods and modeling techniques for description of cell population heterogeneity.** *Biotechnol Adv* 2011, **29:**575–599.
2. Avery SV: **Microbial cell individuality and the underlying sources of heterogeneity.** *Nat Rev Microbiol* 2006, **4:**577–587.
3. Muller S, Harms H, Bley T: **Origin and analysis of microbial population heterogeneity in bioprocesses.** *Curr Opin Biotechnol* 2010, **21:**100–113.
4. Enfors SO, Jahic M, Rozkov A, Xu B, Hecker M, Jurgen B, Kruger E, Schweder T, Hamer G, O'Beirne D, Noisommit-Rizzi N, Reuss M, Boone L, Hewitt C, McFarlane C, Nienow A, Kovacs T, Trägårdh C, Fuchs L, Revstedt J, Friberg PC, Hjertager B, Blomsten G, Skogman H, Hjort S, Hoeks F, Lin HY, Neubauer P, Van der Lans R, Luyben K, *et al*: **Physiological responses to mixing in large scale bioreactors.** *J Biotechnol* 2001, **85:**175–185.
5. Hewitt CJ, Nebe-Von Caron G, Axelsson B, McFarlane CM, Nienow AW: **Studies related to the scale-up of high-cell-density E. coli fed-batch fermentations using multiparameter flow cytometry: effect of a changing microenvironment with respect to glucose and dissolved oxygen concentration.** *Biotechnol Bioeng* 2000, **70:**381–390.
6. Díaz M, Herrero M, García LA, Quirós C: **Application of flow cytometry to industrial microbial bioprocesses.** *Biochem Eng J* 2010, **48:**385–407.
7. Mattanovich D, Borth N: **Applications of cell sorting in biotechnology.** *Microb Cell Fact* 2006, **5:**12.
8. Lara AR, Galindo E, Ramirez OT, Palomares LA: **Living with heterogeneities in bioreactors: understanding the effects of environmental gradients on cells.** *Mol Biotechnol* 2006, **34:**355–381.
9. Delvigne F, Boxus M, Ingels S, Thonart P: **Bioreactor mixing efficiency modulates the activity of a prpoS::GFP reporter gene in E. coli.** *Microb Cell Fact* 2009, **8:**15.
10. Bylund F, Collet E, Enfors SO, Larsson G: **Substrate gradient formation in the large-scale bioreactor lowers cell yield and increases by-product formation.** *Bioproc Eng* 1998, **18:**171–180.
11. Lewis JG, Learmonth RP, Watson K: **Role of growth phase and ethanol in freeze-thaw stress resistance of Saccharomyces cerevisiae.** *Appl Environ Microbiol* 1993, **59:**1065–1071.
12. Klis FM, Boorsma A, De Groot PW: **Cell wall construction in Saccharomyces cerevisiae.** *Yeast* 2006, **23:**185–202.
13. Gasch AP: **The environmental stress response: a common yeast response to environmental stresses**. In *Yeast Stress Responses*, Topics in Current Genetics, Volume 1. Edited by Hohmann S, Mager WH. Heidelberg: Springer; 2002:11–70. Hohmann S. (Series Editor).
14. Zakrzewska A, van Eikenhorst G, Burggraaff JE, Vis DJ, Hoefsloot H, Delneri D, Oliver SG, Brul S, Smits GJ: **Genome-wide analysis of yeast stress survival and tolerance acquisition to analyze the central trade-off between growth rate and cellular robustness.** *Mol Biol Cell* 2011, **22:**4435–4446.
15. Lidstrom ME, Konopka MC: **The role of physiological heterogeneity in microbial population behavior.** *Nat Chem Biol* 2010, **6:**705–712.
16. Ferrer-Miralles N, Domingo-Espin J, Corchero JL, Vazquez E, Villaverde A: **Microbial factories for recombinant pharmaceuticals.** *Microb Cell Fact* 2009, **8:**17.
17. Cormack BP, Bertram G, Egerton M, Gow NA, Falkow S, Brown AJ: **Yeast-enhanced green fluorescent protein (yEGFP)a reporter of gene expression in Candida albicans.** *Microbiology* 1997, **143:**303–311.
18. Day RN, Davidson MW: **The fluorescent protein palette: tools for cellular imaging.** *Chem Soc Rev* 2009, **38:**2887–2921.
19. Regenberg B, Grotkjaer T, Winther O, Fausboll A, Akesson M, Bro C, Hansen LK, Brunak S, Nielsen J: **Growth-rate regulated genes have profound impact on interpretation of transcriptome profiling in Saccharomyces cerevisiae.** *Genome Biol* 2006, **7:**R107.
20. Fazio A, Jewett MC, Daran-Lapujade P, Mustacchi R, Usaite R, Pronk JT, Workman CT, Nielsen J: **Transcription factor control of growth rate dependent genes in Saccharomyces cerevisiae: a three factor design.** *BMC Genomics* 2008, **9:**341.
21. Brauer MJ, Huttenhower C, Airoldi EM, Rosenstein R, Matese JC, Gresham D, Boer VM, Troyanskaya OG, Botstein D: **Coordination of growth rate, cell cycle, stress response, and metabolic activity in yeast.** *Mol Biol Cell* 2008, **19:**352–367.
22. Warner JR, Vilardell J, Sohn JH: **Economics of ribosome biosynthesis.** *Cold Spring Harb Symp Quant Biol* 2001, **66:**567–574.
23. Mateus C, Avery SV: **Destabilized green fluorescent protein for monitoring dynamic changes in yeast gene expression with flow cytometry.** *Yeast* 2000, **16:**1313–1323.
24. Roostalu J, Joers A, Luidalepp H, Kaldalu N, Tenson T: **Cell division in Escherichia coli cultures monitored at single cell resolution.** *BMC Microbiol* 2008, **8:**68.
25. Slavov N, Botstein D: **Coupling among growth rate response, metabolic cycle, and cell division cycle in yeast.** *Mol Biol Cell* 2011, **22:**1997–2009.
26. *Growth rate response*. [http://genomics-pubs.princeton.edu/grr/].
27. Sumner ER, Avery AM, Houghton JE, Robins RA, Avery SV: **Cell cycle- and age-dependent activation of Sod1p drives the formation of stress resistant cell subpopulations within clonal yeast cultures.** *Mol Microbiol* 2003, **50:**857–870.
28. Brauer MJ, Saldanha AJ, Dolinski K, Botstein D: **Homeostatic adjustment and metabolic remodeling in glucose-limited yeast cultures.** *Mol Biol Cell* 2005, **16:**2503–2517.
29. Cipollina C, Alberghina L, Porro D, Vai M: **SFP1 is involved in cell size modulation in respiro-fermentative growth conditions.** *Yeast* 2005, **22:**385–399.
30. Ando A, Nakamura T, Murata Y, Takagi H, Shima J: **Identification and classification of genes required for tolerance to freeze-thaw stress revealed by genome-wide screening of Saccharomyces cerevisiae deletion strains.** *FEMS Yeast Res* 2007, **7:**244–253.
31. Delvigne F, Brognaux A, Francis F, Twizere JC, Gorret N, Sorensen SJ, Thonart P: **Green fluorescent protein (GFP) leakage from microbial biosensors provides useful information for the evaluation of the scale-down effect.** *Biotechnol J* 2011, **6:**968–978.
32. Kneen M, Farinas J, Li Y, Verkman AS: **Green fluorescent protein as a noninvasive intracellular pH indicator.** *Biophys J* 1998, **74:**1591–1599.
33. Van Hoek P, Van Dijken JP, Pronk JT: **Effect of specific growth rate on fermentative capacity of baker's yeast.** *Appl Environ Microbiol* 1998, **64:**4226–4233.
34. Carlsen M, Jochumsen KV, Emborg C, Nielsen J: **Modeling the growth and proteinase A production in continuous cultures of recombinant Saccharomyces cerevisiae.** *Biotechnol Bioeng* 1997, **55:**447–454.
35. Flikweert MT, Kuyper M, van Maris AJ, Kotter P, van Dijken JP, Pronk JT: **Steady-state and transient-state analysis of growth and metabolite production in a Saccharomyces cerevisiae strain with reduced pyruvate-decarboxylase activity.** *Biotechnol Bioeng* 1999, **66:**42–50.
36. George S, Larsson G, Olsson K, Enfors SO: **Comparison of the baker's yeast process performance in laboratory and production scale.** *Bioproc Eng* 1998, **18:**135–142.
37. Porro D, Sauer M, Branduardi P, Mattanovich D: **Recombinant protein production in yeasts.** *Mol Biotechnol* 2005, **31:**245–259.
38. Casabadan MJaC SN: **Analysis of gene control signals by DNA fusion and cloning in *Escherichia coli*.** *J Mol Biol* 1980, **138:**179–207.

39. van Dijken JP, Bauer J, Brambilla L, Duboc P, Francois JM, Gancedo C, Giuseppin ML, Heijnen JJ, Hoare M, Lange HC, Madden EA, Niederberger P, Nielsen J, Parrou JL, Petit L, Porro D, Reuss M, Van Riel N, Rizzi M, Steensma HY, Verrips CT, Vindelov J, Pronk JT: **An interlaboratory comparison of physiological and genetic properties of four *Saccharomyces cerevisiae* strains.** *Enzyme Microb Technol* 2000, **26:**706–714.
40. Watson N: **A new revision of the sequence of plasmid pBR322.** *Gene* 1988, **70:**399–403.
41. Bolivar F, Rodriguez RL, Greene PJ, Betlach MC, Heyneker HL, Boyer HW, Crosa JH, Falkow S: **Construction and characterization of new cloning vehicles. II. A multipurpose cloning system.** *Gene* 1977, **2:**95–113.
42. Suga M, Isobe M, Hatakeyama T: **Cryopreservation of competent intact yeast cells for efficient electroporation.** *Yeast* 2000, **16:**889–896.
43. Gari E, Piedrafita L, Aldea M, Herrero E: **A set of vectors with a tetracycline-regulatable promoter system for modulated gene expression in Saccharomyces cerevisiae.** *Yeast* 1997, **13:**837–848.
44. Murray JA, Scarpa M, Rossi N, Cesareni G: **Antagonistic controls regulate copy number of the yeast 2 mu plasmid.** *EMBO J* 1987, **6:**4205–4212.
45. Verduyn C, Postma E, Scheffers WA, Van Dijken JP: **Effect of benzoic acid on metabolic fluxes in yeasts: a continuous-culture study on the regulation of respiration and alcoholic fermentation.** *Yeast* 1992, **8:**501–517.
46. Kacmar J, Zamamiri A, Carlson R, Abu-Absi NR, Srienc F: **Single-cell variability in growing Saccharomyces cerevisiae cell populations measured with automated flow cytometry.** *J Biotechnol* 2004, **109:**239–254.
47. Johnson RA, Richard DW: *Applied multivariate statistical analysis*. Upper Saddle River: Pearson International Edition; 2007.

doi:10.1186/1475-2859-11-94
Cite this article as: Carlquist *et al.*: Physiological heterogeneities in microbial populations and implications for physical stress tolerance. *Microbial Cell Factories* 2012 **11**:94.

5. Chapter

Combined approach of principal component and interval analysis to evaluate population heterogeneity in batch fermentation experiments of *S. cerevisiae*

Heins A.L. [1], Lencastre Fernandes R. [2], Carlquist M.[4], Lundin, L.[3], Sørensen S. [3], Gernaey V.K. [2], Eliasson Lantz A.[1]

[1] Department of Systems Biology, Technical University of Denmark, 2800 Kongens Lyngby, Denmark

[2] Department of Chemical and Biochemical Engineering, Technical University of Denmark, 2800 Kongens Lyngby, Denmark

[3] Department of Biology, Section of Microbiology, University of Copenhagen, 2100 DK, Copenhagen, Denmark

[4] Department of Chemistry, Division of Applied Microbiology, Lund University, 221 00 Lund, Sweden

Written as method paper

Status: Manuscript in preparation

Abstract

Process development and optimization often involves the evaluation of an industrial biotechnological production process in conditions which are different from the standard conditions employed for production to explore the applicability range of the production host/system. Here an approach is presented to evaluate the influence of different conditions on single cell growth and cell robustness distributions using a dual reporter strain of *S. cerevisiae* in batch cultivations. Using the abilities of the strain - possessing a built-in growth reporter expressing a GFP fluorescent protein under the control of a ribosomal promoter - growth heterogeneities were investigated on single cell level using flow cytometry. By the application of freeze-thaw stress additionally cell membrane robustness could be studied under the different batch conditions. To evaluate the large amount of data resulting from 12 different batch experiments following the different growth phases, principal component analysis (PCA) was applied after the development of a method for the objective description of single cell fluorescence distributions. In general it was found that the glucose concentration seems to have a major influence on general physiology as well as on single cell property distribution, whereas a change in oxygen level and pH only seem to exhibit minor influences. Cells from aerobic low gravity cultivations exhibiting two batch growth phase were found to be mostly robust and responding to changing growth conditions. In contrast to that anaerobic low gravity cultivations as well as aerobic and anaerobic high gravity cultivations only exhibited one growth phase and showed generally lower robustness especially towards the end of the batch cultivation and lower growth rates could be found.

Keywords: batch cultivation, reporter strain, GFP fluorescence, cell robustness, flow cytometry, principal component analysis, interval analysis

5.1 Introduction

To achieve an efficient industrial biotechnological production process which is robust and high-yielding, it is essential to optimize both the cell factory and the cultivation conditions. This often also includes the performance of experiments under conditions that are different from the standard conditions to explore the scope of application of the process. Hereby generally all process parameter that are normally controlled at a specific set point can be varied, like pH, substrate concentration, substrate feed rate, oxygen level, temperature, aeration and gas flow rate. For instance recently the influence of environmental parameter on the production of exopolysaccharide in *Lactobacillus reuteri*[1] was studied using a factorial

design experiment. Similarly, the general evaluation of the influence of different environmental conditions on various cell properties like transcriptome, growth or intracellular pH was the subject of many studies [2–4].

A change in environmental conditions can have influence on the growth, cell metabolism, general physiology and stress level of the cells[5–7] used in the production process which in turn might influence the yields as outcome of the process in either a negative or a positive way. Additionally the nowadays well accepted phenomenon of population heterogeneity, which is known to especially influence large scale cultivation processes, might show a different impact on the production. Generally, population heterogeneity is known to decrease yields, rise by-product formation, induce stress responses but also has positive effects like facilitating the adaption of a cell population to new environmental conditions[8–11]. The heterogeneity of cell populations arises due to non-ideal mixing in large scale as well as in bench scale bioreactors which causes gradients of e.g. substrate, pH and oxygen. Thus microbial cells that circulate throughout the reactor experience rapid changes in environmental conditions which might pose stress on them and affect their metabolism leading to formation of single cell distributions of cell characteristics and activities (e.g. respiration, product efficiency)[12]. Consequently the population of cells used for the production of e.g. biomass, recombinant proteins or bulk products rather exhibits individual properties than homogenous behavior which cannot be described by averaged values[13].

Therefore tools like flow cytometry hat enable the measurement of distributions of single cell properties are increasingly employed[14,15] to investigate broth samples taken during bioprocesses at-line or online in automated setups with a flow chamber connected to the bioreactor and the flow cytometer[16,17]. Flow cytometry is a high throughput technique that allows the measurement of different properties of up to 10000 cells per second including cell size (FSC), side scatter which can be correlated to cell morphology and fluorescence originating from stains respectively from the cells themselves (reporter strains)[15,18]. As a consequence big amounts of data can be collected which are nowadays mostly evaluated subjectively using mean or coefficient of variance (CV) values which fail to describe the whole picture of the single cell distribution (e.g. of shifts and subpopulations)[14]. Furthermore, flow cytometry results are typically plotted as biplots of mostly fluorescence and FSC respectively single parameter histograms showing relative cell count in every fluorescence channel, which shows the whole population but the plots can only be subjectively compared.

In this study a method combining interval analysis of fluorescence histogram plots, - a technique which has been employed earlier for the description of biplots[7]- with principal component analysis is presented which allows objective data description. Principal component analysis transforms the original variables, based on singular value decomposition, into a new set of uncorrelated factors (principal components) that account for the maximum proportion of the variance in the data, with each component being a linear combination of the original observed variables. The first principal component is the linear combination of variables that accounts for the largest proportion of variance in the data, the following one accounts for the second highest and so forth[19].

Single cell differences were evaluated using flow cytometry employing a dual *S. cerevisiae* reporter strain expressing a chromosomal integrated stable GFP[7]. The GFP fluorescence is controlled by the ribosomal promoter RPL22a whose expression was found to be growth correlated[20]. Furthermore the applicability of the strain was successfully shown by monitoring changes in growth during the different phases in batch experiments[7]. Additionally, the strain can also be used as indicator for membrane robustness after applying freeze-thaw stress to broth samples, due to a strong correlation between membrane intactness and the intracellular GFP fluorescence level[7].

This study aims at developing a method to objectively describe the large amount of data resulting from flow cytometry analysis which can be used to understand the correlation between the population structure and the environmental variables (glucose and oxygen availability) in the dynamic environment of a batch cultivation. Hereby GFP fluorescence correlated to growth as well as cell membrane robustness using the dual *S. cerevisiae* reporter strain FE440 was evaluated using flow cytometry. The study focuses on the analysis of a data set originating from a total of 12 *S. cerevisiae* batch cultivations with variable pH, glucose and oxygen concentrations.

5.2 Materials and Methods

5.2.1 Strain

The strain FE440, used in this study, is a dual reporter strain (for growth and cell membrane robustness) based on the *S. cerevisiae* wildtype strain CEN.PK 113-5D[7]. The strain was stored in a 15% glycerol stock in liquid media at −80 °C.

5.2.2 Cultivation conditions

Precultures. A single colony of *S. cerevisiae* FE440 grown on a YNB plate (0.73 % Yeast nitrogen base w/o amino acids and $(NH_4)_2SO_4$ (Difco, USA), 20 g/L D-Glucose, 20 g/L Bacto Agar adjusted to pH 5.8 with NaOH) was used to inoculate a 0.5 L baffled shake flask with 100 ml of defined mineral medium[21]. Precultures were grown in an orbital shaken incubator set to 150 rpm and 30°C until reaching mid exponential phase (approximately 10 h) and directly used to inoculate the bioreactor.

Batch cultivations. 12 Batch cultivations with varying pH, oxygen level and glucose concentration have been performed (for list of conditions, see table 1) using 1 L bioreactors (Sartorius, B. Braun Biotech International, GmbH, Melsungen, Germany) with a working volume of 1 L. The pH and DOT electrodes (Mettler Toledo, OH, USA) were calibrated according to standard procedures provided by the manufacturer using a two point calibration (pH 4 and 7, gassing with Oxygen (100%) and with Nitrogen (0%)). The growth medium used was either a defined mineral medium containing 5 g/L $(NH_4)_2SO_4$, 3 g/L KH_2PO_4, 0.1 g/L $MgSO_4*H_2O$, 1 ml/L trace metal solution, 1 ml/L vitamin solution, 50 µL Sigma 204 Antifoam and 5 or 25 g/L glucose[21] or a modified medium with 10 g/L $(NH_4)_2SO_4$, 3 g/L KH_2PO_4, 0.3 g/L $MgSO_4*H_2O$, 2 ml/L trace metal solution, 2 ml/L vitamin solution, 50 µL Sigma 204 Antifoam and 300 g/L glucose[22]. The OD_{600} for inoculation was 0.001 when using 5 g/L and 25 g/L glucose and 0.01 when using 300 g/L glucose. The pH was controlled to 4 or 5 using 2M NaOH. Temperature, aeration and stirring were kept constant at 30 °C, 1v/vm and 600 rpm. Cultivations were either performed under aerobic conditions using oxygen or under anaerobic conditions using nitrogen for sparging.

Table 1 – conditions of performed batch fermentation: Varying pH (4 and 5), glucose concentration (5g/L, 25g/L and 300g/L glucose) and aeration (100% oxygen and 0% oxygen). * indicates that duplicates exist for this condition. Moreover a cross marks (+) cultivations that have been analysed both on fresh and frozen cells.

Order of run		pH	Glucose [g/L]	Oxygen level [%]
7		4	5	100
5	*	4	5	0
8		4	25	100
4		4	25	0
2	*	4	300	100
1	*	4	300	0
9	*+	5	5	100
11	*+	5	5	0
10	*+	5	25	100
6	*+	5	25	0
3	+	5	300	100
12	+	5	300	0

Samples for OD_{600}, high performance liquid chromatography (HPLC), dry weight (DW) and flow cytometry analysis were withdrawn every second hour following growth on glucose, and when observed also for growth on ethanol as well as in the stationary phase, and every hour during the diauxic shift. Samples for OD_{600} and DW were analysed directly, whereas filtered samples for HPLC were kept at -20 °C. Samples for flow cytometry were mixed with glycerol to a final concentration of 15% and stored in a -80 °C freezer. Additionally, flow cytometry analysis was also performed on fresh samples for selected conditions (see crosses in table 1), where the fermentation broth was mixed with 15% glycerol and samples kept on ice until analysis (maximum one hour).

5.2.3 Sample analysis

OD, DW and HPLC. Growth was monitored by measuring OD_{600} with a Shimadzu UV mini 1240 spectrophotometer (Shimidzu, Kyoto, Japan). For dry weight measurements 5 ml of the filtered and washed cultivation broth were dried for 20 min at 150 W in a microwave, cooled down in a desiccator and afterwards weighted on an analytical balance[23]. The concentration of glucose, acetate, ethanol, glycerol and pyruvate was determined by HPLC (Agilent 1100, Agilent Technologies, CA, USA) with a 300 mm × 7.8 mm Aminex HPX-87H ion exchange column (Bio-Rad, Hercules, CA, USA), refractive index detector (RID Agilent 1200, Agilent Technologies, CA, USA) and UV detector (Agilent 1100, Agilent Technologies, CA, USA)

set to 210 nm. The mobile phase was 5 mM H_2SO_4 (aq.), with a temperature of 60°C and a flow rate of 0.6 mL/min. The composition of the off-gas from batch cultivations was monitored by a MS gas analyzer with multiplexer (Thermo Prima SigmaV).

Flow cytometry. A FACSAria™ III (Becton-Dickinson, NJ, USA) flow cytometer was used for single-cell analysis. Excitation wavelength for the laser was set to 488 nm. Two scattering channels (FSC and SSC) and two fluorescent detection channels were used in the analysis. Fluorescence emission levels were measured using a band pass filter at 530±30 nm. Light scattering and fluorescence levels were standardised using 2.5 µm fluorescent polystyrene beads. Samples for flow cytometry were centrifuged for 1 min at 3000 g and 4 °C, resuspended in 0.9 % saline solution and directly analysed. 10,000 events were recorded. CS&T beads (Cytometer Setup and Tracking beads) (Becton Dickinson, USA) were used for the automated QA/QC of the machine performance.

5.2.4 Data treatment and statistics

Processing and analysis of the flow cytometry data was done using MatLab® R2013a (The MathWorks, Inc., Natick, MA, USA).

The raw data files, extracted as fcs files by the flow cytometer FACSvantage SE software, were imported into MatLab®, using the fcs data reader function (by L.Balkay, University of Debrecen, Hungary, available on MatLab® File Exchange website). The HPLC data was collected in an excel file and imported into MatLab. The data from the fcs files was extracted and saved into mat files including the recorded GFP fluorescence for all performed experiments. For the evaluation of GFP fluorescence data histogram plots for the GFP fluorescence samples were generated using the hist function and followed by plotting the relative cell count per channelnumber (1024 recording channels). In the following the histogram plot area was divided into five different parts and the percentage of GFP fluorescent cells in each of the parts calculated. The percentage values have been collected in a matrix for all conditions respectively for pH 5 for fresh and frozen analysed cells. Afterwards principal component analysis (PCA) was performed to get an overview of the data and to detect a possible underlying pattern. Prior to this autoscaling and centering of the data was performed. Results have been plotted as score and loading plots for the first two principal components and the fluorescence patterns have been evaluated and the main clusters were manually gated.

5.3 Results

12 cultivations with the *S. cerevisiae* reporter strain FE440 have been carried out under different conditions, varying pH (4 and 5) , glucose concentration (5g/L, 25g/L and 300g/L) and aeration (100% O_2 or 100% N_2). First the general physiology under different conditions will be shortly discussed followed by the presentation and analysis of GFP fluorescence profiles throughout the batch experiments. Thereby the in this study presented method combining principal component analysis and interval analysis will be shortly explained. Afterwards its application will be demonstrated comparing the GFP fluorescence for pH 5 for cells kept on ice (referred to as fresh cells) and also after exposure to freeze-thaw stress (referred to as frozen cells). The latter can provide information about cell membrane robustness, as earlier a strong inverse correlation between growth and cell membrane robustness was observed[7]. Afterwards GFP fluorescence for frozen cells for all performed batch cultivations will be compared.

5.3.1 Physiological characteristics of the batch cultivations

The *S. cerevisiae* reporter strain FE440 was cultivated in batch experiments applying 12 different conditions (see table 1). Figure 1 shows four representative profiles: two profiles for pH 5 and 5 g/L of glucose both under aerobic and anaerobic conditions, and one profile at pH 5 and 25 g/L of glucose under aerobic conditions (low gravity cultivation), and one profile at pH 5 and 300g/L glucose under aerobic conditions (high gravity cultivation).

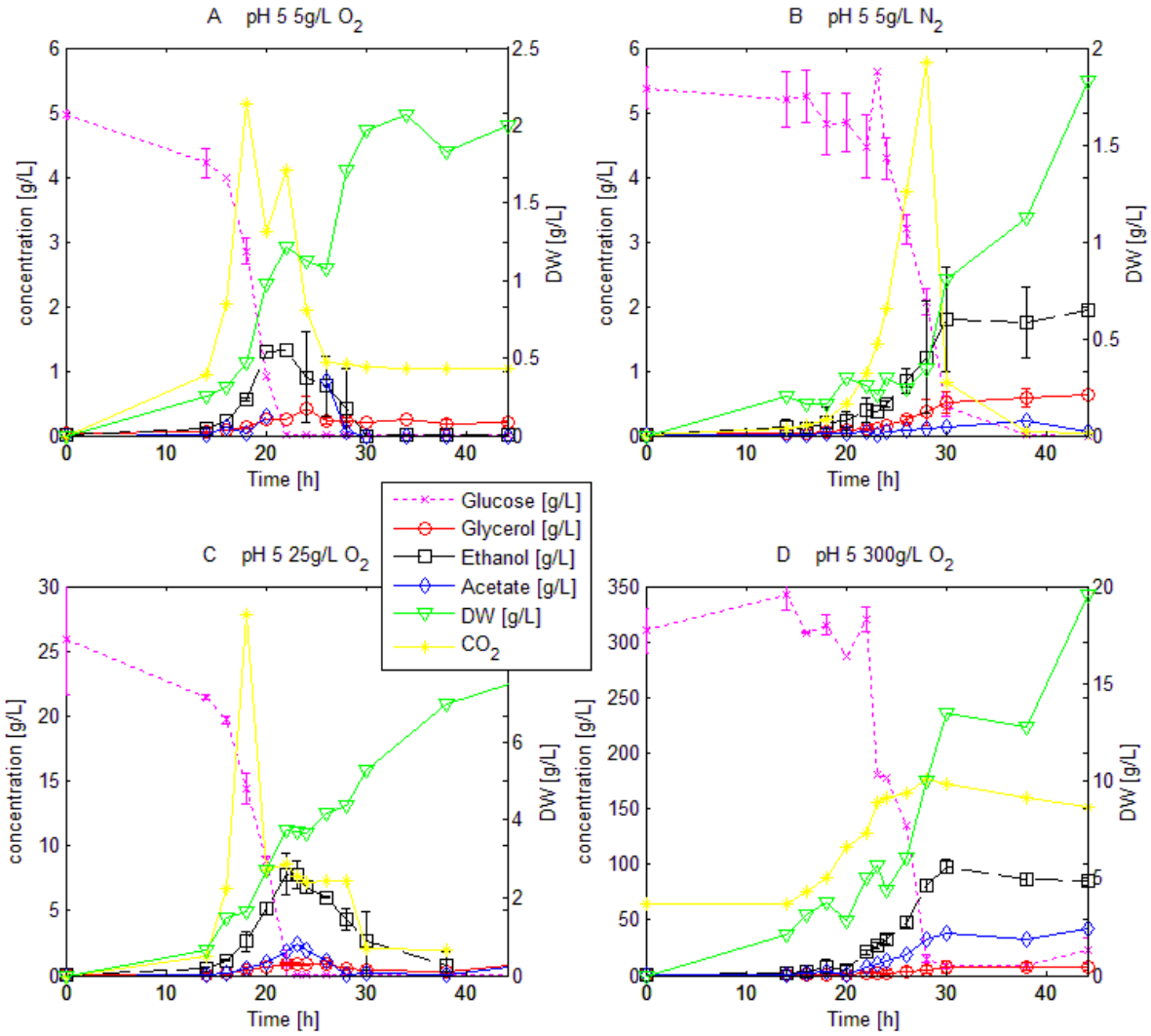

Figure 1 – **physiology profile for four representative conditions**, pH 5 5g/L O_2 (A); pH 5 5g/L N_2 (B); pH 5 25g/L O_2 (C) and pH 5 300g/L O_2 (D), showing the profile of batch cultivations for the *S. cerevisiae* reporter strain FE440 for off-gas CO_2, the major metabolites (glucose, ethanol, glycerol and acetate) and cell dry weight. All values are presented including the standard deviation.

The batch physiology profile for aerobic low gravity cultivations (5 g/L and 25 g/L) at both tested pH values, here represented by the profiles at pH 5 under aerobic conditions with 5 g/L of glucose (A) as well as 25 g/L of glucose (B) showed two growth phases, growth on glucose accompanied by ethanol production and after the diauxic shift growth on the earlier produced ethanol. The hereby found growth rates were consistent with literature[22,24–26] and during growth on glucose the growth rates were generally higher than during growth on ethanol (around 75% lower, see appendix, table 2). Both phases were accompanied by a rise in CO_2

and biomass production as well as glycerol and acetate production during growth on glucose. Glycerol and acetate were also found in other studies to accompany overflow metabolism[27,28]. In the second growth phase on ethanol, the produced acetate was consumed whereas the glycerol concentration remained constant. The diauxic shift took place after around 20-22h and the cultures reached stationary phase after around 30-33h.

In contrast to that, anaerobic low gravity cultivations (5g/L and 25g/L) as well as aerobic and anaerobic high gravity cultivations (300g/L glucose) exhibited only one growth phase consuming the glucose in the medium while producing ethanol. The growth rates for anaerobic low gravity cultivations were consistent with literature[26] and in general lower than for the corresponding aerobic cultivations, whereas for high gravity cultivations, apart from the fact that the growth rates were in general lower than for low gravity cultivations, no clear growth rate trend could be seen. Compared to Odman *et al.* (2009)[22], who found 0.17+/-0.01 h^{-1} for aerobic high gravity cultivations at pH 5, the growth rates observed here were slightly higher (see appendix, table 2). After glucose depletion the ethanol remained constant and consequently no diauxic shift was seen. Also for these cultivations growth was accompanied by a rise in CO_2 level, increasing biomass concentration as well as production of acetate and glycerol, though in higher amounts than for aerobic low gravity cultivations which is in agreement with other studies[27,28]. Different compared to aerobic low gravity cultivations was that the acetate as well as the ethanol were not consumed after production. The cultures reached steady state after around 30h.

Furthermore the yields for the major metabolites as well as the carbonbalance were calculated for the performed cultivation (see appendix, table 2). All carbonbalances could be closed with at least 88% (referring to the one fermentation out of 12 were most carbon was missing). The missing carbon can possibly be explained by ethanol evaporation, as earlier seen by Eliasson *et al.* (2000)[29].

5.3.2 Introduction of the method describing growth correlated GFP fluorescence and membrane robustness originating from a dual reporter strain

In the following sections first the new method for objective description and comparison of flow cytometry data will be introduced using a part of the data set, i.e. the experiments performed at pH 5, comparing growth correlated GFP fluorescence for cells kept on ice, referred to as fresh cells, with GFP fluorescence of freeze-thawed cells. The fluorescence of freeze-thawed cells, referred to as frozen cells, shows information about cell membrane

robustness as a strong correlation between intracellular GFP level and cell membrane integrity could be observed after subjecting cell samples to freeze-thaw stress[7]. Afterwards the application of the method will be demonstrated comparing fluorescence of frozen cells and thereby membrane robustness for all performed conditions.

5.3.2.1 Case one: Cell membrane robustness and growth correlated GFP fluorescence under different conditions at pH 5

For the six different fermentation conditions performed at pH 5 cells were kept on ice (fresh cells) as well as subjected to freeze-thaw stress until flow cytometry analysis to evaluate growth correlated GFP fluorescence of cells with intact cell membrane respectively the influence of freeze-thaw stress on membrane robustness. As it is general practice in single cell studies first GFP fluorescence distributions were plotted as histogram plots for fresh cells following the different time points of the batch cultivation under the different growth conditions (figure 2).

In general the shape of the GFP fluorescence remained the same throughout the batch cultivations, featuring one sharp main population with slight tailing towards higher fluorescence. Also comparing the different conditions no distinct differences could be found. Solely the tailing got more distinct with higher glucose concentration as well as when the cultivations were performed under anaerobic instead of aerobic conditions. Moreover, the mean fluorescence level abided the same throughout the batch for the high gravity cultivations, around 400 for aerobic respectively 350 for anaerobic cultivations, as well as for the anaerobic low gravity cultivations (around 330-350). In contrast to that the mean fluorescence slightly declined for aerobic low gravity cultivations when the glucose was depleted (from around 350-360 to 320-330) and cells underwent diauxic shift, leading to redistribution of cellular components. Afterwards, at the beginning of the ethanol consumption phase the GFP fluorescence further decreased before remaining constant until ethanol depletion. This fluorescence pattern was also found during batch cultivations for characterising the strain FE440[7].

Considering the level of heterogeneity within the GFP fluorescence distribution, meaning the broadness of the distribution, an increase was found with increasing cultivation time especially after glucose depletion.

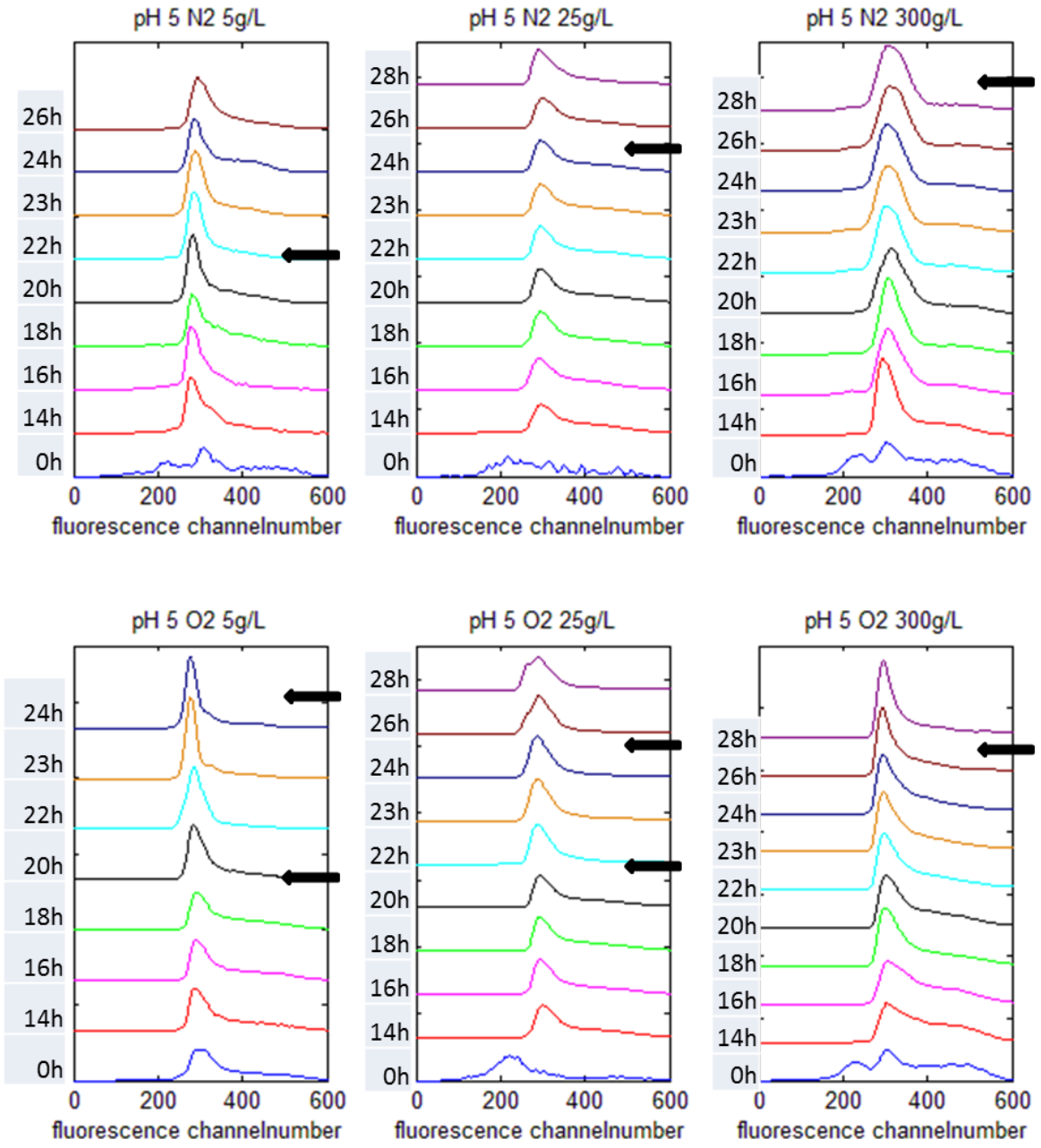

Figure 2 – Growth correlated GFP fluorescence histograms for fresh cells at pH 5 in different growth phases, during batch experiments with different conditions (aerobic and anaerobic, glucose concentration 5g/L, 25g/L or 300g/L). The black arrow next to the histogram plots marks the time when glucose is depleted respectively the second one marks when ethanol is depleted for the experiments where growth on ethanol took place.

To compare the GFP fluorescence distribution of fresh *S. cerevisiae* cells to cells that were subjected to freeze-thaw stress (frozen cells) in a more quantitative way than the above used histogram plots for the different performed conditions and at different time points within each batch cultivation, an interval analysis was developed. Thereby the fluorescence distribution histograms, which represent channel number fluorescence against cell count, were divided into five channel number intervals (1-200, 200-400, 400-600, 600-800 respectively 800-1024) and the percentage of cell count in each interval was calculated (figure 3A). Results can be illustrated as a barplot, which contains one bar for each batch sampling time point, adding up to 100% when combining the percentage of cells in each of the five intervals of the histogram (figure 3B).

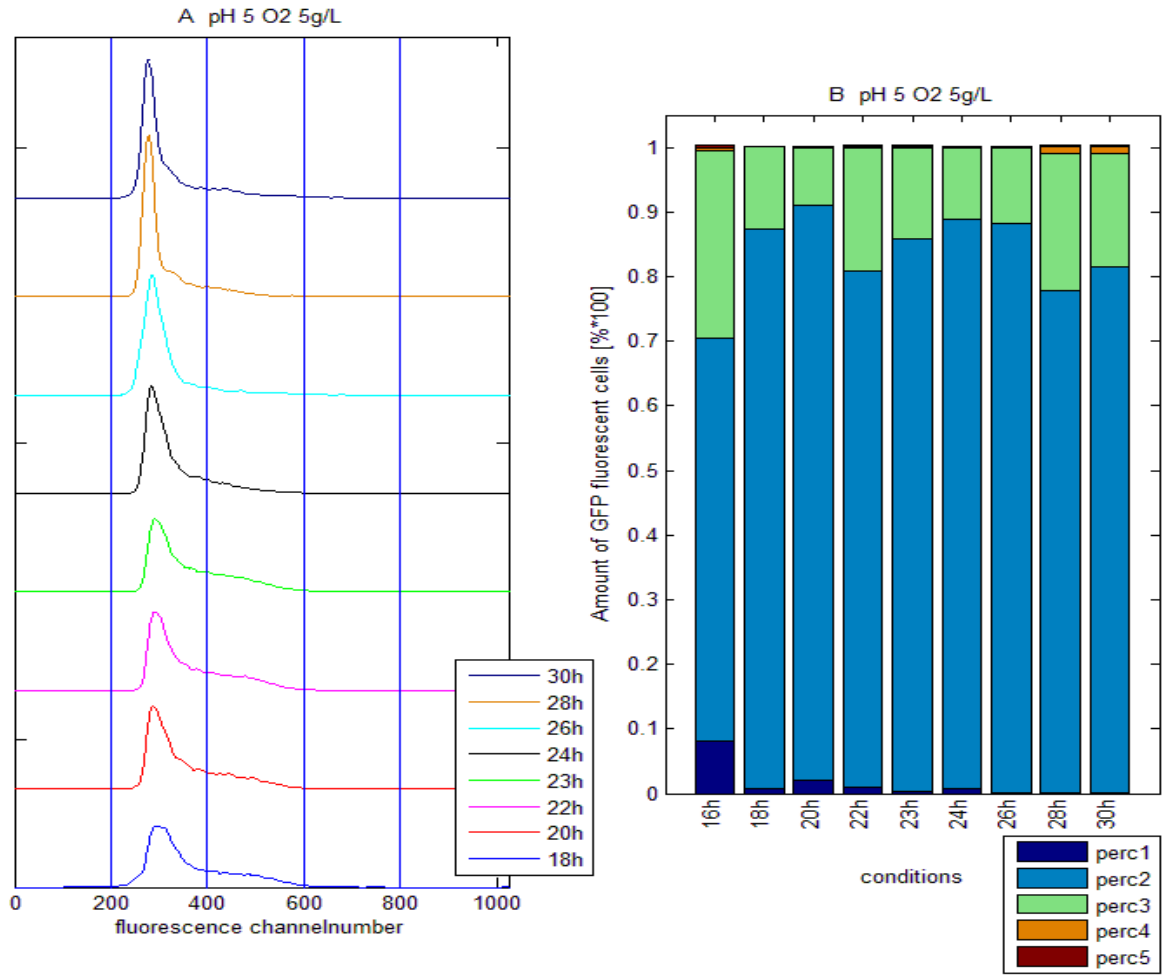

Figure 3 – Example demonstrating GFP fluorescence conversion from histogram to barplot for interval analysis: for pH 5 O_2 5g/L during the different growth phases of a batch experiments. The left plot (A) shows histogram plots throughout the batch which are divided into five intervals (indicated by blue lines). The right plot shows the corresponding barplot (B), displaying the percentage of fluorescent cells in each of the five intervals.

As a second step, for the comparison of the bars corresponding to different sampling points of each experiment as well as sampling points within the same experiment, principal component analysis (PCA) on the percentage of fluorescent cells found in each interval for each data point was performed.

Five principal components were found with the first two explaining 72% of the variance. Results are presented as a score plot for the first two principal components (figure 4). Two main clusters could be gated, one circular cluster (figure 4, red) covering mostly the first quadrant of the score plot and one elongated circular cluster covering parts of the second to fourth quadrant (figure 4, black). Considering the loading plot (figure 5) the red cluster covered conditions that exhibit a high percentage of fluorescence in the first interval and a fairly low percentage of fluorescence in intervals three and five. The remaining intervals exhibit a normal to low percentage of fluorescence. The black cluster, however, included conditions in the upper left part with high fluorescence percentage in the second interval and increasing fluorescence percentage in intervals three and five going towards the lower right part (figure 5). Intervals one and four did not seem to have much influence in this cluster.

In the black cluster samples for all freshly analysed GFP fluorescence samples as well as frozen samples for the standard conditions, pH 5, aerobic conditions and 5 g/L of glucose, and pH 5, anaerobic conditions and 25 g/L glucose could be found. Hereby, the samples for fresh cells clustered mostly in the upper left corner of the cluster in a line facing the right lower corner because they mostly exhibited fluorescence in the second interval but also showed some fluorescence in the third interval. As mentioned in the section above the fluorescence in the third interval, characterising the fluorescent bump seen on the right hand side from the main peak in figure 2, increased with increasing glucose concentration and is also more distinct for anaerobic than aerobic cultivations. The latter is also shown by the location of the conditions further down towards the lower right corner of the cluster. pH 5 anaerobic with 25 g/L glucose exhibited values for later time points that were slightly apart from the main line due to a slightly higher fluorescence seen in interval three. Further down in the cluster on the line facing the lower right corner the samples for the two frozen conditions can be found exhibiting similar fluorescence as fresh samples but with a higher fluorescence percentage in intervals one and three instead of two whereas for fresh cells the opposite is true. This is consistent with earlier findings of Carlquist *et al.* (2012)[7], who found a subpopulation division for frozen cells in a high and low subpopulation representing cells with intact respectively

disrupted membrane as a consequences of freeze thaw stress. Considering the different growth phases during the batch, illustrated by the increasing size of the markers for the samples in the PCA, in general for fresh cells no significant difference can be seen apart from a small downshift in fluorescence for later time points for aerobic low gravity cultivations which was also seen from the histogram plots (figure 4).

The red cluster included the remaining frozen GFP fluorescence samples, but interestingly samples taken close to glucose depletion almost consistently, apart from aerobic high gravity cultivations, spread in the closer vicinity of the border to the black cluster (figure 4). Hereby the aerobic cultivation with 25 g/L and the anaerobic cultivation with 5 g/L (low gravity cultivations) exhibited a similar fluorescence profile to fresh cells (high vicinity of samples to the border of the black cluster) but with higher fluorescence in the first and third interval in the exponential growth phase which was later shifting down to the first and mostly second interval (figure 4). For the anaerobic high gravity cultivation the GFP fluorescence was high (mostly fourth interval) at the beginning of the cultivation, but with also a subpopulation of cells with fluorescence in the second interval. During exponential growth on glucose the fluorescence shifted down (mostly first, second and third interval) and decreased even further after glucose depletion (mostly first and second interval). For aerobic high gravity cultivation a similar but even stronger trend was seen with a significant downshift in fluorescence during exponential growth on glucose (third interval to mostly first and second) and even more distinct after glucose depletion (mostly first interval).

In general, when comparing anaerobic and aerobic cultivations no clear trend can be seen that would indicate that anaerobic or aerobic cultivations exhibit similar characteristics. Opposite to this, cultivations with different glucose concentration can be grouped in high and low gravity cultivations exhibiting different GFP fluorescence characteristics.

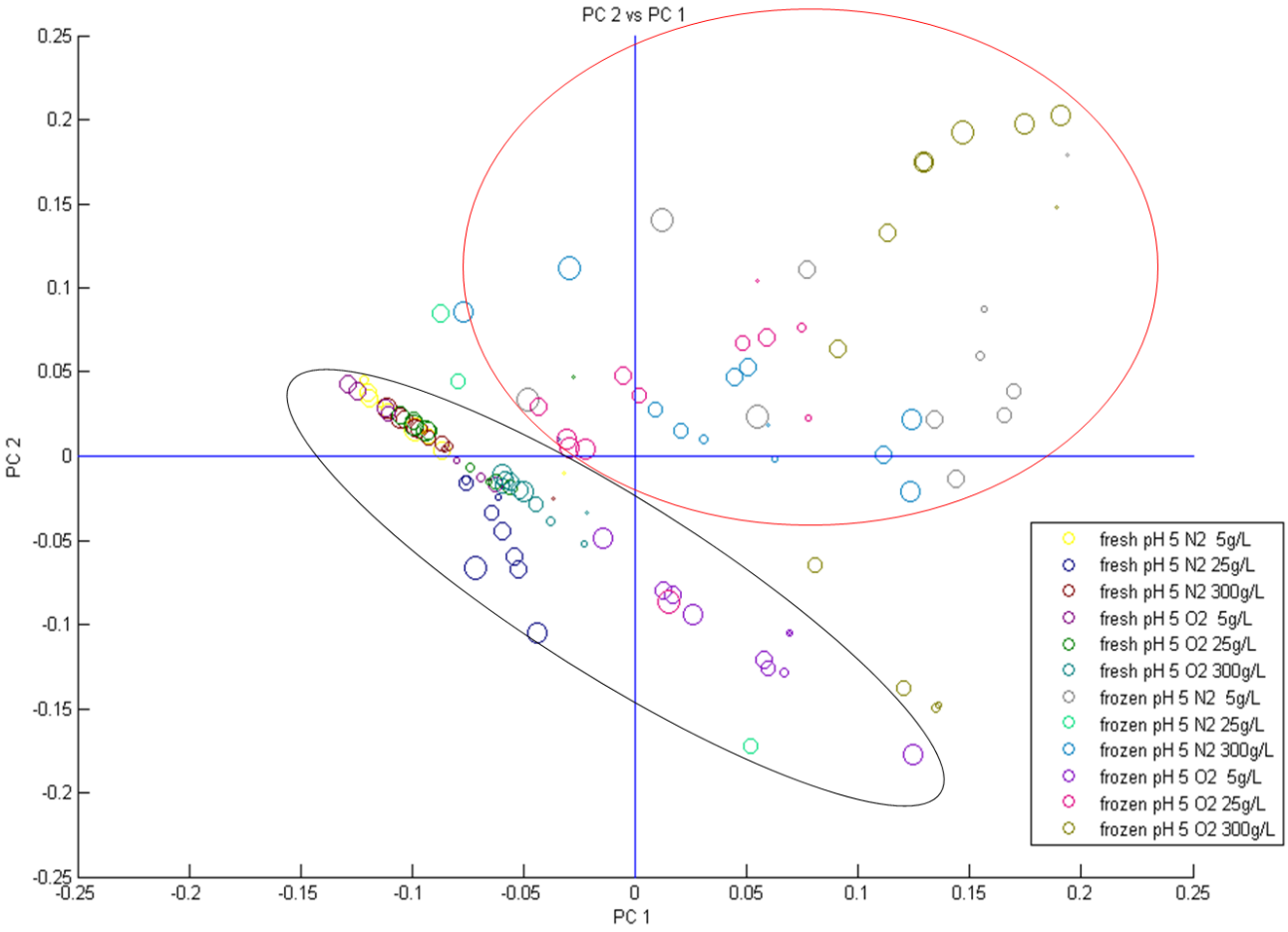

Figure 4 – Score plot for PCA (Principal component analysis) of GFP fluorescence for the comparison of fresh and freeze-thawed cells for batch experiments performed at pH 5. Four principal components have been found. The scores for the first two principal components (together 72% of variance explained) are plotted against each other. The black and red circles indicate gates for the cluster seen in the distribution. The increasing marker size for each experiment is indicating samples taken at later time points in a batch experiment.

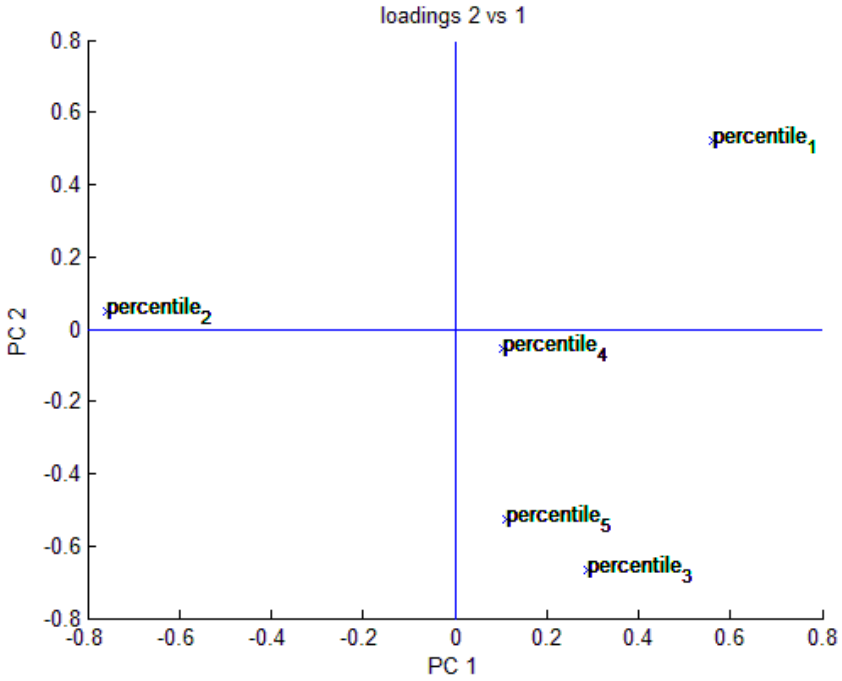

Figure 5 – Loading plot for PCA (Principal component analysis) of GFP fluorescence for the comparison of fresh and freeze-thawed cells for batch experiments performed at pH 5. Four principal components have been found. The loadings for the first two principal components (together 72% of variance explained) are plotted against each other.

5.3.2.2 Case two: GFP fluorescence distributions of frozen cells for all performed experiments

As a second case study the developed method is applied for the comparison between frozen cells of all performed batch conditions. Five principal components were found with the first two explaining 74% of the variance. Results are again presented as a score plot for the first two principal components (figure 6). Three main clusters could be gated (figure 6, red, green and black), all with oval shape. The biggest one (figure 6, red) covered the bottom area of the score plot (quadrant two and three). The two smaller ones (figure 6, green and black) lay in the top part of the score plot, the black one covered the intersection between the first and the fourth quadrant whereas the green one pointed right downwards on the intersection between the first and the second quadrant. Considering the loading plot (figure 7) the red cluster covered conditions that exhibit a high percentage of fluorescence in the first interval and low until middle percentage of fluorescence in intervals three, four and five. Interval two in this case did not show significant fluorescence in this cluster. In contrast to that the black cluster covered conditions that exhibited higher fluorescence in the second interval as well as some in

interval three four and five but only minor in the first interval. Consequently for the conditions that were found in the green cluster the major part of the GFP fluorescence percentage was found in intervals three, four and five, with increasing fluorescence in the third interval when clustered closer to the right lower border of the cluster (figure 6 and 7).

The black cluster contained low gravity cultivations for both pH values apart from some earlier time points of the anaerobic cultivations with 5 g/L and 25 g/L glucose at pH 5 and the aerobic cultivation with 5 g/L glucose at pH 5. However the aerobic cultivations were found to settle in the vicinity of the black and green cluster. In the black cluster cells mostly showed similar fluorescence to fresh cells (fluorescence in the second interval) especially for pH 4. But with increasing pH and under aerobic conditions also a subpopulation division is found with fluorescence in the first and third interval, which is increasing in the low interval towards the end of the cultivations, especially after glucose depletion. Therefore, later sampling points were found to be closer to the red cluster.

The red cluster included anaerobic high gravity cultivations for pH 4 and partly pH 5, the middle time points for anaerobic low gravity cultivation (5 g/L) at pH 5 as well as the aerobic high gravity cultivation for pH 5. For these conditions cells were found to exhibit fairly high fluorescence in the first interval, being largely affected by the freeze-thaw procedure. It needs to be mentioned, though, that these conditions at the beginning of the batch, before exponential growth on glucose set in, also resulted in a population of cells with high fluorescence in the third and fourth interval (figure 6). Samples were in this case found in the upper part of the cluster in the vicinity of the black and the green cluster. First during growth on glucose as well as even more after its depletion the fluorescence decreases sharply.

The green cluster contained, apart from single time-points of anaerobic cultivations at the beginning of the batch cultivation, the aerobic high gravity cultivations for pH 4 as well as the middle time-points for anaerobic high gravity and aerobic low gravity cultivation (5 g/L glucose) at pH 5. These conditions are consequently characterised by a fluorescence distribution in the middle fluorescence range, but with increased fluorescence in the third interval for the high gravity cultivation at pH 4. Furthermore, as for the other clusters the GFP fluorescence level mostly decreased with glucose depletion, moving the fluorescence percentage to lower intervals respectively to the borders of the cluster facing the red or black cluster (figure 6).

In general, as in the section above comparing fresh and frozen cells, it could be concluded that anaerobic and aerobic cultivations exhibited similar fluorescence distributions. Furthermore also the distributions at different pH did not differ significantly. However as for the comparison of fresh and frozen cells the distributions changed with changing glucose concentration and a clear division between high and low gravity cultivations was found.

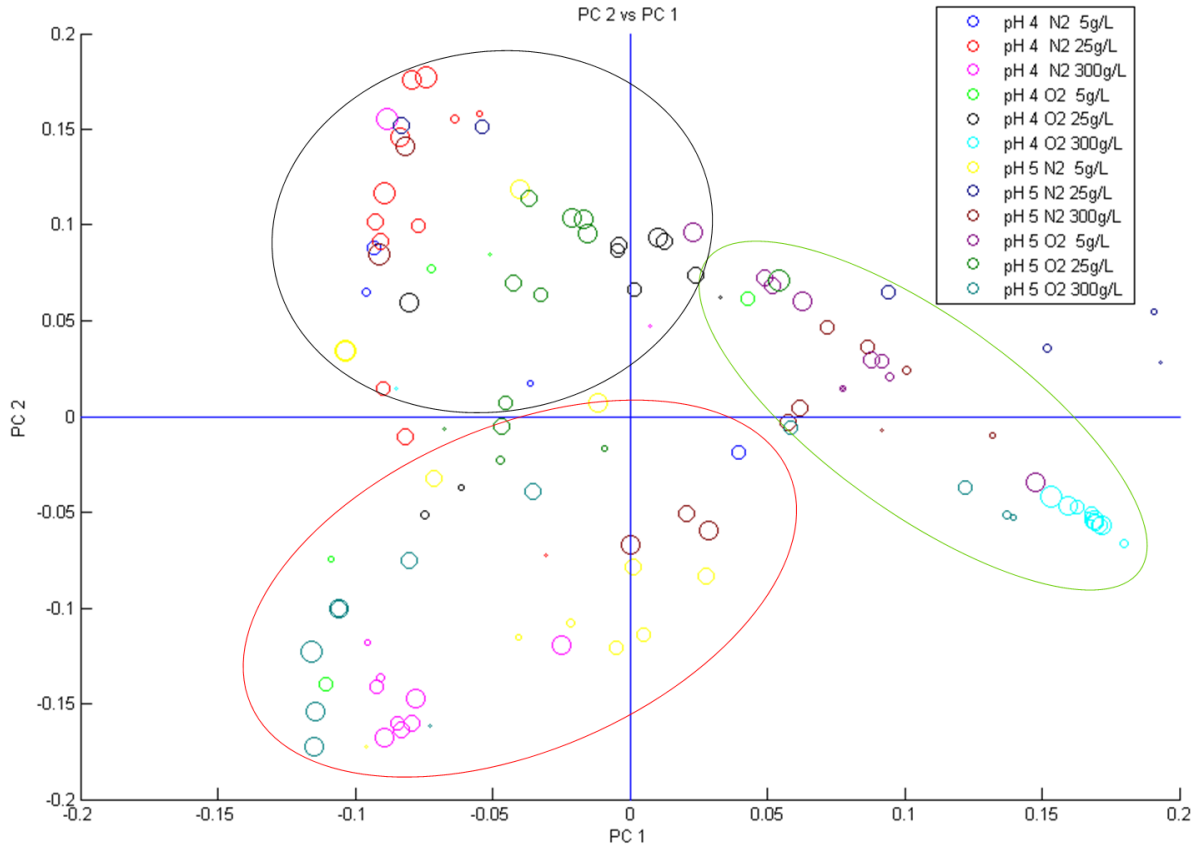

Figure 6 – Score plot for PCA (Principal component analysis) of GFP fluorescence after applying freeze-thaw stress for all performed batch experiments. Four principal components have been found. The scores for the first two principal components (together 74% of variance explained) are plotted against each other. The black, red and green circles indicate gates for the cluster seen in the distribution. The increasing marker size for each experiment is indicating samples taken at later time points.

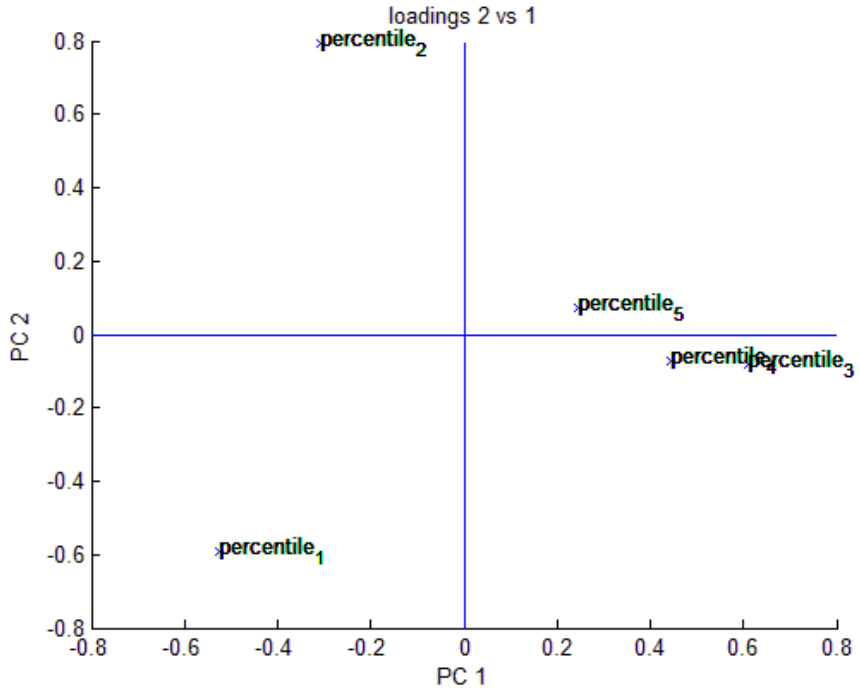

Figure 7 – Loading plot for PCA (Principal component analysis) of GFP fluorescence after the application of freeze-thawed cells for all performed batch experiments. Four principal components have been found. The loadings for the first two principal components (together 74% of variance explained) are plotted against each other.

5.4 Discussion

Different growth and stress conditions in a bioreactor are generally found to influence the physiology of microbial cells and thereby the underlying population heterogeneity distributions[7,30,31]. Here we successfully developed a method employing principal component and interval analysis to investigate single cell physiology of the *S. cerevisiae* dual reporter FE440 in batch cultivations under different conditions. With the used approach the problem of interpretation of the considerable amounts of data resulting from the flow cytometry analysis could be scaled down and single cell growth heterogeneities and cell membrane robustness could be evaluated.

5.4.1 Usefulness of the approach for data analysis

The use of flow cytometry to follow single cell distributions of growth and cell membrane robustness in different batch growth phases and under different conditions created multidimensional data especially for the flow cytometry analysis that needed to be converted to a comparable format. Principal component analysis (PCA) can help to reduce the amount of

variables by creating new variables that makes it easier to compare data points to each other[33]. Data like flow cytometry data exhibiting distributions of 10000 counted cell events at every sampling point throughout the batch are difficult to be converted to meaningful variables that can be used as input for the PCA, as e.g. taking simple mean fluorescence values would fail to describe the whole population dynamics. Therefore it was chosen to introduce an interval analysis that has been used in a similar way in an approach to evaluate biplots of GFP fluorescence and cell size (FSC) before[7]. Histograms were divided into five fluorescence areas and the percentage of fluorescence cells in each interval compared to the fluorescence in the whole histogram was calculated. In this way more descriptive information could be gathered compared to simple mean values, also capturing possible shifts of the fluorescent population, shapes that spread over more than one interval and appearance of subpopulations while scaling down multiple data points to five values per sample. This facilitated the comparison between different conditions because now by using PCA single values containing cell distribution information could be created instead of the whole distribution.

5.4.2 Fluorescence distributions for growth and cell membrane robustness

The GFP fluorescence originating from the dual reporter system was analysed comparing fresh and frozen cells for conditions performed at pH 5 as well as comparing frozen cells for all performed experiments. In general for aerobic low gravity cultivation at pH 5 fresh analysed cells can be used to follow the different phases (growth on glucose, ethanol and stationary phase) of a batch cultivation as also found earlier[7]. For fresh analysed cells in anaerobic low gravity and high gravity cultivations no significant difference between the different growth phases could be seen. For high gravity cultivations especially, this might be due to the fact that cells are generally more stressed and a constant high expression of ribosomal related genes is detected due to adjustment to first the high viscosity glucose concentration, also seen in a longer lag-phase/phase of slow growth, as well as afterwards due to constant reorganization towards the new growth environment (e.g. low glucose concentration, limited oxygen during growth, stationary phase). However, when comparing cells exposed to freeze-thaw stress to evaluate cell membrane robustness to fresh cells clear differences between cells were seen.

Fresh cells at pH 5, as mentioned above, had intact membranes, exhibiting almost constant fluorescence levels, but seem to be more metabolically stressed or show other/higher growth activity when grown in anaerobic low gravity or high gravity cultivations than in aerobic low

gravity cultivations. This is supported by the bump with higher fluorescence for these conditions, which is stronger developed for higher glucose concentration especially under anaerobic conditions. However this is in disagreement with the growth rates derived from general physiology data which were found to be significantly lower for high gravity cultivations, which should in principle be reflected by the GFP expression. Therefore the reporter system seems to show limitation in its applicability under extreme growth conditions in which cells are potentially highly stressed. When exposing cells grown under different conditions at pH 5 to freeze-thaw stress (frozen cells), low gravity cultivations mostly resemble fresh cells considering the main fluorescent population but especially during exponential growth on glucose they seem to contain a small amount of cells in a lower fluorescent subpopulation. These cells seem to be highly affected in membrane integrity, which might be due to open membrane pores during exponential growth because, interestingly, these cells seem to recover when the culture reaches stationary phase in all cases. A reason for this might be that cells in this phase are preparing for coping with nutrient limitation and depletion and are therefore more robust[7]. A similar effect is also seen for cells grown in high gravity cultivation, but towards the end of the exponential growth phase on glucose the whole fluorescent cell population seems to be highly affected in membrane integrity because the fluorescence drops sharply and remains low during stationary phase. Possibly the high stress level cells experience and that they try to cope with the high glucose concentration is affecting them strongly when they reach the opposite extreme of the already above mentioned nutrient limitation or depletion.

When taking frozen cells under all performed conditions into account mostly the same trends as for pH 5 can be seen so that it seems as the pH and oxygen level do not have a big influence on cell membrane robustness, whereas the glucose concentration highly affects the freeze-thaw tolerance.

5.4.3 Conclusion and Outlook

In conclusion comparing the influences of pH, oxygen level and glucose concentration on growth heterogeneity and membrane robustness glucose seems to be the major influence, and this mean that further studies should be focused on developing a deeper understanding of the underlying phenomenon behind this observation e.g. by applying pulses of glucose to chemostat cultures. Thereby its influence on single cell physiology could be studied in a steady growth environment and potentially it could be combined with cell sorting of different

subpopulations of different robustness to deeper investigate their physiology. These studies are also of interest for industrial production processes because glucose is widely used as a substrate.

Furthermore, combining PCA and interval analysis for the evaluation/comparison of flow cytometry data provides a lot of information that can potentially be used in process optimization. This could be especially interesting when using high throughput setups like parallelized microbioreactors as well as experiments involving automated sampling e.g. using a sampling robot.

5.5 References

1. Arsköld, E. *et al.* Environmental influences on exopolysaccharide formation in Lactobacillus reuteri ATCC 55730. *Int. J. Food Microbiol.* **116,** 159–167 (2007).

2. Rohe, P., Venkanna, D., Kleine, B., Freudl, R. & Oldiges, M. An automated workflow for enhancing microbial bioprocess optimization on a novel microbioreactor platform. *Microb. Cell Fact.* **11,** (2012).

3. Fazio, A. *et al.* Transcription factor control of growth rate dependent genes in Saccharomyces cerevisiae: a three factor design. *BMC Genomics* **9,** (2008).

4. Valli, M., Sauer, M., Branduardi, P., Borth, N. & Porro, D. Intracellular pH Distribution in Saccharomyces cerevisiae Cell Populations , Analyzed by Flow Cytometry Intracellular pH Distribution in Saccharomyces cerevisiae Cell Populations , Analyzed by Flow Cytometry. *Appl. Environ. Microbiol.* **71,** 1515–1521 (2005).

5. Lara, A. R. *et al.* Transcriptional and metabolic response of recombinant Escherichia coli to spatial dissolved oxygen tension gradients simulated in a scale-down system. *Biotechnol. Bioeng.* **93,** 372–385 (2006).

6. Schweder, T. *et al.* Monitoring of genes that respond to process-related stress in large-scale bioprocesses. *Biotechnol. Bioeng.* **65,** 151–159 (1999).

7. Carlquist, M. *et al.* Physiological heterogeneities in microbial populations and implications for physical stress tolerance. *Microb. Cell Fact.* **11,** (2012).

8. Bylund, F., Collet, E., Enfors, S.-O. & Larsson, G. Substrate gradient formation in the large-scale bioreactor lowers cell yield and increases by-product formation. *Bioprocess Eng.* **18,** (1998).

9. Enfors, S. O. *et al.* Physiological responses to mixing in large scale bioreactors. *J. Biotechnol.* **85,** 175–185 (2001).

10. George, S., Larsson, G., Olsson, K. & Enfors, S.-O. Comparison of the Baker's yeast process performance in laboratory and production scale. *Bioprocess Eng.* **18,** 135–142 (1998).

11. Sumner, E. R. & Avery, S. V. Phenotypic heterogeneity: differential stress resistance among individual cells of the yeast Saccharomyces cerevisiae. *Microbiology* **148,** 345–351 (2002).

12. Avery, S. V. Microbial cell individuality and the underlying sources of heterogeneity. *Nat. Rev. Microbiol.* **4,** 577–587 (2006).

13. Fernandes, R. L. *et al.* Experimental methods and modeling techniques for description of cell population heterogeneity. *Biotechnol. Adv.* **29,** 575–599 (2011).

14. Díaz, M., Herrero, M., García, L. a. & Quirós, C. Application of flow cytometry to industrial microbial bioprocesses. *Biochem. Eng. J.* **48,** 385–407 (2010).

15. Buziol, S. *et al.* New bioreactor-coupled rapid stopped-flow sampling technique for measurements of metabolite dynamics on a subsecond time scale. *Biotechnol. Bioeng.* **80,** 632–636 (2002).

16. Zhao, R., Natarajan, A. & Srienc, F. A flow injection flow cytometry system for on-line monitoring of bioreactors. *Biotechnol. Bioeng.* **62,** 609–617 (1999).

17. Rieseberg, M., Kasper, C., Reardon, K. F. & Scheper, T. Flow cytometry in biotechnology. *Appl. Microbiol. Biotechnol.* **56,** 350–360 (2001).

18. Wold, S., Esbensen, K. & Geladi, P. Principal component analysis. *Chemom. Intell. Lab. Syst.* **2,** 37–52 (1987).

19. Regenberg, B. *et al.* Growth-rate regulated genes have profound impact on interpretation of transcriptome profiling in Saccharomyces cerevisiae. *Genome Biol.* **7,** (2006).

20. Verduyn, C., Postma, E., Scheffers, W. a & Van Dijken, J. P. Effect of benzoic acid on metabolic fluxes in yeasts: a continuous-culture study on the regulation of respiration and alcoholic fermentation. *Yeast* **8,** 501–517 (1992).

21. Odman, P., Johansen, C. L., Olsson, L., Gernaey, K. V & Lantz, A. E. On-line estimation of biomass, glucose and ethanol in Saccharomyces cerevisiae cultivations using in-situ multi-wavelength fluorescence and software sensors. *J. Biotechnol.* **144,** 102–112 (2009).

22. Olsson L, N. J. On Line and in situ Monitoring of Biomass in Submerged Cultivations. *Trends Biotechnol.* **15,** 517–522 (1997).

23. Papini, M., Nookaew, I., Siewers, V. & Nielsen, J. Physiological characterization of recombinant Saccharomyces cerevisiae expressing the Aspergillus nidulans phosphoketolase pathway: validation of activity through 13C-based metabolic flux analysis. *Appl. Microbiol. Biotechnol.* **95,** 1001–1010 (2012).

24. Van Maris, a J. *et al.* Modulating the distribution of fluxes among respiration and fermentation by overexpression of HAP4 in Saccharomyces cerevisiae. *FEMS Yeast Res.* **1,** 139–149 (2001).

25. Bakker, B. M. *et al.* The mitochondrial alcohol dehydrogenase Adh3p is involved in a redox shuttle in Saccharomyces cerevisiae. *J. Bacteriol.* **182,** 4730–4737 (2000).

26. Costenoble, R., Valadi, H., Gustafsson, L., Niklasson, C. & Franzén, C. J. Microaerobic glycerol formation in Saccharomyces cerevisiae. *Yeast* **16,** 1483–1495 (2000).

27. Radler, F. & Schtitz, H. Glycerol production of various strains of Saccharomyces. *Am. Inst. Chem. Eng.* 5–9 (1981).

28. Eliasson, A. *et al.* Anaerobic Xylose Fermentation by Recombinant Saccharomyces Mineral Medium Chemostat Cultures. *Appl. Environ. Microbiol.* **66,** 3381–3386 (2000).

29. Lidstrom, M. E. & Konopka, M. C. The role of physiological heterogeneity in microbial population behavior. *Nat. Chem. Biol.* **6,** 705–712 (2010).

30. Müller, S., Harms, H. & Bley, T. Origin and analysis of microbial population heterogeneity in bioprocesses. *Curr. Opin. Biotechnol.* **21,** 100–113 (2010).

5.6 Appendix

Table 2 - Collection of yields in [cmole/cmole] for the major metabolites (ethanol, acetate and glycerol), CO_2 and dry weight as well as the carbon-balance for all performed batch experiments including standard deviation where duplicates exist.

conditions	**pH 4**						**pH 5**					
	5g/L		**25g/L**		**300g/L**		**5g/L**		**25g/L**		**300g/L**	
	N_2	**O_2**	**N_2**	**O_2**	**N_2**	**O_2**	**N_2**	**O_2**	**N_2**	**O_2**	**N_2**	**O_2**
Ys/x [cmole/cmole]	0.23	0.22 ±0.0	0.18	0.27	0.15 ±0.02	0.08 ±0.01	0.14 ±0.01	0.3 ±0.0	0.16 ±0.06	0.17 ±0.01	0.1	0.15 ±0.01
Ys/e [cmole/cmole]	0.33	0.38 ±0.03	0.37	0.35	0.42 ±0.02	0.54 ±0.03	0.49 ±0.01	0.39 ±0.04	0.44 ±0.05	0.4 ± 0.09	0.39	0.42 ±0.06
Ys/g [cmole/cmole]	0.16	0.02 ±0.01	0.07	0.02	0.02 ±0.01	0.05 ±0.01	0.09 ± 0.0	0.08 ±0.03	0.06 ±0.04	0.03 ±0.01	0.08	0.03 ±0.01
Ys/a [cmole/cmole]	0.01	0.06 ±0.03	0.01	0.01	0.02 ±0.01	0.05 ±0.03	0.09 ±0.06	0.07 ±0.04	0.03 ±0.01	0.12 ±0.05	0.01	0.01 ±0.06
Ys/CO_2 [cmole/cmole]	0.24	0.2 ±0.03	0.24	0.3	0.34 ± 0.0	0.2 ±0.0	0.18 ±0.03	0.18 ±0.0	0.3 ±0.0	0.23 ±0.03	0.4	0.27 ±0.03
Carbonbalance	**0.97**	**0.88 ±0.02**	**0.87**	**0.95**	**0.95 ±0.02**	**0.92 ±0.05**	**0.99 ±0.05**	**0.98 ±0.09**	**0.99 ±0.11**	**0.95 ±0.05**	**0.97**	**0.88 ±0.13**
$\mu_{glucose}$ [h^{-1}]	0.26	0.36 ±0.07	0.29	0.34	0.17 ±0.06	0.16 ±0.06	0.21 ±0.01	0.38 ±0.01	0.30 ±0.08	0.35 ±0.05	0.23	0.18 ±0.07
$\mu_{ethanol}$ [h^{-1}]	-	0.06 ±0.02	-	0.09	-	-	-	0.1 ± 0.001	-	0.04 ±0.0	-	-

6. Chapter

Population heterogeneity distributions in *E. coli* and *S. cerevisiae* continuous cultivations as a response to growth rate and glucose perturbation

Anna-Lena Heins[1], Ted Johanson[1], Shanshan Han[2], Rita Lencastre Fernandes[3], Luisa Lundin[2], Gitte E Charbon[2], Magnus Carlquist[1,4], Krist V. Gernaey[3], Søren J. Sørensen[2], and Anna Eliasson Lantz[1,§]

[1] Department of Systems Biology, Technical University of Denmark, 2800 Kongens Lyngby, Denmark

[2] Department of Biology, Section of Microbiology, University of Copenhagen, 2100 DK, Copenhagen, Denmark

[3] Department of Chemical and Biochemical Engineering, Technical University of Denmark, 2800 Kongens Lyngby, Denmark

[4] Present address: Department of Chemistry, Division of Applied Microbiology, Lund University, 221 00 Lund, Sweden

[§]Corresponding author

Written as journal paper

Status: Submitted

Abstract

S. cerevisiae and *E. coli* growth reporter strains based on the expression of Green Fluorescent Protein (GFP) were grown at different growth rates in glucose-limited chemostats to investigate population heterogeneity in steady state and the effects of concentrated glucose pulses at single-cell level using flow cytometry. Flow cytometry was thereby used for acheiving a quantitative description thus going clearly beyond normal qualitative assessment of single cell properties. For *E. coli* cells at both low and high growth rates as well as for the slow growing yeast, slight up-shifts in fluorescence were seen after introduction of a glucose pulse, indicating that gene regulation of the promoters primarily responded to upshifts to glucose excess. Slow growing cells responded stronger to the transient glucose excess than fast growing cells. Cell membrane robustness was also investigated by analysing changes in GFP fluorescence after exposure to freeze-thaw stress. Both yeast and *E. coli* cells were seen to be heavily influenced by the freezing procedure at high dilution rates, showing subpopulations with lower fluorescence than the main population, whereas at low dilution rates they were more resilient. In addition, the glucose pulses had an instant effect in protecting parts of the cell population of the rapidly growing yeast cells ($D=0.3\ h^{-1}$) against membrane damage. This was not seen for the slower growing yeast and *E. coli* cells ($D=0.05\ h^{-1}$ respectively $D=0.1\ h^{-1}$). New tools were established to quantify population heterogeneity using a combination of fluorescent growth reporter strains and mathematical methods. By calculating peakwidth and coefficient of variation (CV) of the population distributions, information on the spread of the population was obtained in a quantitative manner. The slope of the cumulative distribution function (cdf) plots was used to quantify shifts over time and differences in peak shape. Together these methods offer a less arbitrary way of quantifying flow cytometry data and population heterogeneity.

Keywords: Population heterogeneity, glucose pulse, reporter strain, freezing effect, flow cytometry

6.1 Introduction

The optimization of industrial cultivation processes requires a comprehensive analysis and understanding of the physiology of the host strain throughout the cultivation. Traditionally, this is performed on averaged cell characteristics from samples containing millions of cells[1,2]. However, microbial cells exhibit an intrinsic cell-to-cell variability that is influenced by the cultivation parameters but also in itself affect the overall performance of the process[3]. In addition, large scale

cultivations introduce spatial heterogeneity through gradients of e.g. dissolved oxygen, substrate, temperature and pH exposing microbial cells to rapid changes in environmental conditions as they circulate throughout the reactor[4,5]. These dynamic conditions pose metabolic stress on the cells, which affects their metabolism and the inherent population heterogeneity[6]. Although this heterogeneity has been found to be harmful for cultivation processes by reducing yields and increasing by-product formation, there are also indications that it may be beneficial as it facilitates a quick adaption to novel conditions[2,7,8]. Transient metabolic responses of microorganisms to rapid changes in nutrient availability have been addressed in several studies based on average population data[9–12]. It has been shown that external perturbations can have many deleterious effects such as disturbing optimal enzyme activity levels and metabolic fluxes, destabilizing cellular structures, affecting chemical gradients and the intracellular pH. But, it has also been shown, that it can lead to higher stress tolerance especially in slow growing cells[4,13–16]. The concomitant stress responses that follow a perturbation are typically transient at the gene expression level and lead to new steady state levels similar to pre-perturbation conditions even in the presence of a persistent stress[17]. The magnitude and duration of the transcriptional responses correspond with the duration and magnitude of the perturbation[18,19]. Although stress responses upon perturbation have been studied, little is known about how changing environments affect population heterogeneity or how different subpopulations contribute to the cultivation process[3].

We have previously looked into how population heterogeneity of batch grown *S. cerevisiae* cells is affected by freeze-thaw stress by comparing the GFP fluorescence, cell size as well as morphology of fresh and frozen cells[6]. Whereas the cell size did not change, clear differences were seen in the GFP fluorescence including the formation of subpopulations that were not present in fresh samples. Especially cells in the exponential growth phase on glucose were susceptible to freeze-thaw damage, while the slower growing cells in the ethanol growth phase were far more resilient[6]. This was in accordance with literature where, in general fast growing cells are found to be more susceptible to freeze-thaw stress[20], whereas slower growing cells tend to redistribute cellular resources towards stress tolerance functions[14,21,22].

The aim of the present study was to gain deeper insight into how microbial population heterogeneity related to growth and cell membrane robustness is influenced by growth rate and changing nutrient availability, hence verifying the effect of industrial-like fluctuating conditions on cell physiology. To enable this, reporter strains for the industrially relevant model organisms *S.*

cerevisiae[6] and *E. coli*[23] were employed and the cell responses analysed and mathematically quantified at single cell resolution. The reporter systems are based on expression of green fluorescent protein (GFP) coupled with ribosomal or ribosomal related promoters as these type of promoters normally are considered to be related to growth and translational activity[24]. The *S. cerevisiae* reporter system (FE440) may in addition be used for analysis of cell membrane robustness as a loss of GFP signal in cells has been seen to be coupled with permeabilised cell membranes[6]. This dual reporter feature makes the reporter strain an interesting tool for further investigations of cell robustness and growth responses to changes in nutrient availability. The *E. coli* reporter system (MG1655/pGS20fisGFPAAV) was selected based on its ability to rapidly respond to changing environmental conditions, avoiding a 'memory' effect on the evolution of gene expression as seen in a prior investigation[23]. Furthermore, it has been demonstrated that the behaviour of both reporter systems depends on the operating mode of the bioreactor[6,25]. The state of the individual cells is reflected in the expression of the reporter protein, which can be followed by its fluorescence by using flow cytometry. Furthermore, by applying freeze-thaw stress prior to flow cytometry analysis, membrane robustness can be examined.

The use of flow cytometry generates large amounts of data as it enables the analysis of thousands of cells per second acquiring and recording big amounts of data related to several different properties (as forward scatter, side scatter and fluorescence) per cell. However, data collected in this way are generally illustrated as single parameter histograms or in plots where two parameters are correlated, such as biplots, scatterplots or contourplots[26,27]. This makes data interpretation subjective and it becomes difficult to compare samples. Here we present new tools to quantify population heterogeneity using a combination of reporter strains and mathematical methods.

6.2 Materials and Methods

S. cerevisiae reporter strain FE440[6] and *E. coli* MG1655/pGS20PfisGFPAAV[23] were used throughout this study. The integrated *S. cerevisiae* reporter system (FE440) is based on expression of the stable eGFP, exhibiting a bright signal, under the control of the ribosomal RPL22a promoter[6]. The *E. coli* reporter system (MG1655/pGS20fisGFPAAV) is of a slightly different nature using the *fis* promotor to express an unstable green fluorescent protein from a low copy number plasmid[23]. The *fis* promoter controls the expression of a transcriptional activator that in turn activates the bacterial ribosomal promoter *rrnB* P. The destabilized GFPAAV variant of GFP was chosen as it

permits the observation of rapid downshifts, however, a plasmid based expression system was deemed necessary to achieve a sufficiently high GFP fluorescence[23]. In all *E. coli* cultivations, 25 μg/mL of chloramphenicol (stock concentration: 50 mg/ml in 96% ethanol) was added to the medium to keep the selection pressure.

6.2.1 Cultivation conditions

Pre-culture. *S. cerevisiae*: A single colony was picked from a plate with minimal medium and used to inoculate a 0.5 L baffled shake flask with 100 ml of defined mineral medium containing 7.5 g/L $(NH_4)_2SO_4$, 14.4 g/L KH_2PO_4, 0.5 g/L $MgSO_4*H_2O$, 2 ml/L trace metal solution, 1 ml/L vitamin solution and 10 g/L glucose [28]. The pre-culture was incubated in an orbital shaker at 150 rpm and 30°C until mid-exponential phase (approximately 10 h) and directly used for inoculation.

E. coli: The *E. coli* inoculum was obtained by a two-step procedure. First, a single colony from a fresh LB plate was used to inoculate a 100 mL Luria-Bertani broth containing shake flask at 37ºC and was grown overnight. A serial dilution with 10-fold steps was then prepared from the overnight culture and the tubes were incubated at 37ºC for 6 to 8 hours in an orbital shaker (180 rpm). The optical density was subsequently measured and the tube grown to an OD_{600} between 0.4 and 0.6 was used to inoculate the bioreactors.

Chemostats. *S. cerevisiae*: Aerobic, glucose-limited, level-based chemostats with 5 different dilution rates (D= 0.05/0.1/0.2/0.25/0.3 h^{-1}) were performed in duplicates using 1 L bioreactors (Sartorius, B. Braun Biotech International, GmbH, Melsungen, Germany) with a working volume of 1 L. pH and DOT electrodes (Mettler Toledo, OH, USA) were calibrated according to standard procedures provided by the manufacturer using two point calibration (pH 4 and 7, gassing with oxygen (100%) and nitrogen (0%), respectively). The growth medium was a defined mineral medium according to Verduyn *et al.* (1992)[28] with 5 g/L glucose. The OD_{600} for inoculation was 0.001. The pH was adjusted and kept constant at 5.0 using 2 M NaOH. Temperature, aeration and stirring were kept constant at 30°C, 1 v/vm and 600 rpm.

E. coli: Glucose-limited chemostat cultures were inoculated with an OD_{600} of 0.01 and operated at 37 °C in the same bioreactor setup as for yeast but with a working volume of 0.6 L. The growth medium was a defined mineral medium[29] containing 4.5 g/L glucose, 2 g/L Na_2SO_4, 2.468 g/L $(NH_4)_2SO_4$, 0.5 g/L NH_4Cl, 14.6 g/L K_2HPO_4, 3.6 g/L $NaH_2PO_4*H_2O$, 1 g/L $(NH_4)_2$-H-Citrate, 50

µL Sigma 204 Antifoam and 0.1 g/L thiamine. After autoclavation, 3 mL $MgSO_4$, 1 mL trace metal solution and 25 µg/ml chloramphenicol (stock concentration: 50 mg/L, diluted in 96 % ethanol) was sterile filtered (0.2 µm) into the medium. The trace metal solution contained 0.5 g/L $CaCl_2*H_2O$, 0.18 g/L $ZnSO_4*7H_2O$, 0.1 g/L $MnSO_4*H_2O$, 20.1 g/L Na_2EDTA, 16.7 g/L $FeCl_3*6H_2O$, 0.16 g/L $CuSO_4*5H_2O$ and 0.18 g/L $CoCl_2*6H_2O$. Aeration and agitation speed were kept constant at 1 v/vm and 1000 rpm to avoid oxygen limitation.

The batch phase of both yeast and *E. coli* cultivations was followed by OD_{600} measurement for determination of biomass concentration and continuous analysis of the off-gas composition by a Mass spectrometer (Prima Pro Process MS, Thermo Fisher Scientific, Winsford UK). After glucose depletion, detected as a rapid drop in the CO_2 content of the off gas, the cultures were switched to chemostat mode by applying a feed with the same medium as used for the batch with the flow rate set to achieve the desired dilution rate. The volume was kept constant by a level based outlet. Steady state was considered established when dry weight, dissolved oxygen tension (DOT) and exhaust gas concentration (CO_2) had remained constant for at least three residence times. After confirming steady state, all cultures were perturbed by addition of a concentrated glucose solution corresponding to a final bioreactor concentration of 1 g/L for *S. cerevisiae* and 0.45 g/L for *E. coli*. After addition of glucose the cultivations were followed by frequent sampling (sampling time depending on the organism, see result section).

Samples were withdrawn for OD_{600}, high performance liquid chromatography (HPLC), dry weight (DW) and flow cytometry analysis. Samples for OD_{600} and DW were analysed directly, HPLC samples were sterile filtered and stored at -20 °C. Samples for flow cytometry were mixed with glycerol to a final concentration of 15% and frozen and stored in a -80 °C freezer. For yeast, flow cytometry analysis was also performed on fresh samples for two of the dilution rates (D= 0.05 h^{-1} and 0.3 h^{-1}), where broth was mixed with 15% glycerol and kept on ice until analysis (maximum one hour).

6.2.2 Freezing test of *E. coli* samples

A freezing test was performed in shake flasks using the same minimum medium as in chemostat cultivation. Triplicate samples were collected from each growth phase and each sample was divided into three sub-samples: one was measured directly, one flash frozen in liquid nitrogen with 15%

glycerol and one more slowly frozen in a -80°C freezer, also with 15% glycerol. To avoid non-desirable degradation during the sample treatment, 20 samples were thawed at a time, then centrifuged, and re-suspended in 0.9% NaCl. The maximum lag time between the first and the 10th analysed sample was 10 min, during which it was assumed that the intracellular GFP concentration was not influenced by the sample preparation. This was verified by re-analysing the first sample after the last, givingidentical results.

6.2.3 Sample analysis

OD, DW and HPLC. Growth was monitored by measuring the OD_{600nm} with a Shimadzu UV mini 1240 spectrophotometer (Shimadzu, Kyoto, Japan). Dry weight measurements were performed on 5 mL cultivation broth according to Olsson and Nielsen (1997)[29]. The concentrations of glucose, acetate, ethanol, glycerol and pyruvate in the broth of the *S. cerevisiae* cultivations were determined by HPLC as earlier described by Carlquist *et al.* (2012)[6]. The *E. coli* cultivations were in addition analysed for lactate and formate, and the glucose concentration was measured by an enzymatic (hexokinase) colorimetric procedure (ABX Pentra Glucose HK CP).

Flow cytometry. A FACSAria™ III (Becton-Dickinson, NJ, USA) flow cytometer was used for single-cell analysis of both yeast and bacteria. Excitation wavelength for the laser was set to 488 nm. Two scattering channels (FSC and SSC) and one fluorescent detection channels were used in the analysis. Fluorescence emission levels were measured using a band pass filter at 530±30 nm. Light scattering and fluorescence levels were standardised using 2.5 µm fluorescent polystyrene beads. Samples for flow cytometry were kept on ice (fresh cells) respectively thawed on ice (frozen cells), afterwards centrifuged for 1 min at 3000 g and 4 °C, resuspended in 0.9 % saline solution and directly analysed. *E. coli* cells used for investigation of pH effects on GFP fluorescence were instead resuspended in 100 mM phosphate buffer at either pH 5.5 or pH 7, incubated 20 minutes at room temperature and kept on ice until analysis. 20,000 and 30,000 events were recorded for yeast and *E. coli* respectively. CS&T beads (Cytometer Setup and Tracking beads) (Becton Dickinson, USA) were used for the automated QA/QC of the machine performance.

6.2.4 Data analysis

Processing and analysis of the flow cytometry raw data was performed using MatLab ® R2010b (The MathWorks, Inc., Natick, MA, USA). The raw data was extracted as fcs files and loaded into MatLab with the help of the readfsc function (by L. Balkay, University of Debrecen, Hungary,

available on MatLab central file sharing). The HPLC data was collected in an excel file and imported into MatLab. The data from the fcs files was extracted and saved into mat files including the recorded GFP fluorescence and the FSC for each steady state and pulse experiment. The cumulative cell distribution function (cdf) from the 1024 recording channels of the flow cytometer was fitted to the data of the GFP fluorescence using the hist function, and afterwards applying the cdfplot function. By applying the hist function to the 1024 recording channels cell count was saved for all channels and plotted as channel number fluorescence for the GFP detector. Biplots for FSC and GFP were created using this function. For achieving better quantitative data for the distributions of GFP, the peakwidth at baseline level was calculated by searching for the borders of the peak, which were considered as at least 25 cell counts per channel number to disregard the noise level of the flow cytometer. By subtracting the channel numbers for the higher and lower border the peakwidth was determined. Furthermore, the mean function was used to calculate the Mean FSC and Mean GFP fluorescence. The normalized GFP was estimated by dividing the mean GFP by the mean FSC. By dividing the peakwidth by the Mean GFP the coefficient of variance (CV) of the distribution was generated. Finally the slope of the cdfplot was estimated by fitting a line to the exponential part of the cumulative distribution of the GFP fluorescence histograms by using the polyfit function with a degree of one. For frozen pulse samples the sub-population percentage was computed by dividing the histogram plot into three areas, a low, middle and a high fluorescent area. The areas were set in relation to the local minimum in the histogram between two sub-populations, which was calculating using the min function. The middle fluorescence range was excluded to avoid biased data and then the sub-population percentage in the low and high range was calculated by dividing the cell amount in the sub-population by the total cell amount found in the two fluorescence ranges. As a result of having duplicate datasets for all samples, all values and estimated parameters were stated showing replicates.

Table 1 - List of abbreviations

Symbol	Description	Unit
Cdf	Cumulative distribution function	-
CV	Coefficient of variation	[%]
D	Dilution rate	h^{-1}
FSC	Forward Scatter	-
GFP	Green flourescent protein	-
$\mathbf{r_S}$	Specific substrate uptake rate	[g glucose/g cells /h]
$\mathbf{r_{Ethanol}}$	Specific ethanol production rate	[g ethanol/g cells /h]
RT	Residence time	[h]
SSC	Side Scatter	-
$\mathbf{Y_{SX}}$	Growth yield on the fed substrate	[c_{mole}/c_{mole}]
$\mathbf{Y_{SCO2}}$	Yield of CO_2 on the fed substrate	[c_{mole}/c_{mole}]
$\mathbf{Y_{SEth}}$	Yield of ethanol on the fed substrate	[c_{mole}/c_{mole}]
$\mathbf{Y_{SGly}}$	Yield of glycerol on the fed substrate	[c_{mole}/c_{mole}]
$\mathbf{Y_{SAce}}$	Yield of acetate on the fed substrate	[c_{mole}/c_{mole}]
$\mathbf{Y_{spyr}}$	Yield of pyruvate on the fed substrate	[c_{mole}/c_{mole}]

6.3 Results

To investigate the influence of growth rate and glucose excess on microbial population heterogeneities in growth and cell membrane robustness, glucose pulses were introduced to glucose-limited continuous cultivations with *S. cerevisiae* reporter strain FE440[6] and *E. coli* reporter strain MG1655/pGS20PfisGFPAAV[23] after characterization of steady state.

Cultivations with both low and high dilution rates were performed to compare responses of cells in fully respiratory versus respiro-fermentative growth. The low dilution rates corresponded to approximately 13% of the maximum specific growth rate (i.e. D = 0.05 and 0.1 h^{-1}) and the high dilution rates to about 77% (D = 0.3 and 0.51 h^{-1}) for *S. cerevisiae* and *E. coli*, respectively. In addition, an additional dilution rate, 0.36 h^{-1}, which roughly corresponded to the rate where overflow metabolism sets in in *E. coli* [30] as well as three dilution rates in between high and low for yeast, were included in the evaluation to further examine the influence of growth rate.

6.3.1 Physiology and GFP fluorescence distribution for *S. cerevisiae* cells at steady-state conditions

To ensure the accuracy of the performed *S. cerevisiae* cultivations, the yields on glucose for steady state yeast cultivations were calculated for cell mass, CO_2, ethanol and acetate as well as the uptake and production rate of glucose and ethanol, all shown in table 2. Carbon balances were calculated from the yield coefficients to confirm data consistency.

Table 2 - Yields (ratios of cell mass, CO_2, ethanol and acetate produced on amount of consumed substrate) and carbon balances, as well as consumption respectively production rates for glucose and ethanol for aerobic glucose-limited continuous cultivations of *S. cerevisiae* FE440 at different dilution rates (D= 0.05/0.1/0.2/0.25/0.3 h^{-1}). All data are presented as mean values including standard deviations and originate from two independent cultivations and include samples taken over a minimum of three distinct residence times.

Chemostat parameter	**D=0.05 h^{-1}**	**D=0.1 h^{-1}**	**D=0.2 h^{-1}**	**D=0.25 h^{-1}**	**D=0.3 h^{-1}**
Y_{SX} [cmole/cmole]	0.58±-0.02	0.56± 0.06	0.60± 0.01	0.35± 0.02	0.22± 0.01
Y_{SCO2} [cmole/cmole]	0.53± 0.02	0.40± 0.04	0.38± 0.01	0.35± 0.01	0.27± 0.01
Y_{SEth} [cmole/cmole]	-	-	-	0.22± 0.01	0.42± 0.01
Y_{SAce} [cmole/cmole]	-	-	-	-	0.01± 0.00
r_S [g/gh]	0.10± 0.01	0.20±0.02	0.38± 0.00	0.82± 0.05	1.61± 0.05
$r_{Ethanol}$ [g/gh]	-	-	-	0.16± 0.00	0.52± 0.00
Carbon balance	**1.11± 0.05**	**0.96± 0.10**	**0.98± 0.01**	**0.94± 0.03**	**0.92± 0.01**

For the dilution rates below D = 0.25 h^{-1} the yield on biomass, Y_{SX}, was around 55-60%, which is consistent with literature data for respiratory metabolism[31]. No accumulation of metabolites was detected indicating an absence of overflow metabolism, which is in accordance with earlier observations[32]. For the two higher dilution rates (D = 0.25 h^{-1} and 0.3 h^{-1}) Y_{SX} was significantly lower and accompanied by accumulation of ethanol as well as small amounts of acetate at the highest dilution rate (D = 0.3 h^{-1}), also seen in Diderich *et al.* (1999)[33]. These results were in agreement with previous results where the onset of respiro-fermentative metabolism for CEN.PK113-7D was found to be 0.28 h^{-1} [34]. The Y_{SCO2} decreased with increasing dilution rate, whereas r_S as well as $r_{Ethanol}$ increased, which are results that are also in agreement with Postma *et al.* (1989)[32] and Van Hoek *et al.* (1998)[34]. In general, all yields showed low standard deviations and confirmed steady state on the physiological level as well as high reproducibility between replicates.

Carbon balances for all the cultivations closed within a maximum error of 6% apart from the highest and lowest dilution rates, where a deviation of 8 respectively 11% was found. This variation in the carbon balance could be explained by a slightly higher, respectively lower, biomass yield compared to earlier studies and as well that there was no glycerol produced[34,35].

Using flow cytometry the distribution for the GFP fluorescence as well as morphological and cell size parameters (FSC and SSC) were investigated using freshly harvested cells. The GFP fluorescence versus forward scatter (FSC) distributions (figure 1 A and B) for the two dilution rates, D= 0.05 h^{-1} and D= 0.3 h^{-1}, had slightly different subpopulation distributions for the GFP fluorescence. Both dilution rates varied within an interval of 100-600 fluorescence channel numbers and had cells grouped into two subpopulations, high and low fluorescence, respectively. However, the high fluorescence subpopulation covered a broader fluorescence range in the 0.05 h^{-1} cultivations (approx. 300-600 compared to 400-600 fluorescence channel numbers). FSC, which usually correlates with particle size, stayed within a range of 800-1000 for the majority of cells at both dilution rates. However, at D=0.05 h^{-1} a minor subpopulation with smaller cell size (FSC=300-600) was observed.

To facilitate an unbiased, quantitative interpretation of the heterogeneous responses seen in the study we decided to introduce additional parameters describing population heterogeneity in growth and cell robustness. These parameters were: coefficient of variation (CV) for mean GFP, peakwidth and the slope of the cumulative distribution curve (table 3). The mean fluorescence can hereby describe general trends of the averaged GFP distribution. Additionally, the peakwidth at baseline level as well as the CV, which is calculated by dividing the mean fluorescence by the peakwidth, can be used to describe the spread and variation of the population. By considering the slope of the cumulative distribution, hints about potential subpopulations can be provided.

In general, fluorescence distributions for cells grown at high dilution rates were more narrow and distinct, compared to cells grown at low dilution rates (figure 1E and F), which was confirmed by the peakwidth value (table 3). Also, the lower dilution rates showed more variation in the distribution, which indicates a higher degree of population heterogeneity. Using the other way to quantify the heterogeneity of the cell fluorescence by plotting the cumulative distribution and calculate the value of its slope (cdf-plot, figure 1G and H and table 3). A lower slope was seen for D=0.05 h^{-1} (0.0062 +/- $2.2 \cdot 10^{-4}$ compared to 0.0095+/- $5.2 \cdot 10^{-4}$ for 0.3 h^{-1}). This indicates a broader

distribution for the low dilution rate. The mean GFP fluorescence was slightly higher for the higher dilution rate, 456.9+/- 28.3 and 464.6+/- 20.3 fluorescence channel numbers, for D=0.05 and 0.3 h^{-1}, respectively. After normalizing mean GFP fluorescence with mean cell size, i.e. fluorescence per cell size unit, the value obtained for D= 0.05 h^{-1} (0.49) and D= 0.3 h^{-1} (0.50), were almost the same, which indicated that the observed difference in fluorescence was related to differences in cell size.

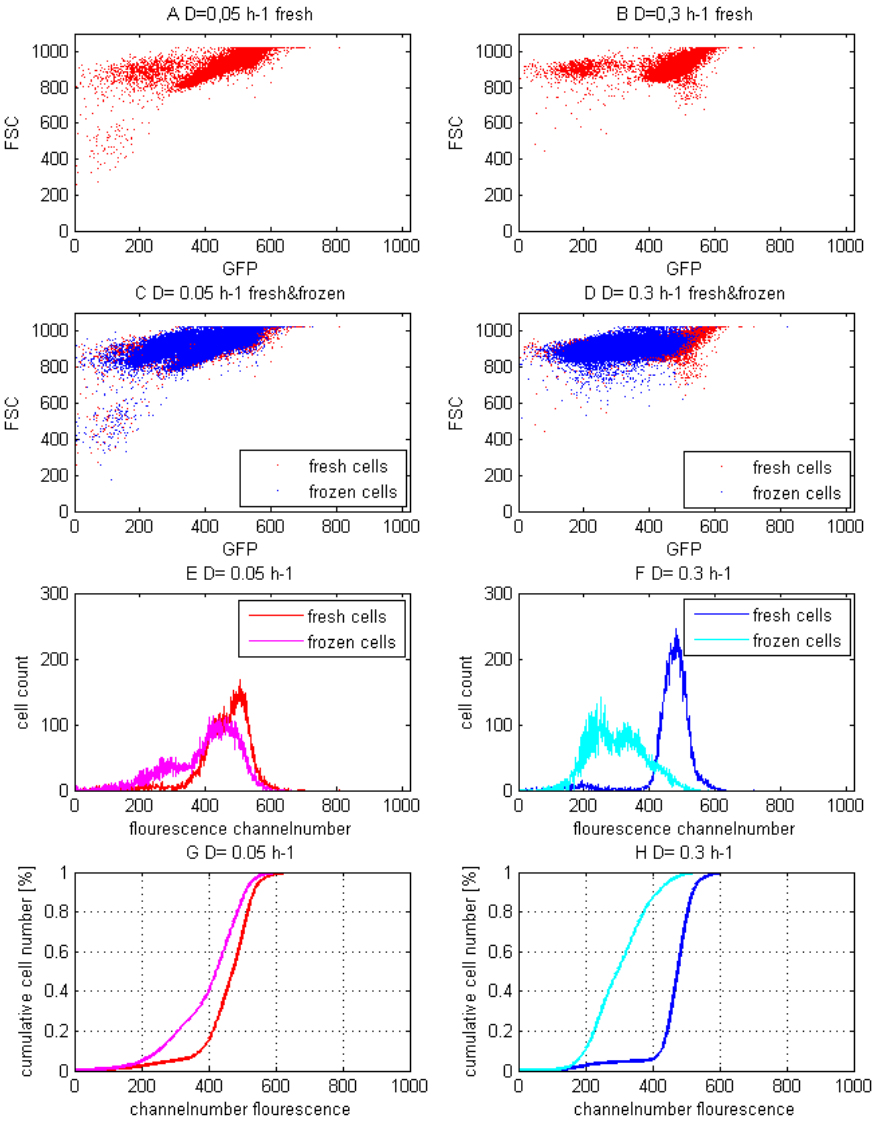

Figure 1 - Fluorescence and size distributions for fresh and frozen yeast cells at steady-state conditions: Biplots for FSC against GFP for fresh cells grown at D= 0.05 h^{-1} (A) and D= 0.3 h^{-1} (B) and for comparison between fresh and frozen cells for both dilution rates (C and D). Also GFP fluorescence represented as cell count against channel number fluorescence (E and F) and cdfplots of cumulative cell number against channel number fluorescence (G and H) for D= 0.05 h^{-1} and D=

0.3 h^{-1} for fresh and frozen *S. cerevisiae* FE440 cells in steady state in aerobic glucose-limited chemostat. All plots represent average values from samples taken after three different residence times.

Table 3 - Heterogeneity at steady state conditions for fresh yeast cells: quantitative values for measure of GFP fluorescence heterogeneity for D= 0.05 h^{-1} and D= 0.3 h^{-1} represented as Mean GFP with the corresponding CV, the slope of cdf plots and peakwidth.

Parameter	**0.05**	**0.3**
Mean GFP	456.9± 28.3	464.6± 20.3
CV GFP	0.18	0.16
Slope cdf plot	$0.0062\pm 2.2\cdot10^{-4}$	$0.0095\pm 5.2\cdot10^{-4}$
Peakwidth	271± 15.6	227± 42.4

6.3.2 Cell membrane robustness for cells from steady state conditions

The *S. cerevisiae* reporter allows the identification of subpopulations with high and low membrane robustness to freeze-thaw stress as an inverse correlation of GFP signal to membrane integrity has been found[6].

Thus, the application of freeze-thaw stress made it possible to obtain more information on the robustness characteristics of the population in the bioreactor.

The main underlying reason for reduced cellular florescence after freezing was suspected to be a reduction in GFP fluorescence due to a shift towards lower intracellular pH due to leaking membranes and the low extracellular pH, which was kept at 5. However, actual loss of intracellular GFP may also be a cause. To evaluate the mechanism further yeast cells were permeabilised with Amphotericin B followed by incubation in buffers with different pH before flow cytometery analysis. Amphotericin B is an antifungal drug, which binds with ergosterol in the cell membranes, thereby forming transmembrane channels[36]. These channels allow ion leakage, but are too small for proteins to pass. Flow cytometry analysis of the permeabilised yeast cells exhibited a linear decrease in fluorescence as the external pH dropped below 7 (data not shown). As the values obtained for incubations with a buffer at pH 5 were equal to those seen for frozen cells, it was

concluded that the reduction in fluorescence caused by freezing is dominated by changes in intracellular pH.

To investigate how growth rate affects membrane integrity, samples from the five dilution rates D=0.05/0.1/0.2/0.25/0.3 h^{-1} were frozen in 15% glycerol at -80°C before flow cytometry analysis and compared to data from fresh cells.

Cells growing at high and low dilution rates were differently affected by freeze-thaw stress, as can be seen from the FSC-GFP biplots and fluorescence histograms in figure 1C-F. For D = 0.05 h^{-1} the shape of the distribution as well as the fluorescence range remained the same after freezing and only a slight increase in the lower fluorescence population was seen. However, for D = 0.3 h^{-1} the fluorescence shifted considerably towards lower values and the fluorescence distribution also broadened. As a result, the mean GFP fluorescence remained almost constant after freezing for D= 0.05 h^{-1} (409.0 +/-14.3) but decreased for the high dilution rate to 295.4 +/- 6.9 (highlighted with red circles in figure 2). This leads to the conclusion that cells growing with a low growth rate (D= 0.05 h^{-1}) are more robust towards freeze-thaw stress.

To further investigate how growth rate influences freeze-thaw stress tolerance and the level of population heterogeneity; mean GFP, mean GFP normalized by cell size as well as CV of mean GFP, the slope of the cdf plot and the peakwidth were calculated for all 5 dilution rates and plotted in figure 2. Similar mean GFP fluorescence (figure 2A) was found for frozen cells from all dilution rates, except for D= 0.05 h^{-1}, where the mean fluorescence was higher. From FSC data it was seen that the cell size decreased with increasing growth rate until the respiro-fermentative metabolism sets in, after which it sharply increased (data not shown). To remove the effect of cell size on mean fluorescence, the fluorescence was normalized with cell size. A steep increase in the normalized mean GFP was seen when going from 0.05 to 0.1 h^{-1}. Thereafter, the value remained almost constant for growth rates up to where respiro-fermentative metabolism sets in (0.25 h^{-1}). Interestingly, above this growth rate, the normalized GFP fluorescence decreased sharply.

The CV of the GFP distribution, which indicates the level of population heterogeneity, showed a similar but opposite trend with a higher level of heterogeneity for D=0.05 and D=0.3 h^{-1} than the dilution rates in between. In general, GFP fluorescence distributions for cells grown at 0.1 h^{-1} and 0.2 h^{-1} were more narrow (peakwidth, figure 2B). This can be seen in the cdfplots whose slopes were highest for D= 0.1 h^{-1} and lower for 0.2 and 0.25 h^{-1} (figure 2B). For D= 0.05 h^{-1} and 0.3 h^{-1}

the GFP fluorescence distribution was broader, resulting in higher peakwidths compared to the other dilution rates.

Though the peak characteristics are different for D = 0.05 h^{-1} and 0.3 h^{-1}, the slope of the cdfplots were similar for these two growth rates (figure 2B). Compared to fresh cells (figure 1E), the distribution for frozen cells grown at 0.05 h^{-1} was broader with a more distinct low fluorescent subpopulation, though keeping the same shape, resulting in a similar value of the slope of the cdfplot. For a diltuion rate of 0.3 h^{-1} the slope of the cdfplot for frozen cells was considerably lower and the shape of the distribution changed with broad tailing towards higher fluorescence and a division into two distinct subpopulations (figure 1F).

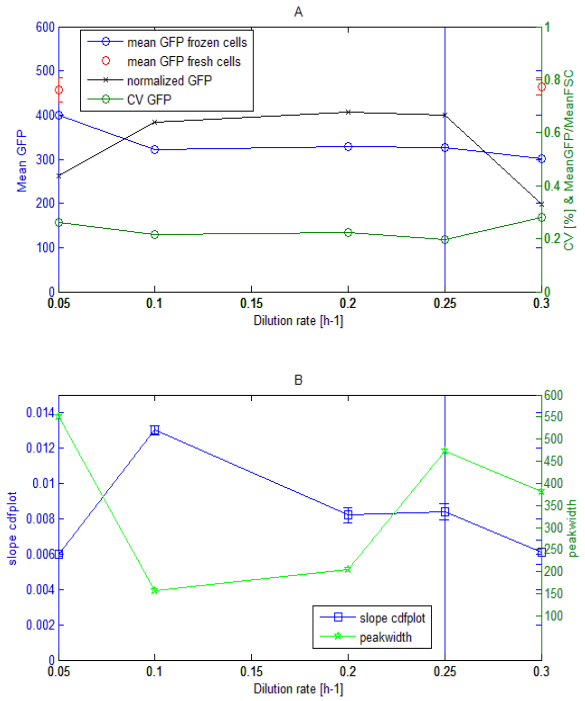

Figure 2 - The effect of growth rate on fluorescence and heterogeneity for yeast cells exposed to freeze-thaw stress: Mean GFP fluorescence distribution as well as GFP fluorescence normalized by cell size together with the corresponding coefficient of variance (A) as well as the peakwidth and the slope of the cdfplot (B) for *S. cerevisiae* cells at steady-state conditions in aerobic glucose-limited chemostat for D= 0.05 h^{-1}, 0.1 h^{-1}, 0.2 h^{-1}, 0.25 h^{-1} and D= 0.3 h^{-1}. The plots represent average values from samples taken after three different residence times. The blue line in both plots indicates the critical dilution rate where respiro-fermentative metabolism sets in.

In order to investigate population heterogeneity dynamics after a glucose perturbation of a steady state culture, single cell analysis of samples frequently taken following the pulse using flow cytometry was applied. The physiological responses as well as the distribution of individual cell responses are presented in the following two sections.

6.3.3 Influence of glucose perturbation on *S. cerevisiae* physiology and GFP fluorescence heterogeneity

A glucose pulse of 1 g/L was introduced to the steady states at the different dilution rates and FSC, GFP fluorescence and HPLC data were recorded over the duration of each perturbation.

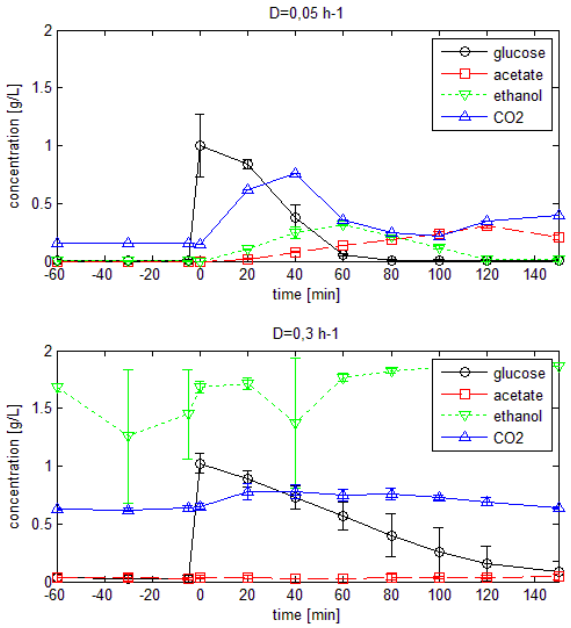

Figure 3 - Time profiles of physiological response: to a 1 g/L glucose pulse in aerobic glucose-limited chemostats of *S. cerevisiae* growing with a dilution rate of 0.05 h^{-1} (top) and 0.3 h^{-1} (bottom). Glucose (g/L, black), CO_2 (v/v %, blue), ethanol (g/L, green) and acetate (g/L, red) concentrations are shown during the duration of the perturbation.

The lower dilution rates, 0.05 h^{-1} (figure 3) as well as 0.1 h^{-1} and 0.2 h^{-1} (data not shown) displayed a batch like behavior with a sharp increase in CO_2 production, overflow metabolism and concomitant ethanol and acetate accumulation when perturbed with a 1 g/L glucose pulse, thus corroborating what was observed by Visser *et al.* (2004)[37]. In contrast, the respiro-fermentative

chemostats (0.25 and 0.3 h^{-1}), only showed a very slight increase in CO_2 generation, consumed the extra glucose at a much slower rate and did not react with an increased ethanol or acetate production.

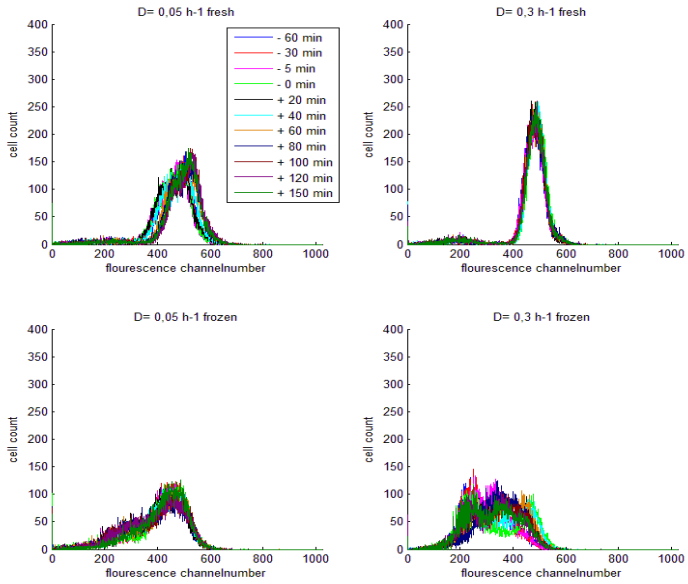

Figure 4 - Time profiles of GFP fluorescence distribution for *S. cerevisiae* fresh cells and cells exposed to freezing: GFP fluorescence represented as cell count against channel number fluorescence of *S. cerevisiae* FE440 before, during and after a 1 g/L glucose pulse in aerobic glucose-limited chemostats for D= 0.05 h^{-1} (left) and D= 0.3 h^{-1} (right) shown as comparison for fresh (top) and frozen cells (bottom). The plots represent time points between -60 min to +150 min after the pulse.

Figure 4 shows the responses of the D= 0.05 h^{-1} and 0.3 h^{-1} steady states to a 1 g/L glucose pulse with regards to GFP fluorescence. From the fluorescence histogram data for fresh cells (figure 4 top) it can be seen that the pulse caused a slight shift towards higher fluorescence for cells grown at 0.05 h^{-1}, whereas cells grown at 0.3 h^{-1} where not influenced. This is also seen in the mean fluorescence, which remained constant for the higher rate and increased for cells grown at the lower rate until around 30-40 min after the pulse (figure 5A fresh). CV and peakwidth (figure 5B and C fresh) indicated a somewhat higher heterogeneity for the low growth rate. However, there was not seen any influence from the pulse, as the values were constant over time. On the contrary, the slope of the cdfplot (figure 5D fresh) increased as a consequence of glucose perturbation for D=0.3 h^{-1}

and decreased for D=0.05 h^{-1}. The change in the slope of the cdf plot may be attributed to a decline in the low fluorescence subpopulation for cells grown at D=0.3 h^{-1} and an increase for cells grown at D=0.05 h^{-1} (see figure 4), whereas the main subpopulation remained constant. Coinciding with glucose depletion (compare with figure 3) the slope returned to the steady state value for both dilution rates.

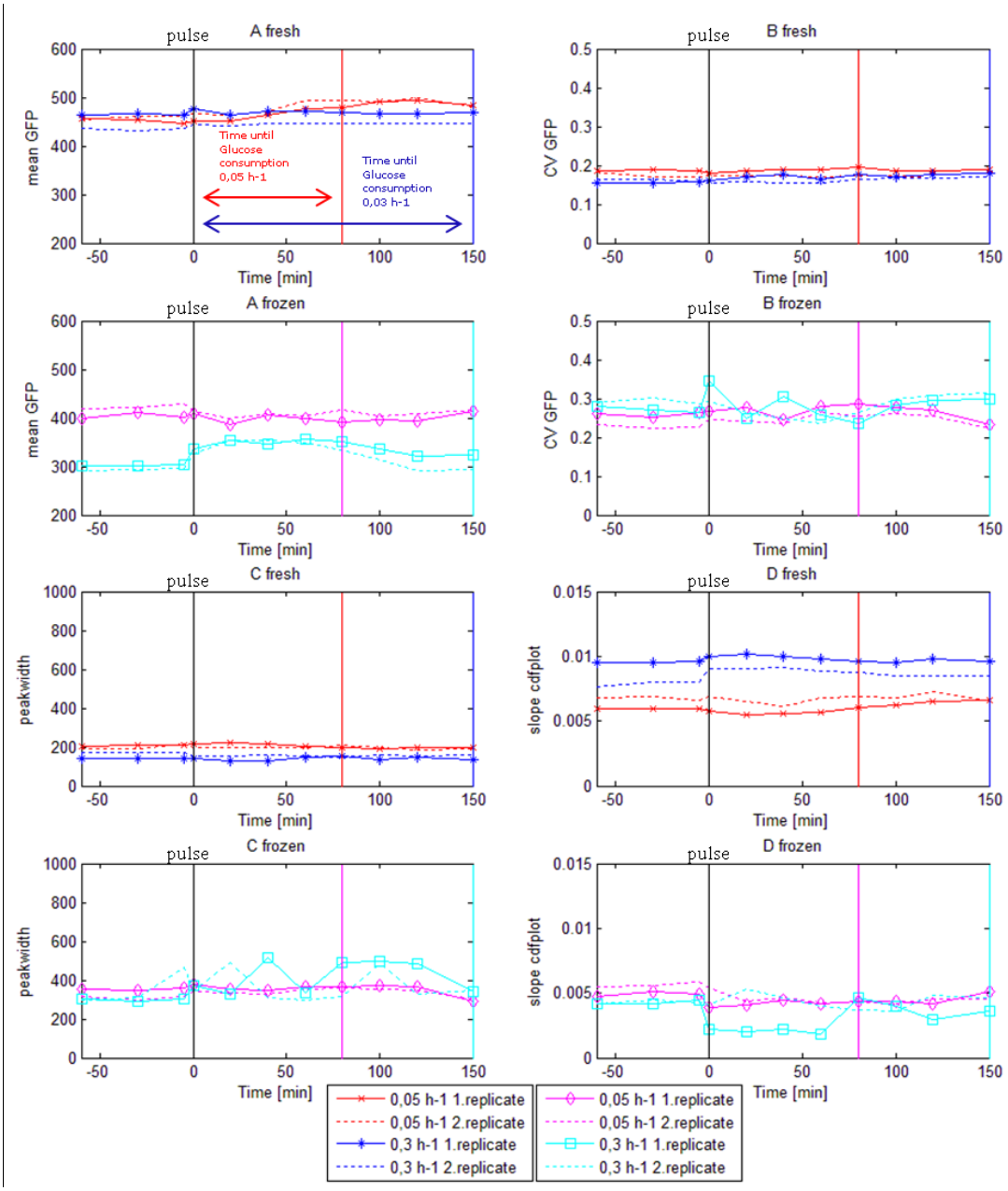

Figure 5 - Heterogeneity following glucose perturbation for fresh and frozen yeast cells: Mean GFP fluorescence (A) as well as CV of GFP fluorescence (B), peakwidth (C) and slope of the cdfplots (D) plotted against time following a 1 g/L glucose pulse for *S. cerevisiae* FE440 in aerobic

glucose-limited chemostats for D= 0.05 h^{-1} and D= 0.3 h^{-1} for fresh (red and blue) and frozen cells (magenta and cyan). The red, blue, magenta and cyan coloured vertical lines indicate the time when the pulsed glucose is consumed for the respective experiment, whereas the black line marks the time of the glucose pulse. Dotted lines represent replicate cultivations.

6.3.4 Influence on cell robustness by glucose perturbation of *S. cerevisiae* cultivations

A distinct difference could be seen after the addition of the glucose pulse when fluorescence histograms for fresh and frozen cells from D=0.05 h^{-1} and D=0.3 h^{-1} cultivations were compared. Frozen samples of cells from the 0.05 h^{-1} cultivation had similar GFP fluorescence distributions before and after the glucose pulse. Hence, glucose perturbation did not seem to have a significant influence on the membrane integrity of cells grown at the low growth rate (figure 4 and 5). In contrast, frozen samples from cells grown at 0.3 h^{-1} were significantly affected. The high fluorescence subpopulation increased as a response to the pulse (figure 4) and this was also reflected as an increase in the mean GFP value (figure 5A frozen). Even though the mean GFP of the cells grown at 0.3 h^{-1} still was more affected by the freezing compared to the mean GFP of cells grown at 0.05 h^{-1}, the addition of glucose seemed to protect the fast growing cells towards freeze-thaw stress to some extent.

In comparison to the uniform and constant population distribution seen when analysing fresh cell samples a much broader population distribution was seen for frozen cells, which got even more pronounced after the addition of a glucose pulse as seen from the values for CV, peakwidth and slope of the cdf plot (figure 4 and 5).

To further elucidate the effect of the pulse on subpopulation distribution, the relative fraction of the low and high fluorescence subpopulation was calculated at different time points (figure 6). The low fluorescence subpopulation contributed with 80% and the high fluorescence sub-population with 20% during steady-state conditions for cells grown at 0.3 h^{-1}. When glucose was added, this changed to an approximately equal distribution. For cells grown at 0.05 h^{-1}, the subpopulation distribution was unaffected by the pulse and composed of approx. 20% low fluorescence and 80% high fluorescence cells.

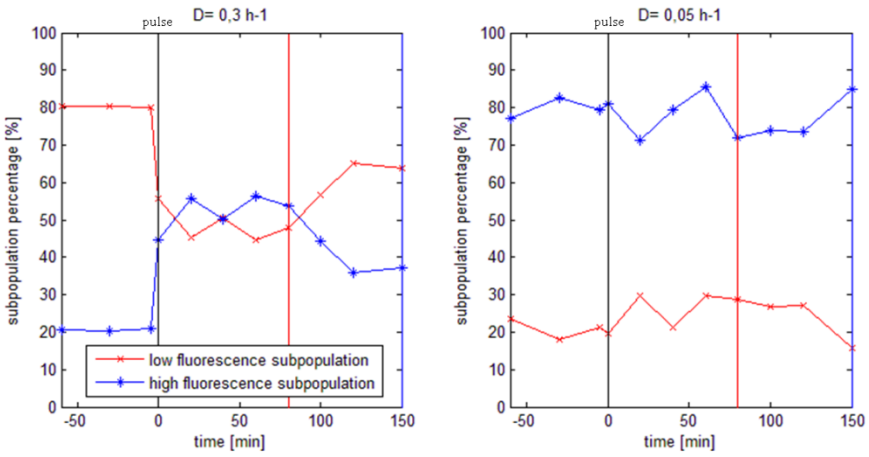

Figure 6 - Subpopulation distribution dynamics following glucose perturbation for yeast cells exposed to freezing: percentage for low (red) and high (blue) fluorescence subpopulation plotted against time following a 1g/L glucose pulse for *S. cerevisiae* FE440 in aerobic glucose-limited chemostats for frozen cells grown with D= 0.3 h^{-1} and D= 0.05 h^{-1}. The red and blue coloured vertical lines are indicating the time when the pulsed glucose is consumed in the 0.05 h^{-1} and 0.3 h^{-1} cultivations respectively. The black line is indicating the time of the glucose pulse.

6.3.5 Freeze-thaw stress as a tool to investigate membrane robustness in *E. coli* cells

The use of a GFP reporter strain in combination with freeze-thaw stress as a tool to map the distribution of membrane robustness has earlier not been applied to *E. coli* cells. Hence, to evaluate the potential with the methodology, shake flasks cultivations of the *E. coli* reporter strain were performed and samples taken for each growth phase. Flow cytometry analysis was performed on both fresh and frozen cells. To verify whether the freezing has resulted in leaky membranes and if this could be detected as a reduction in the GFP signal, cell samples for analysis of GFP fluorescence where kept in buffers at different pH ranging from pH 7.5 down to pH 5.5.

Frozen cells analysed at pH 7 displayed fluorescence patterns very similar to those seen for fresh cells, independent of growth phase and freezing method (data not shown). When analyzing at different pH the fluorescence distribution remained the same with and without freezing for *E. coli* cells analysed at a pH between 6.5 and 7.5 (figure 7). In contrast, the GFP fluorescence of freeze-thawed cells increasingly declined with lower pH when the cells were resuspended in buffers below pH 6. This behaviour is in accordance with what was seen for yeast cells and is also in agreement with the known pH dependence of GFP[38]. We consequently concluded that freeze-thaw stress is

also applicable for *E. coli* membrane robustness investigations. In the following, for logistic reasons it was decided to use the GFP measurement at pH 7 as the reference measurement for intact cells rather than to analyse on fresh cells. Hence, for analysis of membrane robustness distributions in samples from the continuous *E. coli* cultivations, all GFP fluorescence measurements were performed on frozen cells at both pH 5.5 and 7.

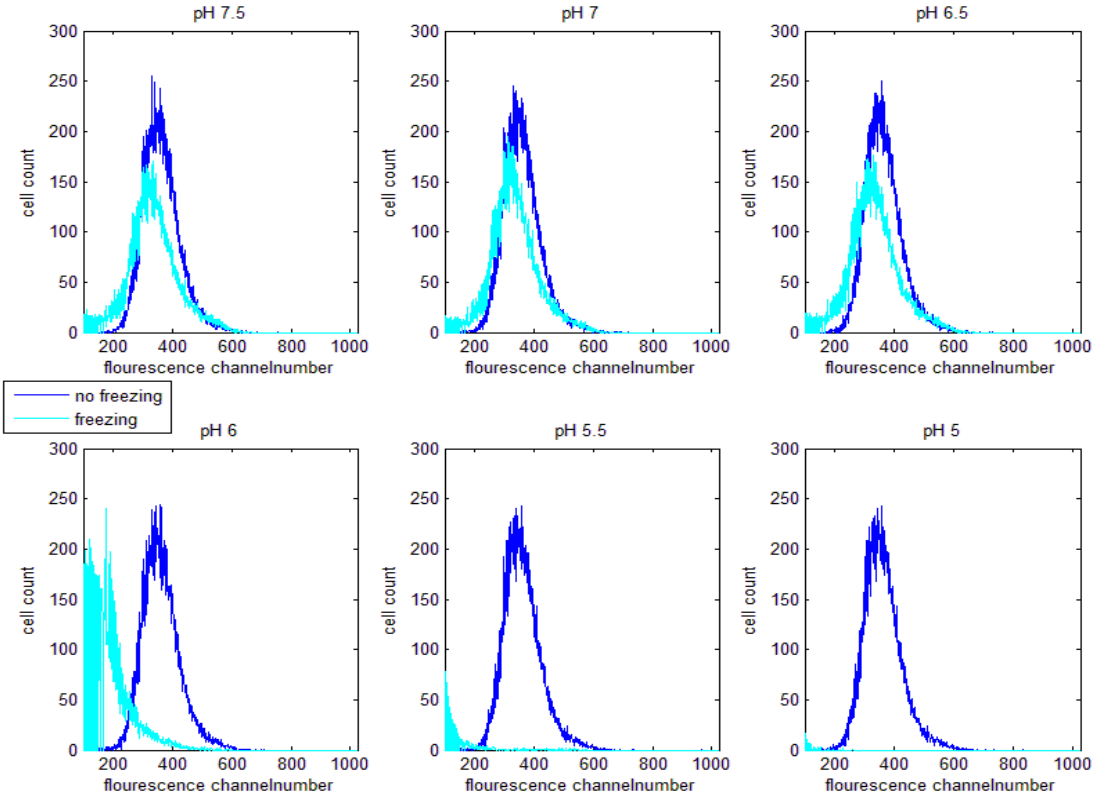

Figure 7 - Effect of freeze-thaw stress on GFP signal distribution of bacterial cells at different pH: Histogram plots for GFP fluorescence of the *E.coli* reporter strain at different pH's between 5.5 and 7.5. Each subplot shows non-frozen cells (blue) compared to frozen cells (cyan) at the same pH.

6.3.6 Physiology and GFP fluorescence distribution of *E. coli* cells at steady-state conditions

Yields on glucose for cell mass, CO_2 and all metabolites produced in significant amounts, as well as the computed uptake rate of glucose for steady state cultivations of *E. coli* are displayed in table 3. Carbon balances were calculated from the yield coefficients to confirm data consistency.

The biomass yields on glucose were about 0.44 cmole/cmole for the low dilution rate and 0.57 cmole/cmole for the higher ones. Though showing the same trend, our yields were lower than those reported in literature for *E. coli* K12 on the same medium. where an Y_{SX} of about 0.6 cmole/cmole has been reported for lower dilution rates (below 0.4 h^{-1}).The biomass yield was seen to increase with increasing dilution rate to reach a maximum of 0.69 cmole/cmole before tapering off at even higher rates[39]. Similarly to *S. cerevisiae*, at the low growth rates (D=0.1 h^{-1} and D= 0.36 h^{-1}) the *E. coli* cultivations had strictly respiratory metabolism with no acetate formation. Literature data suggests a shift to respiro-fermentative growth at a dilution rate above about 0.4 h^{-1} with concomitant acetate production [40]. However, this was not seen in the present study as only a small amount of acetate was observed for the highest growth rate (D= 0.51 h^{-1}). This observation is consistent with Qiang Hua *et al* (2004)[22] where no acetate excretion was found at detectable levels. Additionally, their biomass yields were found to be similar to our data but the CO_2 yields were comparably higher. Lactate was only seen in very low concentrations (< 0.1g/L) in the medium (data not shown), whereas formate formation was found for the higher dilution rates. Surprisingly also small amounts of glycerol were found to be produced in all tested dilution rates. The low standard deviations of the calculated yields, in addition to carbon balances closing with a maximum error of 5%, demonstrate a high data consistency in the present study.

Table 3 - Yield coefficients and carbon balance as well as glucose consumption rate at different dilution rates for aerobic glucose-limited chemostats of *E. coli* MG1655/pGS20PfisGFPAAV (+/-standard deviation). Data are presented as mean values and originate from samples taken over at least three different residence times. Each dilution rate was carried out as a biological duplicate (D=0.1 h^{-1}) or as a single measurement (D=0.36 h^{-1} and D=0.51 h^{-1}).

Chemostat parameter	D=0.1 h-1	D=0.36 h-1	D=0.51 h-1
YSX [cmole/cmole]	0.44± 0.02	0.58± 0.02	0.56± 0.02
YSCO2 [cmole/cmole]	0.49± 0.00	0.37± 0.00	0.36± 0.00
YSAce [cmole/cmole]	0.001± 0.00	0.001± 0.0005	0.003± 0.001
YSGly [cmole/cmole]	0.007± 0.002	0.003± 0.00	0.004± 0.001
YSFor [cmole/cmole]	-	0.03± 0.003	0.03± 0.001
rS [g/gh]	0.18± 0.09	0.78± 0.04	0.94± 0.00
Carbonbalance	0.95± 0.02	0.98± 0.02	0.96± 0.02

Subsequently, the effect of growth rate on GFP expression and population heterogeneity was investigated. From the FSC-GFP biplots (figure 8 A, B, C) it can be seen that the population spanned over a large FSC range (around 600 channel numbers) both for cells analysed at pH 5.5 and 7, which shifted towards higher values with increasing growth rate. A similar population distribution was seen for the GFP fluorescence at the different dilution rates (figure 8), however there was a significant difference between samples analysed at pH 5.5 and 7. Whereas intact cells (pH 7) only exhibited one fluorescent population with a narrow distribution and low CV (table 5), cells analysed at pH 5.5 showed a lower fluorescence subpopulation in addition to the main fluorescent subpopulation that resembled the one for intact cells (figure 8 D, E, F). Moreover, the low fluorescent subpopulation got more pronounced with increasing dilution rate, which can be seen in the increasing CV and peakwidth (table 5). Irrespective of the pH a slight shift in the main population towards higher fluorescence was observed for the higher growth rates (D= 0.36 h^{-1} and D= 0.51 h^{-1}). Consequently, the mean fluorescence for cells grown at the two higher dilution rates and analysed at pH 7 was higher (438.43+/-4.22 and 422.49+/-7.08) (table 5) than for cells grown at D= 0.1 h^{-1} (377.50+/-17.33). The lower peakwidth of cell distributions for cells grown at the higher growth rates of 0.36 h^{-1} and 0.51 h^{-1} indicated a lower heterogeneity in rapidly growing cells. When analysis of GFP fluorescence was performed at pH 5.5, the mean fluorescence initially increased when the dilution rate was raised from D= 0.1 h^{-1} to D= 0.36 h^{-1}, but decreased again at D= 0.51 h^{-1} which can be explained by the more pronounced low fluorescent subpopulation observed at higher dilution rates. The slope of the cdfplot (table 5) remained unchanged irrespectively of the pH used for analysis and the dilution rate at which cells where grown, confirming that the fluorescence distribution only changed in the low channel numbers whereas the shape of the main fluorescent subpopulation remained the same (figure 8).

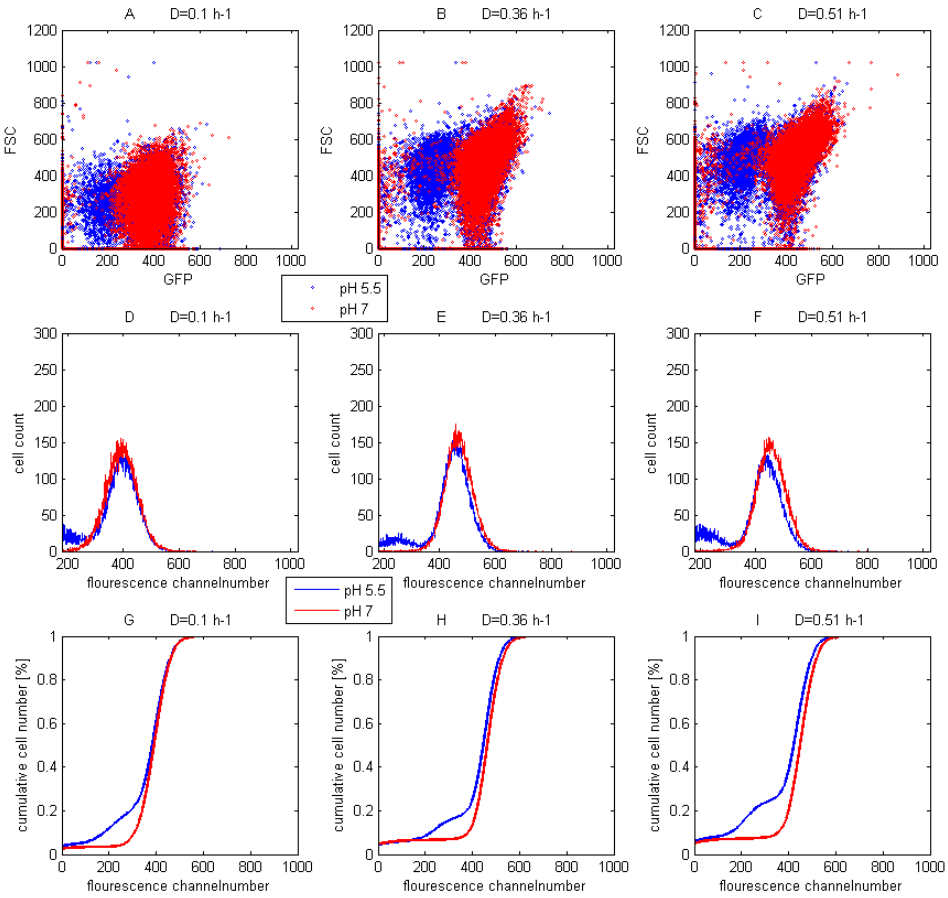

Figure 8 - Fluorescence and size distributions for frozen *E.coli* cells at steady-state conditions at pH 5.5 and 7: Biplots for FSC against GFP for frozen cells at pH 5.5 (blue) and 7 (red) grown at D = 0.1 h^{-1} (A), D = 0.36 h^{-1} (B) and D = 0.51 h^{-1} (C). Also GFP fluorescence represented as cell count against channel number fluorescence (D, E and F) and cdfplots of cumulative cell number against channel number fluorescence (G, H and I) for D= 0.1 h^{-1}, D= 0.36 h^{-1} and D= 0.51 h^{-1} frozen *E.coli* cells at pH 5.5 and 7 in steady state in aerobic glucose-limited chemostat. The plots represent average values from samples taken after three different residence times.

Table 5 - Quantitative values for population heterogeneity of GFP fluorescence: represented as CV, mean GFP, peakwidth and slope of the cdfplots and including the standard deviation for steady-states of frozen cells at pH 5.5 and 7 for D =0.1 h^{-1}, 0.36 h^{-1} and 0.51 h^{-1}, respectively.

Parameters	0.1 h^{-1}	0.36 h^{-1}	0.51 h^{-1}
Mean GFP	379.86± 29.34	407.83± 23.17	370.67± 14.53
pH 5.5	377.50± 17.33	438.43± 4.22	422.49± 7.08

pH 7			
CV GFP			
pH 5.5	0.32	0.35	0.39
pH 7	0.24	0.28	0.29
GFP peakwidth			
pH 5.5	402.67± 9.36	419.67± 17.96	444.00± 2.65
pH 7	262.23± 12.50	232.67± 4.5	230.33± 5.13
Slope of cdfplots			
pH 5.5	$0.006\pm 4.84\cdot10^{-4}$	$0.007\pm 6.04\cdot10^{-4}$	$0.006\pm 3.25\cdot10^{-4}$
pH 7	$0.007\pm 2.48\cdot10^{-4}$	$0.007\pm 1.84\cdot10^{-4}$	$0.007\pm 5.74\cdot10^{-5}$

6.3.7 Influence of the glucose pulse on physiology and GFP distribution in *E. coli* at pH 5.5 and pH 7

The responses of aerobic, glucose-limited *E. coli* cultures to sudden glucose excess were investigated by perturbing the steady-state cultures with 0.45 g/L glucose pulses. At time point zero, glucose was added and the dynamics of the extracellular metabolite and intracellular fluorescence levels followed over three hours. The pulsed glucose was depleted after 30 min for D=0.1 h^{-1} and after 37 min for both D =0.36 h^{-1} and D =0.51 h^{-1} (figure 9). No acetate formation or formation of other metabolites were detected as a consequence of the pulse at 0.1 h^{-1}, which was consistent with earlier findings for respiratory metabolism.[28] Small amounts of acetate due to overflow metabolism as well as glycerol were already present in the cultivation broth at steady-state for D=0.36 h^{-1} and D=0.51 h^{-1}.

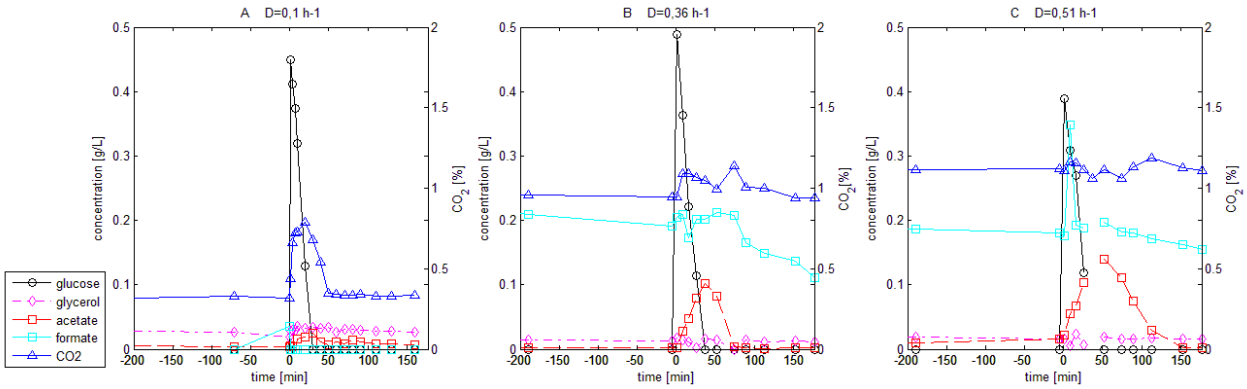

Figure 9 - Perturbation profile of *E. coli* cultivations following a 0.45 g/L glucose pulse: Profiles for aerobic glucose-limited chemostats at D = 0.1 h^{-1} (A), 0.36 h^{-1} (B), 0.51 h^{-1} (C). Glucose (g/L, black), acetate (g/L, red), glycerol (g/L, pink), CO_2 (v/v%, blue) and formate (g/L, green).

For the high dilution rates, D =0.36h^{-1} and D = 0.51h^{-1}, the acetate concentration increased up to 0.1g/L respectively 0.15g/L as a consequence of the pulse together with a rise in CO_2. After glucose depletion, the acetate was consumed connected to a second rise in CO_2 level. The reduction of the acetate level was slower for D = 0.51 h^{-1} than for D =0.36 h^{-1}, as the cells were already growing with overflow metabolism and were unable to re-assimilate the produced acetate. The acetate was in this case probably diluted out rather than consumed by the cells. Formic acid levels before the pulse were around 0.2g/L and seemed to only respond with a slight increase. Thereafter its concentration slowly decreased probably due to dilution.

Considering the GFP fluorescence analysed at pH7 (corresponding to values for intact cells), the pulse caused a slight shift towards higher fluorescence for all three dilution rates, which resulted in slightly elevated mean fluorescence values (figure 10 A). As the pulses abated, the fluorescence returned after a short period with increased population variance (CV, figure 10C) to steady state levels. This rise in variance is co-occurring for all three dilution rates and might for the high ones be connected to acetate growth. No population segregation was found for either of the three dilution rates and the peak shapes, considering the peakwidth and slope of the cdfplot (figure 10 D and G), remained constant during the pulses. There was only a slight observed decrease in the slope after nutrient depletion for D = 0.1h^{-1} after glucose depletion and for the two higher dilution rates after acetate depletion.

When GFP was analysed at pH 5.5 to assess membrane robustness, the effect of the pulse could easily be seen with clear differences between slow and fast growing cells. For the two higher dilution rates a second distinct phase was also seen for the GFP signal mirroring the overall trend of the CO_2 evolution - corresponding to acetate re-assimilation. This indicates that the reporter strain had a response fast enough to capture both the glucose and the acetate phase. For the low dilution rate the mean fluorescence remained constant apart from a slight drop during growth on the pulsed glucose. Furthermore, cells growing at the higher dilution rates of 0.36 h^{-1} and 0.51 h^{-1}, showed a more dynamic response to the glucose addition than the low dilution rate. This could be seen in the slight increase in peakwidth for the faster growing cells during both glucose and acetate growth, in contrast to the almost constant peakwidth for the slow growth condition (figure 11 D). Also the CV of the GFP at D = 0.1 h^{-1} remained constant apart from a steep increase after the glucose perturbation followed by an asymptotic decrease during the glucose consumption. In contrast to that the level of heterogeneity for the two higher dilution rates decreased after the glucose perturbation and then rose above steady state level during the acetate consumption phase. Slow growing cells were characterized by a generally higher and constant slope of the cdfplot, apart from a small drop after the glucose perturbation indicating an increase in heterogeneity induced by the pulse (figure 11H). In contrast fast growing cells decreased their heterogeneity with the pulse, seen by a slight increase in slope. However when growing on acetate the slope dropped steeply followed by a slow return to steady state level after acetate depletion indicating that fast growing cells were strongly affected when growing on acetate.

Cells analysed for membrane robustness at pH 5.5 showed a bigger population spread as well as a higher level of overall heterogeneity considering peakwidth and CV (figure 11 C, D, E and F) than when just analysed for growth heterogeneity (at pH 7). Additionally the carbon source seemed to influence the membrane robustness (at pH 5.5) at high growth rates which was not revealed when analysing intact cells at pH 7 (figure 11 A and B). Furthermore, membrane robustness affected cells (at pH 5.5) also required a longer time, which increased with increasing dilution rate, to return to steady state levels.

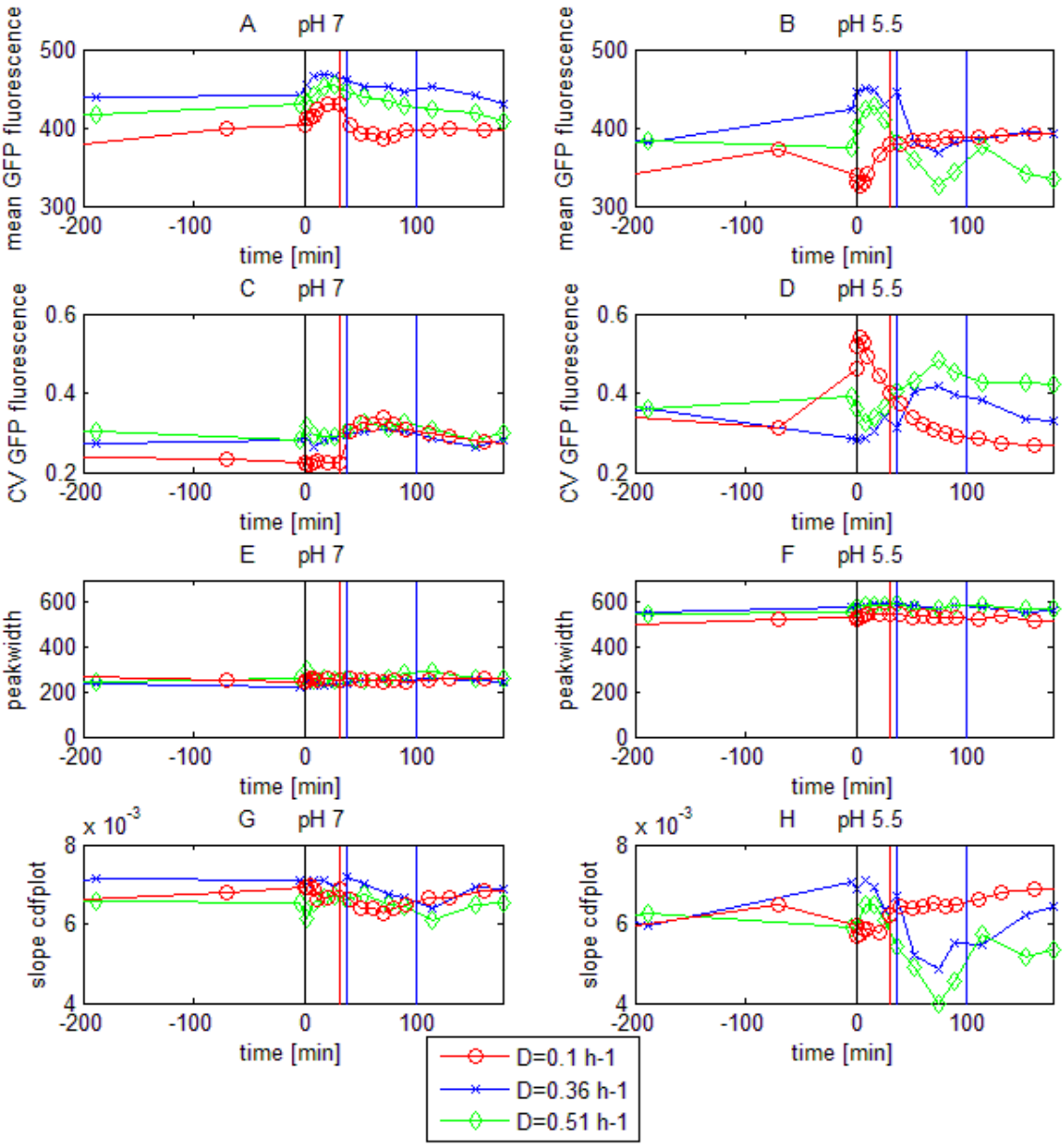

Figure 10 - Effects of glucose perturbation on heterogeneity of *E.coli* at pH 5.5 and 7: measured by mean fluorescence (A and B), CV (C and D), peak width (E and F), and cdfplot slope (G and H) of *E. coli* glucose-limited chemostats plotted against time following a 0.45 g/L glucose pulse at D = 0.1 h^{-1} (red), 0.36 h^{-1} (blue), 0.51 h^{-1} (green). The first red, blue and green coloured vertical lines indicate the time when the pulsed glucose was consumed in the respective experiment, whereas the black line indicates the time of the glucose pulse. The second blue line indicates the end of the acetate growth phase.

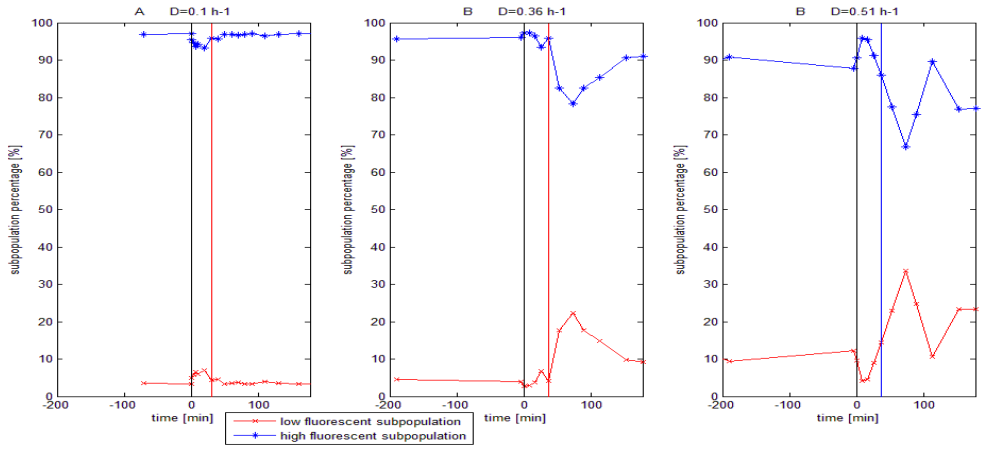

Figure 11 - Subpopulation distribution dynamics following glucose perturbation for *E.coli* cells exposed to freezing at pH 5.5: percentage for low (red) and high (blue) fluorescence subpopulation plotted against the time following a 0.45 g/L glucose pulse for *E.coli* in aerobic glucose-limited chemostats for frozen cells grown with D = 0.1 h^{-1}(A), D = 0.36 h^{-1}(B) and D = 0.51 h^{-1} (C) at pH 5.5. The red and blue colored vertical lines are indicating the time when the pulsed glucose is consumed in the 0.1 h^{-1}, 0.36 h^{-1} and 0.51 h^{-1}cultivation respectively. The black line is indicating the time of the glucose pulse.

To further investigate the effect of the pulse on membrane robustness subpopulation distributions (samples analysed at pH 5.5), the relative fraction of the low and high fluorescence subpopulation was calculated at different time points (figure 11). For D = 0.1 h^{-1} the high fluorescent subpopulation (intact membranes) compromised around 97% of the whole population under steady state conditions. With perturbation the low fluorescent subpopulation (damaged membranes) increased up to around 7 %, but with glucose depletion the distribution returned to steady state values. For D = 0.36 h^{-1} the same subpopulation distribution in steady state and trend during glucose growth could be seen. However, during acetate growth after glucose depletion the percentage of the high subpopulation (intact cells) decreased further to around 78% and only slowly returned to steady state values after its depletion. The same trend was also found during acetate growth for the highest dilution rate, although after its depletion the steady state level was not fully reached again during the analysis window (low/high subpopulation: 20%/80%). In contrast to the two other dilution rates the fraction of the high fluorescent subpopulation (intact cells) increased with the pulse to up to 95% compared to steady state (around 90%).

6.4 Discussion

Cellular heterogeneity is present in all living things from simple bacteria, to eukaryotic and mammalian cells. To explore how cell-to-cell variability in growth and membrane robustness (investigated as a consequence of freeze-thaw stress) are affected by growth rate and sudden variation in glucose concentration, fluorescent reporter strains of *S. cerevisiae* and *E. coli* were grown in continuous cultivations at different dilution rates. Both high and low dilution rates were employed and the population distributions followed during steady state and after the introduction of a glucose pulse. The glucose pulse was applied to mimic the fluctuating conditions cells experience in industrial scale bioreactors. With our investigations we successfully described and compared microbial responses to environmental perturbations at the single-cell level for slow and fast growing *E. coli* and *S. cerevisiae* cells. The introduction of new tools allowed us to perform a detailed, quantitative characterization of population heterogeneity properties.

6.4.1 Quantification of heterogeneity

As unsynchronized microbial cultures are heterogeneous, averaged response values fail to describe the influence of different subpopulations[1]. The currently most used method for single cell analysis is flow cytometry, which allows simultaneous quantification of thousands of individual cells per second[41]. As mentioned earlier, flow cytometry data are generally illustrated as single parameter histograms or in plots where two parameters are correlated[26,27]. By using classical histograms and biplots and by calculating mean GFP fluorescence, general traits of the GFP distribution can be observed. However, this type of data treatment provides a qualitative description rather than a quantitative one and the selection of parameters and divisions of subpopulations are based on subjective interpretations, which points to the need for more objective standards for the quantification of population heterogeneity. To achieve this the shape of the distribution values were enumerated using simple statistical and mathematical functions, which permits the peakwidth and the CV, based on peakwidth divided by the mean GFP fluorescence, to be used to describe population heterogeneity. The wider the peak and the bigger the CV, the more heterogeneous is the population. The appearance of subpopulations, shifts over time and differences in peak shape can be illustrated by using a cumulative distribution, which can be quantified via its slope. So the higher the slope, the narrower the distribution will be and the lower the population heterogeneity. The challenge, depending on the study, however lies in determining which or what combination of parameter/s that can reveal relevant and the most descriptive information from the torrent of data. For example a rapid change in peakwidth can either be related to a more aligned population in

general or to an appearance of a subpopulation (which is related to more heterogeneity in general). Hence it can be necessary, especially when expecting subpopulations, to consider peakwidth and slope of the cdfplot together to avoid false argumentation. In conclusion, by using the newly developed parameters or a combination of them a cell population can be described more objectively and more detailed than using conventional trend plots. A set of parameter values are also easier to comprehend than rows of distribution plots because they are represented as single values for sampling points that can be plotted over time (figure 5 and 10) similar to general physiology data.

6.4.2 Freezing as a tool to determine membrane robustness

Freezing is well known to affect and damage microbial cells. Cooling and thawing rates have a significant influence on the amount of damage inflicted[42]. Furthermore, faster growing cells are more susceptible to freeze-thaw stress,[20] whereas slower growing cells tend to redistribute cellular resources towards stress tolerance functions[14,21,22]. But freezing can also be consciously employed to reveal information about the population structure of cells related to membrane robustness under different environmental conditions as done in our study. We have previously looked into freezing effects in yeast on fluorescence distributions and shape of cells by comparing freshly analysed cells versus cells frozen before analysis[6].Whereas there was no observable effect on cell morphology, clear differences were seen for the GFP fluorescence including the formation of subpopulations at different fluorescence levels. The underlying cause of the decreasing fluorescence in yeast cells subjected to freeze-thaw stress was further investigated in this study and found to be mainly due to a pH drop caused by an equalization of the external and internal pH via membrane pores/holes as freeze-thawed yeast cells displayed a fluorescence similar to that of fresh cells when the external pH was kept at pH 7, which then linearly decreased as the external pH dropped below 7. This is in accordance with earlier observations where fluorescent proteins, especially the green and yellow variants, showed to be severely affected by acid shifts close to the physiological pH[43]. The fact that the applied freezing procedure reproducibly generates pores in the membranes that allow exchange of ions between the intracellular and extracellular space, but that are too small to allow the fluorescent proteins to pass, permits the usage of freeze-thawing for studying membrane robustness heterogeneity. The methodology was also successfully applied for investigation of membrane robustness heterogeneity in *E. coli* cells and hence seem to be applicable for different microorganisms.

6.4.3 Influence of growth rate

The yeast growth reporter strain has previously been shown to be growth related in a batch study when comparing the fast growth in the glucose phase with the slower growth in the ethanol phase[6]. However, in batch cultivations the effect of growth rate versus use of carbon source on GFP expression cannot be separated. In the current study, where continuous cultivations were employed to facilitate investigation of the influence of growth rate separately, we did not observe an increase in GFP fluorescence for intact cells with increasing dilution rate as expected. Instead, the mean fluorescence level was fairly constant with the exception of an increase at the lowest dilution rate (0.05 h^{-1}). However, after normalising with FSC, which is correlated with cell size in yeast, a clear increasing trend was observed up until D=0.25 h^{-1}, whereafter the fluorescence/FSC sharply declined. This would indicate that the "expression per cell volume" increased with growth rate in the respiratory phase. Yet, as observed previously in the shift from respiro-fermentative growth on glucose to respirative growth on ethanol[6], the particular type of metabolism seems to have a strong influence on the ribosomal promoter associated fluorescence as indicated by the sharp decline above 0.25 h^{-1}, which marks the onset of respiro-fermentative growth.

A similar pattern was seen for the *E. coli* reporter, though prior to normalisation with cell size which in this case might be due to the small size not accurately being predicted by the FSC (it rather gives information about the morphology[41]). However it is known that *E. coli* cells increase slightly in length and width when growing under nutrient richer conditions[44]. Therefore the rising steady-state GFP fluorescence for intact cells with dilution rate for the two lower growth rates (D= 0.1 h^{-1} and D =0.36h^{-1}) (figure 8) cannot strictly be described by higher "expression per cell volume" but is also influenced by other factors. Afterwards the GFP fluorescence remained constant respectively slightly declined depending on the growth rate. Whether the GFP expression was reduced due to change in metabolism with the onset of overflow metabolism or due to reduction in plasmid counts remains unclear. However plasmid counts of low copy number plasmids have previously been shown to decrease at high dilution rates in *E. coli* chemostats[45].

Growth rate had a clear influence on membrane robustness population distributions for both yeast and *E. coli* cells. The slower growing cells were largely unaffected by the freezing procedure, whereas for the rapidly growing cells a shift towards lower fluorescence was seen, which was more pronounced for yeast than for *E. coli*. In accordance, small cells have earlier been seen to be less

susceptible to freeze damage than larger cells when the freezing is performed at slow freezing rates, similar to those applied at the present study[46].

6.4.4 Influence of glucose perturbation

The influence of the fluctuating environmental conditions cells experience in industrial scale reactors was further explored by analysing responses to transient changes from glucose limitation to glucose excess and back. Fresh samples from the yeast cultivations showed a slight shift in fluorescence intensity at the lower dilution rate (D=0.05 h^{-1}), but a constant intensity at the higher dilution rate (0.30 h^{-1}). This seems intuitive, as any shift in metabolism after a relief of glucose limitation must be bigger for slower growing cells. This trend was also seen for *E. coli* cells, and though all cells irrespective of dilution rate reacted to the pulse with an upshift in fluorescence, the reaction got more pronounced with decreasing dilution rate (figure 10). Our results indicate that while the growth rate was only found to introduce small changes to the expression of our reporter genes in yeast and *E. coli*, clear up-regulations were observed after the introduction of the glucose pulses. This indicates that the gene regulations of the promoters are primarily responding to environmental shifts rather than growth rate at steady state conditions.

With regards to cell membrane integrity, cell population distributions were largely unchanged after the pulse in samples from the low dilution rate cultivations. However, in strong contrast, samples from the high dilution rate cultivations displayed significant shifts in the population distributions as a response to the pulses (figure 5 and 6). Interestingly, after the introduction of the pulse a larger part of the population maintained the fluorescence. This behaviour was mirrored by the *E. coli* cells. At the low dilution rate (D= 0.1 h^{-1}) the *E. coli* GFP fluorescence barely shifted with the pulse, whereas as the dilution rate increased (D= 0.36 h^{-1} and D= 0.51 h^{-1}), the shifts became more pronounced (figure 10 and 11). The bacterial cells responded with an upshift in fluorescence, i.e. increased ratio of cells with intact cell membranes, in the glucose consumption phase but the amount of intact cells declined increasingly with rising dilution rate (for the two higher dilution rates) respectively remained constant for acetate consumption for D=0.1 h^{-1}. This exemplifies the high toxicity of acetate which seems to increase with increasing dilution rate whereas ethanol for yeast cell rather seems to function as freezing protectant, what has also been found earlier in batch cultures of S. cerevisiae[20]. Figure 4 shows how the yeast population distribution changed responding to glucose perturbation after the freeze-thaw cycle. At the low dilution rate there was a

slight shift to lower fluorescence and a widening of the peak. In contrast, the high dilution rate population showed a dramatic peak widening and a shift to a lower fluorescence for a large part of the population. Why the pulse seems to protect some of the faster growing cells from freeze-thaw damage is not straight forward to explain. The only thing connected to the physiology of the cells that can react on the time-scales of the almost instantaneous changes observed is the intra-cellular metabolite levels. One could surmise that the fast growing cells, already primed for over-flow metabolism, quickly absorbed the glucose and perhaps even produced some storage carbohydrates, e.g. trehalose which in yeast is found to accumulate as response to freeze stress[47]. An intracellular shift in metabolite concentrations might very well affect the physics of the freezing process offering additional protection to the cell membrane.

6.4.5 Potential with the reporter strains and future outlook

High-throughput, single-cell gene expression studies are vital for elucidating the dynamics and contributions of heterogeneous cell populations. In general, the new tools presented here combines reporter strains and mathematical methods to explore subpopulation dynamics in changing environments. Changes that traditionally were only subjectively quantified by comparing classical histograms can be now be objectively quantified and analyzed using these mathematical tools. The tools can be used to facilitate analysis and interpretation of cytomics data and provide insight for the generation of future strategies for the improvement of performance and robustness of industrial scale cultivations.

Acknowledgement

The Danish Council for Strategic Research is gratefully acknowledged for financial support in the frame of the project "Towards robust fermentation processes by targeting population heterogeneity at microscale" (project number 09-065160). ERA-IB (ERA-NET Industrial Biotechnology) is gratefully acknowledged for financial support in the frame of the project "Targeting population heterogeneity at microscale for robust fermentation processes" (project number EIB.08.031).

6.5 References

1. Fernandes, R. L. *et al.* Experimental methods and modeling techniques for description of cell population heterogeneity. *Biotechnol. Adv.* **29,** 575–599 (2011).

2. Avery, S. V. Microbial cell individuality and the underlying sources of heterogeneity. *Nat. Rev. Microbiol.* **4,** 577–87 (2006).

3. Müller, S., Harms, H. & Bley, T. Origin and analysis of microbial population heterogeneity in bioprocesses. *Curr. Opin. Biotechnol.* **21,** 100–113 (2010).

4. Lara, A. R., Galindo, E., Ramírez, O. T. & Palomares, L. A. Living With Heterogeneities in Bioreactors Living With Heterogeneities in Bioreactors. *Mol. Biotechnol.* **34,** (2006).

5. George, S., Larsson, G., Olsson, K. & Enfors, S.-O. Comparison of the Baker's yeast process performance in laboratory and production scale. *Bioprocess Eng.* **18,** 135–142 (1998).

6. Carlquist, M. *et al.* Physiological heterogeneities in microbial populations and implications for physical stress tolerance. *Microb. Cell Fact.* **11,** (2012).

7. Bylund, F., Collet, E., Enfors, S.-O. & Larsson, G. Substrate gradient formation in the large-scale bioreactor lowers cell yield and increases by-product formation. *Bioprocess Eng.* **18,** (1998).

8. Enfors, S. O. *et al.* Physiological responses to mixing in large scale bioreactors. *J. Biotechnol.* **85,** 175–185 (2001).

9. Taymaz-Nikerel, H., van Gulik, W. M. & Heijnen, J. J. Escherichia coli responds with a rapid and large change in growth rate upon a shift from glucose-limited to glucose-excess conditions. *Metab. Eng.* **13,** 307–318 (2011).

10. Schweder, T. *et al.* Monitoring of genes that respond to process-related stress in large-scale bioprocesses. *Biotechnol. Bioeng.* **65,** 151–159 (1999).

11. Yosef, N. & Regev, A. Impulse control: Temporal dynamics in gene transcription. *Cell* **144,** 886–896 (2011).

12. Ronen, M. & Botstein, D. Transcriptional response of steady-state yeast cultures to transient perturbations in carbon source. *Proc. Natl. Acad. Sci. U. S. A.* **103,** 389–394 (2006).

13. Mashego, M. R., van Gulik, W. M., Vinke, J. L., Visser, D. & Heijnen, J. J. In vivo kinetics with rapid perturbation experiments in Saccharomyces cerevisiae using a second-generation BioScope. *Metab. Eng.* **8,** 370–383 (2006).

14. Zakrzewska, A. *et al.* Genome-wide analysis of yeast stress survival and tolerance acquisition to analyze the central trade-off between growth rate and cellular robustness. *Mol. Biol. Cell* **22,** 4435–4446 (2011).

15. Kresnowati, M. T. a P. *et al.* When transcriptome meets metabolome: fast cellular responses of yeast to sudden relief of glucose limitation. *Mol. Syst. Biol.* **2,** (2006).

16. Wu, L. *et al.* Short-Term Metabolome Dynamics and Carbon , Electron , and ATP Balances in Chemostat-Grown Saccharomyces cerevisiae CEN . PK 113-7D following a Glucose Pulse. *Appl. Environ. Microbiol.* **72,** 3566–3577 (2006).

17. Gasch, A. P. & Werner-Washburne, M. The genomics of yeast responses to environmental stress and starvation. *Funct. Integr. Genomics* **2,** 181–192 (2002).

18. Delvigne, F., Boxus, M., Ingels, S. & Thonart, P. Bioreactor mixing efficiency modulates the activity of a prpoS::GFP reporter gene in E. coli. *Microb. Cell Fact.* **8,** (2009).

19. Gasch, a P. *et al.* Genomic expression programs in the response of yeast cells to environmental changes. *Mol. Biol. Cell* **11,** 4241–4257 (2000).

20. Lewis, J. G., Learmonth, R. P. & Watson, K. freeze-thaw stress resistance of Role of Growth Phase and Ethanol in Freeze-Thaw Stress Resistance of Saccharomyces cerevisiae. *Appl. Environ. Microbiol.* **59,** (1993).

21. Brauer, M. J. *et al.* Coordination of Growth Rate , Cell Cycle , Stress Response , and Metabolic Activity in Yeast. *Mol. Biol. Cell* **19,** 352–367 (2008).

22. Hua, Q., Yang, C., Oshima, T., Mori, H. & Shimizu, K. Analysis of Gene Expression in Escherichia coli in Response to Changes of Growth-Limiting Nutrient in Chemostat Cultures Analysis of Gene Expression in Escherichia coli in Response to Changes of Growth-Limiting Nutrient in Chemostat Cultures. *Appl. Environ. Microbiol.* **70,** (2004).

23. Han, S., Delvigne, F., Brognaux, A., Charbon, G. E. & Sørensen, S. J. Design of growth-dependent biosensors based on destabilized GFP for the detection of physiological behavior of Escherichia coli in heterogeneous bioreactors. *Biotechnol. Prog.* **29,** 553–563 (2013).

24. Regenberg, B. *et al.* Growth-rate regulated genes have profound impact on interpretation of transcriptome profiling in Saccharomyces cerevisiae. *Genome Biol.* **7,** (2006).

25. Han, S., Delvigne, F., Brognaux, A., Charbon, G. E. & Sorensen, S. J. Design of growth-dependent biosensors based on destabilized GFP for the detection of physiological behavior of Escherichia coli in heterogeneous bioreactors. *Biotechnol. Prog.* (2013). doi:10.1002/btpr.1694

26. Kacmar, J., Zamamiri, A., Carlson, R., Abu-Absi, N. R. & Srienc, F. Single-cell variability in growing Saccharomyces cerevisiae cell populations measured with automated flow cytometry. *J. Biotechnol.* **109,** 239–254 (2004).

27. Attfield, P. V, Choi, H. Y., Veal, D. a & Bell, P. J. Heterogeneity of stress gene expression and stress resistance among individual cells of Saccharomyces cerevisiae. *Mol. Microbiol.* **40,** 1000–1008 (2001).

28. Verduyn, C., Postma, E., Scheffers, W. a & Van Dijken, J. P. Effect of benzoic acid on metabolic fluxes in yeasts: a continuous-culture study on the regulation of respiration and alcoholic fermentation. *Yeast* **8,** 501–517 (1992).

29. Olsson, L., Schulze, U. & Nielsen, J. On-line bioprocess monitoring – an academic discipline or an industrial tool? *TrAC Trends Anal. Chem.* **17,** 88–95 (1998).

30. Nahku, R. *et al.* Specific growth rate dependent transcriptome profiling of Escherichia coli K12 MG1655 in accelerostat cultures. *J. Biotechnol.* **145,** 60–65 (2010).

31. Van Dijken JP *et al.* An interlaboratory comparison of physiological and genetic properties of four Saccharomyces cerevisiae strains. *Enzyme Microb. Technol.* **26,** 706–714 (2000).

32. Postma, E., Verduyn, C., Scheffers, W. A. & Dijken, J. P. V. A. N. glucose-limited chemostat cultures of Enzymic Analysis of the Crabtree Effect in Glucose-Limited Chemostat Cultures of Saccharomyces cerevisiae. *Appl. Environ. Microbiol.* **55,** 468–477 (1989).

33. Diderich, J. a. Glucose Uptake Kinetics and Transcription of HXT Genes in Chemostat Cultures of Saccharomyces cerevisiae. *J. Biol. Chem.* **274,** 15350–15359 (1999).

34. Hoek, P. Van, Dijken, J. P. Van & Pronk, J. T. Effect of Specific Growth Rate on Fermentative Capacity of Baker ' s Yeast Effect of Specific Growth Rate on Fermentative Capacity of Baker ' s Yeast. *Appl. Environ. Microbiol.* **64,** (1998).

35. Larsson, C., von Stockar, U., Marison, I. & Gustafsson, L. Growth and metabolism of Saccharomyces cerevisiae in chemostat cultures under carbon-, nitrogen-, or carbon- and nitrogen-limiting conditions. *J. Bacteriol.* **175,** 4809–4816 (1993).

36. Medoff, G., Kobayashi, G. S., Kwan, C. N., Schlessinger, D. & Venkov, P. Potentiation of Rifampicin and 5-Fluorocytosine as Antifungal Antibiotics by Amphotericin B. *Proc. Natl. Acad. Sci. U. S. A.* **69,** 196–199 (1972).

37. Visser, D. *et al.* Analysis of in vivo kinetics of glycolysis in aerobic Saccharomyces cerevisiae by application of glucose and ethanol pulses. *Biotechnol. Bioeng.* **88,** 157–167 (2004).

38. Robey, R. B. *et al.* pH-dependent fluorescence of a heterologously expressed Aequorea green fluorescent protein mutant: in situ spectral characteristics and applicability to intracellular pH estimation. *Biochemistry* **37,** 9894–9901 (1998).

39. Kayser, A., Weber, J., Hecht, V. & Rinas, U. Metabolic flux analysis of Escherichia coli in glucose-limited continuous culture. I. Growth-rate-dependent metabolic efficiency at steady state. *Microbiology* **151,** 693–706 (2005).

40. Nanchen, A., Schicker, A. & Sauer, U. Nonlinear Dependency of Intracellular Fluxes on Growth Rate in Miniaturized Continuous Cultures of Escherichia coli Nonlinear Dependency

of Intracellular Fluxes on Growth Rate in Miniaturized Continuous Cultures of Escherichia coli †. *Appl. Environ. Microbiol.* **72,** 1164–1173 (2006).

41. Díaz, M., Herrero, M., García, L. a. & Quirós, C. Application of flow cytometry to industrial microbial bioprocesses. *Biochem. Eng. J.* **48,** 385–407 (2010).

42. Mazur, P. Freezing of living cells: mechanisms and implications. *Am. J. Physiol.* **247,** 125–142 (1984).

43. Chudakov, D. M., Matz, M. V, Lukyanov, S. & Lukyanov, K. A. Fluorescent Proteins and Their Applications in Imaging Living Cells and Tissues. *Physiol. Rev.* **90,** 1103–1163 (2010).

44. Chien, A.-C., Hill, N. S. & Levin, P. A. Cell size control in bacteria. *Curr. Biol.* **22,** 340–349 (2012).

45. Seo, J. H. & Bailey, J. E. Continuous cultivation of recombinant Escherichia coli: Existence of an optimum dilution rate for maximum plasmid and gene product concentration. *Biotechnol. Bioeng.* **28,** 1590–1594 (1986).

46. Gervais, P. Cell Size and Water Permeability as Determining Factors for Cell Viability after Freezing at Different Cooling Rates. *J. Biotechnol.* **70,** 268–272 (2004).

47. Mahmud, S. A., Hirasawa, T. & Shimizu, H. Differential importance of trehalose accumulation in Saccharomyces cerevisiae in response to various environmental stresses. *J. Biosci. Bioeng.* **109,** 262–266 (2010).

7. Chapter

Combined use of fluorescent dyes and a whole cell biosensor to monitor the effect of acetate on single-cell heterogeneity of *E. coli* in aerobic batch cultures by flow cytometry

Luisa Lundin[1*], Anna-Lena Heins[2 *], Inês Nunes[1], Shanshan Han[1], Rita Lencastre Fernandes[3], Gitte E Charbon[1], Waleed Abu Al-Soud[1], Krist V Gernaey[3], Søren J Sørensen[1], Anna Eliasson Lantz[2§]

[1] Department of Biology, Section of Microbiology, University of Copenhagen, 2100 DK, Copenhagen, Denmark

[2] Department of Systems Biology, Technical University of Denmark, 2800 Kongens Lyngby, Denmark

[3] Department of Chemical and Biochemical Engineering, Technical University of Denmark, 2800 Kongens Lyngby, Denmark

[§]Corresponding author

*These authors contributed equally to the work

Written as journal paper

Status: Manuscript in preparation

Abstract

The appearance of acetate as a by-product in large scale bioprocesses with *E. coli* is found to decrease the biomass yield as well as to be toxic to cells, which has several different effects e.g. large induction of stress responses. However, the underlying cell phenomena are poorly explored. Here the time-resolved cellular heterogeneity profile of *E. coli* strain MG1655 during batch growth on acetate and glucose as carbon sources was studied by applying a growth reporter strain expressing a destabilized GFP together with different fluorescent activity stains targeting particular features (viability and metabolic activity). The obtained results from flow cytometry analysis suggested that, cells are more heterogeneous in growth as well as stronger metabolically challenged during growth on acetate than when growing on glucose. Furthermore, also compared to acetate growth after diauxic shift, when growing on acetate as sole carbon source, population heterogeneity was found to be more significant with the presence of subpopulations. Interestingly considering the subpopulation distribution some cells seem to be more robust than the rest of the population when growing on acetate.

In conclusion cellular heterogeneity was evident if not only plotted in traditional averaged data plots and noticeable in all measured parameters. The developed approach enabled a deeper study of heterogeneity during growth on the favoured substrate glucose as well as on the toxic acetate. The use of a combination of activity fluorescent dyes proved to be an accurate and fast alternative and supplement to the employment of a fluorescent growth reporter strain. However the choice of combination of stains should be well considered depending on which particular population traits to aim for.

Keywords: Flow cytometry, Biosensor, Physiology on acetate, Heterogeneity, GFP fluorescence, Stains, metabolic activity, viability, objective data analysis

7.1 Introduction

The use of living cells for the production of biomass or products such as bulk chemicals (e.g. 1,3-propanediol, ethanol), enzymes and pharmaceutical proteins (e.g. insulin) has gained increasingly importance over the last decade[1]. *E. coli* is the most commonly used bacterial production host for proteins, because of its ability of inexpensive, easy and fast expression of proteins[2].

Nowadays it is widely known, that microbial cell populations in industrial scale, biotechnological production processes, though originating from pure, isogenic cultures, are heterogeneous. Due to non-ideal mixing gradients of e.g. substrate, dissolved oxygen and pH arise which create local

microenvironments that are experienced by the cells traveling throughout the reactor[3–5]. This experience of a fluctuating environment induces dynamic cell responses both genetic, metabolic and physiological[6] level and causes the development of cell population heterogeneity in bioprocesses[7]. Increased population heterogeneity may lead to reduced yields and productivity as well as elevated by-product formation[4,5,8]. For instance, formation of acetate as the major by-product in *E. coli* fermentation when glucose is the carbon source, has been seen to decrease the biomass yield in large scale cultivation due to repeated production/re-assimilation when the cells move from zones of high glucose and low oxygen concentration to zones with low glucose and high oxygen saturation[9,10]. Hence, zones with different acetate concentration are formed, which is undesirable as an acetate concentrations above 2 g/L is already toxic for cells[11], having several negative effects on growth, biomass and recombinant protein production and, as mentioned above, leads to a detrimental effect on process performance as well as to significant induction of stress responses[12,13]. However, the underlying cellular phenomena are poorly understood and potential occurrence of less productive or less robust subpopulations would reduce the overall process efficiency. This points to the need for investigating the physiology at subpopulation level, especially cell viability and robustness towards stress, and population dynamics of *E. coli* cells growing with acetate as sole carbon source[10]. Once a deeper understanding for differences between cells in a population has been gained, strategies for process optimization, favoring beneficial subpopulations may be developed.

Ordinary bioprocess monitoring often relies solely on population-based average measurements which by not distinguishing co-existing cell behaviors, are unable to reflect the heterogeneity among individual cells within a population[14]. Flow cytometry (FC) has been applied to discover and monitor cell-to-cell differences, cellular mechanisms and regulatory circuits at single-cell level[15] by applying fluorescent stains as well as reporter strains expressing a fluorescence protein whose expression can be correlated to a gene product of interest[7]. Furthermore, the application of more than one fluorescent stain simultaneously unveils functional differences between bacterial cells, and as so population heterogeneity[16]. This enables the study of the physiological state of bacteria with a high resolution achieving distributions of the measured parameters, and these methodologies have also been applied to study heterogeneity of microbial populations grown in batch cultures[17,18].

A big variety of fluorescence stains targeting different cellular properties are commercially available allowing the assessment of population heterogeneity. The redox dye, 5-cyano-2,3-ditolyl tetrazolium chloride (CTC), is reduced by electron transport activity to a water insoluble, intracellular red fluorescent formazan and has commonly been used for monitoring the respiratory

activity of cells[19–21]. The still relatively unused stain, redox sensor green (RSG) is a vitality stain that becomes fluorescent (green) when altered by bacterial reductases[22] and as many of these are part of the electron transport system, this stain has also been employed as an indicator of the respiratory ability of bacteria[23]. The membrane permeable, asymmetrical cyanine dye, SYBR green, binds readily to nucleic acids in cells and it has been applied in flow cytometry to among other things quantify bacteria in crude environmental samples[24,25]. As a counterpart to activity measurements, the propidium iodide (PI) dye has commonly been used as a membrane integrity indicator. It is a nucleic acid stain that is also membrane impermeable and therefore employed to detect cells with disrupted membranes in bacterial populations[26]. Cells that are not metabolically active, lack the ability to exchange ions through the membrane, due to lack of membrane potential. The bis-(1,3-dibarbituric acid)-trimethine oxanol ($DiBAC_4(3)$) dye has the ability to enter depolarized cells and, while retained inside, turns green[27].

As mentioned above, potential cellular heterogeneities in bioreactors may also be investigated by the combined use of FC analysis and the microbial population itself as reporter[28]. The green fluorescent protein (GFP) is a small bioluminescent protein that is used as promoter activity reporter in many bacteria and yeast cells, not interfering with cell growth[29,30]. The high degree of stability of the wild type GFP might pose a problem in some experiments where transient gene expression is studied. Non-active, non-viable or dormant microbial cells containing stable GFP would continue to express the fluorescent signal even in the absence of promoter gene expression and over many cell generations[31]. It has been reported that the addition of an AAV-tag to the C-terminal of the template $GFP_{mut3.1}$, reduces its half-life from 24 h to 60 min, forming a destabilized form of GFP[32]. A growth reporter (biosensor strain) with the gene encoding a destabilized GFP variant (AVV) fused to the *E. coli* ribosomal promoter *rrnB* P1P2[33] was used in the present study. This promoter is known to be growth rate regulated and responsive to nutrient starvation[34].

In this study, the effect of acetate on physiological heterogeneity and viability of *E. coli* was investigated under two different conditions in batch culture; while growing on acetate as sole carbon source eliminating the effect of glucose as well as while consuming acetate after diauxic shift. Additionally physiology was compared to growth on glucose. To assess population heterogeneity, we applied a combination of five different fluorescent stains, CTC, RSG, SYBR green, $DiBAC_4$ and PI, and an *E. coli* growth reporter strain expressing a destabilized GFP. The change of the state of the individual cells in the microbial population throughout the batch

experiment was analyzed by FC and quantified using simple mathematical tools. We hypothesize that acetate strongly affects the percentage of metabolically active cells.

7.2 Material and Methods

7.2.1 Strains

A biosensor strain based on the expression of destabilized GFP under the control of the *rrnB* P1P2 promoter, namely, MG1655/pGS20PrrnBGFPAAV, was used to illustrate the growth dynamics of a bacterial population in batch cultures[35]. The recombinant strain MG1655 bearing pGS20PrrnB, i.e. a strain containing the same plasmid with the *rrnB* promoter but without the *gfp* gene, was used as the control strain for the growth studies and flow cytometric measurements.

7.2.2 Flow cytometry

All bacterial cells were analysed using a FACSAria™ III (Becton Dickinson, USA) flow cytometer. The system includes two lasers with minimum laser power of 10 mW with the specific wavelengths of 488 nm and 561 nm. Two scattering channels (FSC and SSC) and two fluorescent detection channels (530/30 nm and 610/20 nm) were used in the analysis. The amplification voltages on the detectors were set based on negative and positive controls (stained, non-stained, viable and non-viable bacterial populations) to better visualize the populations and were as followed: FSC – 301V; SSC – 316 V; 530/30 nm – 520 V and 610/20 – 582 V. The detection thresholds were set in FSC and SSC in order to eliminate background noise.

The flow cytometer (FC) specific software was used in combination with CS&T beads (Cytometer Setup and Tracking beads) (Becton Dickinson, USA) for the automated QA/QC of the machine performance. All results obtained with the FCM were saved as fcs files.

7.2.3 Staining procedure and validation

Five activity stains were used in this study: 5-cyano-2,3-ditolyltetrazolium chloride (CTC) (Sigma-Aldrich, Germany), SYBR Green (SYBR) (Invitrogen, USA), Propidium Iodide (PI) (Sigma-Aldrich, Germany), Bis-(1,3-dibutylbarbituric acid) trimethine oxonol ($DiBAC_4(3)$) (Molecular probes, USA) and Redox Sensor Green (RSG) (Invitrogen, USA). For each staining procedure, 1 µL of stain was added to 100 µL of sample suspended in 0.9% of saline solution. The final stain concentrations were 1x for SYBR, 0.05 mg/mL for PI, 0.5 mM for CTC and 0.001 mM for both $DiBAC_4(3)$ and RSG. The CTC staining was incubated for 1 hour at 37ºC. The SYBR staining was

incubated for 20 minutes and $DiBAC_4(3)$, PI and RSG for 10 minutes at room temperature. The stains were protected from the light during the whole procedure.

With the aim to investigate if staining results vary during sample handling, a validation procedure was performed, which allowed the optimization of the sample handling prior to staining and subsequent flow cytometric analysis. The biosensor MG1655/pGS20PrrnBGFPAAV was grown in shake flasks using 100 mL of the defined minimal media[36] with addition of either glucose (5 g/L) or acetate (2 g/L) as a carbon source. The medium used during these validation procedures was supplemented with 25 μg/mL of chloramphenicol (dissolved in 96% ethanol, stock concentration: 10 mg/ml). The cultures were grown at 37ºC in an orbital shaker at 140 rpm. Samples were taken every hour until the cultures reached the stationary phase. The optical density at 600nm (OD_{600}) of the cultures was measured with a UV/Vis photometer (Biophotometer 6131, Eppendorf AG, Germany) at each time point. The staining procedure was applied to samples immediately, after 30 and 60 minutes of ice incubation as well as after 30 and 60 minutes of room temperature incubation. Flow cytometry methods (FC) was used to detect the growth dependent GFP expression of the biosensor and the fluorescent signal of the cells after staining.

Two-way analysis of variance (ANOVA) was applied to the obtained mean fluorescence signals, using the GraphPad Prism 5 (GraphPad, Inc, USA) software. A significance level of 0.05 was employed. Thus, adequate incubation times and temperatures were chosen when no significant differences ($p>0.05$) were observed between the results obtained immediately after sampling and after the different tested incubation conditions. Based on the validation results, the samples for staining with RSG, SYBR green and PI should be kept on ice until flow cytometric measurements. For the DiBAC4(3) staining, the samples collected during the first ten hours of growth in batch were placed at room temperature and on ice after this time point. The samples to be stained with CTC were kept at room temperature. Proper dilution increases staining efficiency and accuracy, so based on calibration curves relating the OD_{600} and the number of events recorded in the flow cytometer, samples with an OD_{600} above 0.2 were diluted 10 times before staining.

7.2.4 Preculture preparation

The inocula used to start the batch cultures were obtained by a two-step procedure. First, a single colony of the biosensor MG1655/pGS20PrrnBGFPAAV strain grown a fresh LB plate was used to inoculate a flask containing 100 ml of LB medium and incubated at 37 ºC incubated overnight. Secondly, a dilution series with 10-fold steps in LB medium was prepared from the overnight culture, and grown for 6 to 8 hours at 37ºC on an orbital shaker (160 rpm). Subsequently the OD_{600}

was measured for the whole dilution series, and the one with a $0.4 < OD_{600} < 0.6$ was used to inoculate the bioreactors. The medium used in the pre-cultures was supplemented with 25 µg/mL of chloramphenicol (dissolved in 96% ethanol, stock concentration: 10 mg/ml). The same procedure was used to prepare the inoculum of the control strain.

7.2.5 Batch cultivation

Batch cultivations of the biosensor MG1655/pGS20PrrnBGFPAAV strain were performed using 5 g/L glucose or 2 g/L acetate as carbon source. The growth medium used was a defined mineral medium[36]. After autoclavation, 3 mL $MgSO_4$, 1 mL trace metal solution and 25 µg/ml chloramphenicol were added by sterile filtration (0.2 µm). All cultivations were performed using 1-liter bioreactors (Sartorius, B. Braun Biotech International, GmbH, Melsungen, Germany) with a working volume of 1 L. The pH and DOT electrodes (Mettler Toledo, USA) were calibrated according to standard procedures provided by the manufacturer using a two-point calibration (pH 4 and 7 respectively gassing with air (100%) or nitrogen).

The inoculum achieved from the pre-cultivation was used to inoculate the bioreactor to a final OD_{600} of 0.005 for both carbon sources. The pH was controlled at pH 7 using 2 M NaOH and 2 M HCl. Temperature, aeration and stirring were kept constant at 37°C, 1v/v/m and 1000 rpm, to avoid oxygen limitation. A mass spectrometer (Prima Pro Process MS, Thermo Fisher Scientific, Winsford UK) was used for continuous analysis of the off-gas composition.

Samples for OD_{600} measurements, high performance liquid chromatography (HPLC), dry weight (DW) measurements and flow cytometry analysis were withdrawn periodically every 1.5 or 2 hours. Samples for OD_{600} and DW were analyzed directly, whereas filtrated samples for HPLC were kept at -20 °C until measurement. Samples for flow cytometry were kept on ice or at room temperature until analysis (see "Staining procedure and validation").

7.2.6 OD, DW and HPLC

Growth was followed with OD_{600} measurements using a Shimadzu UV mini 1240 spectrophotometer (Shimidzu, Kyoto, Japan). For dry weight measurements 5 ml of the cultivation broth was filtered, washed and dried for 20 min at 150W in a microwave, cooled down in desiccators and afterwards weighed on an analytical balance[37]. The concentrations of glucose, succinate, acetate, ethanol, glycerol, lactate, formate and pyruvate were determined by HPLC (Agilent 1100, Agilent Technologies, CA, USA) with a 300 mm × 7.8 mm Aminex HPX-87H ion exchange column (Bio-Rad, Hercules, CA, USA), refractive index detector (RID Agilent 1200,

Agilent Technologies, CA, USA) and UV detector (Agilent 1100, Agilent Technologies, CA, USA) set to 210 nm. The mobile phase was 5 mM H_2SO_4 (aq.), temperature 60°C and flow rate 0.6 mL/min.

7.2.7 Data analysis

Processing and analysis of the flow cytometry raw data was performed using MatLab ® R2010b (The MathWorks, Inc., Natick, MA, USA). The raw data were extracted as fcs files and loaded into MatLab with the readfsc function (by L. Balkay, University of Debrecen, Hungary, available on MatLab central file sharing). The HPLC data were collected in an excel file and imported into MatLab. The data from the fcs files were extracted and saved into mat files including the recorded fluorescence for the different staining, GFP fluorescence and the FSC and SSC. The cumulative cell distribution function (cdf) from the 1024 recording channels of the flow cytometer was fitted to the fluorescence data using the hist function and afterwards applying the cdfplot function. By applying the hist function to the 1024 recording channels cell count was saved for all channels and plotted as channel number fluorescence for the used detector of the flow cytometer. Biplots for FSC and fluorescence (GFP and stains) were created using this function. With the help of the function FindGate (by M. McClean, Princeton University, USA, available on MatLab central file sharing) all data have been gated for the main bacterial size population. For better quantitative data for the fluorescence distributions (GFP and stains), the peakwidth at baseline level was calculated by searching for the borders of the peak, which were considered as at least 5 cell counts per channel number to disregard the noise level of the flow cytometer. By subtracting the channel numbers for the higher and lower border the peakwidth was determined. Furthermore, the mean function was used to calculate the mean fluorescence (GFP and stains). By dividing the peakwidth by the mean fluorescence (GFP and stains) the coefficient of variance (CV) of the distribution was generated. Finally the slope of the cdfplot was estimated by fitting a line to the exponential part of the cumulative distribution of the fluorescence histograms (GFP and stains) by using the polyfit function with a degree of one. For SYBR, RSG and CTC for cells grown on acetate the sub-population percentage was computed by dividing the histogram plot into three areas, a low, middle and a high fluorescent area. The areas were set in relation to the local minimum in the histogram between two sub-populations, which was calculated using the min function. The middle fluorescence range was excluded to avoid biased data and then the sub-population percentage in the low and high range was calculated by dividing the cell amount in the sub-population by the total

cell amount found in the two fluorescence ranges. Due to having triplicate datasets for all samples, all values and estimated parameters are stated showing error bars.

7.3 Results

In order to study the effect of acetate on the development of growth heterogeneity, a reporter strain based on the expression of destabilized GFP (AAV) under control of the ribosomal *rrnB* P1P2 promoter was grown in triplicate batch cultures with glucose and acetate as carbon source respectively. Additionally, the physiological status was examined via application of five different fluorescent stains (CTC, RSG, SYBR green, $DiBAC_4$ and PI) targeting basic metabolic needs of bacterial cells. Using flow cytometry, fluorescence of the reporter strain and stains was followed over time throughout the phases of the batch cultures and afterwards compared. For control purposes the same reporter strain without the *gfp* gene was grown in batch culture on glucose.

7.3.1 Cellular growth physiology

The yields of biomass, CO_2 as well as of acetate (for glucose cultivations) on the substrate (glucose or acetate) for the performed cultivations were calculated (see table 1). To test data consistency, carbon balances were computed from the yield coefficients. All data originate from three biological replicates, of which the mean as well as the standard deviation (stdev) was estimated.

Table 1- Yields and carbon balance of triplicate cultivations of the strain MG1655/pGS20PrrnBGFPAAV (biosensor) with glucose respectively acetate as substrate in comparison with a control strain MG1655/pGS20PrrnB . Results ± stdev are shown separately for the control and the biosensor strain. Y_{SX}, Y_{SAC} and Y_{SC} are respectively the yields of biomass, acetate and carbon dioxide on glucose, as well as Y_{SX} and Y_{SC} on acetate.

Yield	$Control_{glucose}$	$Biosensor_{glucose}$	$Biosensor_{acetate}$
$Y_{SX\ [cmole/cmole]}$	0.65 ± 0.02	0.64 ± 0.07	0.28 ± 0.02
$Y_{SC\ [cmole/cmole]}$	0.31 ± 0.02	0.34 ± 0.02	0.10 ± 0.03
$Y_{SAc\ [cmole/cmole]}$	0.08 ± 0.01	0.08 ± 0.04	-

All yields for the glucose cultivations are in agreement with earlier studies[36,38]. Moreover, the yields of the biosensor strain did not differ significantly from the control strain with no GFP expression (table 1). The carbon balance for cultivations with glucose as the substrate could be closed within 1.05±0.00 and 1.06±0.04, for the control and the biosensor strain, respectively.

Both strains showed a typical growth behavior with glucose as substrate (figure 1A for the biosensor, data for the control strain not shown). After a phase of slow growth/lag phase (around 6h), an exponential growth phase with glucose consumption accompanied by the production of acetate, biomass and CO_2 followed. Both strains exhibited almost the same maximum specific growth rate, which was $\mu_{max} = 0.72\ h^{-1} \pm 0.03$ for the control strain, and $\mu_{max} = 0.70\ h^{-1} \pm 0.02$ for the biosensor. With glucose depletion after around 10 h, the cells underwent diauxic shift, upon which the prior produced acetate was consumed. In this phase biomass was further accumulated, though with a lower rate compared to when glucose was the substrate ($\mu_{acetate} = 0.1\ h^{-1} \pm 0.02$). Stationary phase was reached after approximately 14 h. No other metabolites than the above mentioned could be detected.

Compared to growth on glucose, when growing on acetate (figure 1B) the biosensor exhibited a longer phase of slow growth/lag phase (around 17h), where after acetate was consumed accompanied by biomass production until depletion after around 35h. The maximum specific growth rate ($\mu_{max} = 0.15\ h^{-1} \pm 0.04$) as well as the biomass production (final value: 1g/L) was lower, resulting in 50% lower biomass yield (table 1), than for growth on glucose (final value: 2g/L), though comparable with growth on acetate after diauxic shift. Also the CO_2 production was comparably low for all time points (fig. 1B) also resulting in around 66% less CO_2 yield compared to glucose cultivation (table 1). No other metabolites could be identified. When calculating the carbon balance for the biosensor grown on acetate, around 61% of the carbon was missing, though the biomass yield is consistent with the findings of Andersen and Von Meyenburg (1980)[39] as well as with Steinsiek *et al.* (2011)[38]. From the HPLC chromatograms, an unidentified peak could be seen, which may be oxaloacetate (data not shown). A possible reason is that oxaloacetate was over-produced through the bypass of isocitrate dehydrogenase in acetate grown cultures, and was central to successful adaption and growth on acetate[40].

7.3.2 GFP fluorescence during growth on glucose and acetate

To follow growth related heterogeneities over time in the different batch cultures, the GFP expression of the growth reporter strain was measured by flow cytometry. The mean values for GFP fluorescence for the strain growing on glucose (A) respectively acetate (B) are presented in figure 1.

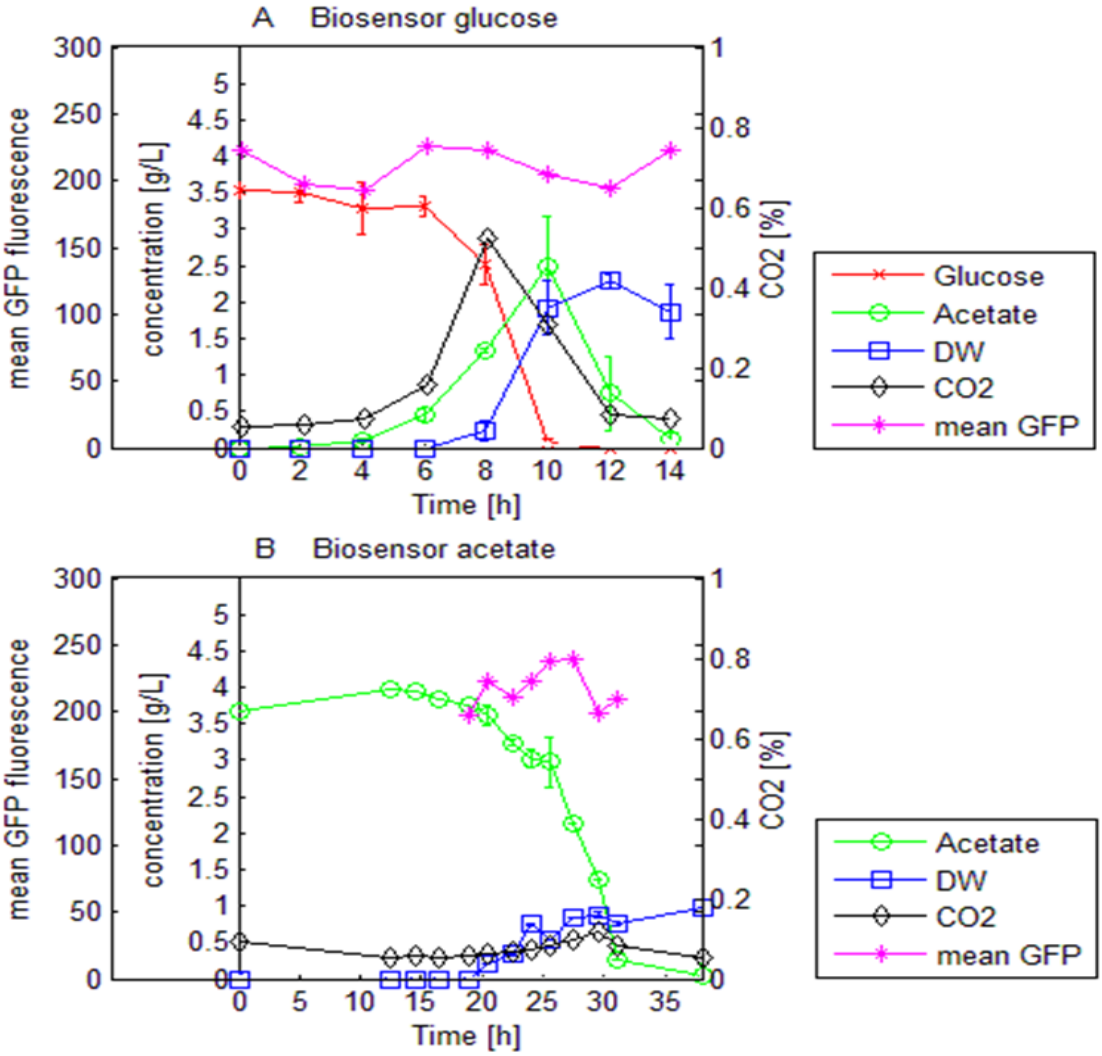

Figure 1 - Physiology and mean GFP fluorescence along time for the strain MG1655/pGS20PrrnBGFPAAV (biosensor) in batch cultivation growing with glucose (A) respectively acetate as carbon source (B). Time profiles are shown for biomass, substrate concentration (g/L), CO_2 (%), mean GFP fluorescence (arbitrary units) as well as acetate concentration (g/L). All values are provided including standard deviation originating from triplicate cultivations.

The biosensor signal (GFP expression) was rather low throughout the cultivations, which also has been observed for similar cultivations earlier[33]. However, a similar trend for both glucose and acetate grown cells could be observed, as the fluorescent signal slightly increased during the exponential growth phase and subsequently decreased again towards the end of the cultivation (figure 1 and 2). For the cultivations with glucose as substrate, the mean fluorescence already

decreased slightly during the second growth phase, the exponential growth on acetate (mean and stdv 194±10.87) compared to exponential growth on glucose (mean and stdv 212.46±37.69) thereby exhibiting lower mean fluorescence values than for exponential growth on acetate as sole carbon source (mean and stdv 220±21.36), which can also be seen considering histogram plots throughout the cultivations (figure 2).

7.3.3 Physiological status evaluation by fluorescent staining

To gain further insight into the physiological state of the strain at a single cell level during growth on acetate in comparison to glucose and to assess the effect acetate has on the degree of population heterogeneity, a combination of fluorescent stains were applied, targeting the membrane status and chosen metabolic activities.

7.3.3.1 Membrane status assessment

The assessment of the cellular membrane status was made using PI and $DiBAC_4(3)$. For both stains a very low percentage of positive stained cells were detected, hence indicating that cells had intact membranes and maintained the membrane potential for all growth conditions applied in this study (data not shown). However, it was noticed that the amount of PI positive cells showed a slight increase at the beginning of the exponential growth phase for both, cells growing on acetate respectively glucose as sole carbon source, whereas this increase was not observed when cells grew on acetate after diauxic shift.

7.3.3.2 Metabolic activity assessment

To gain a deeper understanding of metabolic heterogeneity for growth on acetate and glucose and to highlight eventual subpopulations, the DNA and vitality stains: SYBR green, CTC and RSG were applied. The metabolic activity changes over time for both carbon sources were monitored by measuring the fluorescence distribution for cells grown on glucose (figure 2A-D) and on acetate (figure 2E-H) along the growth curve. Due to differences in growth rate, data from all batch growth phases are presented for the strain growing on glucose whereas for the strain growing on acetate most of the presented results are related to the exponential phase.

The histogram profiles for the CTC stain (figure 2A, E) were distinct different for cells growing on the two different carbon sources. For cells from pure acetate cultures, the CTC distribution was broader compared to cells from glucose cultures, hence more heterogeneous and displayed a small subpopulation exhibiting a higher respiratory activity than the main population. Furthermore, for the main population, a lower fluorescence signal was observed for cells grown on acetate compared to

cells grown on glucose. Interestingly, when cells grew on acetate after diauxic shift, no subpopulation was found and the mean fluorescence was higher than when acetate was added to the medium as sole carbon source. When staining with RSG (figure 2 B, F), only small differences between the cells growing on the different carbon sources could be observed. A somewhat higher signal was displayed for the strain growing on glucose. Furthermore, as for CTC, subpopulations were seen for the cells growing in acetate, but only at the beginning of the growth curve and not during acetate growth after diauxic shift.

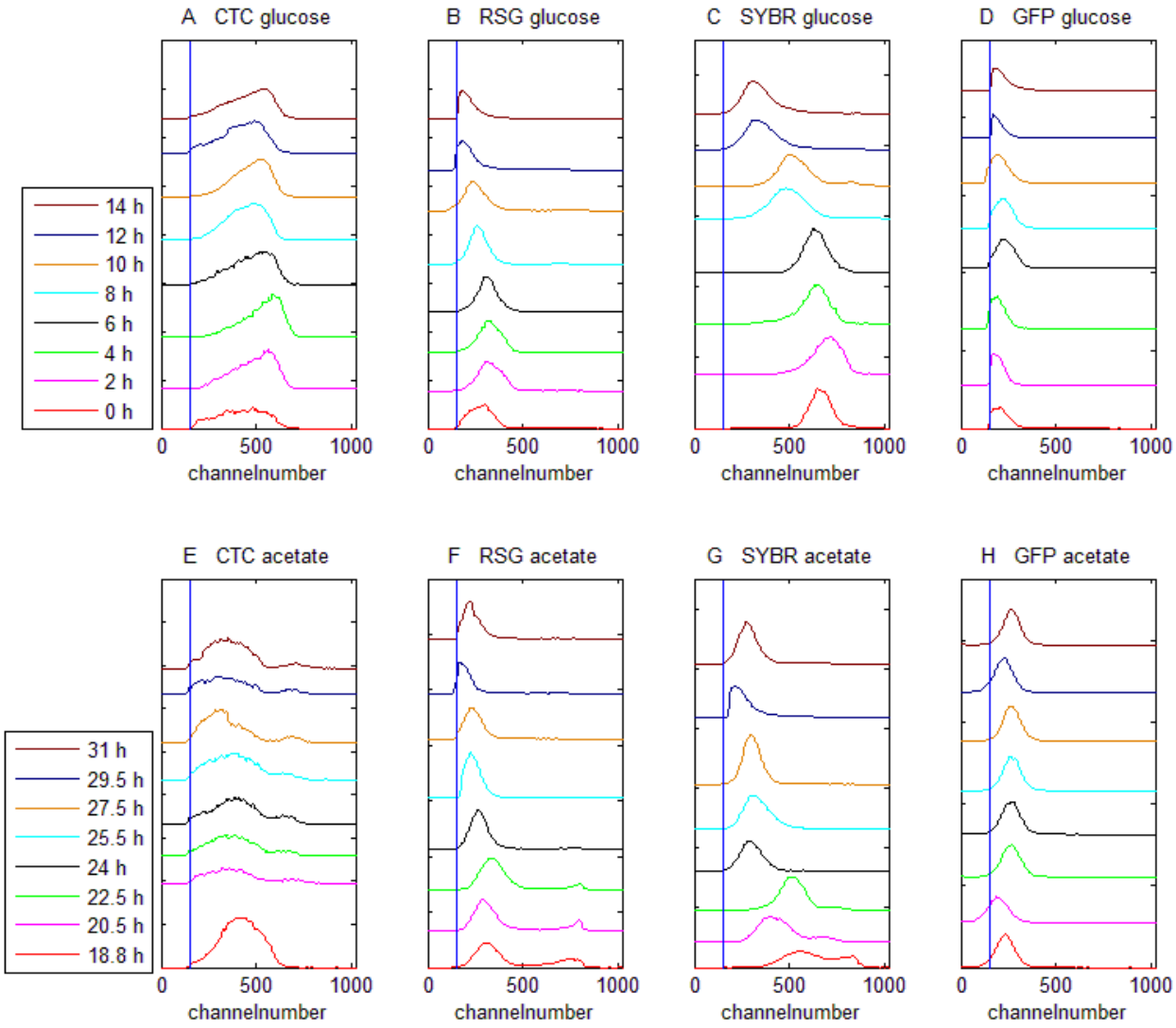

Figure 2 - Fluorescence distribution plots stacked offset for SYBR, CTC, RSG and GFP for the strain MG1655/pGS20PrrnBGFPAAV (biosensor) in batch cultivation growing with glucose (A, B, C and D) or acetate (D, E, F and H) as carbon source. Each graph represents fluorescence distributions of samples of the particular stain from different time points following the

batch. The blue line in the graphs is indicating the negative control without the corresponding stain. For glucose cultivations, exponential growth on glucose was seen between 6 and 10h, growth on acetate between 10 and 14h, where after the cells entered stationary phase. For the acetate cultivations, the samples presented are all from exponential growth phase.

Clear differences were seen for SYBR fluorescence between the populations growing on acetate and on glucose (figure 2 C, G). For cells grown on glucose, the DNA/RNA content (expressed as SYBR fluorescence) was high from the beginning, but shifted down after around 8 h, coinciding with the end of exponential growth phase on glucose and further decreased during the transition to stationary phase (after around 12 h). For the cells grown on acetate as sole carbon source, the signal fluctuated significantly during exponential growth. Compared to growth on glucose, the DNA/RNA content as analyzed using SYBR was generally lower for growth on acetate as sole carbon source as well as during acetate consumption after diauxic shift.

7.3.4 Heterogeneity of the populations grown on glucose and acetate

Since histogram plots (figure 2) only allow a qualitative description of the fluorescence levels, the distributions of GFP, CTC, RSG and SYBR fluorescence for each sampling point were quantitatively analysed by calculating parameters supplementary to the mean fluorescence, the coefficient of variance (CV), the peakwidth as well as the slope of the cumulative distribution plot (cdfplot slope) (Heins *et al.*, chapter 6) allowing an objective interpretation of the results (figure 3). The slope of the cdfplot, which is calculated of the exponential part of the cumulative distribution (see example for CTC data in figure 4), as well as the peakwidth, meaning the width of the peak at baseline level, provide information about the shape of a distribution (Heins *et al.*, chapter 6). Additionally both parameters also give insight about potential subpopulations. A non-purely exponential shape of the cdfplot representing plateaus will be seen if subpopulations are present (as in figure 4 D or B) and will be reflected in changes of the slope of the plot. In combination with the cdfplot slope a rise in peakwitdh can also point towards appearance of subpopulations. The CV is calculated by dividing the peakwidth by the mean fluorescence and provides information about the level of heterogeneity of the distribution, as well as about reproducibility of the performed cultivations (Heins *et al.*, chapter 6). Opposite to the CV and the peakwidth, there is an inverse relation of the slope values to the level of heterogeneity as a wider peak represents a lower slope.

Considering the CV (figure 3A and D), it is clear that the cells grown on acetate in comparison to growth on glucose yields more heterogeneity between replicate cultivations, though the level of

heterogeneity within the distribution for growth on glucose and acetate is similar in the beginning of the exponential phase, except for CTC, where a lower CV was seen for the glucose cultivation (0.23 for glucose, compared to 0.34 for acetate). This was also valid when cells grew on acetate after glucose depletion (figure 3 A). Furthermore, the CV increased during exponential growth on glucose for GFP fluorescence, RSG and SYBR, which may be connected to an increasing peakwidth (figure 3B) whereas it remained constant for CTC. Constant values for the calculated CV were also seen for all stains and GFP fluorescence for growth on acetate, which can be connected to constant peakwidths. For the glucose cultivation after glucose depletion, where cells consumed the produced acetate, the peakwidth stabilised and values were similar to the ones for the cultivations where acetate was the sole substrate.

The slope of the cdfplot for GFP, RSG and SYBR fluorescence declined throughout exponential growth on glucose while it remained constant for SYBR (figure 3C and F). For growth on acetate, both when acetate was added from the start as carbon source as well as after diauxic shift in the glucose cultivations, similar values were found and no changes in the slope values were observed throughout the cultivations for neither GFP nor any of the stains, thereby confirming the observations on heterogeneity level seen using the other parameters. The only exception was the CTC fluorescence, for which lower slope values for cells from growth on acetate after diauxic shift were seen than for cells from the pure acetate cultivations. When considering the whole cdfplot (figure 4) it can be seen, more pronounced than in figure 2, that the distributions for cells grown on glucose and acetate exhibit differences in the peakshape. For the CTC data, in general, little shifts and peakshape changes were observed, in glucose and acetate which is in concordance with the slope observations in figure 3C and F. The only exception is a subpopulation in the acetate batch (highlighted by the bump in the plot) with higher fluorescence than the main population also visible in figure 2. Compared to CTC, some shifts are seen in the RSG data for cells growing on glucose, indicating more heterogeneity. The fluorescence is shifting up from the start of batch and down again with exponential growth on glucose and acetate growth after diauxic shift. In the acetate cultivations similar shifts can be seen and additionally a subpopulation is clearly visible, which is more pronounced in the beginning of exponential growth on acetate. SYBR shows in general more heterogeneity in the fluorescence level (bigger shifts) as also seen in figure 2 coincidental with exponential growth on glucose and acetate (after diauxic shift as well as pure acetate culture). While cells grow on acetate as only carbon source there are also subpopulations visible whereas growth on acetate after diauxic shift does not exhibit this behavior.

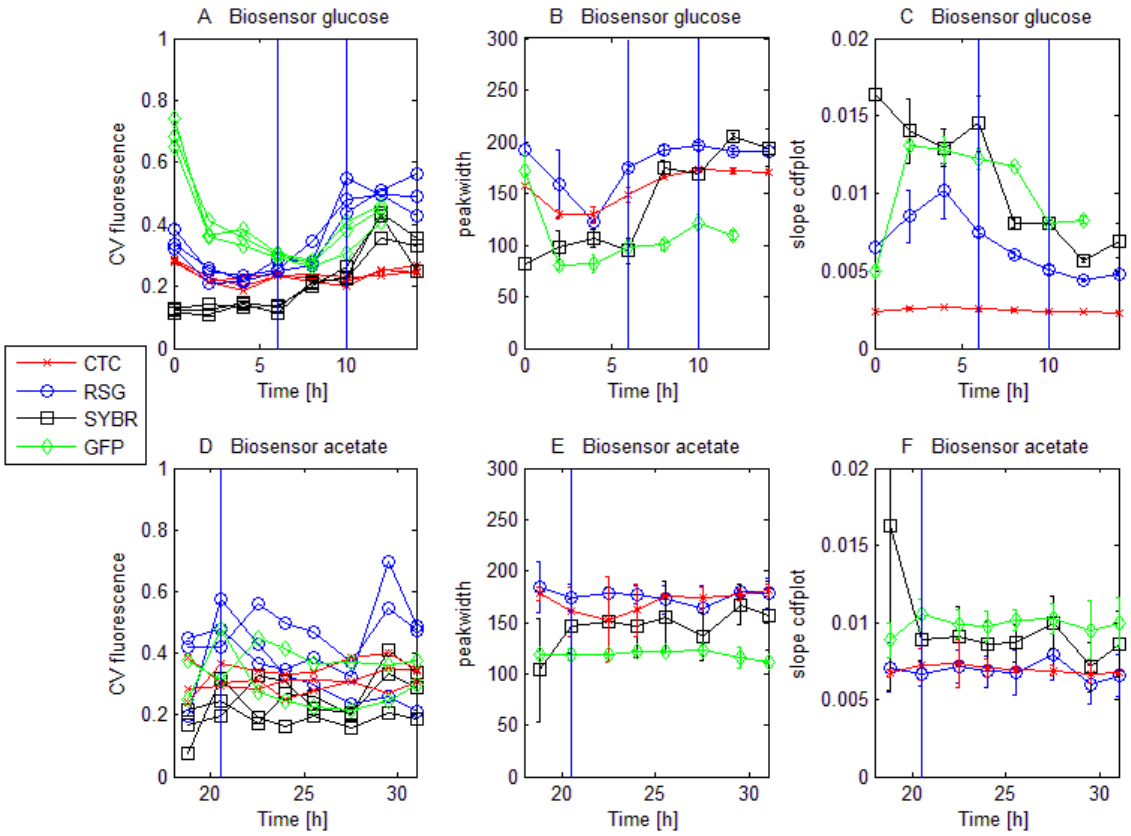

Figure 3 - CV, peakwidth* and slope of cdfplot for CTC, RSG, SYBR and GFP fluorescence distributions for the strain MG1655/pGS20PrrnBGFPAAV (biosensor) in batch cultivations: with glucose (A, B and C) or acetate as carbon source (D,E and F). All values, apart from CV, where all replicates are plotted, are provided including standard deviation originating from triplicate cultivations. The first blue line is indicating the start of the exponential growth phase on glucose (A, B and C) respectively acetate (D, E and F) and the second blue line glucose depletion (A, B and C). Acetate is in both cases depleted with the last presented sample.

*The peakwidth for CTC refers to the width of the whole peak including subpopulations, whereas for RSG the subpopulation is not included. For GFP and SYBR no clear subpopulations were detected so the peakwidth refers to the whole peak.

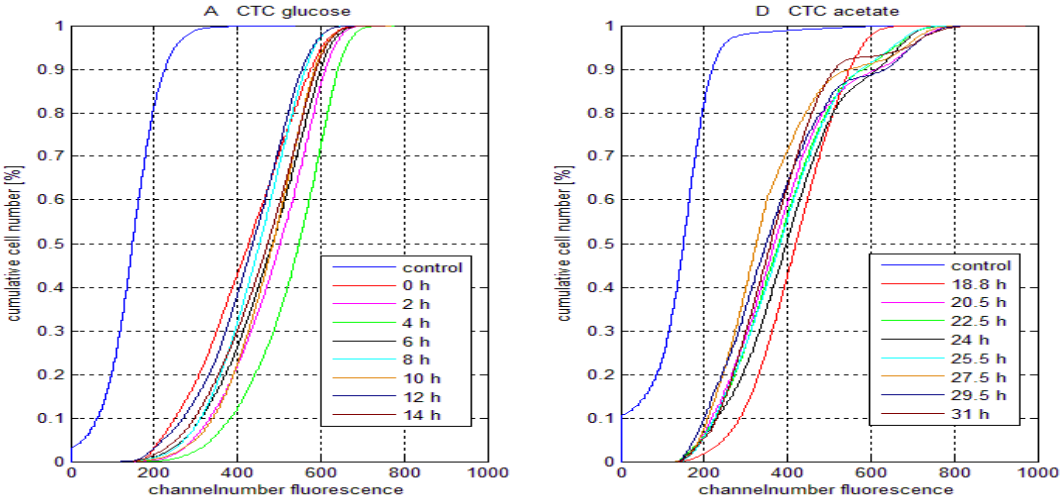

Figure 4 - cdfplots for CTC fluorescence for the strain MG1655/pGS20PrrnBGFPAAV (biosensor) in batch cultivations: with glucose (A) or acetate as carbon source (D). Each graph represents cumulative fluorescence distributions from different time points following the batch.

7.3.5 Subpopulation distributions for glucose and acetate grown cells

As mentioned in the sections above, two of the applied stains, namely CTC and RSG, exhibited two subpopulations (see figure 2 and 4), when growing on acetate whereas for glucose only one main population could be detected. These subpopulations were gated and in figure 5 the relative fractions of the high and low fluorescent subpopulation following the batch are depicted. Additionally, the same gating was applied for SYBR because the whole population was moving, although no clear subpopulation division was seen.

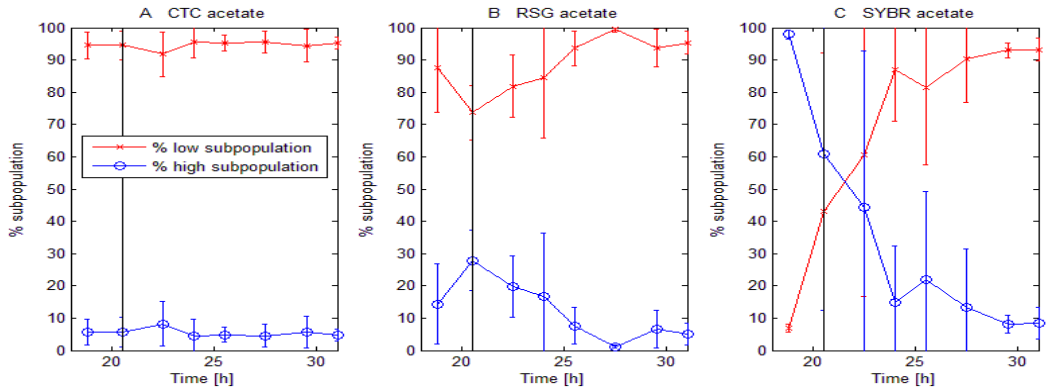

Figure 5 - Subpopulation distribution for CTC, RSG and SYBR fluorescence for the strain MG1655/pGS20PrrnBGFPAAV (biosensor) in batch cultivation growing with acetate as carbon source. Blue represents the high fluorescent population and red the low fluorescent population,

whereas the black line indicates the start of the exponential growth phase on acetate. All values originate from triplicate cultivations and are provided including standard deviation.

For CTC the subpopulation distribution remained constant throughout the batch, with a low fluorescent main population, comprehending around 90% of the cells and a small fraction of cells with a higher fluorescence (around 10%). Contrarily, for RSG the relative ratio of the low fluorescent subpopulation increased with exponential growth from around 80% to almost 100% with acetate depletion, whereas the opposite trend was seen for the high fluorescent subpopulation. For SYBR as mentioned above, no distinct subpopulation division was visible; it was rather the whole population moving. Prior to the start of exponential growth the percentage of the population with low fluorescence was only around 10%. Then the relative fraction of the low fluorescent subpopulation for the SYBR stained cells increased throughout the cultivation to finally include around 90% of the cells. The standard deviations for calculations of the relative fractions of subpopulations for SYBR stained cells were high compared to calculations for data from CTC and RSG staining, indicating less reproducible results between replicates thus higher staining heterogeneity.

7.4 Discussion

Heterogeneity at the single-cell level is often not deeper investigated as traditional studies of microbial populations rely on data averaged across thousands or millions of cells in a sample[41]. To enable robust high-yielding bioprocesses it is important to consider and improve the understanding of microbial population heterogeneity and how population dynamics are influenced by environmental conditions[7]. In the present study five different stains targeting metabolic traits in combination with a GFP-reporter strain were successfully applied for single-cell analysis and mapping of population distributions over time in *E. coli* batch cultivations on the substrates acetate and glucose.

7.4.1 Influence of acetate on heterogeneity of the population in different growth phase compared to glucose

Growth of *E. coli* on acetate is inhibited even at very low concentrations, e.g. 0.5 g/l [42], and this inhibition becomes very significant in a defined medium when acetate is used as sole carbon source[43]. It is also known that bacterial populations become more asynchronous under stress and contain cells at all stages of the division cycle[44], leading to a higher level of heterogeneity. Hence,

the hypothesis was that the enhanced stress during growth on acetate would lead to increased heterogeneity of the population, compared to growth on glucose. Our data support this, as in general wider and thereby more heterogeneous population distributions with slightly lower mean fluorescence (for stains as well as the reporter fluorescence) were observed for acetate grown cells. However, the difference between the two carbon sources was smaller than expected. In general, comparing acetate growth after diauxic shift to growth on acetate as sole carbon source the cell population distributions exhibited similar traits, however, the mean fluorescence was more similar to fluorescence levels for cells grown on glucose and no subpopulation development was detected after diauxic shift. Interestingly, a small portion of cells that are more robust and tolerant to acetate stress seem to exist, since for some of the applied stains subpopulations with higher respiratory activity than the main population were found (figure 2 and 5). Moreover, it is interesting to note that regardless of the carbon source, hardly any cells with compromised or depolarized membrane (data from PI and $DiBAC_4(3)$ staining), and therefore regarded as non-viable or dormant, were detected. Concludingly, considering the long phase of slow growth/lag-phase in the acetate cultivations, cells seem to be stressed and need time to adjust to the harsh growth conditions, but the acetate is not so toxic that it influences the viability of the cells.

7.4.2 Connection observed between metabolic activity using stains and physiology including the use of growth reporter strains

In general, in glucose cultures, the cells appeared to respire more actively (RSG and CTC data) and to synthesize nucleic acids (SYBR green data) before the start of the exponential growth phase (figure 1 and 2). Afterwards the respiratory activity as well as the synthesis of nucleic acid decreased with time and when the cells grew on the prior produced acetate all metabolic activities decreased further before reaching a constant level with the beginning of the stationary phase. The same trend over the batch growth phases as for the stains could also be followed with the growth reporter strain. The GFP fluorescence increased with the beginning of the exponential phase on glucose, indicating active synthesis of ribosomal RNA, before declining during acetate growth and reaching a plateau with the beginning of the stationary phase.

Discrepancies were found between the results obtained with CTC and RSG. Although both strains are used to detect respiratory activity, the RSG distributions exhibited more heterogeneity than the CTC distributions (figure 4). The distinct difference between acetate and glucose grown cells seen for cells stained with CTC, i.e. more heterogeneous distribution seen for cells from acetate cultivations, in addition to the existence of a small subpopulation with a higher respiratory level,

was not observed when staining with RSG. However, in general both stains showed a slightly lower respiratory activity when growing on acetate than during growth on glucose. This might be connected to the lower growth rate on acetate, which implies a slower metabolism and thereby lower respiratory activity. This is also supported by the results for SYBR green, demonstrating that cells exhibit a higher rate of DNA/RNA production when growing with a higher growth rate on glucose than when growing on acetate. Surprisingly the growth reporter strain revealed slightly higher GFP fluorescence levels during exponential growth on acetate compared to glucose. This fact is contradictory to the observation of the higher fluorescent signal for SYBR green from cells grown on glucose than from cells grown on acetate and to the generally accepted belief that fast growing cells have a higher number of ribosomal operons resulting in a higher synthesis rate of rRNA than cells growing at a slower growth rate[34]. One explanation might be that glucose exhibits a repression effect on the ribosomal activity. Potentially the strain's machinery is working harder to cope with the harsh conditions in the presence of acetate, as reflected in higher average ribosomal activity (figure 1) and the RSG and SYBR data (figure 2 B,F,C and G). Further investigations are required to fully understand the mechanisms involved in these phenomena.

7.4.3 Conclusions and recommendations with regards to the usefulness of the applied stains

CTC has frequently been used to define the amount of "active" bacteria in samples of diverse origin[45,46]. So far a direct correlation between the amount of cells that are actively respiring, growing and dividing and the amount of cells that reduced enough dye to be detected could not be verified, though a good correlation between colony forming units (CFU) and CTC positive cells regardless of the growth phase was found[47]. The use of CTC is controversial since a possible toxic effect to the cells due to lowered counts of positive cells compared to other studies cannot be obviated. Also an unified protocol for the application of CTC is missing which makes it hard to compare the obtained results reported in different publications[48]. RSG is altered by active reductases in the cells[22], some of which are part of the electron transport system[23] and therefore enables the assessment of bacterial respiratory and metabolic activity. In conclusion considering our results although both stains are aiming at displaying respiratory activity, differences were seen between them, why the choice of which one to utilize should be taken with care depending on the application. Whereas RSG shows a higher sensitivity and correlates especially for growth on glucose better with SYBR fluorescence, CTC was able, although exhibiting lower sensitivity, to display small highly respiring subpopulations.

The two stains targeted to access membrane status, PI and $DiBAC_4(3)$, demonstrated very low, not statistically significant, fractions of positive stained cells. However, it was noticed that the percentage of PI positive cells increased at the onset of exponential growth for both growth on glucose and on acetate. These observations appear to corroborate the existence of false positives when bacteria are actively growing as previously observed in environmental bacterial samples by Shi et al. 2007 and considering that PI false positives have also been detected in stressed cultures of *S. cerevisiae*[50]. In conclusion, PI should be used with care when assessing viability of cells under dynamic growth conditions, therefore $DiBAC_4(3)$ may be more suitable as a vitality indicator in batch cultures.

7.4.4 Potential of the combined use of reporter strains together with stains

The physiological state of microorganisms can be affected by a number of environmental factors, which consequently may influence the performance of bioprocesses. An understanding of the state of the individual cells is thus needed to achieve high process efficiency. Traditional cultivation data reflect the general metabolic ability of the production strains but do not illustrate single cell differences. Using rapid fluorescent staining procedures and reporter strains combined with FC provided fast information on cellular physiological status changes and population distributions. Although this approach was comprehensive, by just choosing one of the stains or in combination with the growth reporter strain and analyze the distributions quantitatively would already reveal significant information about population heterogeneity and provide a important complement to the traditional methods used in industry to monitor batch cultures.

Acknowledgement

The Danish Council for Strategic Research is gratefully acknowledged for financial support in the frame of the project “Towards robust fermentation processes by targeting population heterogeneity at microscale” (project number 09-065160). ERA-IB (ERA-NET Industrial Biotechnology) is gratefully acknowledged for financial support in the frame of the project “Targeting population heterogeneity at microscale for robust fermentation processes” (project number EIB.08.031). Part of the work presented here is sponsored by the Portuguese Foundation for Science and Technology by project SFRH/BD/43996 within the QREN-POPH and through the European Social Fund.

7.5 References

1. Demain, A. L. The business of biotechnology. *Ind. Biotechnol.* **3,** 269–283 (2007).

2. Demain, A. L. & Vaishnav, P. Production of recombinant proteins by microbes and higher organisms. *Biotechnol. Adv.* **27,** 297–306 (2009).

3. Lara, A. R. *et al.* Transcriptional and metabolic response of recombinant Escherichia coli to spatial dissolved oxygen tension gradients simulated in a scale-down system. *Biotechnol. Bioeng.* **93,** 372–385 (2006).

4. George, S., Larsson, G., Olsson, K. & Enfors, S.-O. Comparison of the Baker's yeast process performance in laboratory and production scale. *Bioprocess Eng.* **18,** 135–142 (1998).

5. Larsson, G. *et al.* Substrate gradients in bioreactors: origin and consequences. *Bioprocess Eng.* **14,** 281–289 (1996).

6. Avery, S. V. Microbial cell individuality and the underlying sources of heterogeneity. *Nat. Rev. Microbiol.* **4,** 577–587 (2006).

7. Fernandes, R. L. *et al.* Experimental methods and modeling techniques for description of cell population heterogeneity. *Biotechnol. Adv.* **29,** 575–599 (2011).

8. Bylund, F., Collet, E., Enfors, S.-O. & Larsson, G. Substrate gradient formation in the large-scale bioreactor lowers cell yield and increases by-product formation. *Bioprocess Eng.* **18,** (1998).

9. Enfors, S. O. *et al.* Physiological responses to mixing in large scale bioreactors. *J. Biotechnol.* **85,** 175–185 (2001).

10. Luli, G. W. & Strohl, W. R. Comparison of Growth, Acetate Production, and Acetate Inhibition of Escherichia-Coli Strains in Batch and Fed-Batch Fermentations. *Appl. Environ. Microbiol.* **56,** 1004–1011 (1990).

11. Gschaedler, a, Robas, N., Boudrant, J. & Branlant, C. Effects of pulse addition of carbon sources on continuous cultivation of Escherichia coli containing a recombinant E. coli gapA gene. *Biotechnol. Bioeng.* **63,** 712–720 (1999).

12. Eiteman, M. A. & Altman, E. Overcoming acetate in Escherichia coli recombinant protein fermentations. *Trends Biotechnol.* **24,** 530–536 (2006).

13. Shiloach, J. & Fass, R. Growing E. coli to high cell density--a historical perspective on method development. *Biotechnol. Adv.* **23,** 345–357 (2005).

14. Dhar, N. & McKinney, J. D. Microbial phenotypic heterogeneity and antibiotic tolerance. *Curr. Opin. Microbiol.* **10,** 30–38 (2007).

15. Fritzsch, F. S. O., Dusny, C., Frick, O. & Schmid, A. Single-Cell Analysis in Biotechnology, Systems Biology, and Biocatalysis. *Annu. Rev. Chem. Biomol. Eng. Vol 3* **3,** 129–155 (2012).

16. Nebe-von-Caron, G., Stephens, P. J., Hewitt, C. J., Powell, J. R. & Badley, R. a. Analysis of bacterial function by multi-colour fluorescence flow cytometry and single cell sorting. *J. Microbiol. Methods* **42,** 97–114 (2000).

17. Quiros, C., Herrero, M., Garcia, L. A. & Diaz, M. Application of flow cytometry to segregated kinetic modeling based on the physiological states of microorganisms. *Appl. Environ. Microbiol.* **73,** 3993–4000 (2007).

18. Rezaeinejad, S. & Ivanov, V. Heterogeneity of Escherichia coli population by respiratory activity and membrane potential of cells during growth and long-term starvation. *Microbiol. Res.* **166,** 129–135 (2011).

19. Prorot, A., Eskicioglu, C., Droste, R., Dagot, C. & Leprat, P. Assessment of physiological state of microorganisms in activated sludge with flow cytometry: application for monitoring sludge production minimization. *J. Ind. Microbiol. Biotechnol.* **35,** 1261–1268 (2008).

20. Rodriguez, G. G., Phipps, D., Ishiguro, K. & Ridgway, H. F. Use of a fluorescent redox probe for direct visualization of actively respiring bacteria. *Appl. Environ. Microbiol.* **58,** 1801–1808 (1992).

21. Belkova, N. L., Tazaki, K., Zakharova, J. R. & Parfenova, V. V. Activity of bacteria in water of hot springs from Southern and Central Kamchatskaya geothermal provinces, Kamchatka Peninsula, Russia. *Microbiol. Res.* **162,** 99–107 (2007).

22. Gray, D. Y., Chueng, C. & Godfrey, W. Bacterial vitality detected by a novel fluorogenic redox dye using flow cytometry. *Abstr. Am. Soc. Microbiol. Meet.* **Washington,** (2005).

23. Kalyuzhnaya, M. G., Lidstrom, M. E. & Chistoserdova, L. Real-time detection of actively metabolizing microbes by redox sensing as applied to methylotroph populations in Lake Washington. *ISME J* **2,** 696–706 (2008).

24. Zipper, H., Brunner, H., Bernhagen, J. & Vitzthum, F. Investigations on DNA intercalation and surface binding by SYBR Green I, its structure determination and methodological implications. *Nucleic Acids Res.* **32,** (2004).

25. Noble, R. T. & Fuhrman, J. A. Use of SYBR green I for rapid depifluorescence counts of marine virus and bacteria. *Aquat. Microb. Ecol.* **14,** 113–118 (1998).

26. Strauber, H. & Muller, S. Viability states of bacteria--specific mechanisms of selected probes. *Cytom. A* **77,** 623–634 (2010).

27. Laflamme, C., Lavigne, S., Ho, J. & Duchaine, C. Assessment of bacterial endospore viability with fluorescent dyes. *J. Appl. Microbiol.* **96,** 684–692 (2004).

28. Delvigne, F. *et al.* Green fluorescent protein (GFP) leakage from microbial biosensors provides useful information for the evaluation of the scale-down effect. *Biotechnol. J.* **6,** 968–978 (2011).

29. Sorensen, S. J., Burmolle, M. & Hansen, L. H. Making bio-sense of toxicity: new developments in whole-cell biosensors. *Curr. Opin. Biotechnol.* **17,** 11–16 (2006).

30. Andersen, J. B. *et al.* New unstable variants of green fluorescent protein for studies of transient gene expression in bacteria. *Appl. Environ. Microbiol.* **64,** 2240–2246 (1998).

31. Leveau, J. H. J. & Lindow, S. E. Predictive and Interpretive Simulation of Green Fluorescent Protein Expression in Reporter Bacteria. *J. Bacteriol.* **183,** 6752–6762 (2001).

32. Miller, W. G., Leveau, J. H. J. & Lindow, S. E. Improved gfp and inaZ broad-host-range promoter-probe vectors. *Mol. Plant-Microbe Interact.* **13,** 1243–1250 (2000).

33. Han, S., Delvigne, F., Brognaux, A., Charbon, G. E. & Sorensen, S. J. Design of growth-dependent biosensors based on destabilized GFP for the detection of physiological behavior of Escherichia coli in heterogeneous bioreactors. *Biotechnol. Prog.* (2013). doi:10.1002/btpr.1694

34. Jin, D. J., Cagliero, C. & Zhou, Y. N. Growth rate regulation in Escherichia coli. *FEMS Microbiol. Rev.* **36,** 269–287 (2012).

35. Han, S., Delvigne, F., Brognaux, A., Charbon, G. E. & Sørensen, S. J. Design of growth-dependent biosensors based on destabilized GFP for the detection of physiological behavior of Escherichia coli in heterogeneous bioreactors. *Biotechnol. Prog.* **29,** 553–563 (2013).

36. Xu, B., Jahic, M. & Blomsten, G. Glucose overflow metabolism and mixed-acid fermentation in aerobic large-scale fed-batch processes with Escherichia coli. *Appl. Microbiol. Biotechnol.* **51,** 564–571 (1999).

37. Olsson L, N. J. On Line and in situ Monitoring of Biomass in Submerged Cultivations. *Trends Biotechnol.* **15,** 517–522 (1997).

38. Steinsiek, S., Frixel, S., Stagge, S. & Bettenbrock, K. Characterization of E. coli MG1655 and frdA and sdhC mutants at various aerobiosis levels. *J. Biotechnol.* **154,** 35–45 (2011).

39. Andersen, K. B. & von Meyenburg, K. Are growth rates of Escherichia coli in batch cultures limited by respiration? *J. Bacteriol.* **144,** 114–123 (1980).

40. Cozzone, A. J. & El-Mansi, M. Control of isocitrate dehydrogenase catalytic activity by protein phosphorylation in Escherichia coli. *J. Mol. Microbiol. Biotechnol.* **9,** 132–146 (2005).

41. Avery, S. V. Microbial cell individuality and the underlying sources of heterogeneity. *Nat. Rev. Microbiol.* **4,** 577–587 (2006).

42. Nakano, K., Rischke, M., Sato, S. & Markl, H. Influence of acetic acid on the growth of Escherichia coli K12 during high-cell-density cultivation in a dialysis reactor. *Appl. Microbiol. Biotechnol.* **48,** 597–601 (1997).

43. Koh, B. T., Nakashimada, U., Pfeiffer, M. & Yap, M. G. S. Comparison of Acetate Inhibition on Growth of Host and Recombinant Escherichia-Coli K12 Strains. *Biotechnol. Lett.* **14,** 1115–1118 (1992).

44. Gilbert, P., Collier, P. J. & Brown, M. R. Influence of growth rate on susceptibility to antimicrobial agents: biofilms, cell cycle, dormancy, and stringent response. *Antimicrob. Agents Chemother.* **34,** 1865–1868 (1990).

45. Bartosch, S., Mansch, R., Knötzsch, K. & Bock, E. CTC staining and counting of actively respiring bacteria in natural stone using confocal laser scanning microscopy. *J. Microbiol. Methods* **52,** 75–84 (2003).

46. Servais, P. Are the actively respiring cells (CTC+) those responsible for bacterial production in aquatic environments? *FEMS Microbiol. Ecol.* **35,** 171–179 (2001).

47. Creach, V., Baudoux, A. C., Bertru, G. & Le Rouzic, B. Direct estimate of active bacteria: CTC use and limitations. *J. Microbiol. Methods* **52,** 19–28 (2003).

48. Nielsen, J. L., Kragelund, C. & Nielsen, P. H. Combination of fluorescence in situ hybridization with staining techniques for cell viability and accumulation of PHA and polyP in microorganisms in complex microbial systems. *Methods Mol Biol* **599,** 103–116 (2010).

49. Shi, L. *et al.* Limits of propidium iodide as a cell viability indicator for environmental bacteria. *Cytometry. A* **71,** 592–598 (2007).

50. Davey, H. M. & Hexley, P. Red but not dead? Membranes of stressed Saccharomyces cerevisiae are permeable to propidium iodide. *Environ. Microbiol.* **13,** 163–171 (2011).

8. Chapter

Systematic approach for evaluation of continuous scale down fermentation of *S. cerevisiae* combining a newly developed two compartment setup with a PBM and unstructured model

Anna-Lena Heins[1*], Rita Lencastre Fernandes[2*], Krist V. Gernaey[2] and Anna Eliasson Lantz[1,§]

[1] Department of Systems Biology, Technical University of Denmark, 2800 Kongens Lyngby, Denmark

[2] Department of Chemical Engineering, Technical University of Denmark, 2800 Kongens Lyngby, Denmark

*These authors contributed equally to the work

[§]Corresponding author

Written as journal paper

Status: Manuscript in preparation

Abstract

In this paper the combined approach of modeling and experimental work is presented to demonstrate its usefulness to aid in and facilitate process development and optimization. A new scale down setup to simulate large scale continuous cultivations was developed consisting of two stirred tank reactors connected to each other (volume ratio 1:6), one representing the feeding zone (small reactor, feed inlet) with high glucose concentration and low oxygen, whereas the other one represents the remaining reactor volume (featuring the outlet), with high oxygen and lower substrate concentration. As a first step a two compartment model based on an earlier developed population balance model (PBM) coupled to an unstructured model[1] was used to describe the development of the bulk concentrations and cell size distributions in the cultivation broth. Thereafter the scale down system, which can be performed as a continuous culture, was run in the lab using the same conditions as used in the model. This included the assessment of different dilution rates ($D = 0.05\ h^{-1}$ and $D = 0.2\ h^{-1}$), glucose concentrations (50 g/L and 300 g/L) as well as different recirculation times between the two compartments (0.1 L/h and 3L/h). General physiology was evaluated as well as flow cytometry was used to quantify single cell properties including cell size and GFP respectively BFP fluorescence originating from two fluorescent reporter strains, a growth and an ethanol reporter. These reporter strains were applied for the deeper investigation of growth and cell robustness characteristics as well as ethanol growth distributions of cells traveling between the two compartments. All results, for the model and the experiments are compared to the performance of a one compartment, conventional chemostat. Results underline the utility for the here presented combined approach as well as the use of continuous scale down reactors for process investigations as insides concerning single cell characteristics of the process are revealed which are normally hidden when applying classical continuous cultivation setups in lab scale without deeper modeling or data analysis inquiry.

Keywords: population balance model, population heterogeneity, reporter strain, yeast, two compartment bioreactor setup, mathematical modeling, continuous scale down reactor

8.1 Introduction

Nowadays, the advances in modeling allow the model based description of single cell physiology in biotechnological industrial fermentation processes[2]. Therefore, a systematic approach using modeling in combination with lab scale experiments can be used to perform and in the end facilitate

process optimization[3]. Hereby modeling can assist in setting the range of interesting experiments, evaluate experimental data, find the performance optimum and create a framework for future process development. In turn experiments are then used to collect data in setups simulating large scale processes, and to validate modeling results. It is important to point out that the model validation step is indeed one of the most important parts of a modeling study.

Large scale fed-batch and continuous cultivations are widely used in the biotechnology industry for the production of pharmaceuticals, biomass and proteins (e.g. insulin)[4,5]. The steadily increasing demand for sustainable production also raises the demand for high yielding biotechnological production processes using robust strains which consequently needs to be well characterized and controllable. This and the fact that a cell population in a bioreactor is in fact heterogeneous, which makes population properties rather distributed than following as earlier assumed averaged characteristics[6], makes process optimization crucial. Spatial population heterogeneity can have several different causes. However, gradients of process parameters (e.g. substrate concentration, pH and oxygen) arising in large scale fermentation due to non-ideal mixing, and thus the development of zones representing different extracellular environments, were found to be one of the major causes of poplation heterogeneity. For example the use of Rushton turbines, one of the most common impellers used in industrial bioprocesses, has been observed to generate compartments within the reactor due to high axial flow barriers created by the turbine[7]. Consequently, lowered yields and a rise in by-product formation are obtained[8,9]. Especially substrate gradients contribute to this phenomenon because cells traveling throughout the reactor experience substrate concentrations that may range from high concentrations close to the feed port to very low concentrations in zones more distant to the feed port. It was found for *Escherichia coli*[10,11] that this is connected with an elevated stress response, especially when cells pass the feeding zone.

A crude and simple way of assessing the degree of spatial population heterogeneity in a bioreactor is the compartment model approach. In such approach, it is assumed that the bioreactor is divided into different zones due to the non-ideal mixing patterns. Exchange flows connect the compartments (zones), and the higher the exchange flow between compartments, the closer to the ideal mixing case one is, i.e. a one compartment set-up. In the other extreme, the system can be represented using Computational Fluid Dynamics simulations, where a very large number of nearly infinitely small volume elements is considered. In a compartment model approach, an ideal mixing behavior, and thus a continuous stirred tank reactor (CSTR) description, can be assumed for each compartment

(i.e. spatial zone). Besides consisting of a straightforward way for describing non-ideal mixing in large scale reactors, a compartment model approach has the advantage of being easily translated into laboratory experimental setups by using scale down reactors.

Scale down reactors are nowadays frequently used for process development and optimization and have been shown to be a valuable tool for the study of gradients of substrate, oxygen[12] and pH in large scale fermentation processes[13]. Different setups of scale down reactors have been used depending on the process /application. Most common are stirred tank reactors (STR) connected to plug flow reactors (PFR) or two STRs connected to each other [14] because both setups allow the creation of gradients of various reactor parameters in a well-controlled environment which is especially useful for studying population heterogeneity. Several studies investigated glucose gradients and the consequent population heterogeneity e.g. during aerobic ethanol production[15] which revealed the induction of stress responses close to the perturbation zone as well as by-product formation in *S. cerevisiae* as well as *E. coli*[16] (PFR connected to STR). Sweere *et al.* (1988)[17] investigated the effects of fluctuating glucose concentration on a *S. cerevisiae* physiology, applying different circulation times and volume ratio of the two reactors, while the feed was only added to the reactor with the smaller volume. It resulted in the same findings as for George *et al.* (1993)[15] in the setup with STR and PFR connected. Later Delvigne *et al.* (2006a, 2006b & 2006c)[18–20] developed, for both *E. coli* and *S. cerevisiae,* a combination of stochastic microbial growth and bioreactor mixing models to explore the hydrodynamic effect of the bioreactor on microbial growth which allowed explanation of the scale down effect associated with glucose fluctuations. By combining the two model parts the authors obtained the profile of concentrations that a cell was subjected to during its cultivation in the bioreactor. Common to all used setups is that they are performed in fed-batch mode, with one reactor representing the feeding zone and the other one the perturbation zone (either PFR with perturbation at inlet or STR with different conditions compared to the other one).

In this study, substrate gradients, which are often seen in large scale industrial fermentation, are simulated and the effect of the operating conditions (dilution rate and glucose feed concentration) are evaluated using, to our knowledge for the first time a scale down reactor system for aerobic glucose limited continuous cultivation. The existence of gradients is assumed to result in a compartmentalization of the reactor (i.e. delimited spatial zones can be defined). This

compartmentalization is translated into a set-up consisting of two compartments of different volume, one representing the feeding zone of an industrial scale reactor and one representing the remaining reactor volume where the bioreactor outlet is located. This study addresses firstly an *in silico* investigation of the dynamics of a yeast population cell size distribution during a continuous large scale fermentation, where a compartmentalization of the reactor can be assumed. The performed computer simulations rely on an adaption of a previously described population balance model (PBM) coupled to an unstructured model describing the bulk concentrations in the cultivation media[1].

Following the *in silico* study, the corresponding experimental investigation was performed by running glucose-limited continuous cultivations using a growth and an ethanol metabolism *S. cerevisiae* reporter strain. Yeast single cell physiology and robustness will be assessed using flow cytometry analysis. Apart from exhibiting general growth physiology the two strains used in this study were reporter strains which typically express a protein or enzyme whose activity can be easily assayed[21]. In the major part of the cultivations performed in this study, the growth reporter strain FE440 was used: it expresses a green fluorescent protein (GFP) from a ribosomal promoter which was correlated to single cell growth[22]. In some cultivations, an ethanol reporter Sc-PCK1-B expressing a blue fluorescent protein (TagBFP) from a phosphoenolpyruvate carboxykinase promoter (inactive when glucose is present, part of gluconeogenesis) whose expression is correlated to ethanol consumption (Johansen et al., unpublished) was utilized. Additionally, when applying freeze-thaw stress to cells sampled from the fermentation broth membrane robustness could be investigated[22]. Consequently using flow cytometry analysis revealed not only distributions of cell size and morphology, but also growth and ethanol consumption characteristics of thousands of single cells per second. Thus, in addition to conventional growth physiology different expression profiles of cells traveling throughout the scale down system were investigated.

8.2 Materials and Methods

8.2.1 Strains and Chemicals

The *S. cerevisiae* reporter strain FE440[22] expressing a green fluorescent protein (GFP) controlled by the ribosomal protein RPL22a promoter and thus correlated to growth was mainly used throughout this study. The ethanol reporter strain Sc-PCK1-B (Johansen et al. (2013), unpublished) expressing a blue fluorescent protein (BFP) controlled by the phosphoenolpyruvate carboxykinase promoter

and thereby correlated to ethanol growth/non glucose growth (glucose repression/derepression). All chemicals used during the study were obtained from Sigma Aldrich (St. Louis, USA).

8.2.2 Cultivation conditions

Pre-culture. A single colony of the growth reporter FE440 respectively the ethanol reporter strain Sc-PCK1-B was picked from a plate with minimal medium and used to inoculate a 0.5 L baffled shake flask with 100 ml of defined mineral medium containing 7.5 g/L $(NH_4)_2SO_4$, 14.4 g/L KH_2PO_4, 0.5 g/L $MgSO_4*H_2O$, 2 ml/L trace metal solution, 1 ml/L vitamin solution and 10 g/L glucose[23]. The pre-culture was incubated in an orbital shaker set to 150 rpm at 30°C until mid-exponential phase (approximately 10 h) and directly used for inoculation.

Chemostats One compartment: Aerobic level-based chemostats were run with the growth reporter strain FE440 according to a factorial design plan using 1 L bioreactors (Sartorius, B. Braun Biotech International, GmbH, Melsungen, Germany) with a working volume of 1 L. The glucose concentrations in the feed were 50 g/L or 300 g/L and the dilution rates were D= 0.05 and 0.2 h^{-1} as well as including a center point with D = 0.125 h^{-1} and 125 g/L glucose. The experiments were performed in duplicates (except for the center point). pH and DOT electrodes (Mettler Toledo, OH, USA) were calibrated according to standard procedures provided by the manufacturer using two point calibration (pH 4 and 7, gassing with oxygen (100 %) and nitrogen (0 %), respectively). The growth medium was a defined mineral medium according to Verduyn *et al.* (1992)[23] with 5 g/L glucose for the batch phase and 50 g/L, 125 g/L respectively 300 g/L glucose for the feed in continuous mode. The OD_{600} for inoculation was 0.001. The pH was adjusted and kept constant at 5.0 using 2 M NaOH. Temperature, aeration and stirring were kept constant at 30° C, 1 v/vm and 600 rpm.

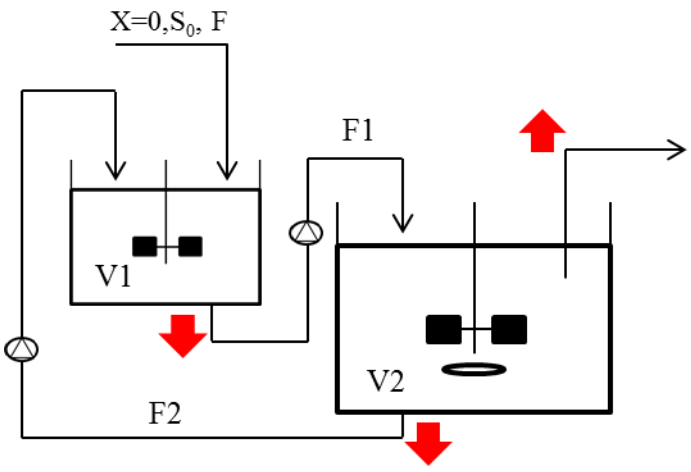

Run	G_{Feed} [g/L]	D [h^{-1}]	Recirculation flow F2 [L/h]
A*	300	0.05	0.1
B	300	0.2	0.1
C	300	0.05	3.0
D	300	0.2	3.0
E*	50	0.05	0.1
F**	50	0.2	0.1
G	50	0.05	3.0
H*	50	0.2	3.0
I*	125	0.125	1.45

Figure 1 – setup for two compartment experiments: V1 represents the 0.5L reactor with the feed inlet and no oxygen sparging, V2 represents the remaining reactor volume with the waste outlet and the oxygen supply. Between the two reactors a recirculation is set up (F1 and F2) and samples are taken at three different points, the waste outlet, at the beginning of F1 as well as at the beginning of F2. The red arrows mark sampling points.

Table 1 – Overview of factorial design plan: Factorial design with varying glucose feed concentration (50 g/L, 125 g/L and 300 g/L), dilution rate (D= 0.05 h^{-1}, 0.125 h^{-1} and 0.2 h^{-1}) and recirculation flow between the two reactors (0.1 L/h, 1.45 L/h and 3 L/h). The asterix respectively double asterix marks the experiments that have been performed with the growth reporter strain respectively with both strains.

Two compartment: Aerobic level-based chemostats with different dilution rates (D = 0.05 and 0.2 h^{-1}as well as D = 0.125 h^{-1} as center point), glucose feed concentration (50 g/L, 125 g/L and 300 g/L) and recirculation flow (0.1 L/h, 1.45 L/h and 3 L/h) between the two reactors were performed for selected conditions (marked with an asterix for the growth reporter strain respectively two asterix for performance with both strains, table 1) according to a factorial design experiment plan (see table 1). A 5 L reactor (V2) connected to a 0.5 L reactor (V1) (Sartorius, B. Braun Biotech International, GmbH, Melsungen, Germany) was used with a ratio of the working volume of V1 = 1/6*V2. The 0.5 L reactor (V1) hereby represented the feeding zone with feed addition and no sparging of oxygen whereas the 5 L reactor (V2) corresponded to the remaining reactor volume. The 5 L reactor contained the outlet of the system and was sparged with oxygen. Between the two reactors a

recirculation was applied (F1 and F2), whereas the recirculation flow rate from V2 to V1 (F2) was varied according to the factorial design plan. The pH and DOT electrodes (Mettler Toledo, OH, USA) were calibrated in the same way as for the one compartment and also the growth medium was a defined mineral medium according to Verduyn *et al.* (1992) [23] with 5 g/L glucose for the batch phase and 50 g/L respectively 125 g/L or 300 g/L glucose for the feed in continuous mode. The OD_{600} for inoculation was 0.001. The pH was adjusted and kept constant in both reactors at 5.0 using 2 M NaOH. Temperature, aeration and stirring were kept constant at 30°C, 1 v/vm and 600 rpm.

For both setups, the one and two compartment setup, the batch phase was followed by OD_{600} measurement and continuous analysis of the off-gas composition by a Mass spectrometer (Prima Pro Process MS, Thermo Fisher Scientific, Winsford UK). After glucose depletion, detected as a rapid drop in the CO_2 content of the off gas, the cultures were switched to chemostat mode with the desired dilution rate by applying a feed with the same medium as used for the batch but containing 50 g/L, 125 g/L respectively 300 g/L glucose . The volume was kept constant by a level based outlet for both the one and two compartment experiments. Steady state was considered established when dry weight, dissolved oxygen tension (DOT), metabolites and exhaust gas concentration (CO_2) had remained constant for at least three residence times. For the ethanol reporter strain, and additional fed-batch phase was integrated into the process after glucose depletion to validate if the same steady state was reached as when the continuous mode was started with a lower biomass concentration after the batch. Therefore, a feed with 300 g/L glucose at a growth rate of 0.1 h^{-1} was applied until a biomass concentration of 25 g/L was reached.

Samples were withdrawn for OD_{600}, high performance liquid chromatography (HPLC), dry weight (DW) and flow cytometry analysis. Samples for OD_{600} and DW were analyzed directly, HPLC samples were sterile filtered and stored at -20 °C. Samples for flow cytometry were mixed with glycerol to a final concentration of 15 % and frozen and stored in a -80°C freezer. The sampling frequency was once every residence time until the 9^{th} residence time starting with the 0^{th} residence time directly after switching to chemostat mode, as well as three samples during exponential growth in batch mode. For the one compartment experiments samples where withdrawn at the outlet whereas for the two compartment experiments samples were additionally withdrawn on both outlets of the recirculation lines (V1 and V2, see figure 1, marked with an arrow).

8.2.3 Sample analysis

OD, DW and HPLC. Growth was monitored by measuring OD_{600} with a Shimadzu UV mini 1240 spectrophotometer (Shimidzu, Kyoto, Japan). Dry weight measurements were performed on 5 ml cultivation broth according to Olsson and Nielsen (1997)[24]. The concentrations of glucose, acetate, ethanol, glycerol and pyruvate in the broth were determined by HPLC as earlier described by Carlquist *et al.* (2012)[22].

Flow cytometry. A FACSAria™ III (Becton-Dickinson, NJ, USA) flow cytometer was used for single-cell analysis of both yeast and bacteria. Excitation wavelength for the laser was set to 488 nm. Two scattering channels (FSC and SSC) and two fluorescent detection channels were used in the analysis. Fluorescence emission levels were measured using a band pass filter at 530±30 nm for GFP and 450±20 nm for BFP. Light scattering and fluorescence levels were standardised using 2.5 µm fluorescent polystyrene beads. Samples for flow cytometry were centrifuged for 1 min at 3000 g and 4 °C, resuspended in 0.9 % saline solution and directly analysed. 10,000 events were recorded for yeast. CS&T beads (Cytometer Setup and Tracking beads) (Becton Dickinson, USA) were used for the automated QA/QC of the machine performance.

8.2.4 Data analysis

Processing and analysis of the flow cytometry raw data was performed using MatLab ® R2013a (The MathWorks, Inc., Natick, MA, USA). The raw data was extracted from the flow cytometer as fcs files and loaded into MatLab with the help of the readfsc function (by L. Balkay, University of Debrecen, Hungary, available on MatLab central file sharing). The HPLC data were imported from excel. The data from the fcs files was saved into mat files including the recorded GFP fluorescence and the FSC for each experiment. By application of the hist function to the 1024 recording channels cell count was saved for all channels and histogram plots generated. For better quantitative description of the GFP distributions, the mean function was used to calculate the mean FSC and mean GFP fluorescence. By dividing the standard deviation of the GFP distribution by the mean GFP the coefficient of variance (CV) of the distribution was generated.

8.2.5 Modeling Aspects

A two-stage PBM (population balance model) previously developed for a batch cultivation[1], was adapted to describe a continuous cultivation in a one- and two-compartment set-up (see figure 1). Cell total protein content (a measure of cell size) is used as model variable. In the case of the two compartment set-up presented in this work, four population balance equations are necessary (two

cell stages x two compartments). Furthermore, the dilution terms taking into account the transport between compartments, inlet and outlet are included in the PBM equations for both the case of one- and two-compartment models. The PBM equations for a two compartment model are presented in Appendix 1 (Eq. A1-1 to A1-4). For further details on the formulation of a PBM and the various model kernels forming the PBM equations, the paper by Lencastre Fernandes *et al.*, (2013)[1] should be consulted. The same boundary and initial conditions as proposed for the batch cultivation model are used for both compartments.

Based on the trajectory of the estimated critical sizes along a batch cultivation[1] the budding and division critical sizes were defined as continuous functions of the concentrations of glucose or ethanol, in a given compartment, according to the following assumptions:

- If the concentration of glucose, in a given compartment, is equal to or above 0.1 g/l, growth on glucose is assumed for that compartment, and the critical budding ($\mu_{B)}$ and division (μ_D) sizes are calculated based on the glucose concentration according to Eq. A1-6 to A1-7 in Appendix 1
- If the concentration of glucose, in a given compartment, is below 0.1 g/l, growth on ethanol is assumed for that compartment, and the critical budding ($\mu_{B)}$ and division (μ_D) sizes are calculated based on the glucose concentration according to Eq. A1-8 to A1-9 in Appendix 1
- If the concentration of glucose and ethanol, in a given compartment are under $1e^{-6}$ g/l, growth in that compartment is assumed to be zero. An estimated value for the saturation constant of the overall growth process (corresponding to half of the maximum specific growth rate) is 0.15 g/l[25].
- The partition shape parameters (necessary for defining the birth kernel in the PBM equations) are assumed to change according to the growth mode (glucose or ethanol) observed in a given compartment: for glucose growth, $\alpha=\beta=50$, for ethanol growth $\alpha=30$ and $\beta=60$. The nature of these values is further discussed in Lencastre Fernandes *et al. (*2013)[1].

In order to further describe the bulk concentration of glucose, ethanol and oxygen in the cultivation media, in each compartment, an unstructured model was coupled to the PBM (see Eq. A1-10 to A1-15). As presented for the experimental set-up (see figure 1), the glucose feed corresponds to the inlet in compartment one, and the oxygen supply takes place exclusively in compartment two. As

proposed for the batch model [1], the substrate dependent term in the growth kernel (λ(Z)) is evaluated, in this case, for each of the compartments (see Eq. A1-19).

The model was implemented and solved in MatLab® Release2012b, and the fixed-pivot method was used for discretization of the PBM equations. The unstructured and PBM models are solved iteratively, following a solution procedure similar to the one proposed for the batch model[1].

8.3 Results and discussion

8.3.1 Comparison of the modeling results with the experimental setup

To simulate gradients often seen in large scale cultivations and the consequent development of compartments with different microenvironment inside a reactor that influences the single cell behavior a 2-compartment setup was developed (figure 1). It consists of two reactors with a volume ratio 1:6. The smaller reactor (V1) represents the feeding zone with feed addition and no sparging of oxygen, whereas the bigger reactor (V2) corresponds to the remaining reactor volume containing the outlet, considerably lower glucose concentration and sparging with oxygen. A circulation loop (with flow F1 and F2, respectively) ensured the exchange between the two reactors, where the recirculation from V2 to V1 (F2) was varied according to the factorial design plan (table 1). Overall dilution rates (calculated for the whole working volume of both reactors) of D = 0.05 h^{-1} and 0.2 h^{-1}, in addition to a center point corresponding to D = 0.125 h^{-1} were applied. The dilution rates in the two compartments were different than the overall dilution rate and an overview of the resulting flows and dilution rates (based on the flow per volume in the respective compartment) in each of the compartments for the experimentally performed conditions is given in table 2. It needs to be mentioned that due to the volume differences and circulation between the reactors (two compartments) with only one feed inlet, local dilution rates in the compartments can be higher than what is normally possible without experiencing a wash-out of biomass.

Different operating conditions were evaluated *in silico* using a factorial design plan, of which afterwards selected conditions were performed experimentally (table 1). These included two cases (A and E) run with D = 0.05 h^{-1} and 50 g/L respectively 300 g/L of glucose feed both with low recirculation flow rate between the reactors. Furthermore to be able to evaluate effect of a higher overall dilution rate on the cell population structure, also cases F and H, corresponding to a low and high recirculation flow rate respectively, were included in the experimental study. In the case H oscillations were found when performing simulations as well as for the center point (case I) which

was also chosen to be carried out as a middle range condition between the extremes. Additionally to the comparison of the model and the two compartment setup all results are also compared to the corresponding one compartment chemostat experimental cultivation and model simulation.

Table 2 – Overview of dilution rates in each of the compartments for experimental conditions: the overall dilution rates were D= 0.05 h^{-1}, 0.125 h^{-1} and 0.2 h^{-1} with flows estimated for the working volume of the two compartments in total. The dilution rates in each compartment were calculated based on the flows (F1 and F2) between the reactors.

D =0.05 h^{-1}/low recirculation for 50g/L (E) respectively 300g/L feed (A)			
flow rate $_{in}$ for $D_{overall}$ [h^{-1}]	0.175	**D_{V1}[h^{-1}]**	0.55
recirculation flow [L/h]	0.1	**D_{V2}[h^{-1}]**	0.079
D= 0.2 h^{-1}/50g/L feed/ low recirculation (F)			
flow rate $_{in}$ for $D_{overall}$ [h^{-1}]	0.7	**D_{V1} [h^{-1}]**	1.64
recirculation flow [L/h]	0.1	**D_{V2} [h^{-1}]**	0.229
D= 0.2 h^{-1}/50g/L feed/high recirculation (H)			
flow rate in for $D_{overall}$ [h^{-1}]	0.7	**D_{V1} [h^{-1}]**	7.4
recirculation flow [L/h]	3	**D_{V2} [h^{-1}]**	1.057
D=0.125 h^{-1}/125g/L feed/middle recirculation (I)			
flow rate $_{in}$ for $D_{overall}$ [h^{-1}]	0.438	**D_{V1} [h^{-1}]**	3.78
recirculation flow [L/h]	1.45	**D_{V2} [h^{-1}]**	0.539

8.3.2 Variation of general physiology and cell size over time in the two compartment setup in comparison with one compartment chemostats and modeling results

8.3.2.1 General physiology

When looking at the general physiology of the different cases, for all of them steady state was achieved, though after a different number of residence times depending on the conditions. For growth at the high dilution rate, D= 0.2 h^{-1}, the cells generally consumed the fed glucose producing CO_2 and ethanol due to overflow metabolism. When the experiment was performed with low recirculation flow rate (case F, figure 2), the glucose concentration in compartment V1 was around half of the feed concentration along with the production of CO_2 and low amounts of biomass (end value for biomass concentration: around 3 g/L). The dilution rate in compartment V1 was much

higher than the overall dilution rate (table 2). This implies that cells, glucose and ethanol were transported to V2. In this compartment the incoming glucose was readily consumed and ethanol accumulated (ethanol concentration was around 3 g/L). The model simulations supported these observations (figure 3), and further suggested that cells in V2 have not switched to ethanol growth: a high budding index (around 60%) was predicted for both compartments, and the predicted cell size distributions were similar, although slightly smaller cells were observed in V2 as it would be expected as found by earlier studies[26,27] as lower glucose concentrations were observed. In both compartments no other metabolites were found in significant amounts.

When applying a high recirculation flow rate between the compartments (case H), both compartments exhibited the same concentration profiles. This was expected and predicted by the model simulations, as the high exchange between compartments is closer to the one-compartment case (i.e. where ideal mixing and homogeneity in the reactor is assumed). The glucose fed to V1 was readily consumed, CO_2 was produced as well as small amounts of biomass (around 12 g/L) and ethanol (around 5 g/L). In the model simulations an oscillatory behavior was observed, in particular for the budding index profile for both compartments and the oxygen profile for compartment V2. These oscillations are a result of a continuous shift between glucose and ethanol growth modes: as the budding and division critical sizes (and consequently the growth rate) decrease gradually following the glucose concentration. When the glucose concentration reaches the threshold value, the partition shape parameters change resulting in the generation of new smaller cells, which grow slower leading to an accumulation of glucose and when the glucose concentration again rises above the threshold value the shape parameters change once again leading to an accumulation of bigger cells and thus a faster growth rate and faster consumption of glucose (leading to a decrease of the glucose concentration). These oscillations were not visible in the experimental results. It remains to be studied whether the oscillations are exclusively due to a model artifact (due to the assumptions that were made) or they take place in reality, but the frequency of the experimental sampling was too low to capture this phenomenon.

When lowering the dilution rate and elevating the glucose feed concentration (case I, center point), a similar picture as for the high dilution rate (case H) was observed. Whereas there was no difference in biomass concentration between the two compartments (up to around 25g/L), the ethanol level was different. The fed glucose was readily consumed in compartment V1 producing CO_2, biomass and ethanol (around 25g/L). The remaining glucose and ethanol are recirculated and

completely consumed in the compartment V2. The model simulation also predicted oscillations for this case.

For experiments with the low dilution rate (D = 0.05h^{-1}, cases A and E) the fed glucose was only partly consumed in V1 producing ethanol, CO_2 and biomass. The remaining glucose, the formed ethanol and biomass were transported into V2, where significantly higher biomass concentrations were detected. When increasing the feed glucose concentration, an increase in the produced biomass concentration (to around 50 g/L vs 20 g/L), ethanol concentration (around 20 g/L vs 5 g/L) and CO_2 were observed in both compartments, as well as a higher remaining glucose concentration in V1. In contrast to experiments with lower glucose concentration, also small amounts of glycerol were detected in V1 for case A.

The model predictions for case A were not in agreement with the experimental observations. Indeed, while the model predicts a residual glucose concentration in V1, a significant amount was observed after 6 retention times in the experiments. It is however not clear if a steady state has been reached at that point, or if a further decrease of the glucose concentration (to residual levels) would be observed for higher residence times. An explanation for this could be that the cells due to the high glucose concentration are more stressed and hence need longer time to adjust and to reach steady state. It could be a similar phenomenon as seen in high gravity batch cultivations, where a lag phase/phase of slow growth of about 20h is seen before the exponential growth phase starts[28]. This was not incorporated in the model and could thereby lead to different results compared to the experiments.

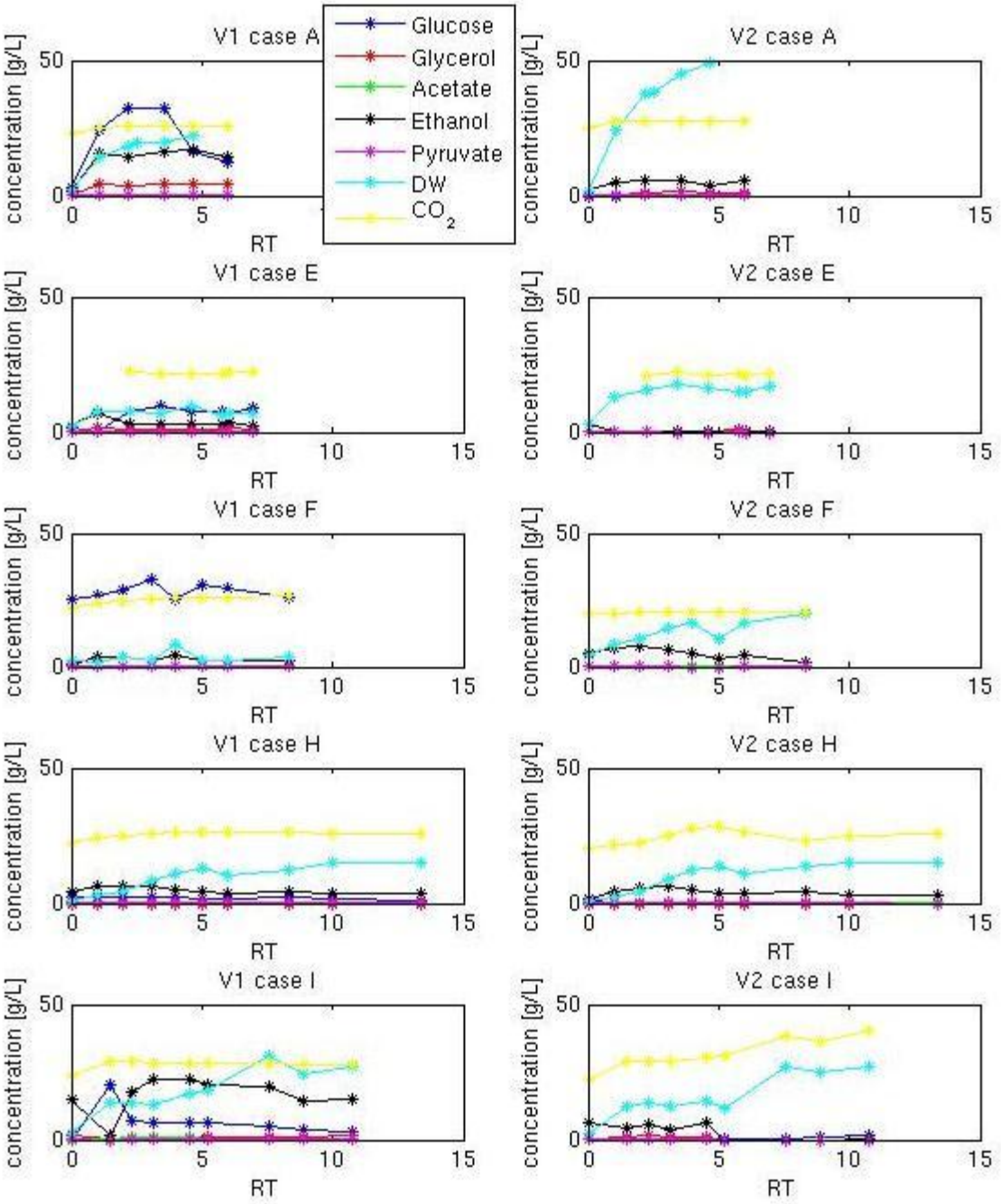

Figure 2 – Variation of glucose, ethanol, glycerol, acetate, pyruvate, biomass and CO_2 for the two compartment experiments: using the growth reporter strain FE440. Results are shown for the experimental performed cases (A, E, H, F, I).

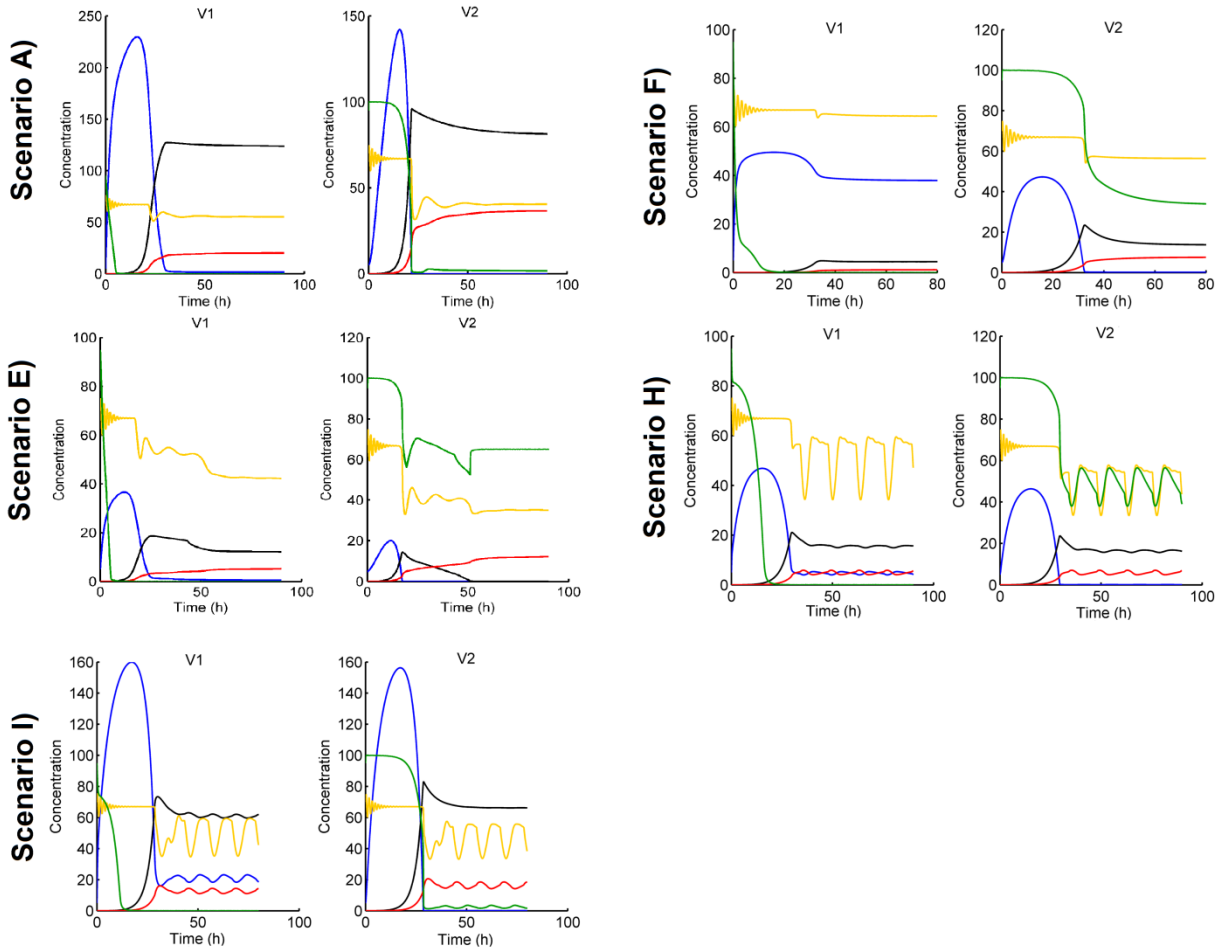

Figure 3 – Variation of glucose, ethanol, glycerol, acetate, pyruvate, biomass and CO_2 for the two compartment model: results are shown for the experimental performed cases (A, E, H, F, I). Blue: glucose; Black: ethanol; Red: biomass; Green: dissolved oxygen; Yellow: budding index

8.3.2.2 Cell size

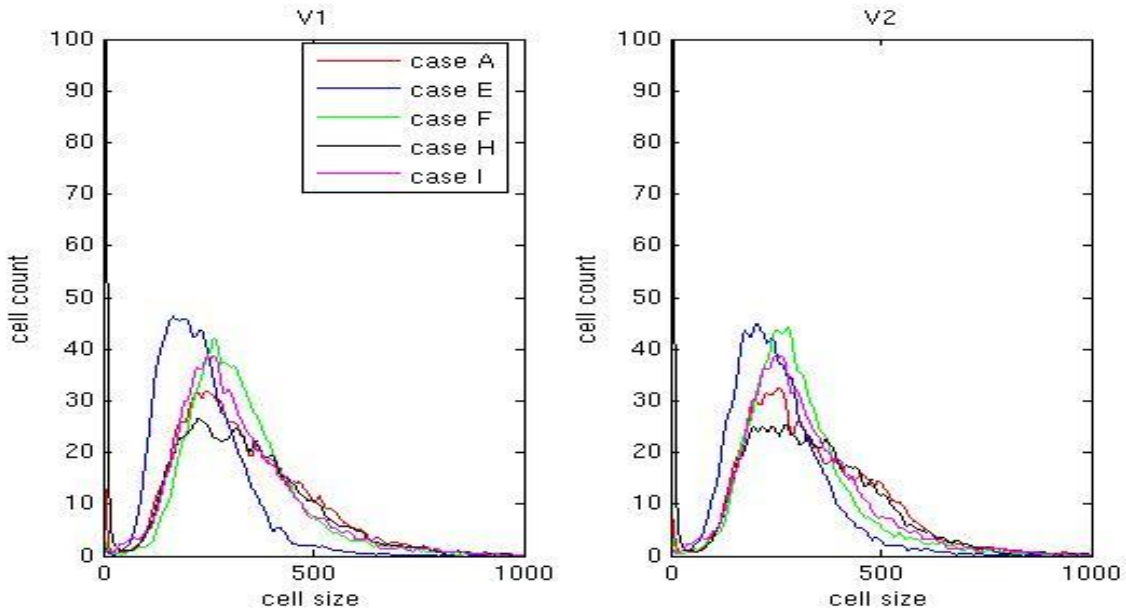

Figure 4 – Variation of the experimental cell size distribution in the two compartments in steady state: using the growth reporter strain FE440. Results are shown for the experimental performed cases (A, E, H, F, I).

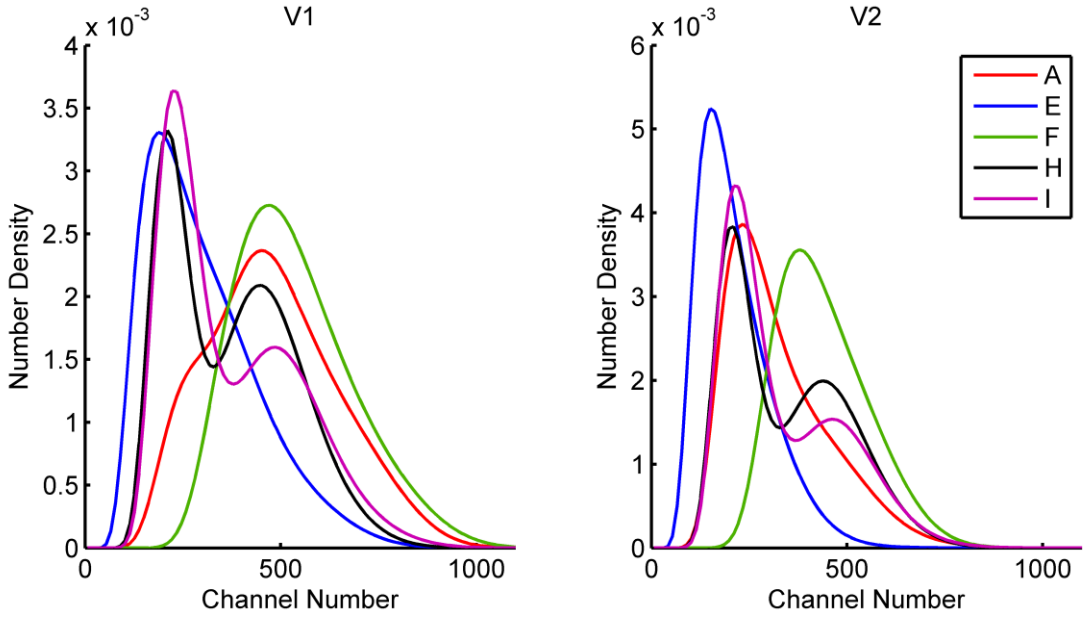

Figure 5 – Variation of the cell size distribution in the two compartments model: Results are shown for the experimental performed cases (A, E, H, F, I).

The cell size distribution changed depending on the conditions when comparing the two compartments and also in comparison with ordinary chemostat cultivations (figure 10 and Appendix 2). For case A, E and I the cell size remained the same for cells in both compartments as well as cells grown in a normal chemostat (one compartment): 338.43+/-0.56 vs 338.12+/-30.63 vs 354.59+/-5.48. The model predictions however suggested that two different cell size distributions would be observed in the two compartments, for case A: a smaller sized population is predicted for V2, while a combined population of smaller and bigger cells would be found in V1 (see table 3). This difference between experimental and model predictions is consistent with the discrepancies found for the physiological data, and thus further suggests that the model may not be suitable for describing high-gravity cultivations. But it also has to be mentioned that high-gravity cultivations were not explicitly included during the model development. However, the smaller cell size predicted in the model could be explained by a change in osmolarity, as it was found earlier that incrasing osmolarity leads to shrinking cells[27].

The cell size distributions measured in V1 for case A, F, H and I (see table 3) correspond to larger cells than for case E and displayed a clear tailing towards high cell sizes. In V2, the distributions for case A and I were broader than for the remaining cases, showing a higher mean cell size (see table 3). For case E, the cell size distribution exhibited a lower mean cell size (see table 3) and more narrow distribution (see table 3) but a similar shape tailing. Indeed, the results suggest that the lowest level of population heterogeneity results from the operating conditions corresponding to the lowest local dilution rates. Oppositely, the highest level of population heterogeneity is found for case H, where the highest local dilutions rates were observed. This suggests that a high local volume exchange contribute significantly to the heterogeneity of the cell population. A high glucose feed concentration may be an additional factor contributing to a higher level of heterogeneity.

The model predictions showed different distributions for case A, H and I in comparison to case F: smaller size populations were predicted for these cases, reflecting the shift of the population in response to a lower glucose concentration. As previously discussed, for these cases higher glucose concentrations were measured in comparison to the model predictions, which was in agreement with the experimentally measured distributions displaying larger cells than shown in the predicted distributions. In comparison with the one compartment model (see appendix 3, figure 13) cell size distributions predicted for cases A, E and F resembled distributions found in the two compartment model for V2, which seems to be expected as the biggest part of the one compartment chemostat

will resembled the compartment V2 with high oxygen concentration and residual glucose concentration. For cases H and I cell size distributions in the one compartment model resemble the subpopulation that showed the higher cell size in the two compartment model, probably due to less changes in the residual glucose concentration predicted in the one compartment reactor.

Table 3 – Parameter calculated for cell size in two and one compartment chemostats found in experiments and predicted by the model: mean fluorescence and coefficient of variance (CV) calculated for cell size. Values for the two compartments are presented for each compartment separately (V1 and V2) and experimental values are given including standard deviation as an average for data collected during three subsequent residence times in steady state.

Parameter		**A**	**E**	**F**	**H**	**I**
Model predictions						
Mean	**V1**	479.03	300.40	535.76	372	373.62
	V2	324.10	213.34	439.29	347	334.61
CV	**V1**	1.06	1.11	1.03	1.09	1.09
	V2	1.08	1.10	1.03	1.09	1.09
Experimental results						
Mean	**V1**	342.12±5.1	230.02±34.51	330.12±0.71	333.79±41.62	343.47±3.6
	V2	345.79±4.6	233.56±4.15	307.13±3.6	306.53±14.48	348.37±41.11
CV	**V1**	0.66	0.46	0.58	0.80	0.58
	V2	0.66	0.43	0.55	0.77	0.62

8.3.3 The effect of compartmentalization on biomass productivity and yields on substrate

From the data in the previous section it is obvious that the degree of compartmentalization, as well as growth rate and feed concentration in a bioreactor have a significant influence on cell physiology. Therefore it is also interesting to investigate the effect on the overall yields on glucose as well as on the productivity of biomass in the experimental performed cases (figure 6). Hereby only the yields of biomass, ethanol and CO_2 were considered because other metabolites produced in low amounts like acetate, glycerol and pyruvate only account for less than 10% in the carbonbalance (data not shown). This is consistent with Postma *et al*. (1989)[29] who found that below D= 0.25 h^{-1} no other byproducts than ethanol were accumulated.

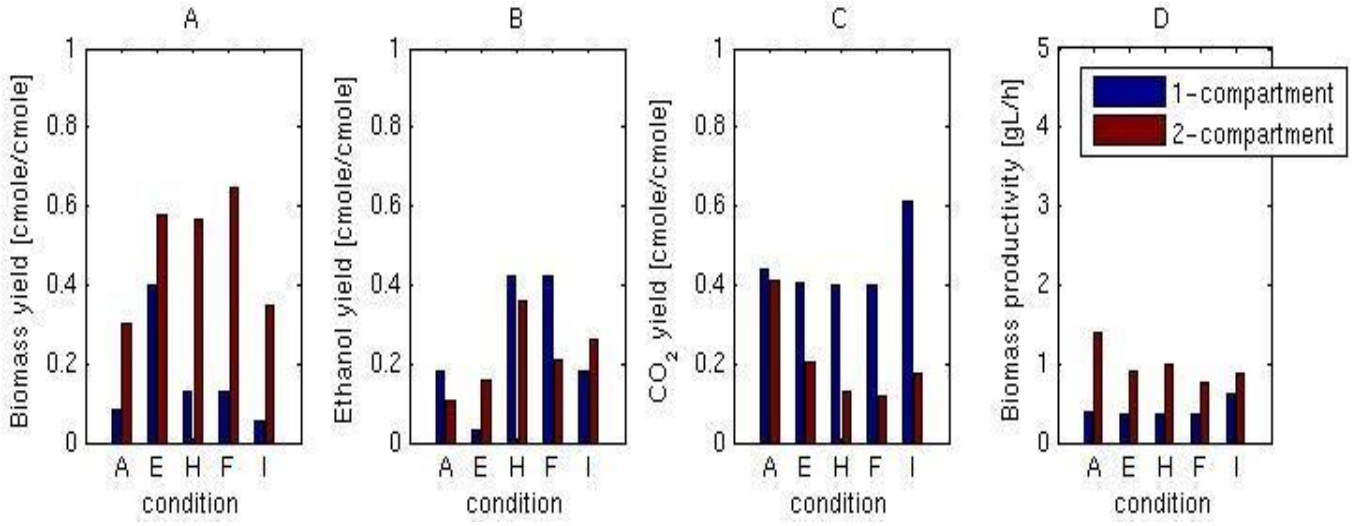

Figure 6 – Biomass, ethanol and CO_2 yields as well as biomass productivity for experiments on glucose: for the one compartment (blue bars) and the two compartment (red bars) experiments in steady state.

The biomass yields for one and two compartment continuous cultivation show significant differences. In general, the biomass yields (figure 6A) and thereby also the biomass productivity (figure 6D) for the two compartment cultivations was higher than for the ordinary chemostat cultures. Whereas for the low dilution rate the difference was only up to 3-fold, for D= 0.2 h^{-1} the difference was around 6-fold. The highest productivity was found for case A in two compartment chemostats whereas the lowest was found in one compartment chemostats for case F and H. The center point (I) exhibited values in between the two other dilution rates. In general, the values found for the two compartment were comparable with biomass yields seen in earlier studies in ordinary chemostats by e.g. van Dijken *et al.* (2000)[30] whereas for the one compartment values were lower than reported in earlier studies. For the ethanol yields (figure 6B) the picture was less clear. Whereas for case A as well as for case F and H the yield in the normal chemostat cultures was higher than for the two compartment cultivations, the opposite was observed for case E as well as for the center point. Also for the CO_2 yields (figure 6C) the one compartment chemostats showed significant higher values than for the two compartment cultivations with the exception of case A for which the yield was almost the same in both setups. Van Dijken *et al.* (2000) as well as van Hoek (1998)[30,31] found that in chemostat cultures the CO_2 yield is decreasing with increasing dilution rate which can also be seen for the two compartment setup whereas it was only true for the center point and the high dilution rate and not for D= 0.05 h^{-1} in the one compartment setup. Considering the recirculation rate, the yields should resemble more the one compartment chemostat with increasing

recirculation rate, which could not be seen from the results. In fact, in the results only the biomass yield decreased whereas the ethanol increased when comparing low and high recirculation rate (case F and H). The same was seen for the increase in glucose feed concentration (case A and E). In large scale cultivations of *S. cerevisiae* it was found that when cells experience a fast change in environmental conditions[32], the biomass yield decreases in line with an increase in ethanol yield, which was not seen in conventional lab scale chemostat cultures. The reason are microenvironments in different parts of the bioreactor due to non-ideal mixing which also makes cells more stressed, which has been followed by the expression of stress related genes[15]. This explains the observed decrease in biomass concentration when the feed concentration increases which imposes a bigger difference in environment between the two compartments. However with a rise in recirculation rate this phenomenon should become less important since the conditions in both compartments become more similar and should in general be more equal to a conventional chemostat, though the opposite was seen from the yields which show similar values as for low recirculation.

8.3.4 The use of reporter strains to gain additional information on cell physiology

To gain further physiological information about the growth, stress level and robustness distributions of the cells traveling throughout the two compartment chemostat as a special feature the strain used in this study was a growth reporter strain expressing a green fluorescent protein (GFP). Its expression was controlled by a ribosomal promoter and was shown to be a useful tool to follow growth characteristics at single cell level[22]. Additionally, the employed growth reporter strain when exposing the cells to freeze-thaw stress can be applied for the investigation of cell membrane robustness, because a strong correlation between intracellular GFP level and cell membrane robustness was found[22].

Furthermore, case F was also performed using an ethanol reporter strain (Johansen, unpublished) to investigate the distinct differences in ethanol level seen between the two compartments in this case. The strain expresses a blue fluorescent protein (BFP), whose expression is controlled by the PCK1 (phosphoenolpyruvate carboxykinase 1) promoter. The promoter codes for the key enzyme of the gluconeogenesis and is hence repressed during growth on glucose/glucose is present and active during growth on ethanol. Therefor the BFP fluorescence can be correlated to growth on ethanol. All cases performed with reporter strains are compared with the corresponding cultivation in an ordinary chemostat.

8.3.4.1 Influence of compartmentalization on cell robustness/cell growth

Growth and cell robustness were studied using the *S. cerevisiae* reporter strain FE440[22]. The experimental studied cases were investigated for GFP fluorescence via flow cytometry and distributions are plotted as histogram plots comparing the distributions for two subsequent residence times (for V1 and V2) for each case as well as distributions for different cases between each other (figure 7). For all cases steady state of the fluorescence level was established. Whereas for cases A, F, I and H only minor variation between different residence times was found, supported by a low standard deviation for calculated parameters for description of the population (table 4), population distributions for case E showed a slightly higher variation (figure 7) with higher standard deviations in the calculations. However, variation between samples in steady state from cells grown at D = 0.2 h^{-1} were bigger than for cells growing at D = 0.125 h^{-1} respectively D = 0.05 h^{-1} (figure 7). This indicates that it takes longer time to stabilize and adjust to the changing environment (high glucose/low oxygen respectively low glucose/high oxygen) when cells grow at a higher dilution rate. Between the two compartments no significant difference in GFP fluorescence could be seen, except of case E, differences between the compartments in calculated values are less than 10% (table 4), although for the cases with low recirculation general physiology in the two compartments was different. The reason for this is probably the longer expression time of GFP compared to the recirculation time between the two compartments. For case E for V2 a broad normal distribution is seen whereas for V1 a slightly broader distribution with two maxima is seen.

However fluorescence distributions for all cases can still be compared between cases. Cases A, F, E (V2) and I exhibited similar steady state characteristics (figure 7) with a broad distribution tailing towards lower fluorescence (figure 7), whereas the tailing is less obvious for cells growing at the high dilution rate, which is also illustrated by lower CV for the GFP distribution at higher dilution rate (table 4). Case H revealed two subpopulations, one high fluorescent containing around 95% of the whole population and one low fluorescent (around 5% of the population).

When comparing the cases to steady state values of ordinary chemostats (Appendix 2, figure 11), two compartment cultivations revealed always lower fluorescence considering the mean (table 3), especially for cases A, F and I. However for cases A and E in normal chemostats, apart from the main population a lower subpopulation respectively subpopulation connected to the main population was found resulting in an increased peak width and slightly lower mean fluorescence than for other cases. This indicates that cells grown in one compartment chemostats are less affected

by freeze-thaw stress than cells grown in a two compartment chemostat. Only when growing with D = 0.05 h^{-1} in an ordinary chemostat a small portion of the cell population seemed to be strongly affected by freeze-thaw stress and the influence became stronger with higher glucose concentration in the feed. At the same conditions in a two compartment chemostat highly effected cells were only found for case E in compartment V1, whereas no subpopulations were found for case A, but the same general trend for the feed concentration was seen. Cells grown in a two compartment chemostat seem to be less robust due to the recirculation. Especially the high recirculation at D= 0.2h^{-1} (case H) generated a small population of cells which are strongly influenced by freezing. Due to this the CV for this case was higher than for the other cases (table 4). However, generally with low recirculation in a two compartment chemostat cells growing at D = 0.2 h^{-1} as well as the middle range dilution rate seem to be less affected by freezing, exhibiting a slightly more narrow distribution connected with a lower CV and higher mean fluorescence (table 4), than cells growing at the low dilution rate. This is interesting since generally it is found that in continuous culture cells growing at a low dilution rate are more robust and tolerant to stress than cells growing with a higher growth rate[33,34].

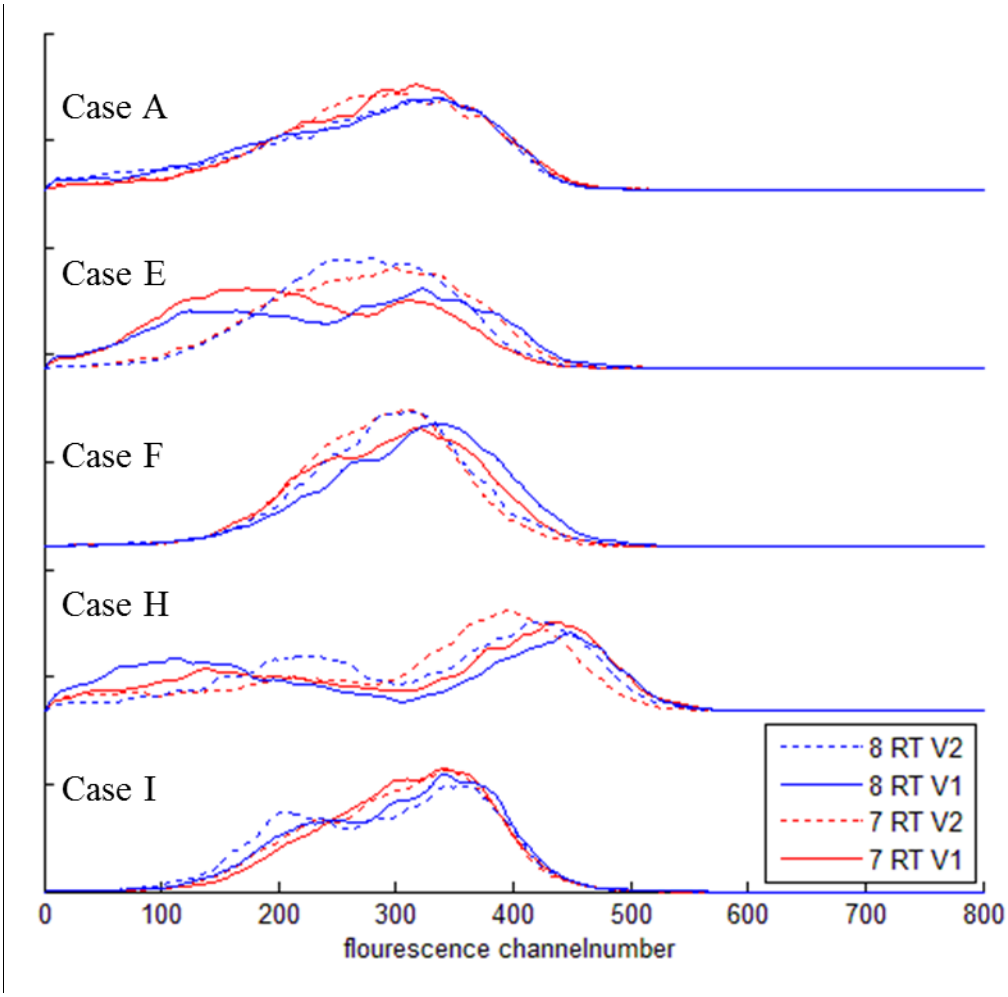

Figure 7 – histogram plots for experimental GFP fluorescence/membrane robustness data in steady state: after applying freeze-thaw stress using the growth reporter strain FE440. Plots are shown as a comparison between the different compartments (V1 and V2) of the two compartment setup and the one compartment setup for two subsequent residence times in steady state.

Table 4 – Parameter calculated for objective description of membrane robustness in two and one compartment experiments: mean fluorescence and coefficient of variance (CV) calculated for GFP fluorescence in the two compartment setup and the one compartment setup. Values for the two compartments are presented for each compartment separately (V1 and V2) and all values are given including standard deviation as an average for three subsequent residence times in steady state.

Parameter		**A**	**E**	**F**	**H**	**I**
Mean	**V1**	268.83± 9.89	222.39± 20.58	308.23±10.34	270.58± 24.19	310.34±10.01
GFP	**V2**	259.57±12.03	280.71± 20.74	295.43± 9.07	303.62± 6.93	298.91±7.49
	Chemostat	342.91± 0.26	288.95 +/-35.57	361.32±27.98	361.32± 27.98	396.64± 3.84
CV	**V1**	0.41	0.52	0.24	0.60	0.24
	V2	0.46	0.56	0.23	0.45	0.26
	Chemostat	0.33	0.42	0.31	0.31	0.21

8.3.4.2 Influence of compartmentalization on ethanol/glucose consumption under chosen conditions

To further investigate physiological differences between the two compartments of the scale down setup an ethanol reporter strain expressing a blue fluorescent protein (BFP) controlled by a PCK1 reporter was cultivated in the system with a dilution rate of D = 0.2 h^{-1}, 50 g/L feed concentration and low recirculation between the two compartments (case F). This condition was chosen because it revealed significant differences in dilution rate as well as ethanol and glucose level between the two compartments. Additionally results are compared to a one compartment chemostat with the same reporter strain.

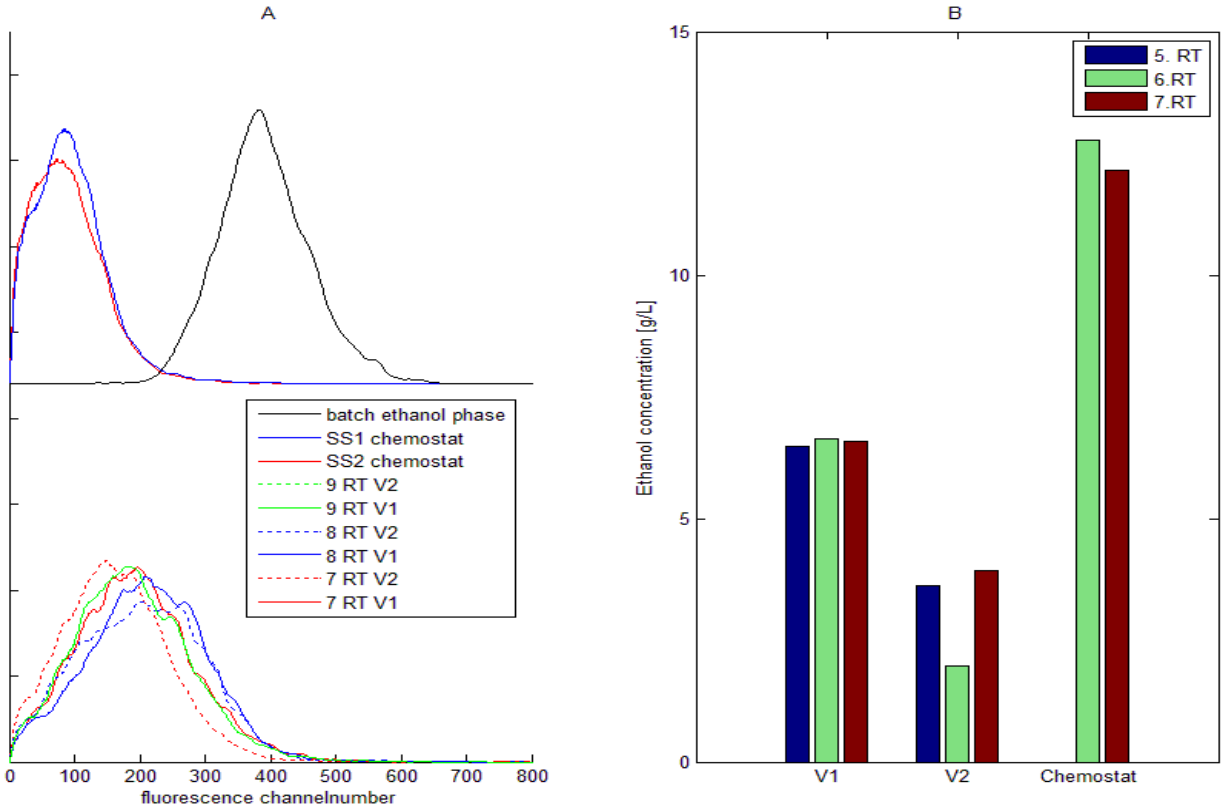

Figure 8 – BFP fluorescence/ ethanol respectively glucose consumption in steady state: using the ethanol reporter strain Sc-PCK1-B. Plots are shown as a comparison between the different compartments (V1 and V2) of the two compartment setup and the one compartment setup for three subsequent residence times in steady state in a histogram plot (A). In addition ethanol concentration values are shown for the samples shown as distribution (B).

Almost no difference in the BFP fluorescence level of the ethanol reporter can be recognized following the two compartments (V1 and V2) over three residence times (figure 8A, histogram). Both compartments exhibited a similar peak width (figure 8A). Only small shape differences in the main part of the fluorescence distribution (figure 8A), which influenced the mean fluorescence (191.25+/- 10.12 vs. 170.84+/- 26.88) were found. Steady state was established for both compartments, although variation of the population was slightly higher in V2 compared to V1 (0.56 vs. 0.50). Also, higher standard deviations were found for samples taken in V2. The higher degree of heterogeneity in the compartment V2 may be due to the higher volume and because no feeding was applied in this compartment so that some cells show a starvation response and some grow on

ethanol. In comparison to an ordinary chemostat (figure 8) under the same conditions in steady state, the mean BFP fluorescence in the two compartment cultivations was about 64% higher (170.84+/. 26.88 respectively 191.25+/- 10.12 vs. 65.88+/- 6.04) and additionally in general a higher degree of heterogeneity (0.65 respectively 0.50 vs. 0.35), characterized by a broader and less aligned distribution, was seen. Considering physiology data for the ordinary chemostat no ethanol growth was found (data not shown) and the ethanol concentration remained constant and higher than in a two compartment chemostat (figure 8B). Compared to BFP fluorescence from ethanol growth in batch cultivation the fluorescence during the two compartment cultivation was around 50% lower. However, the ethanol concentration was different in the two compartments (figure 8B). These findings indicate that cells in the two compartments utilise ethanol because glucose repression is released but in comparison to the recirculation the release of glucose repression is too slow so that a switch from PCK1 repression to expression cannot be directly captured. For this reason it could be interesting to perform two compartment cultivations with even lower recirculation flow rate. But in general this application of the two compartment setup shows that it reveals characteristics of the cultivation which cannot be captured using a conventional chemostat because the flows as well as concentration differences between the feeding zone and the remaining reactor volume are unknown and therefore the time cells linger in the different compartments is unclear. By applying the here developed scale down system the expression differences cells are found to exhibit in different parts of a large industrial scale reactor can be simulated[9].

8.4 Conclusion and general applicability of approach for future experiments

The here presented approach of modeling in combination with the performance of experimental work showed consistency or at least the same trend in most cases but also limitations, especially under extreme growth conditions (high gravity glucose cultivations). Though in general the approach is still useful for process optimization by applying modeling to get an overview of conditions that might be interesting to perform in lab scale experiments exhibiting special traits like e.g. oscillations found during our simulations. Such an approach can reduce the amount of experiments to be performed because conditions revealing standard characteristics in the model might not need to be performed in the lab.

The experimental setup can be used for studies of production processes in the development phase for e.g. recombinant proteins, to investigate how production is influenced by compartmentalization at different conditions. Furthermore, by applying reporter strains the single cell response e.g. in

stress genes, growth or ethanol growth in the different compartments can be studied. For this purpose it could also be interesting to include more sampling points or study more different recirculation times and dilution rates to test the operating limits of the setup. In comparison to pulse experiments in conventional chemostats, a setup like the here presented one has the advantage that the flows between the two compartments are known, which makes it possible to assess phenomena like the ones seen for the ethanol reporter strain. Furthermore in this setup the repeated exposure of cells to a changing environment is taken into account whereas in perturbation studies this is only achieved by pulsed feed experiments which are rarely reported up to now in physiological investigations of single cells[35].

8.5 References

1. Lencastre Fernandes, R. *et al.* Cell mass and cell cycle dynamics of an asynchronous budding yeast population: experimental observations, flow cytometry data analysis, and multi-scale modeling. *Biotechnol. Bioeng.* **110,** 812–826 (2013).

2. Müller, S., Harms, H. & Bley, T. Origin and analysis of microbial population heterogeneity in bioprocesses. *Curr. Opin. Biotechnol.* **21,** 100–113 (2010).

3. Koutinas, M., Kiparissides, A., Pistikopoulos, E. N. & Mantalaris, A. Bioprocess systems engineering : transferring traditional process engineering principles to industrial biotechnology. *Comput. Struct. biotechnoloy* **3,** (2012).

4. Ferrer-Miralles, N., Domingo-Espín, J., Corchero, J. L., Vázquez, E. & Villaverde, A. Microbial factories for recombinant pharmaceuticals. *Microb. Cell Fact.* **8,** (2009).

5. Chemler, J. a, Yan, Y. & Koffas, M. a G. Biosynthesis of isoprenoids, polyunsaturated fatty acids and flavonoids in Saccharomyces cerevisiae. *Microb. Cell Fact.* **5,** (2006).

6. Lidstrom, M. E. & Konopka, M. C. The role of physiological heterogeneity in microbial population behavior. *Nat. Chem. Biol.* **6,** 705–712 (2010).

7. Vrabel, P., Lans, R. G. J. M. Van Der, Luyben, K. C. A. M., Boon, L. & Nienow, A. W. Mixing in large-scale vessels stirred with multiple radial or radial and axial up-pumping impellers : modelling and measurements. *Biotechnol. Bioeng.* **55,** 5881–5896 (2000).

8. Bylund, F., Collet, E., Enfors, S.-O. & Larsson, G. Substrate gradient formation in the large-scale bioreactor lowers cell yield and increases by-product formation. *Bioprocess Eng.* **18,** (1998).

9. Enfors, S. O. *et al.* Physiological responses to mixing in large scale bioreactors. *J. Biotechnol.* **85,** 175–185 (2001).

10. Larsson, G. *et al.* Substrate gradients in bioreactors: origin and consequences. *Bioprocess Eng.* **14,** 281–289 (1996).

11. Schweder, T. *et al.* Monitoring of genes that respond to process-related stress in large-scale bioprocesses. *Biotechnol. Bioeng.* **65,** 151–159 (1999).

12. Lara, A. R. *et al.* Transcriptional and metabolic response of recombinant Escherichia coli to spatial dissolved oxygen tension gradients simulated in a scale-down system. *Biotechnol. Bioeng.* **93,** 372–385 (2006).

13. Papagianni, M. Methodologies for Scale-down of Microbial Bioprocesses. *J. Microb. Biochem. Technol.* **05,** 1–7 (2011).

14. Papagianni, M., Mattey, M. & Kristiansen, B. Design of a tubular loop bioreactor for scale-up and scale-down of fermentation processes. *Biotechnol. Prog.* **19,** 1498–1504 (2003).

15. George, S., Larsson, G. & Enfors, S.-O. A scale-down two-compartment reactor with controlled substrate oscillations: Metabolic response of Saccharomyces cerevisiae. *Bioprocess Eng.* **9,** 249–257 (1993).

16. Bylund, F., Guillard, F., Enfors, S.-O., Trägårdh, C. & Larsson, G. Scale down of recombinant protein production: a comparative study of scaling performance. *Bioprocess Eng.* **20,** (1999).

17. Sweere, A. P. J. *et al.* Modelling the dynamic behaviour of Saccharomyces cerevisiae and its application in control experiments. *Appl. Microbiol. Biotechnol.* 116–127 (1988).

18. Delvigne, F., Destain, J. & Thonart, P. A methodology for the design of scale-down bioreactors by the use of mixing and circulation stochastic models. *Biochem. Eng. J.* **28,** 256–268 (2006).

19. Delvigne, F., Destain, J. & Thonart, P. Toward a stochastic formulation of microbial growth in relation to bioreactor performances: case study of an E. coli fed-batch process. *Biotechnol. Prog.* **22,** 1114–1124 (2006).

20. Delvigne, F., Lejeune, A., Destain, J. & Thonart, P. Stochastic Models To Study the Impact of Mixing on a Fed-Batch Culture of Saccharomyces cere W isiae. *Biotechnol. Prog.* 259–269 (2006).

21. Fernandes, R. L. *et al.* Experimental methods and modeling techniques for description of cell population heterogeneity. *Biotechnol. Adv.* **29,** 575–599 (2011).

22. Carlquist, M. *et al.* Physiological heterogeneities in microbial populations and implications for physical stress tolerance. *Microb. Cell Fact.* **11,** (2012).

23. Verduyn, C., Postma, E., Scheffers, W. a & Van Dijken, J. P. Effect of benzoic acid on metabolic fluxes in yeasts: a continuous-culture study on the regulation of respiration and alcoholic fermentation. *Yeast* **8,** 501–517 (1992).

24. Olsson, L. & Nielsen, J. On-line and in situ monitoring of biomass in submerged cultivations. *Reviews* **15,** 517–522 (1997).

25. Villadsen, J., Nielsen, J. & Lidén, G. *Bioreaction Engineering Principles*. (Springer US, 2011). doi:10.1007/978-1-4419-9688-6

26. Vanoni, M., Vai, M., Popolo, L. & Alberghina, L. Structural heterogeneity in populations of the budding yeast Saccharomyces Structural Heterogeneity in Populations of the Budding Yeast Saccharomyces cerevisiae. *J. Bacteriol.* **156,** 1282–1291 (1983).

27. Porro, D., Vai, M., Vanoni, M., Alberghina, L. & Hatzis, C. Analysis and modeling of growing budding yeast populations at the single cell level. *Cytometry. A* **75,** 114–120 (2009).

28. Odman, P., Johansen, C. L., Olsson, L., Gernaey, K. V & Lantz, A. E. On-line estimation of biomass, glucose and ethanol in Saccharomyces cerevisiae cultivations using in-situ multi-wavelength fluorescence and software sensors. *J. Biotechnol.* **144,** 102–112 (2009).

29. Postma, E., Verduyn, C., Scheffers, W. A. & Dijken, J. P. V. A. N. glucose-limited chemostat cultures of Enzymic Analysis of the Crabtree Effect in Glucose-Limited Chemostat Cultures of Saccharomyces cerevisiae. *Appl. Environ. Microbiol.* **55,** 468–477 (1989).

30. Van Dijken JP *et al.* An interlaboratory comparison of physiological and genetic properties of four Saccharomyces cerevisiae strains. *Enzyme Microb. Technol.* **26,** 706–714 (2000).

31. Hoek, P. I. M. V. A. N., Dijken, J. P. V. A. N. & Pronk, J. T. Effect of Specific Growth Rate on Fermentative Capacity of Baker ' s Yeast. *Appl. Environ. Microbiol.* **64,** 4226–4233 (1998).

32. George, S., Larsson, G., Olsson, K. & Enfors, S.-O. Comparison of the Baker's yeast process performance in laboratory and production scale. *Bioprocess Eng.* **18,** 135–142 (1998).

33. Brauer, M. J. *et al.* Coordination of Growth Rate , Cell Cycle , Stress Response , and Metabolic Activity in Yeast. *Mol. Biol. Cell* **19,** 352–367 (2008).

34. Zakrzewska, A. *et al.* Genome-wide analysis of yeast stress survival and tolerance acquisition to analyze the central trade-off between growth rate and cellular robustness. *Mol. Biol. Cell* **22,** 4435–4446 (2011).

35. Sunya, S., Bideaux, C., Molina-Jouve, C. & Gorret, N. Short-term dynamic behavior of Escherichia coli in response to successive glucose pulses on glucose-limited chemostat cultures. *J. Biotechnol.* **164,** 531–542 (2013).

1 APPENDIX 1: Equations for model

$\frac{\partial N_{V1}^{NB}(m,t)}{\partial t} + \frac{\partial}{\partial m}\left[r_m(m,Z)N_{V1}^{NB}(m,t)\right] = -\Gamma_B(m\,|Z)\;N_{V1}^{NB}(m,t) + 2\int_m^{m_f}\Gamma_D(m'\,|Z)P(m,m'\,|Z)N_{V1}^{B}(m',t)dm' + \frac{F2}{V1}N_{V2}^{NB}(m,t) - \frac{F1}{V1}N_{V1}^{NB}(m,t)$	**Eq. A1-1**
$\frac{\partial N_{V1}^{B}(m,t)}{\partial t} + \frac{\partial}{\partial m}\left[r_m(m,Z)N_{V1}^{B}(m,t)\right] = -\Gamma_D(m\,|Z)\;N_{V1}^{B}(m,t) + \Gamma_B(m\,|Z)\;N_{V1}^{NB}(m,t) + \frac{F2}{V1}N_{V2}^{B}(m,t) - \frac{F1}{V1}N_{V1}^{B}(m,t)$	**Eq. A1-2**
$\frac{\partial N_{V1}^{NB}(m,t)}{\partial t} + \frac{\partial}{\partial m}\left[r_m(m,Z)N_{V1}^{NB}(m,t)\right] = -\Gamma_B(m\,|Z)\;N_{V1}^{NB}(m,t) + 2\int_m^{m_f}\Gamma_D(m'\,|Z)P(m,m'\,|Z)N_{V1}^{B}(m',t)dm' + \frac{F1}{V2}N_{V1}^{NB}(m,t) - \frac{F2+F}{V2}N_{V2}^{NB}(m,t)$	**Eq. A1-3**
$\frac{\partial N_{V2}^{B}(m,t)}{\partial t} + \frac{\partial}{\partial m}\left[r_m(m,Z)N_{V2}^{B}(m,t)\right] = -\Gamma_D(m\,|Z)\;N_{V2}^{B}(m,t) + \Gamma_B(m\,|Z)\;N_{V2}^{NB}(m,t) + \frac{F1}{V2}N_{V1}^{B}(m,t) - \frac{F2+F}{V2}N_{V2}^{B}(m,t)$	**Eq. A1-4**

$N_{Vi}^{NB}(m_0,t) = \quad N_{Vi}^{NB}(m_f,t) = N_{Vi}^{B}(m_0,t) = {}_{Vi}^{B}(m_f,t) = 0$ $m \in [m_0, m_f]; i = 1,2$	**Eq. A1-5**
$\mu_B = 200\frac{G}{G+K_{\mu S}} + 300$	**Eq. A1-6**
$\mu_D = 400\frac{G}{G+K_{\mu S}} + 550$	**Eq. A1-7**
$\mu_B = 120\frac{E}{E+K_{\mu S}} + 180$	**Eq. A1-8**
$\mu_D = 250\frac{E}{E+K_{\mu S}} + 300$	**Eq. A1-9**

$$\frac{dG_{V1}}{dt} = -r_{G,\max}\frac{G_{V1}}{G_{V1}+K_G}X_{V1} + \frac{F}{V1}G_{feed} - \frac{F1}{V1}G_{V1} + \frac{F2}{V1}G_{V2}$$	**Eq. A1-10**
$$\frac{dG_{V2}}{dt} = -r_{G,\max}\frac{G_{V2}}{G_{V2}+K_G}X_{V2} - \frac{F+F2}{V2}G_{V2} + \frac{F1}{V2}G_{V1}$$	**Eq. A1-11**
$$\frac{dE_{V1}}{dt} = \overbrace{r_{G,\max}\frac{G_{V1}}{G_{V1}+K_G} - \frac{1}{a}\left(\min\left(r_{O,\max}\frac{O_{V1}}{O_{V1}+K_O}, a\cdot r_{G,\max}\frac{G_{V1}}{G_{V1}+K_G}\right)\right)}^{q_G^{Red}=q_G^{Total}-q_G^{Oxid}}\cdot jX_{V1}$$ $$-\frac{1}{k}\left(\min\left(r_{O,\max}\frac{O_{V1}}{O_{V1}+K_O} - \min\left(r_{O,\max}\frac{O_{V1}}{O_{V1}+K_O}, a\cdot r_{G,\max}\frac{G_{V1}}{G_{V1}+K_G}\right), k\cdot r_{E,\max}\frac{E_{V1}}{E_{V1}+K_E}\frac{K_i}{G_{V1}+K_i}\right)\right)X_{V1}$$ $$-\frac{F1}{V1}E_{V1} + \frac{F2}{V1}E_{V2}$$	**Eq. A1-12**
$$\frac{dE_{V2}}{dt} = \overbrace{r_{G,\max}\frac{G_{V2}}{G_{V2}+K_G} - \frac{1}{a}\left(\min\left(r_{O,\max}\frac{O_{V2}}{O_{V2}+K_O}, a\cdot r_{G,\max}\frac{G_{V2}}{G_{V2}+K_G}\right)\right)}^{q_G^{Red}=q_G^{Total}-q_G^{Oxid}}\cdot jX_{V2}$$ $$-\frac{1}{k}\left(\min\left(r_{O,\max}\frac{O_{V2}}{O_{V2}+K_O} - \min\left(r_{O,\max}\frac{O_{V2}}{O_{V2}+K_O}, a\cdot r_{G,\max}\frac{G_{V2}}{G_{V2}+K_G}\right), k\cdot r_{E,\max}\frac{E_{V2}}{E_{V2}+K_E}\frac{K_i}{G_{V2}+K_i}\right)\right)X_{V2}$$ $$+\frac{F1}{V2}E_{V1} - \frac{F2}{V2}E_{V2}$$	**Eq. A1-13**

$$\frac{dO_{V1}}{dt} = -\min\left(r_{O,\max}\frac{O_{V1}}{O_{V1}+K_O}, a\cdot r_{G,\max}\frac{G_{V1}}{G_{V1}+K_G}\right)X_{V1} - \min\left(r_{O,\max}\frac{O_{V1}}{O_{V1}+K_O} - \min\left(r_{O,\max}\frac{O_{V1}}{O_{V1}+K_O}, a\cdot r_{G,\max}\frac{G_{V1}}{G_{V1}+K_G}\right), k\cdot r_{E,\max}\frac{E_{V1}}{E_{V1}+K_E}\frac{K_i}{G_{V1}+K_i}\right)X_{V1} - \frac{F1}{V1}O_{V1} + \frac{F2}{V1}O_{V2}$$	**Eq. A1-14**
$$\frac{dO_{V2}}{dt} = k_L a(O^* - O_{V2}) - \min\left(r_{O,\max}\frac{O_{V2}}{O_{V2}+K_O}, a\cdot r_{G,\max}\frac{G_{V2}}{G_{V2}+K_G}\right)X_{V2} - \min\left(r_{O,\max}\frac{O_{V2}}{O_{V2}+K_O} - \min\left(r_{O,\max}\frac{O_{V2}}{O_{V2}+K_O}, a\cdot r_{G,\max}\frac{G_{V2}}{G_{V2}+K_G}\right), k\cdot r_{E,\max}\frac{E_{V2}}{E_{V2}+K_E}\frac{K_i}{G_{V2}+K_i}\right)X_{V2} + \frac{F1}{V2}O_{V1} - \frac{F2}{V2}O_{V2}$$	**Eq- A1-15**
$$\lambda(Z)_{V_i} = \frac{b}{a}\left(\min\left(r_{O,\max}\frac{O_{V_i}}{O_{V_i}+K_O}, a\cdot r_{G,\max}\frac{G_{V_i}}{G_{V_i}+K_G}\right)\right) + g\left(\overbrace{r_{G,\max}\frac{G_{V_i}}{G_{V_i}+K_G} - \frac{1}{a}\left(\min\left(r_{O,\max}\frac{O_{V_i}}{O_{V_i}+K_O}, a\cdot r_{G,\max}\frac{G_{V_i}}{G_{V_i}+K_G}\right)\right)}^{q_G^{Red}=q_G^{Total}-q_G^{Oxid}}\right) + \frac{l}{k}\left(\min\left(r_{O,\max}\frac{O_{V_i}}{O_{V_i}+K_O} - \min\left(r_{O,\max}\frac{O_{V_i}}{O_{V_i}+K_O}, a\cdot r_{G,\max}\frac{G_{V_i}}{G_{V_i}+K_G}\right), k\cdot r_{E,\max}\frac{E_{V_i}}{E_{V_i}+K_E}\frac{K_i}{G_{V_i}+K_i}\right)\right), \mathrm{i}=1,2$$	**Eq. A1-16**

APPENDIX 2: Experimental data for physiology and cell size and GFP respectively BFP fluorescence distribution data for one compartment

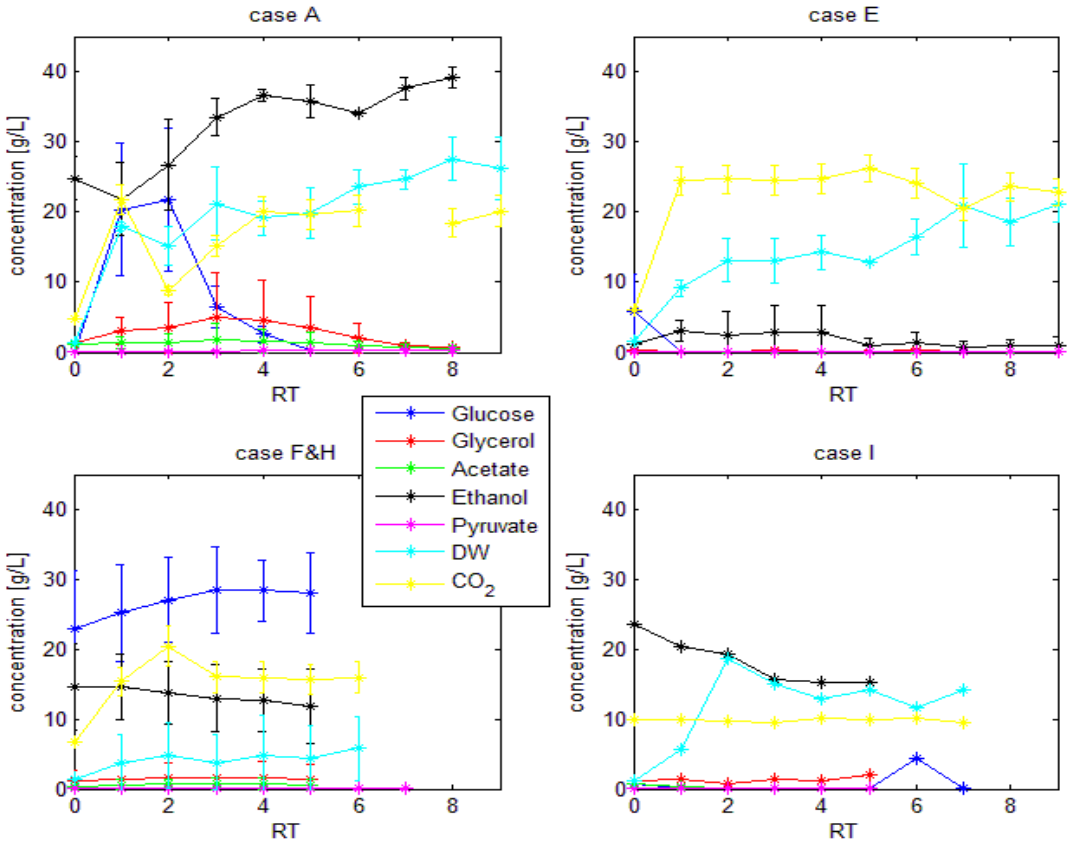

Figure 9 – Variation of glucose, ethanol, glycerol, acetate, pyruvate, biomass and CO_2 for one compartment experiments: using the growth reporter strain FE440. Results are shown for the experimental performed cases (A, E, H, F, I).

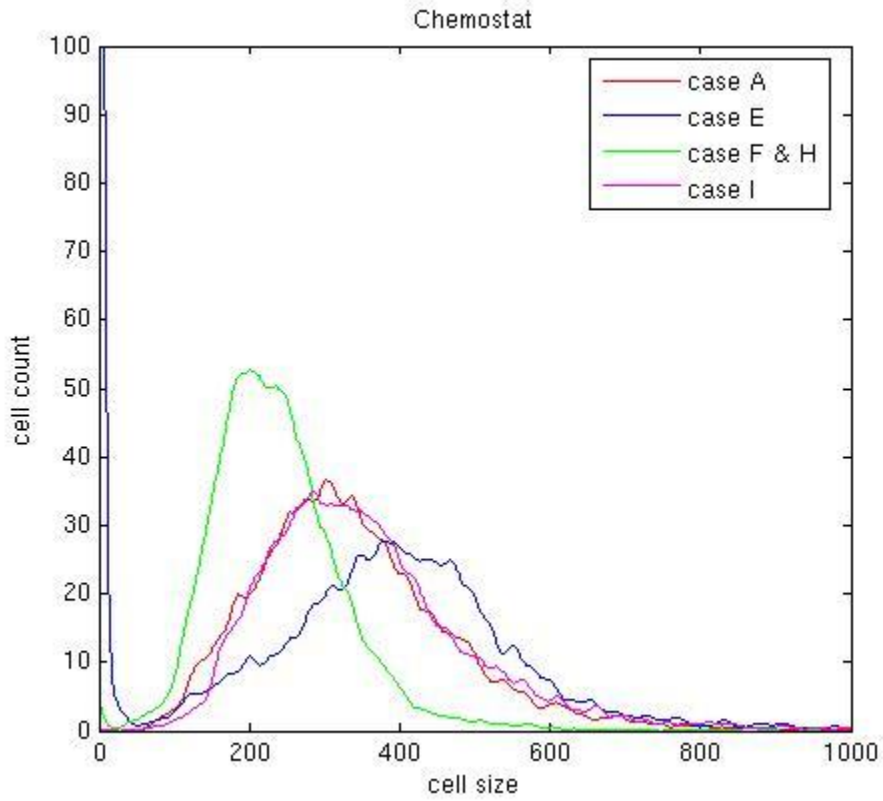

Figure 10 – Variation of the experimental cell size distribution in steady state for one compartment experiments: using the growth reporter strain FE440. Results are shown for the experimental performed cases (A, E, H, F, I).

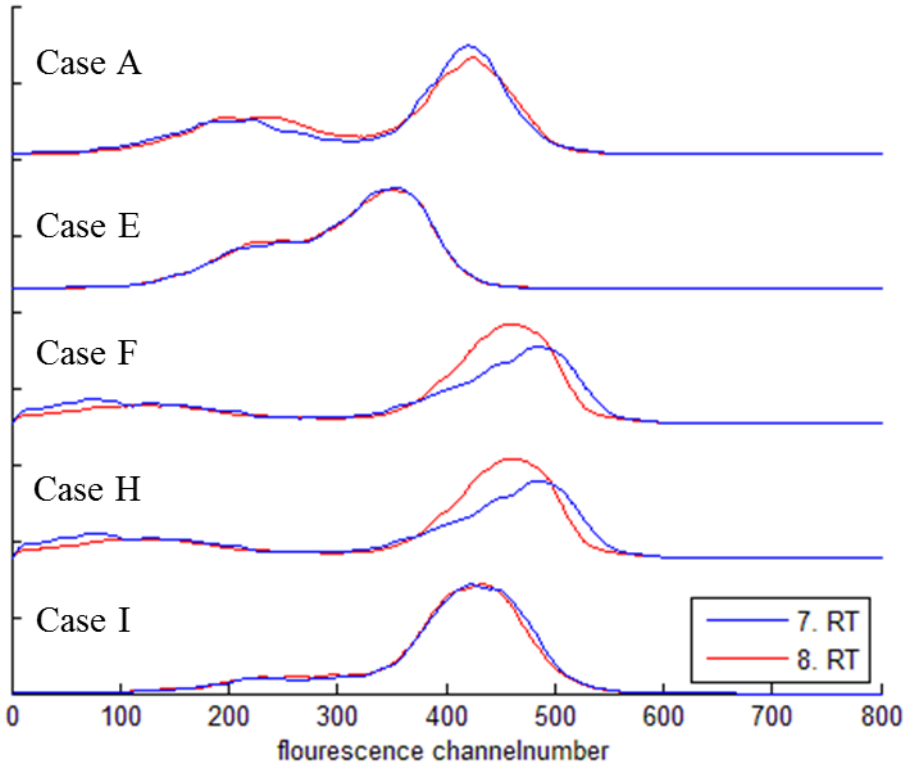

Figure 11 – histogram plots for GFP fluorescence/membrane robustness data in steady state for one compartment experiments: after applying freeze-thaw stress using the growth reporter strain FE440. Plots are shown as a comparison between the different cases (A, E, F, H and I) for two following residence times in steady state.

APPENDIX 3: Modeling data for physiology and cell size distribution for one compartment

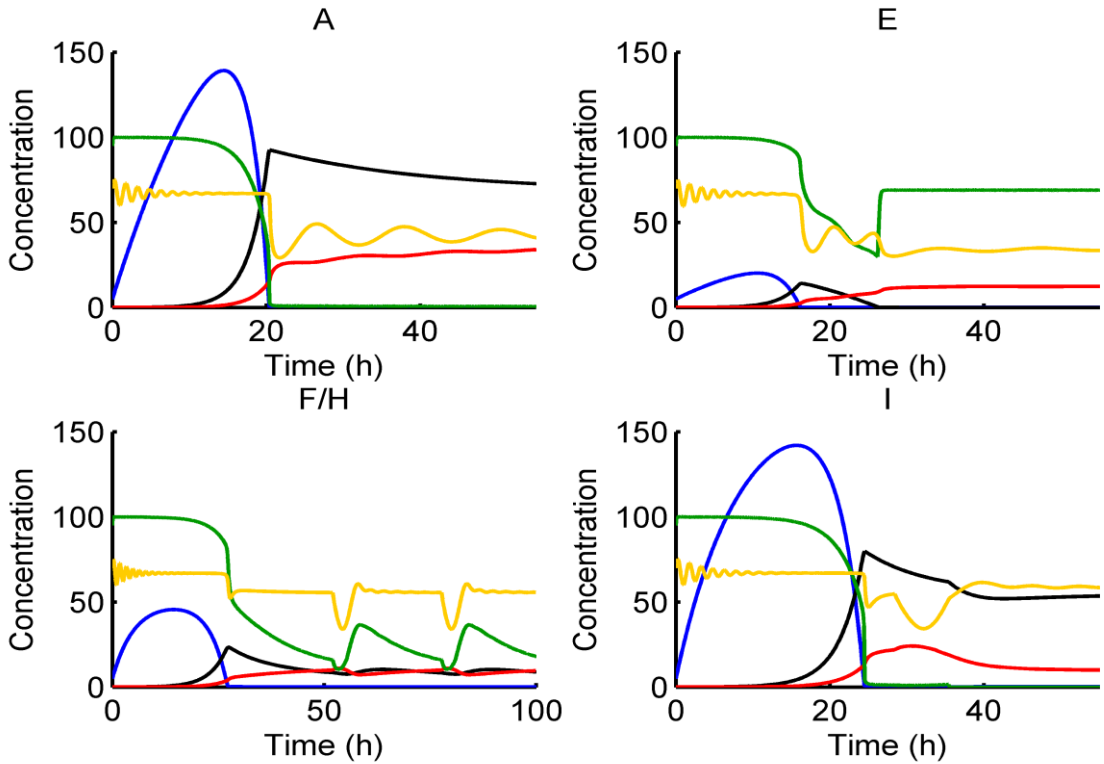

Figure 12 – Variation of glucose, ethanol, glycerol, acetate, pyruvate, biomass and CO_2 for one compartment model: results are shown for the experimental performed cases (A, E, H, F, I). Blue: glucose; Black: ethanol; Red: biomass; Green: dissolved oxygen; Yellow: budding index.

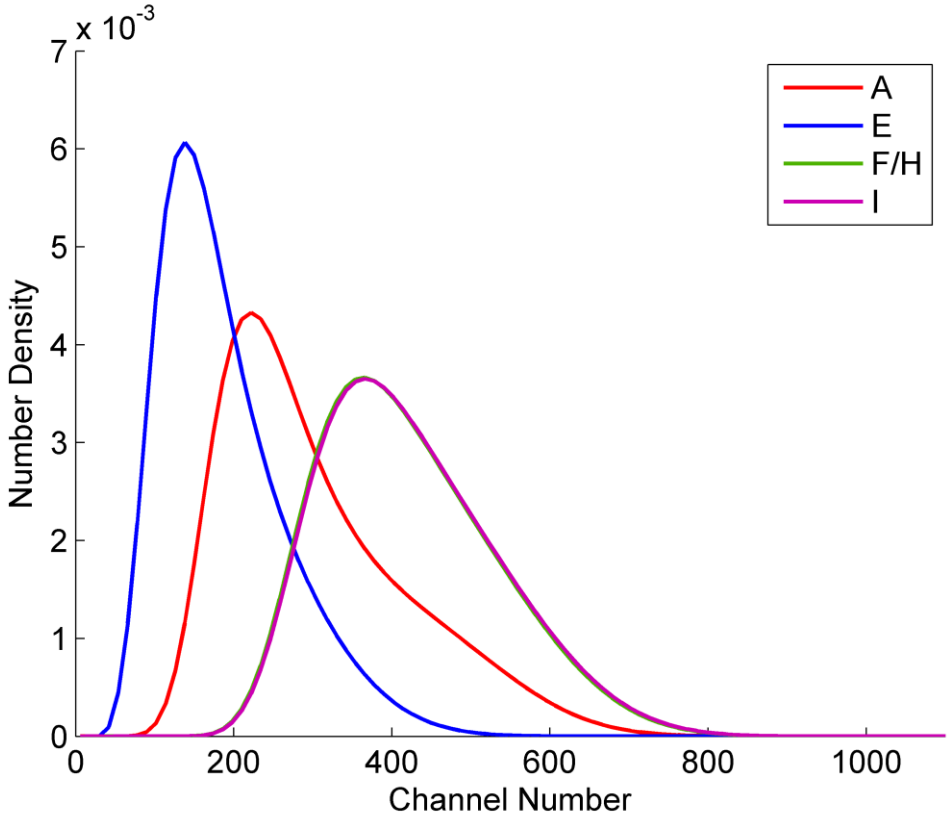

Figure 13 – Variation of cell size distribution for one compartment model: results are shown for the modeled cases (A, E, H, F, I).

9. Chapter

Conclusion and Outlook

9.1 Conclusion

In this chapter the major findings of the work described in this thesis are summed up. The aim was to study the occurrence and consequences of population phenotypic heterogeneity for the two cell factories *E. coli* and *S. cerevisiae* under different modes of bioprocess operation. For this purpose, different analytical and experimental tools were developed and applied. This included new high-throughput methods for quantitative analysis of large volumes of flow cytometry data and the development and validation of new reporter strains to monitor population heterogeneities in growth and cell membrane robustness. The major novelties related to tools applied will be shortly evaluated and summed up in the following sections where after the main physiological findings will be discussed.

9.1.1 Physiological characteristics of *E. coli* and *S. cerevisiae* as reporter strains

Reporter gene technology is powerful for dynamic in vivo measurements of activities of specific promoters, which in turn correlate to specific cell properties. By using modern strain genetic engineering techniques it is possible to place the gene coding for an easily detectable protein under the control of any given promoter[9].

The growth reporters were of slightly different nature for the two organisms. The two *E. coli* reporter strains carried a destabilized GFP version integrated on a low copy number plasmid whose expression was correlated to growth via promoters connected to the activation of the ribosomal polymerase rRNA synthesis (*fis* and *rrnb* promoter) (see figure 1). Therefore the strains allowed following of fast dynamic changes in batch and continuous cultivation as a response to a glucose pulse at different growth rates (see chapter 6 and 7). In contrast, the *S. cerevisiae* reporter strain, which was developed and validated in the scope of this thesis, carried a stable GFP which was chromosomally integrated upstream of the ribosomal promoter *RPL22a* (see figure 2). As a consequence of the stable GFP, but also due to the slower growth of *S. cerevisiae* compared to *E.*

coli the reporter sometimes failed to capture fast changes e.g. as the response to a glucose pulse at high growth rates or showed delayed response due to the maturation time of the GFP (see chapter 6). Due to the same reason possibly also no changes in GFP fluorescence between the two compartments could be detected in the applied scale down system (chapter 8). Additionally, the relatively long time until a stable GFP degrades makes it impossible to see direct switch off of any reporter system. Furthermore the *E. coli* reporter strains were found to be suitable to be used as "growth rate" reporter strains[1] exhibiting a GFP fluorescence expression that can be directly correlated to the growth rate whereas the *S. cerevisiae* reporter strain was more a "growth" or "physiological state" reporter because opposite to original believe (based on transcriptomics data[2]) a rise in growth rate was not directly correlated to a rise in GFP expression. Instead the GFP expression upshift was rather correlated to nutrient upshift. Though, apart from some exceptions (e.g. under extreme growth conditions in high gravity batch cultivation, chapter 5) the strain could still be successfully applied to study growth patterns during e.g. batch cultivation as well as continuous culture. This demonstrates in general that the choice of the reporter gene should be done with caution and the reporter strain preferably well characertised under different conditions that could possibly influence the expression of the gene of interest to eliminate false conclusions in more complex experimental setups.

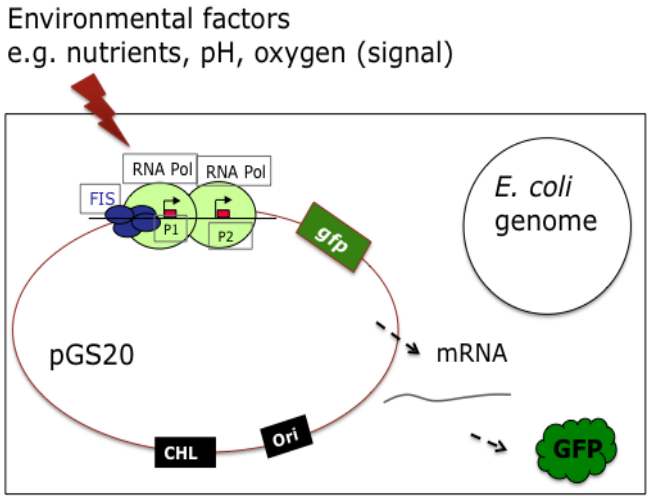

Figure 1 – The *E. coli* growth reporter strains rrnb and fis. The Fis protein has three binding sites in front of the *rrnB P1* promoter. The physical location of *rrnB* P1P2 promoter and *gfp* gene is illustrated. The figure is borrowed from Han *et al.* (2013)[1].

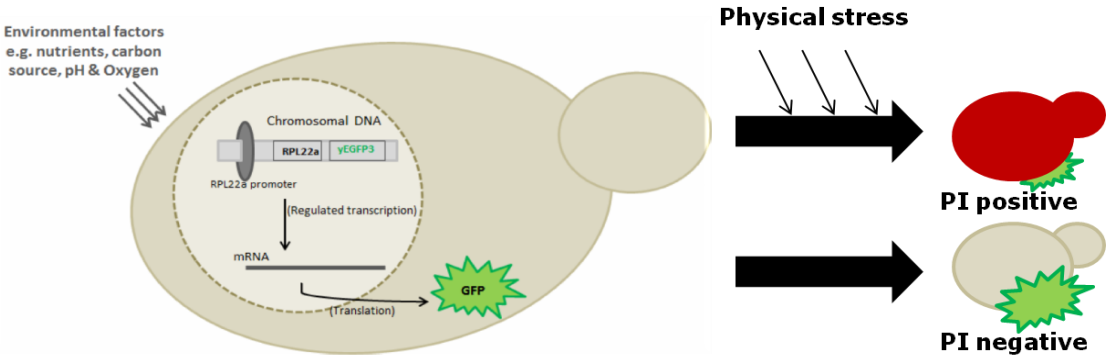

Figure 2 – The dual *S. cerevisiae* growth reporter strain FE440 which can be used to investigate growth related GFP fluorescence as well as when applying freeze-thaw stress to evaluate cell membrane robustness.

Moreover, the *S. cerevisiae* growth reporter strain was found to be a dual reporter strain (see figure 1) revealing information about cell membrane robustness when applying freeze-thaw stress to broth samples and performing the flow cytometry analysis at acidic pH (applied in chapter 4, 5 and 6). Later it was demonstrated that this tool to assess cell membrane robustness is not exclusive for yeast but can also be applied for *E. coli* (chapter 6).

The second applied *S. cerevisiae* reporter strain (applied in chapter 8), an ethanol reporter strain based on the expression of TagBFP under the control of the promoter for the phosphoenolpyruvate carboxykinase 1 (PCK1), was found suitable to monitor ethanol growth of cells in scale down reactors. Due to the pH-independency of TagBFP, however, no information about the cell membrane robustness could be gained. In conclusion, all in this thesis applied reporter strain systems were found to be valuable tools within their scope of applicability to monitor single cell characteristics.

9.1.2 Use of flow cytometry in combination with fluorescent stains and reporter strains for single cell analysis of microbial populations

As a high throughput technique flow cytometry is able to generate large amounts of data points (cell count) within seconds from broth samples representing the cell population inside the bioreactor. It was successfully applied to record data for cell size (FSC), cell morphology (SSC) and fluorescence originating from stains (see chapter 4 and 7) or reporter strains (BFP and GFP based). As summarised above, different fluorescent reporter strains were effectively employed to follow single cell distribution characteristics in cultivation processes of different nature (batch, chemostat and

two compartment reactors). Additionally, different fluorescence stains were successfully used to follow viability (PI and $DiBAC_4$) or metabolic activity (CTC, RSG and SYBR green) of single cells throughout the different phases of batch cultivation (chapter 7). Both approaches revealed useful information about single cell characteristics under different growth conditions, but especially for the stains, the choice of which combination of stains to apply should be made with care depending on which physiological traits to focus on. It is important to note that some stains, although targeting the same cell property e.g. metabolic activity, exhibited slightly different results (chapter 7, RSG and CTC). Hence, it is important to fully investigate the specific target(s) for the stain one want to use.

Some obstacles were experienced during the application of flow cytometry in this work. For example measurements are strongly dependent on the day of measurement which makes it sometimes critical to compare results achieved on different days although calibration beads are applied. Especially, when measuring on fresh samples (non-frozen samples, kept on ice) results can easily vary when the settings are not completely the same. Hereby also storage and treatment of the samples plays a big role. When analysing freeze-thaw stressed cell samples the sample handling procedure should be exactly the same to eliminate other possible influences that can change the fluorescence results especially also when the samples are frozen and thawed, as a different freezing (e.g. fast freezing in liquid nitrogen and slow freezing on ice) and thawing speed also influences the level of cell robustness (unpublished results). Furthermore, using different instruments with different resolution makes an objective data comparison challenging as the underlying mathematical relations needs to be evaluated first. Obviously some of these problems especially concerning sample handling can be circumvented by using an online flow cytometer with an automated sampling unit as already has been applied in a few studies by otehrs and e.g. the cytostat (see chapter 2,[3–5]).

In conclusion flow cytometry is a powerful tool for the investigation of single cell heterogeneities but it also needs to be used with caution to avoid wrong conclusion on recorded data because the output is influenced by the conditions accompanying the measurements. Furthermore as also summed up in chapter 2 both reporter strains and stains or a combination of both show big potential for single cell physiological investigations in both research and industry. Although reporter strains might only be suitable in industry for the development or optimization of bioprocesses since the introduction of a fluorescent protein in a production process might change or influence the production characteristics. Therefore, fluorescent stains targeting different cell properties might in

this case be the choice as also already employed e.g. viability staining as a standard method in fed-batch production processes (see chapter 2).

9.1.3 Setups for the experimental study of population heterogeneity

During this thesis different experimental setups have been used to study population heterogeneity of *S. cerevisiae* and *E. coli,* simulating conditions experienced in large scale cultivations, in lab scale. Batch cultivations were performed as a first approach to characterise the applicability of reporter strains and fluorescence stains as well as for getting an overview of single cell heterogeneities under dynamic conditions. Through the different growth phases fluorescence properties originating from fluorescent stains and reporter strains could be successfully monitored in response to different growth rates and growth environment (e.g. high substrate concentrations during exponential phase, nutrient limitation in stationary phase, overflow metabolism) (chapter 4,5 and 7). To further investigate the responsiveness of the reporter strains featuring growth correlated GFP fluorescence to different growth rates, continuous cultivations were used comparing slow and fast grown cells. Afterwards, the cultures were perturbed with glucose pulses simulating the feeding zone of large scale fed-batch cultivations and the sudden rise in substrate concentration cells experience passing through that zone (chapter 6). Results (see below for summary) were consistent with earlier studies investigating cell responses in large scale fermentation[6,7], which makes pulse experiments in continuous cultivations generally a valuable tool to study gradients. However when applying specialised setups e.g. a two compartment chemostat setup (scale down reactor, chapter 8) which is a different way to simulate the zones seen in large-scale reactors, that arise due to gradients in substrate and oxygen (feeding zone: high glucose/low oxygen level, remaining reactor: lower glucose/higher oxygen level), characteristics that are hidden due to unknown flows between different compartments in a conventional chemostat can be made visible. An example is the ethanol consumption monitored by the application of the ethanol reporter strain which could not be found in a normal chemostat (chapter 8). Furthermore, in a scale down setup cells are confronted to repeated passage through the feeding zone which makes this setup probably better comparable with an industrial large scale setup. Therefore different scale down setups have earlier been frequently applied in single cell research (chapter 2).

9.1.4 Data analysis applying objective methods and in combination with modeling

Already during my summary of literature related to single cell studies simulating large scale fermentation in lab scale to investigate the phenomenon of population heterogeneity the lack of

deeper, systematic and objective/unbiased data analysis and presentation, especially for the big amounts of data collected by flow cytometry analysis, was made evident (chapter 2). This has also been concluded by earlier publications[8–10]. However, general practice for treatment of flow cytometry data is the presentation of biplots or histograms of two related single cell properties respectively single parameter distributions, which are then interpreted subjectively using the bare eye to evaluate population shifts or manual gating (which has been developed and published by others) into positive and negative subpopulations e.g. for fluorescence stains (chapter 2). Also the calculation of mean values and rarely CV (coefficient of variance) is applied, which indeed scales down the complex data distribution data to single values that can be presented as time plots, but also presents significant loss of information about the population shape (e.g. broadness, tailing), appearance of subpopulations and potential shifts of the whole population. Without applying difficult mathematical equations, but just using interval analysis or subpopulation analysis dividing e.g. a histogram or biplot into different fluorescence areas and calculate the percentage or amount of relative fluorescence in each area one can raise the level of data interpretation up in objectivity and detail (chapter 4 and 5). Thereby the amount of output values that needs to be compared can still be held small in comparison to the original data set which simplifies the comparison of different cultivation conditions. Though if the amount of different conditions is large multivariate statistical tools for the comparison of data sets e.g. ANOVA, regression analysis or principal component analysis (PCA) as used in this thesis (chapter 5) can be easily applied (as they are e.g. add-in functions in excel) to verify the significance of differences between datasets. Furthermore, by applying simple mathematical tools new parameters for the objective description of histograms of fluorescence distributions could be derived (chapter 6). As demonstrated in this thesis adding the peak width (at baseline level or at half height) and the slope of the cumulative fluorescence distribution as standard parameters for the distribution description, additionally to the mean fluorescence and the CV, information about distribution heterogeneity in general and about peak shape and subpopulation appearance in specific can be presented in a simple but quantitative manner. Consequently a combination of the derived values can be plotted over time as e.g. general physiology data and still give valuable and objective information about the whole distribution as well as about shifts over time (chapter 6 and 7). Though it needs to be mentioned that depending on the study and the desired level of information (e.g. focus on subpopulation or shifts, or just general trends needed) the combination of parameters needs to be well considered. Furthermore, when only calculating a single parameter it might again scale down data to an average level that fail to describe

the real scenario of the single cell population in the bioreactor throughout time or at a particular sampling point.

Another important approach that could aid to facilitate interpretation and handling of data analysis and process control is combining modeling with experimental work (Chapter 8), which is up to now rarely applied (Chapter 2) but found to have high potential especially for bioprocess optimization[11]. Approaches like this can reduce the experimental space or at least put some borders because the whole range of possible conditions can be evaluated using modeling and afterwards interesting conditions can be picked to be performed experimentally. Results can then be integrated back into the model to increase its predictive power and in the end lead to strategies for process development and optimization.

In conclusion both deeper data analysis especially of complex flow cytometry data and the combination of modeling and experimental work shows great potential for the improvement of industrial scale bioprocesses as well as for population heterogeneity research to investigate small differences of single cell distributions in an unbiased systematic way under experimental interesting conditions.

9.1.5 Summary of major physiological findings related to population heterogeneity

In general the project was based on the hypothesis that because population heterogeneity is a two-sided phenomenon, leading towards decreased yields and an increased by-product formation but on the other hand also to cell populations that could easier adjust to a changing environment, there should be an optimal level of population heterogeneity, which results in high-yielded robust fermentation processes. In the scope of this thesis experiments revealed that to find this optimum the influences of several environmental factors (e.g. substrate, oxygen, pH etc.) on microbial cell factory and its characteristics (e.g. cell size, viability, metabolic activity, cell robustness etc.) need to be evaluated and quantified in depth at first, because things ongoing in a bioreactor are way more dynamic than prior thought (e.g. chapter 4 and 5).

By subjecting growth reporter strains of *E. coli* and *S. cerevisiae* to glucose perturbation (chapter 6), similar trends were seen, which is intriguing when taking into account the very different nature of the two microorganisms. For both microbes it was found that slow growing cells are mostly robust but the intact cells highly responding to the pulse whereas fast growing cells were less robust but intact cells less responding to the pulse. However, when glucose was pulsed it acted as protectant of

cells and increased the membrane robustness of fast growing cells. Some differences between the two microbes were seen, for instance *E. coli* was found to be less sensitive to freeze-thaw stress than yeast.

In batch cultivation of an *E. coli* growth reporter strain combined with the application of different fluorescent stains (chapter 7) it was seen that, although acetate is known to be highly toxic for *E. coli*, single cell physiology does not exhibit severe differences using glucose or acetate as sole carbon source. Cells in both cases were highly viable and metabolic active. Though, for cells grown on acetate as sole carbon a small fraction of the cell population was found to be more robust than the remaining population, which was not seen for cells growing on acetate after diauxic shift. Additionally, when investigating population heterogeneity concerning growth and membrane robustness in a two-compartment chemostat it was revealed that single cell characteristics are significantly influenced depending on the severity of differences between the two compartments (chapter 8).

9.2 Outlook

In continuation of this thesis to get a deeper understanding of how exactly the applied reporter systems function as well as to evaluate the growth and stress response on a deeper level transcriptomics and/or proteomics should be integrated into the analysis of the cultivation processes. Furthermore these methods could also be applied after cell sorting of different subpopulations e.g. of different cell membrane robustness as seen as a response to the pulse or during batch cultivation, to examine the underlying cellular characteristics that result in the development of the different phenotypes in a population. Moreover after successful sorting of cells from the subpopulations, they could be regrown if the sorting procedure allows sterile work. This could aid in strain development and improvement in line with the new upcoming field strain population engineering. All this could possibly be combined with a setup that complements the basic fermentation setups with an online flow cytometer with automated sampling to get online fluorescence data without the gaps that occur between normal sampling points for the different reporter strains as well as for maybe additionally applied fluorescent stains. Also the application of further reporter strains monitoring different cell properties as e.g. a stress reporter strain or even more interesting especially in the industrial perspective a single protein expression reporter strain would be relevant. Furthermore the in this thesis developed scale down system should be deeper characterised testing its borders, e.g. using even lower recirculation, different length or circulation

tubes and different dilution rates. Afterwards the system could also be combined with the above mentioned online flow cytometer and fluorescence stains e.g. for viability and metabolic activity and maybe transcriptomics. Also a comparison with a setup combining a PFR and STR could be of interest to evaluate the different properties. For this purpose the integration of rapid sampling methods similar to a bioscope could be useful. In the end to scale things down and in depth investigation of the single cell behaviour in an isolated environment, microbioreactor studies should be performed.

All possible further studies should obviously also be accompanied by objective, systematic data analysis methods, maybe by using and evolving and the in this thesis introduced mathematical parameters and methods and combine them with modeling approaches. Together all this could lead to the ability of detailed description of population heterogeneity experienced in large scale biotechnological production processes and derived from that the development of control strategies.

9.3 References

1. Han, S., Delvigne, F., Brognaux, A., Charbon, G. E. & Sørensen, S. J. Design of growth-dependent biosensors based on destabilized GFP for the detection of physiological behavior of Escherichia coli in heterogeneous bioreactors. *Biotechnol. Prog.* **29,** 553–563 (2013).

2. Regenberg, B. *et al.* Growth-rate regulated genes have profound impact on interpretation of transcriptome profiling in Saccharomyces cerevisiae. *Genome Biol.* **7,** (2006).

3. Zhao, R., Natarajan, A. & Srienc, F. A flow injection flow cytometry system for on-line monitoring of bioreactors. *Biotechnol. Bioeng.* **62,** 609–617 (1999).

4. Abu-Absi, N. R., Zamamiri, A., Kacmar, J., Balogh, S. J. & Srienc, F. Automated flow cytometry for acquisition of time-dependent population data. *Cytometry. A* **51,** 87–96 (2003).

5. Kacmar, J., Gilbert, A., Cockrell, J. & Srienc, F. The cytostat: A new way to study cell physiology in a precisely defined environment. *J. Biotechnol.* **126,** 163–172 (2006).

6. Bylund, F., Collet, E., Enfors, S.-O. & Larsson, G. Substrate gradient formation in the large-scale bioreactor lowers cell yield and increases by-product formation. *Bioprocess Eng.* **18,** (1998).

7. George, S., Larsson, G., Olsson, K. & Enfors, S.-O. Comparison of the Baker's yeast process performance in laboratory and production scale. *Bioprocess Eng.* **18,** 135–142 (1998).

8. Delvigne, F. & Goffin, P. Microbial heterogeneity affects bioprocess robustness: Dynamic single-cell analysis contributes to understanding of microbial populations. *Biotechnol. J.* **9,** 61–72 (2014).

9. Fernandes, R. L. *et al.* Experimental methods and modeling techniques for description of cell population heterogeneity. *Biotechnol. Adv.* **29,** 575–599 (2011).

10. Lencastre Fernandes, R. *et al.* Cell mass and cell cycle dynamics of an asynchronous budding yeast population: experimental observations, flow cytometry data analysis, and multi-scale modeling. *Biotechnol. Bioeng.* **110,** 812–826 (2013).

11. Koutinas, M., Kiparissides, A., Pistikopoulos, E. N. & Mantalaris, A. Bioprocess systems engineering : transferring traditional process engineering principles to industrial biotechnology. *Comput. Struct. biotechnoloy* **3,** (2012).

10. Appendix

List of publications not included in the thesis

- **Cell mass and cell cycle dynamics of an asynchronous budding yeast population**
  Lencastre Fernandes, Rita ; Carlquist, Magnus ; Lundin, Luisa ; **Heins, Anna-Lena** ; Dutta, Abhishek ; Sørensen, Søren J. ; Jensen, Anker Degn ; Nopens, Ingmar ; Eliasson Lantz, Anna ; Gernaey, Krist
  in journal: Biotechnology and Bioengineering, vol: 110, issue: 3, pages: 812-826, 2013
  Type: Journal article
  Status: Published 2013

- **Applying mechanistic models in bioprocess development.**
  Lencastre Fernandes, Rita ; Bodla, Vijaya Krishna ; Carlquist, Magnus ; **Heins, Anna-Lena** ; Eliasson Lantz, Anna ; Sin, Gürkan ; Gernaey, Krist
  part of: Advances in Biochemical Engineering/Biotechnology, pages: 137–166, 2013, Springer
  Type: Book chapter
  Status: Published 2013

- **Experimental methods and modeling techniques for description of cell population heterogeneity**
  Lencastre Fernandes, Rita ; Nierychlo, M. ; Lundin, L. ; Pedersen, Anne Egholm ; PuentesTellez, P. E. ; Dutta, A. ; Carlqvist, Magnus ; Bolic, Andrijana ; Schäpper, Daniel ; Brunetti, Anna Chiara ; Helmark, Søren ; **Heins, Anna-Lena** ; Jensen, Anker Degn ; Nopens, I. ; Rottwitt, Karsten ;Szita, Nicolas ; van Elsas, J. D. ; Nielsen, P. H. ; Martinussen, Jan ; Sørensen, S. J. ; Eliasson Lantz, Anna ; Gernaey, Krist
  in journal: Biotechnology Advances, vol: 29, issue: 6, pages: 575-599, 2011
  Type: Journal article
  Status: Published 2011